Alma Mater Studiorum – Università di Bologna

DOTTORATO DI RICERCA IN
Ingegneria Civile, Chimica, Ambientale e dei Materiali
Ciclo XXX

Settore Concorsuale:
08/A1 Idraulica, Idrologia, Costruzioni idrauliche e marittime

Settore Scientifico Disciplinare:
ICAR/01 Idraulica

PROPAGATION OF UNCERTAINTY ACROSS MODELING CHAINS TO EVALUATE HYDRAULIC VULNERABILITY IN COASTAL AREAS

Presentata da:
Silvia Unguendoli

Coordinatore Dottorato
Prof. Ing. Luca Vittuari

Supervisore
Prof. Ing. Barbara Zanuttigh

Co-supervisore
Dott. Tiziana Paccagnella

Esame finale anno 2018

Time went by and we had to say goodbye.
No farewell could be the last one,
if you long to meet again.

(Farewell – Avantasia)

Acknowledgments

This thesis is the conclusion of my Philosophiæ Doctorate in Civil, Chemical, Environmental and Materials Engineering at School of Engineering and Architecture of the Bologna University, Italy. This thesis has been carried out at the Regional Environmental Agency of Emilia-Romagna (Arpae), at the Hydro Meteo Climate Service.

Especially, I would like to thanks my advisors Barbara Zanuttigh and Tiziana Paccagnella, for their constructive and continued support and help throughout this project. Thanks to them for always being enthusiastic about my research.

Special thanks also should be given to my colleagues that were a great help during this time and made my days fun and cheerful. Thanks for enduring me, in particular in the most nervous moments.

A special heartfelt thanks goes out to Alessandro, who has had to deal with the brunt of my stressful ways. He has been an anchor, keeping me focused on the goal at hand. Thanks to always being by my side and having believed in me.

I'm also grateful to my old friends for remaining the same even though, by now, we have grown up.

Last, but certainty not least, special thanks to my parents for their encouragements and unconditional support.

Summary

Worldwide, numerous approaches have been developed to deal with extreme events. All of the events that caused damages on the coastal areas have brought to light the importance of an Early Warning System (EWS) in predicting and preparing for coastal risks, thereby minimizing loss of life as well as damage to infrastructure. The concept outlining extreme event-related policies that is widely applied in several nations is the "safety chain".

Coastal flooding and erosion are one of the most serious environmental problems in coastal zones of the Emilia-Romagna region. An accurate and fully informative prediction of sea level (SL) in the time range from one hour to several days is an essential tool for the management of the region and the delivery of reliable and accurate warnings.

Usually, these forecasting systems are composed of interlinked meteorological, wave/oceanographic and morphological coastal models. The Emilia-Romagna Early Warning System (EWS) is a state-of-the-art coastal forecasting system, composed of an operational cascade of numerical models, to provide a forecast up to 72 hours ahead of the sea level height along the entire coastal region (Harley et al., 2016). The integrated modeling system is operational at the Hydro Meteo Climate Service of Arpae, the Regional Environmental Agency of Emilia-Romagna.

When a series of models are used in cascade for the meteorological, oceanographic and coastal predictions, one has to keep in mind that uncertainties associated with each model component propagate through the numerical chain with a collective effect on the final forecasts accuracy. It is not easy to be fully understand the full range and interaction of uncertainties in the forecast systems.

The aim of this thesis is to investigate the propagation of the uncertainties from meteorological to coastal forecasts, in order to obtain a better understanding of the uncertainties associated to the numerical modeling systems. To achieve these goals, the focus has been addressed with two phases of the study.

The first phases focused on the parameter settings of the morphological model XBeach, as source of uncertainties within the model itself. This was done by means of a sensitivity analysis of the model that allowed to characterize how the model responds to changes in input, with an emphasis on finding the input parameters to which outputs are the most sensitive.

Moreover, an estimate of how the uncertainties propagate within the numerical modeling chain was made by means of the ensemble technique. Moving from a single-deterministic to probabilistic forecasts, it is possible to give some useful indication of the forecast reliability. Therefore, the meteorological Limited Area Ensemble Prediction System COSMO-LEPS was used to generate 16 different meteorological forecasts that were used to force the wave\oceanographic models SWAN and ROMS and finally the morphological model XBeach. The study focused on two different storm events both occurred in the autumn 2015-winter 2016 on the Emilia-Romagna coasts.

The results showed that, in both cases, the uncertainties of the wind and pressure fields clearly propagated through to the oceanographic models up to influence the coastal forecasts. The accuracy of the forecasts of the oceanographic and morphological models is largely dependent on the quality in wind data. However, extension of the ensemble approach to the coastal areas showed encouraging results and suggested, as a future development, the possible optimization of the system by using a meteorological ensemble built in such a way as to optimize the spread in terms of the surface variables used to drive the marine-coastal model components.

Table of Contents

Chapter 1 Introduction

This chapter introduces the main problems, motivations and objectives of the research. Storm surges have become one of the most disastrous natural events for the coastal areas. The need for more and more accurate forecasting systems for coastal flooding is growing with the social and touristic relevance of these areas. An overview on the "safety chains" developed to tackle these issues and some considerations on the uncertainties that are propagated within these numerical modeling chains are presented.

1.1 Vulnerability of Coastal areas

At a rough estimate more than 200 million people worldwide live along coastlines less than 5 meters above sea level. By the end of the 21st century this figure is estimated to increase to 400 to 500 million (World Ocean Review , 2017). Therefore, the population densities in coastal regions are about three times higher than the global average (Small and Nicholls, 2003).

The insatiable human attraction to the coast has resulted in rapid expansions in settlements, urbanization, infrastructure, economic activities and tourism in the 20th century and is likely to continue to increase in the 21st century (Jongejan and Ranasinghe, 2009).

As stated by the European Environment Agency (2006) for Europe, population densities of the coastal regions are on average 10 % higher than inland. However, in some countries this figure can be more than 50 %. There are many regions where the coastal population is at least five times the European average density. In several coastal regions of Italy, France and Spain the coverage of built-up areas in the first kilometer coastal strip exceeds 45 %. In these areas further development is occurring in the coastal hinterland.

Major threats for large stretches of European coasts are erosion and flooding. As stated by Martinelli et al (2010) one fifth of the coastline of the European Union is presently eroding away, in a few dramatic cases as much as 20 m a year, the largest percentage of eroding coastline being in Romania (60%), Poland (55%) and in Latvia (33%).

It should be noted that in most of these places, the coastal areas densities strongly increase during the summer period. In particular, about 5 million tourists visit the coastline of the Emilia-Romagna region, located on the northern Italy, every year (Harley et al., 2013). In tandem, the continuous growth of urban artificial surfaces, the development of beach-front infrastructure built to service the visitors and climate change put more and more pressure on these coastal areas.

It is then apparent that large numbers of people will be exposed to flooding by storm surges which are among the most disastrous events that can cause floods in the coastal areas. A storm surge is a meteorologically forced long wave motion which is pushed toward the shore. It is generated by a combination of meteorological forces of the wind shear stress and low air pressure due to a storm and oscillates in the period range of a few minutes to a few days (Gonnert et al., 2001). In some coastal

areas, such floods can be generated by unusual sequences of wind set-up and air pressure variations. In addition, wind driven waves can be superimposed on the storm tide. This rise in sea level can cause severe flooding in coastal areas, particularly when the storm tide coincides with the high tides (Battjes & Gerritsen, 2002).

Over the past centuries, a number of severe coastal floods have destroved many places in the world. This list includes Hurricane Katrina, which struck the coastline of Louisiana in 2005 (Knabb et al., 2005), Cyclone Sidr in the Bay of Bengal in 2007 (Paul, 2009), the 2009 Klaus storm in the Mediterranean Sea (Berlotti et al., 2011), the 2010 Xynthia storm on the west coast of France (Kolen et al., 2013), Hurricane Sandy on the east coast of the USA in 2012 (Galarneau Jr. et al., 2013), Typhoon Haiyan in the Philippines in 2013 (Lagmay et al., 2015) and the 2013/2014 series of winter storms in the UK (Slingo et al., 2014). Whether or not these events have increased in both intensity and frequency in the long term is the subject of considerable debate (Coumou and Rahmstorf, 2012; Peterson et al., 2013). These events had massive impacts, damaging property and resulting in the loss of human lives (e.g., Alovisi et al. 2007) and have raised public awareness and demand for storm hazard mitigation measures (Ciavola et al. 2011).

Italy is particularly exposed to the coastal flooding risk and the Emilia-Romagna coastline has morphological characteristics that make it one of the most vulnerable areas. The regional coasts are characterized by large areas with lower sea level, largely reclaimed and urbanized. Moreover, the avalanching of the dunes, the subsidence and the strong reduction of solid river transport that cause the beach erosion worsen the situation. The coastal littoral of the Emilia-Romagna region was heavily damaged by intense storm events such as the 5-6 February 2015 storm, the November 2012 event named “Halloween Storm” and the event od March 2010 (Perini et al., 2015).

1.2 **Extreme events**

Worldwide, numerous approaches have been developed to deal with extreme events. All of the events that caused damages on the coastal areas have brought to light the importance of an Early Warning System (EWS) in predicting and preparing for the arrival of coastal risks, thereby minimizing loss of life as well as damage to infrastructure. The concept outlining extreme event-related policies that is widely applied in several nations is the “safety chain”.

EWSs give civil protection agencies the necessary time and information in order to prepare themselves and, if needs be, execute the necessary risk-reduction measures (Basher, 2006). It provides advance warning of dangerous events, so that protective actions can be taken. While EWSs for river flooding and tsunamis are operational throughout many affected regions worldwide, the development of EWSs for coastal inundation risk is still in its infancy (Ciavola et al., 2011).

With specific regards to coastal storm hazards, the development of EWSs has until recently focused on hydrodynamic forecasts for vulnerable low-lying areas. Then, numerous countries developed and implemented flood forecast systems (e.g. Flather, 2000; Verlaan et al., 2005; Daniel et al., 2009; Lane et al., 2009; Werner et al., 2009; Ji et al., 2010). Usually, these coastal flood warnings are based on wind, wave and storm surge forecasts produced by meteorological, oceanographic and coastal models.

Some examples of these systems around the world include the Acqua Alta surge forecast system for the Venice lagoon (Bajo and Umgiesser, 2010; Ferrarin et al., 2013; Mariani et al., 2015), the UK joint

Met Office–EA Flood Forecasting Centre (Stephens and Cloke, 2014), the US National Hurricane Center forecast system (Morrow et al., 2014) and the Bangladesh storm surge EWS (Dube et al., 2009).

In Italy, the Regional Agency for Prevention, Environment and Energy of Emilia-Romagna (Arpae) is responsible for issuing coastal flood warnings for the Emilia-Romagna Region, which overlooks the northern Adriatic Sea (Italy). The Emilia-Romagna Early Warning System (EWS) is a state-of-the-art coastal forecasting system, composed of an operational cascade of numerical models, to provide a forecast up to 72 hours ahead of the sea level height along the entire coastal region (Harley et al., 2016). The integrated modeling system is operational at the Hydro Meteo Climate Service of Arpae Emilia-Romagna. A detailed description of the numerical chain it can be found in Chapter 2.

Some studies such as Paul (2009), Stephens and Cloke (2014) and Spencer et al. (2014) demonstrated that, when performing successfully, the early warnings provided by these systems have been credited with having greatly reduced the impacts and loss of life of various extreme events.

1.3 **Forecast uncertainty**

The interactions between atmospheric, oceanic and coastal processes are poorly understood, resulting in large uncertainties in the predictions of coastal flooding, in particular, under extreme conditions (Baart,2011; Zou,2009).

The accuracy of storm surge forecast is likely to be affected by the uncertainties arising from the weather forecast (Ding et al., 2016). Indeed, storm surges are driven by the weather, which is expected to be the dominant source of surge forecast uncertainty. Essentially, the coastal floods due to storm surges can be predicted with an accuracy that depends on the accuracy of the meteorological forecasts

De Moel et al. (2012) state that there is quite some uncertainty in the flood damage simulations, which is rooted in the uncertainty of the input data and model assumptions (Merz et al., 2004; Merz and Thieken, 2009; Apel et al., 2008; De Moel and Aerts, 2011). These sources of uncertainty can relate to both epistemic uncertainty (incomplete knowledge), or aleatory uncertainty (natural variability) (see e.g. Apel et al., 2004).

Quite often, some or all of the model inputs are subject to sources of uncertainty, including errors of measurement, absence of information and poor or partial understanding of the driving forces and mechanisms (Der Kiureghian and Ditlevsen, 2009). Furthermore, the model itself can introduce uncertainty depending on his parameter setting, particularly with the setting of the individual parameters, which are used as input for the model (Heuvelink, 1998). In this way, a numerical model can be highly complex, and as a result its relationships between inputs and outputs may be poorly understood.

As stated by Cloke et al (2009), meteorological input uncertainty is usually assumed to represent the largest source of uncertainty in the prediction of floods with a time horizon of beyond 2–3 days. However, there are in fact many sources of uncertainties further down in the flood forecasting cascade which could also be significant, for example: the corrections and downscaling; spatial and temporal uncertainties as input into the hydrological antecedent conditions of the system (including data assimilation); geometry of the system (including flood defence structures); possibility of infrastructure failure (dykes or backing up of drains); characteristics of the system (in the form of model parameters); and in the limitations of the models available to fully represent processes (for example

surface and sub-surface flow processes in the flood generation and routing). The relative importance of the different types of uncertainty will most likely vary with the time (and lead time) of the forecasts, with the magnitude of the event and catchment characteristics.

Operational and research flood forecasting systems around the world are increasingly moving towards using ensembles of numerical weather predictions, known as ensemble prediction systems (EPS), rather than single deterministic forecasts, to drive their flood forecasting systems.

An ensemble modelling approach addresses this issue by producing not one but several forecasts with the same likelihood to be the correct one. Each forecast uses slightly different initial conditions and/or boundary conditions and/or model physics, with the aim of sampling the range of forecast results which are consistent with the uncertainty in the forecast (Palmer et al., 2004).

Therefore, the ensemble approach allows to estimate the probabilities of various outcomes and to quantify the associated uncertainties by producing a sample of alternative/possible future atmospheric states. Furthermore, it is also possible to assess how the uncertainty propagates from meteorological forecasts to coastal modeling (overtopping and coastal flood) , thereby improving our understanding of the reliability of results (Zou and Reeve, 2009; Dance and Zou, 2010).

The ensemble modeling approach has been widely used in meteorology (e.g. Marsigli et al., 2001, Buizza et al., 2005; Bowler et al., 2008; and references therein) and storm surge studies (Horsburgh et al., 2008; Flowerdew et al., 2010, Ding et al., 2016), but much less so far in coastal engineering.

1.4 **Objectives**

Coastal flooding and erosion are among the most serious environmental problems in coastal zones of the Emilia-Romagna region. An accurate and fully informative prediction of sea level (SL) in the time range from one hour to several days is an essential tool for the management of the region and the delivery of reliable and accurate warnings.

Storm surges are driven by the weather, which is expected to be the dominant source of surge forecast uncertainty. The accuracy of storm surge forecast is likely to be affected by the uncertainties arising from the weather forecast.

The main objective of this thesis is to obtain a better understanding of the uncertainties associated to the complete numerical modeling systems, which are composed of interlinked meteorological, oceanographic and coastal models.

To achieve this goal, three different research issues were investigated.

Morphological model uncertainties: analysis of the uncertainties related to the input parameter of the morphological model XBeach. How does the variation of the input parameter values influence the model outputs?

Propagation of uncertainties: a study to investigate how the uncertainties propagate from the meteorological data to the coastal forecasts, through the whole numerical modeling chain. The analysis is carried out by means of the ensemble technique.

Integrated "Weather-Coastal" Ensemble System: the extension of the ensemble method up to the morphological model has the purpose to evaluate the use of the probabilistic approach also for the coastal forecasting.

1.5 Approach and Outline

The research issues are addressed throughout several chapters, eventually leading to fulfilling the thesis objectives and answering the problem definition.

Chapter 2 presents the configuration of the numerical modeling chain, operational at the Hydro Climate Service of Arpae Emilia-Romagna, with the aim to provide the reader wih a complete overview of the forecasting system. The chapter focuses on the input and output data of each model, providing a clear description of the computational domains and the relative boundary conditions.

Chapter 3 is used to present the case study. This is done with a general description of the Emilia-Romagna coasts and their main features, focusing on the chosen study domain close to the Cesenatico municipality. Also presented are the two storm events that occurred in the autumn 2015- winter 2016 on the Emilia-Romagna littoral, which are investigated in this thesis.

After the comprehensive description of the available forecast models and data, Chapters 4 and 5 present the analysis and the relative results of the project.

The uncertainty analysis is mainly focused on the XBeach model in order to investigate the uncertainties associated to its forecasts. In Chapter 4 it can be found a sensitivity analysis and a proper calibration of the model can be found, with reference to the case study. The analysis was carried out by varying the values of the most important model parameters, analyzing the effect on the model outputs. This study allows to better understand the uncertainties of this model in relation to the different parameter values.

Finally, Chapter 5 presents an estimate of the propagation of the uncertainties by means of the ensemble approach. The technique was extended from the meteorological model COSMO-LEPS, which is already operational at Arpae SIMC, through the oceanographic models SWAN and ROMS, up to the coastal model XBeach. The use of the ensemble method allows to evaluate the forecasts uncertainty and its propagation within the system.

Chapter

2 The operational modeling chain

The ultimate goal of the research is to integrate meteorological models, regional hydrodynamic (waves, tides and surge) models and surf zone hydrodynamic models, to investigate the propagation of the uncertainties within the modeling prediction systems. This chapter presents a detailed description of the models that are part of the operative modeling framework at the Hydro Meteo Climate Service (SIMC) of Arpae Emilia-Romagna.

2.1 Description of the numerical modeling chain

The Emilia-Romagna Early Warning System (EWS) is a state-of-the-art coastal forecasting system that provides a forecast up to 72 hoursahead of the sea level along the entire coastal region (Harley et al., 2016). The integrated modeling system consists of a wave modeling forecasting chain, named MEDITARE (Valentini et. al., 2007) based on the SWAN model (Ris et al., 1994), and an oceanographic model ROMS, implemented on the Adriatic Sea, named ADRIAROMS (Chiggiato and Oddo,2006). Both models are driven by the weather forecast numerical model COSMO (www.cosmo-model.org), forced by the ECMWF model (www.ecmwf.int) with a 7 km resolution. The outputs from the coupled operational meteo-marine chain are used as input data for the coastal model XBeach (Roelvink et al, 2009) that was implemented as part of the FP7-MICORE project activities (www.micore.eu) and integrated in a coastal early warning system for the Emilia-Romagna Region (Harley et al., 2016). The operational chain (Figure 1) provides a deterministic forecast up to 72 hour ahead. A detailed description of each model can be found in the next subsections.

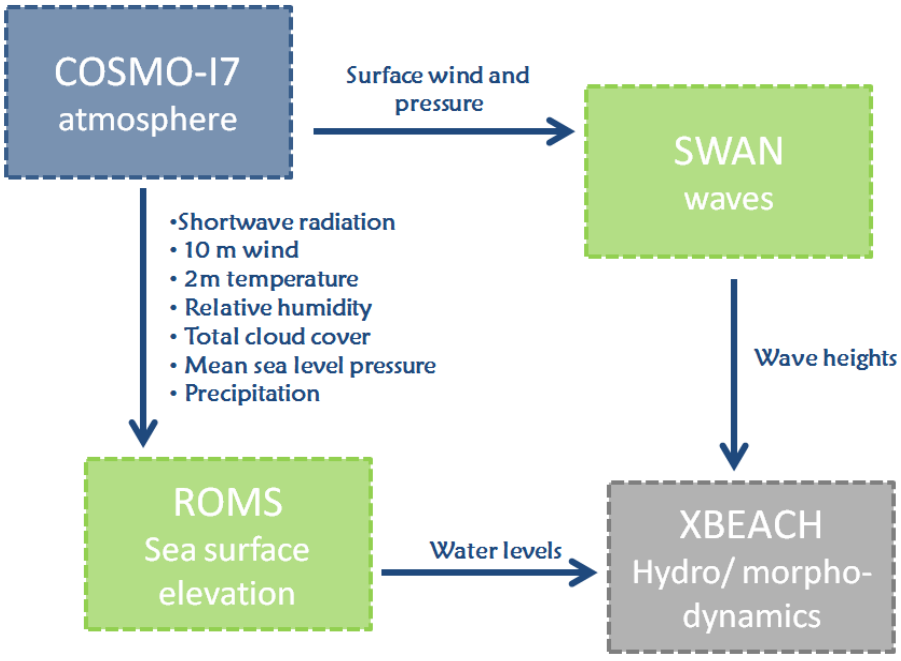

Figure 1 Operational numerical forecasting chain at Arpae SIMC Emilia-Romagna for the coastal Early Warning System.

2.2 **Meteorological model: COSMO**

The COSMO-Model is a non-hydrostatic limited-area atmospheric prediction model, developed by the Consortium for Small-Scale Modelling (COSMO, http://www.cosmo-model.org). It has been designed for both operational numerical weather prediction (NWP) and various scientific applications on the meso-β and meso-γ scale. The COSMO-Model is based on the primitive thermo-hydrodynamical equations describing compressible flow in a moist atmosphere. A variety of physical processes are taken into account by parameterization schemes. COSMO has been developed to meet high-resolution regional forecast requirements of weather services and to provide a flexible tool for various scientific applications on a broad range of spatial scales. By employing 1 to 3 km grid spacing for operational forecasts over a large domain, it is expected that deep moist convection and the associated feedback mechanisms to the larger scales of motion can be explicitly resolved. Meso-γ scale NWP-models thus have the principle potential to overcome the shortcomings resulting from the application of parameterized convection in current coarse-grid hydrostatic models. In addition, the impact of topography on the organization of penetrative convection by, e.g. channeling effects, is represented much more realistically in high resolution non-hydrostatic forecast models. In the beginning, the operational applications of the model within COSMO were mainly on the meso-β scale using a grid spacing of 7 km. The key issue was an accurate numerical prediction of near-surface weather conditions, focusing on clouds, fog, frontal precipitation, and orographically and thermally forced local wind systems.

Since April 2007, several weather centers of COSMO consortium have been running operationally a meso-γ scale version, with a grid-spacing of about 2.8 km. This allows for a direct simulation of severe weather events triggered by deep moist convection, such as supercell thunderstorms, intense mesoscale convective complexes, pre-frontal squall-line storms and heavy snowfall from wintertime mesocyclones.

Lateral boundary conditions can be provided by 1-way nesting from several coarse-grid models, including IFS model from ECMWF, ICON model from the German Weather Service (DWD) and COSMO-model itself.

As for the operational implementation of COSMO model at Arpae-SIMC the main features can be summarized as follows:

- COSMO-I7 is the 7 Km version of COSMO running over the Italian domain twice a day with 40 model levels with a forecast range of 72 hours; it takes the boundary conditions from ECMWF HRES System, while the initial conditions are obtained via a nudging-based data assimilation system.
- COSMO-I2 is the 2.8 km version of COSMO running over the Italian domain twice a day with 50 model levels with a forecast range of 48 hours; both initial and boundary conditions are provided by the fields generated by COSMO-I7.
- COSMO-LEPS is the limited-area Ensemble Prediction System developed at Arpae-SIMC on behalf of the COSMO consortium (Marsigli et al. 2001, Montani et al. 2011). It consists of 16 integrations of the COSMO model running twice a day, at 7 km of horizontal resolution, with 40 model levels and with a forecast range of 132 hours. It takes both initial and boundary conditions from selected members of ECMWF ENS and the integration domain covers central and southern Europe. COSMO-LEPS can be viewed as a dynamical downscaling of ECMWF ENS:

the advantages of global-model ensembles are combined with the high-resolution details gained in limited-area modelling so as to provide a probabilistic guidance for the possible occurrence of high-impact weather. In addition to the ensemble runs, one extra integration is performed taking both initial and boundary conditions from ECMWF HRES: this run is referred to as COSMO-LEPS_Det.

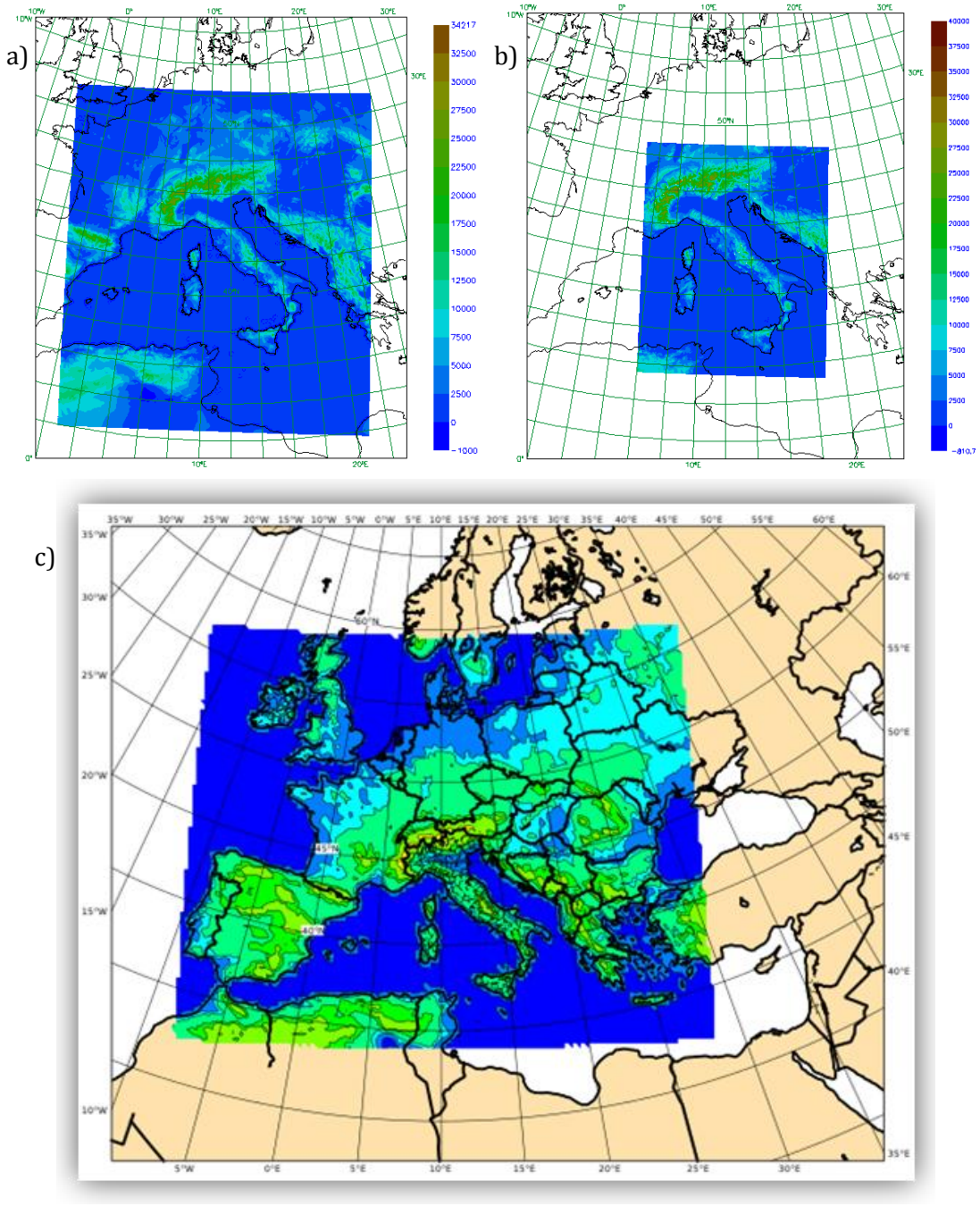

Figure 2 Domains of the meteorological models: a) COSMO-I7, b) COSMO-I2 and c) COSMO-LEPS

In this study the attention is mainly focused on COSMO-LEPS which will provide the forecast fields for the oceanographic models run, in their turn, in ensemble mode, thus enabling the possibility to evaluate the propagation of uncertainty from meteorological down to coastal model. In order to quantify the added value of an ensemble approach with respect to a deterministic one, the

performance of the oceanographic and coastal models nested on COSMO-I7 and COSMO-LEPS_Det will be also investigated.

2.3 **Waves models: SWAN**

The "Sea State" is the description of the properties of sea surface waves, at a given time and place. This might be given in terms of the wave spectrum or more simply in terms of the significant wave height, wave direction, mean and peak period; these information can be obtained by means of numerical models. For this purpose the Hydro-Meteorological Service of the ARPA Emilia-Romagna, ARPA-SIM, uses the SWAN model operationally (www.arpa.emr.it/sim/?mare/). ARPA-SIM Sea State numerical modelling is supported by the contribution of the National Civil Protection Department (www.protezionecivile.it).

The SWAN model is a non-stationary third-generation phase-averaged wave model for the simulation of waves in waters of deep, intermediate and finite depth. SWAN is supported by Rijkswaterstaat (as part of the Ministry of Transport, Public Works and Water Management, The Netherlands) and was developed at Delft University of Technology, Delft (the Netherlands) and where it is undergoing further enhancements. The SWAN model has been released under public domain. The resolution and the bathymetry precision are of primary importance to achieve a really good estimation of the wave height in the coastal area and in the surf zone. The advantage of using this model is related to the following functionalities:

- Wave propagation processes

  – propagation through geographic space,
  – refraction due to spatial variations in bottom and current,
  – shoaling due to spatial variations in bottom and current,
  – blocking and reflections by opposing currents,
  – transmission through, blockage by or reflection against obstacles.
- Wave generation and dissipation processes:

  – generation by wind,
  – dissipation by whitecapping,
  – dissipation by depth-induced wave breaking,
  – dissipation by bottom friction,
  – wave-wave interactions (quadruplets and triads)
- Nesting with WAM, WAVEWATCH III and SWAN itself.

The operational model is driven by the speed and direction of the 10 m wind computed by the Italian implementation of the meteorological model COSMO. The operational system is designed in three steps, the first one is a run over the Mediterranean Sea, with a 25 Km horizontal resolution (1/4°), that produces the boundaries conditions for the following run over the Italian domain, whose resolution is about 8 Km (1/12°) that is approximately equal to the meteorological model one (7 Km horizontal resolution). This run produces the hotstart files necessary for the wave field set-up of the following run and the boundary conditions necessary for nesting run over the Emilia Romagna area with a computational resolution of about 800 m. This nesting technique allows to achieve good results in

limited areas where a really high forecast accuracy is needed. Figure 3 shows the nested computational domains of the SWAN model. The technical specifications of the model are the follows:

Italian scheme (SWAN-ITA):

- geographic domain: 6°-20° (longitude East), 34°-46° (latitude North);
- 10 m wind from COSMO-I7 as forcing;
- computational grid (regular): 1/12 of degree, about 8 Km;
- one forecast each day at 00 UTC. To warm-up the model the hotstart files from the previous run (or a stationary run if they are not available), in order to set-up the wind field, and 24 hours of wind analysis are used;
- forecast range: +72 hours with three-hourly output;
- outputs variables: significant wave height, mean direction, mean and peak period;

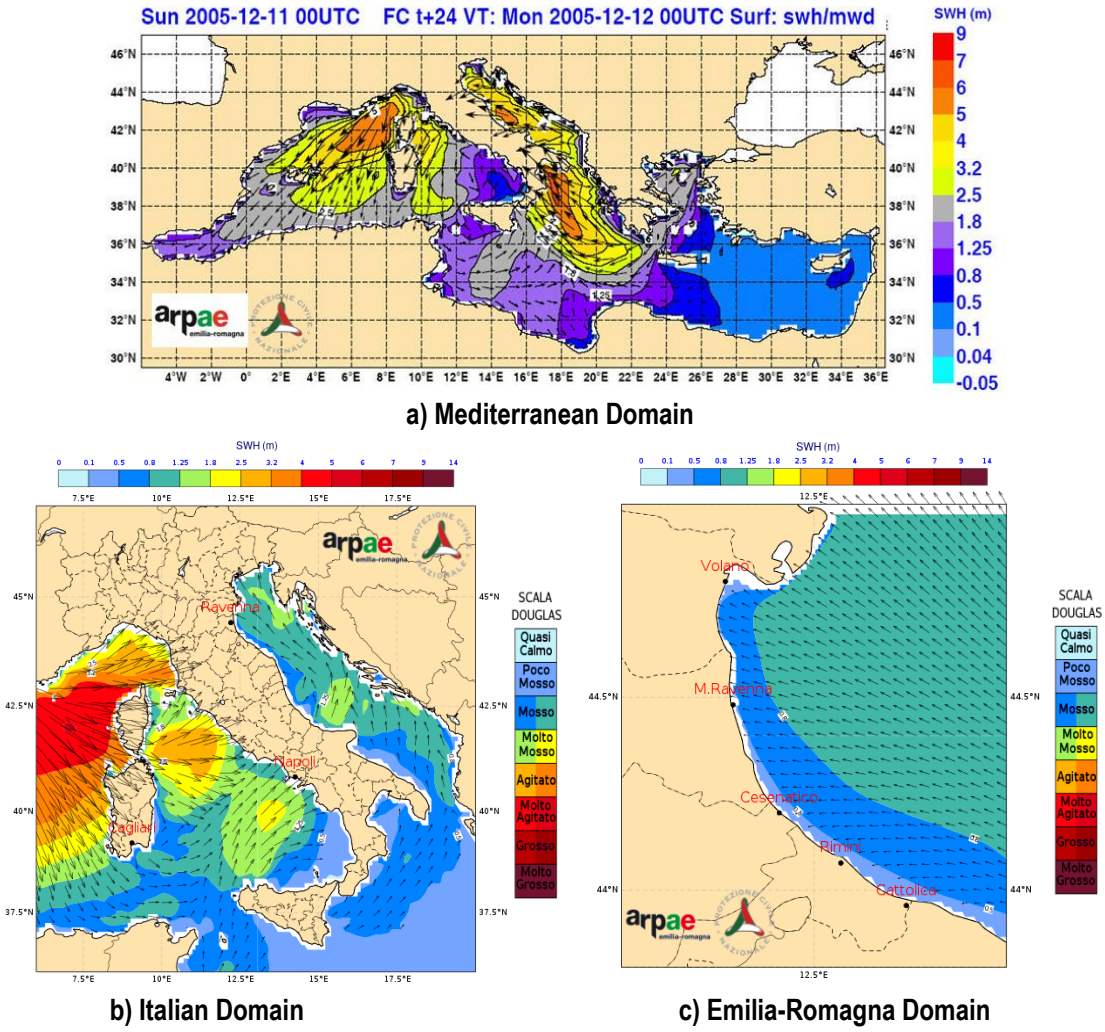

Figure 3 Nested computational domains of the SWAN model. The figure presents an example of the SWAN output of wave predictions for the Mediterranean domain (a), the Italian region (b) and the Emilia-Romagna region (c).

Scheme of nesting over the Emilia Romagna sea (SWAN-EMR):

- geographic domain: 12°-13° (longitude East), 43.8°-45° (latitude North);
- 10 m wind from COSMO-I7 as forcing;

- computational grid (regular): 1/120 of degree, about 800 m;
- one forecast each day at 00 UTC. To warm-up the model the hotstart files from the previous run (or a stationary run if they are not available), in order to set-up the wind field, and 24 hours of wind analysis are used;
- forecast range: +72 hours with hourly output;
- outputs variables: significant wave height, mean direction, mean and peak period;

2.4 Tide and surge model: ROMS

AdriaROMS is the operational ocean forecast system for the Adriatic Sea running at Arpae-SIMC Emilia-Romagna. It is based on the ocean model Regional Ocean Modeling System (ROMS, version 3.0). The system is operational since June 2005 (Chiggiato and Oddo, 2008). The current version, 3.0, is operational since April 2008. AdriaROMS has a regular grid with 2 km horizontal resolution and 20 vertical σ-levels.

Initial conditions were provided by optimal interpolation mapping of CTD casts collected during the August 2006 oceanographic cruise DART06b Dynamics of the Adriatic in Real Time (NR/V Alliance). Surface forcing is guaranteed by the atmospheric limited area model COSMO-I7 (formerly LAMI), non hydrostatic with 7 Km horizontal resolution, that provides tri-hourly shortwave radiation, 10 m wind, 2m temperature, relative humidity, total cloud cover, mean sea level pressure and precipitation. All of them are used to compute momentum, heat and freshwater fluxes and the effect on sea level of the atmospheric pressure. Boundary conditions, to the south, are radiation/relaxation of mean daily forecast of temperature, salinity, currents from the general circulation model of the full Mediterranean MFS, managed by INGV, with superimposed 5 major tidal harmonics (M2,S2, N2, O1, K1), as visible in Figure 4.

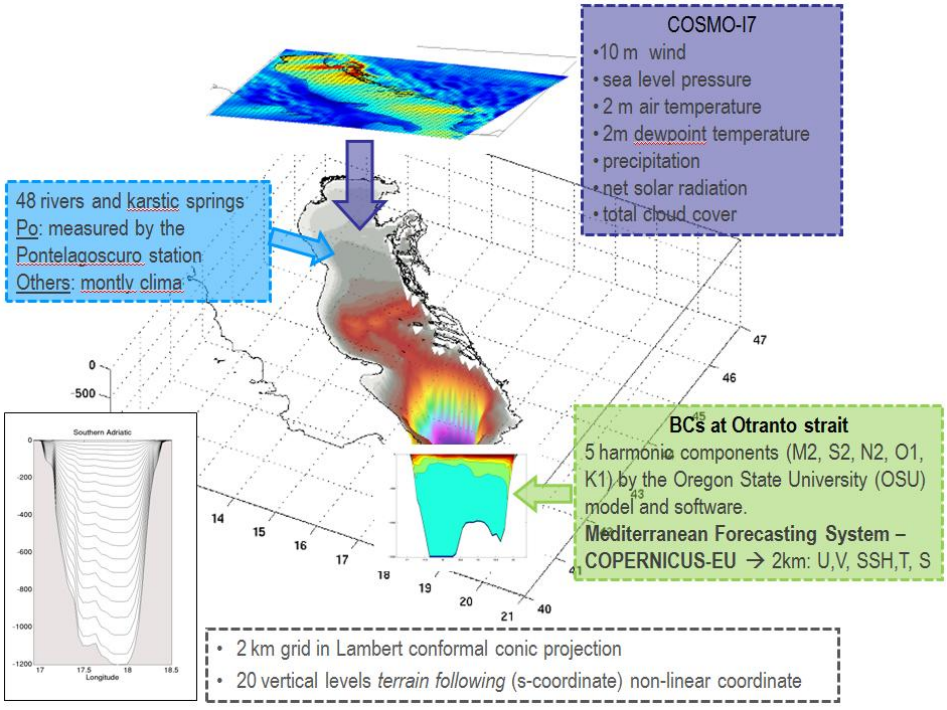

Figure 4 Adriatic domain of the AdriaROMS model, with the indication of the different input data.

Forty eight rivers (and springs) are included as well, using monthly climatological values from Raicich (1996). For the Po river, the biggest, it is used the persistence throughout the forecast.

Technical notes on AdriaROMS 2.0 configuration

- ROMS is a 3D, free surface, hydrostatic, primitive equations, finite difference, fully non linear model that solves the Reynolds-averaged Navier-Stokes equation. (for more info about ROMS kernel see Shchepetkin and McWilliams, 2005 or Haidvogel et al., 2007).
- Non linear terrain-following vertical s-coordinates
- Orthogonal curvilinear horizontal coordinated, staggered on a Arakawa C grid MPDATA family advection scheme (Margolin and Smolarkiewicz, 1998).
- Density based laplacian with spline reconstruction of vertical profiles for the accurate representation of the baroclinic pressure gradient (Shchepetkin and McWilliams, 2003).
- No horizontal viscosity, while a weak horizontal diffusivity, grid-size dependent, is applied by a laplacian operator. Mixing of tracers is along geopotential surfaces while momentum along s-surfaces.
- GLS generic for vertical turbulence closure, as coded in Warner et al. 2005.
- Radiation-relaxation boundary condition for momentum-temperature-salinity from MFS model. Tidal elevation and currents are applied as well, following Flather (1976).
- The shortwave radiation is imposed (LAMI output), the long-wave radiation is estimated via Berliand and Berliand formula (Budiko, 1974), turbulent fluxes via Fairall et al. (2003). No relaxation or correction is applied to the fluxes. The effect of the mean sea level pressure on sea level is considered too.
- Rivers are treated as sources of mass and momentum flux. The evaporation precipitation flux is treated as salinity flux.

The oceanographic numerical model AdriaROMS is used in the operational forecasting suite to compute sea level, temperature, salinity and 3-D current fields of the Adriatic Sea (northern Mediterranean Sea). The model runs over the Adriatic Sea domain once a day with a forecast range of 72 hours. Figure 5 shows an example of the sea surface elevation forecasts available on the Arpae Emilia-Romagna web site, provided by the model AdriaROMS.

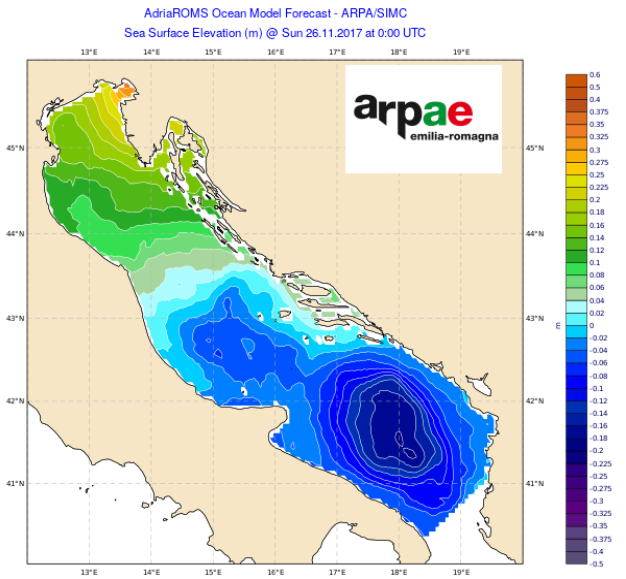

Figure 5 Example of ROMS output of sea level predictions for the Adriatic Sea. The hourly data are available on the Arpae Emilia-Romagna web site (www.arpae.it).

2.5 **Morphological model: XBeach**

The hydro/morpho-dynamic forecasts in the near-shore zone for the Early Warning System of the Emilia-Romagna region are provided by using the morphological model XBeach.

The XBeach model is designed to simulate near-shore hydrodynamics and morpho-dynamics, especially during storms or hurricanes, and is able to predict dune erosion, overwash and breaching of dunes and barrier islands. XBeach is a two-dimensional depth-averaged (2DH) model that solves coupled cross-shore and alongshore equations for wave propagation, flow, sediment transport and bedl evel changes (Roelvink et al., 2009). XBeach is an acronym for "eXtreme Beach behavior model" and is developed by IHE-UNESCO, Delft University of Technology, Deltares and the University of Miami. In contrast to most other numerical models, XBeach computes the near-shore water level variations due to the wave motions, and therefore, an actual swash zone is present in the model. This makes the model suitable for detailed modeling of swash zone processes. XBeach is a 2DH depth-averaged numerical model, however, in this thesis only the one-dimensional version is used.

This subsection gives an overview of the most important aspects of the XBeach model while a comprehensive description of the model, including all equations, can be found in the user manual of XBeach (Roelvink et al., 2015). The XBeach version 18 (revision 4691), also known as the 'Kingsday' release, was applied in this thesis.

2.5.1 Model description

Figure 6 shows the grid conventions used in the XBeach model. The x-axis is oriented towards the coast and the y-axis is directed alongshore. The grid is positioned relative to the world coordinates through the origin of the grid and the rotation angle. A rectilinear or curvi-linear, staggered, non-equidistant grid is applied. Water levels, bed levels, concentrations, wave energy and more are defined in the grid centers. Velocities and sediment transports are defined at the cell interfaces. The bottom level is directed upward as positive, in contrast to some other numerical models (as Delft3D) which define the bottom level in the opposite direction.

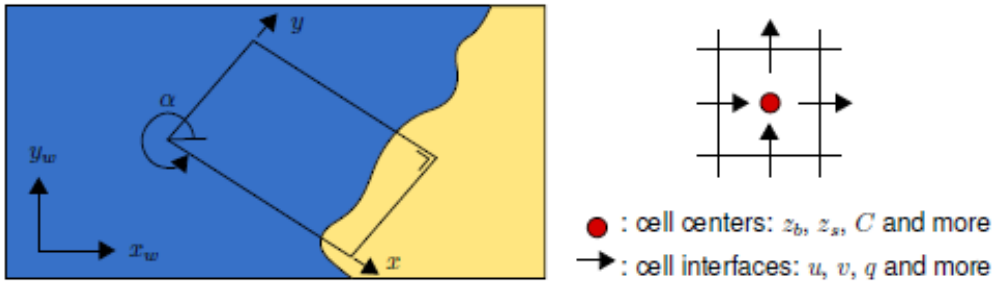

Figure 6 Coordinate system and grid definition, adapted from Roelvink et al. (2009).

In brief, in the XBeach surf-beat mode, the energy from random short waves (on the timescale of the wave groups) acts as a wave driver for the long-wave model. The short-wave energy is obtained by a time dependent version of the wave-action balance equation (Holthuijsen et al., 1989), as described in Equation (1).

$$\frac{\partial A}{\partial t}+\frac{\partial c_x A}{\partial x}+\frac{\partial c_y A}{\partial y}+\frac{\partial c_\theta A}{\partial \theta}=-\frac{D_w}{\sigma} \quad (1)$$

where $A = S_w/\sigma$ is the wave action, S_w represents the wave energy density in each directional bin σ, t is the time, x and y are the horizontal coordinates, c_x, c_y and c_θ are the wave-action propagation speeds in x, y-directions and θ-space, respectively. D_w is the total wave dissipation distributed proportionally over the wave directions. The solution of Equation (1) leads to the calculation of wave radiation stresses $S_{xx,w}$, $S_{xy,w}$, $S_{yy,w}$, which are expressed as products of S_w according to the linear wave theory.

The contribution of the roller radiation stresses, $S_{xx,r}$, $S_{xy,r}$, and $S_{yy,r}$, generated during wave breaking, is evaluated by the solution of the roller energy balance equation, which is expressed similarly to Equation (1). Then the components of wave forcing in each direction, F_x and F_y, are calculated utilizing the radiation stress tensor. For the low-frequency and mean flow, the Generalized Langrangian Mean (GLM) formulation (Andrews and McIntyre, 1978; Walstra et al., 2000) of shallow water equations are utilized (Equations (2, (3 and (4):

$$\frac{\partial u^L}{\partial t}+u^L\frac{\partial u^L}{\partial x}+v^L\frac{\partial u^L}{\partial y}-fv^L-\nu_h\left(\frac{\partial^2 u^L}{\partial^2 x}+\frac{\partial^2 u^L}{\partial^2 y}\right)=\frac{\tau_{sx}}{\rho h}-\frac{{\tau_{bx}}^E}{\rho h}-g\frac{\partial \eta}{\partial x}+\frac{F_x}{\rho h} \quad (2)$$

$$\frac{\partial v^L}{\partial t}+u^L\frac{\partial v^L}{\partial x}+v^L\frac{\partial v^L}{\partial y}-fu^L-\nu_h\left(\frac{\partial^2 v^L}{\partial^2 x}+\frac{\partial^2 v^L}{\partial^2 y}\right)=\frac{\tau_{sy}}{\rho h}-\frac{{\tau_{by}}^E}{\rho h}-g\frac{\partial \eta}{\partial x}+\frac{F_y}{\rho h} \quad (3)$$

$$\frac{\partial \eta}{\partial t}+\frac{\partial hu^L}{\partial x}+u^L\frac{\partial hv^L}{\partial y}=0 \quad (4)$$

where u^L and v^L are the Langrangian velocities, f is the Coriolis coefficient, ν_h is the horizontal viscosity, τ_s and τ_b are the wind and the bed shear stresses, respectively, η is the water level, h is the water depth, g is the gravitational acceleration and ρ is the water density. The sediment transport is represented by a depth-averaged advection-diffusion equation (Galappatti and Vreugdenhil, 1985), as follows (5):

$$\frac{\partial hC}{\partial t}+\frac{\partial hCu^E}{\partial x}+\frac{\partial hCv^E}{\partial t}+\frac{\partial}{\partial x}\left[D_h h\frac{\partial C}{\partial x}\right]+\frac{\partial}{\partial y}\left[D_h h\frac{\partial C}{\partial y}\right]=\frac{hC_{eq}-hC}{T_s} \quad (5)$$

where C is the sediment concentration, u_E and v_E are the Eulerian velocities, D_h is the sediment diffusion coefficient, T_s is the adaptation time (related to the response of sediment to the flow) and C_{eq} is the equilibrium sediment concentration, which is the source term in the equation. The bed level (z_b) changes are calculated by the sediment mass conservation equation (Equation (6):

$$\frac{\partial z_b}{\partial t}+\frac{1}{1-p}\left(\frac{\partial q_x}{\partial x}+\frac{\partial q_y}{\partial y}\right)=0 \quad (6)$$

where p is the sediment porosity, q_x and q_y are the sediment transport rates in each direction, which are calculated based on sediment concentration resulting from Equation (6). A detailed presentation of the governing equations and the boundary conditions of the model is given in Roelvink et al. (2009).

2.5.2 XBeach in the Early Warning System

Within the existing civil protection protocol for the Emilia-Romagna coastline, 3-day wave and water-level forecasts are undertaken daily by Arpae-SIMC through its meteo-marine operational forecasting system and used to force the morphological model XBeach.

Then, XBeach is executed daily at a total of 22 cross-shore profile lines along the Emilia-Romagna coastline, which correspond to eight different coastal sites, including the tourist areas of Rimini, Cesenatico and Riccione. The model provides a daily 3-day forecast of coastal storm hazard at these eight key sites along the Emilia-Romagna coastline (northern Italy).

Two different storm impact indicators, as stated by Harly et al. (2016), are used within the ER-EWS to translate XBeach predictions into indicators of storm hazard, as selected by the regional geological survey and ARPA to monitor storm impacts and compile them into an impact-oriented event database (Perini et al., 2011).

The safe corridor width (SCW) is a measure of the amount of dry beach available between the dune foot and waterline for safe passage by beach users. A threshold SCW of 10m has been selected by end users to separate low-hazard (i.e. “code green”) conditions from medium-hazard (i.e. “code orange”) conditions. A threshold SCW of 5m meanwhile has been selected to separate medium-hazard conditions from high-hazard (i.e. “code red”) conditions.

Moreover, the building–waterline distance (BWD) is a measure of the amount of dry beach available between the seaward edge of a building and the model derived waterline. A threshold BWD of 10m has been selected by end users to separate low-hazard conditions from medium-hazard conditions. A threshold BWD of 0m (i.e. inundation of the building is predicted) has meanwhile been selected to separate medium-hazard conditions from high-hazard conditions.

Chapter

3 Case study

In this subsection a detailed environmental description of the area of interest for this thesis it can be found, focusing on the wave and storm climate of the region and its morphological features. Further, an overview of the past and the actually coastal protections are presented with the aim to provide the necessary background information of the study site. The chapter also presents the two storm events that occurred on the Emilia-Romagna coasts during the autumn 2015-winter 2016, which are investigated in this thesis.

3.1 Description of the case study area: Emilia Romagna littoral

The Emilia Romagna littoral is located in the North East of Italy (Figure 7) and comprises 130 km of low and sandy coast, most of which are strongly urbanized. The Northern boundary of the Region is marked by the Goro branch of the Po River while the townships of Riccione and Cattolica are the south boundary. The coastline is dominated by tourist activities resulting from the several millions of tourists that visit each year, predominantly during the summer months (Harley et al., 2011). A decennial coastal plan for this area was recently published addressing the problem of integrated coastal zone management (Preti, 2009).

The Emilia Romagna beaches face the Northern Adriatic Sea, a relatively shallow epi-continental shelf with low tidal amplitude. It is typically a low energy environment with a mean significant wave height of 0.4 m (Tpeak ≈ 4 s) and a semidiurnal and micro tidal regime (spring tidal range = 0.9 m). A general erosive tendency is mainly caused by the reduced sediment transport rates of the rivers and by the increased anthropogenic subsidence. This, together with building of tourism facilities, has completely altered the beach equilibrium.

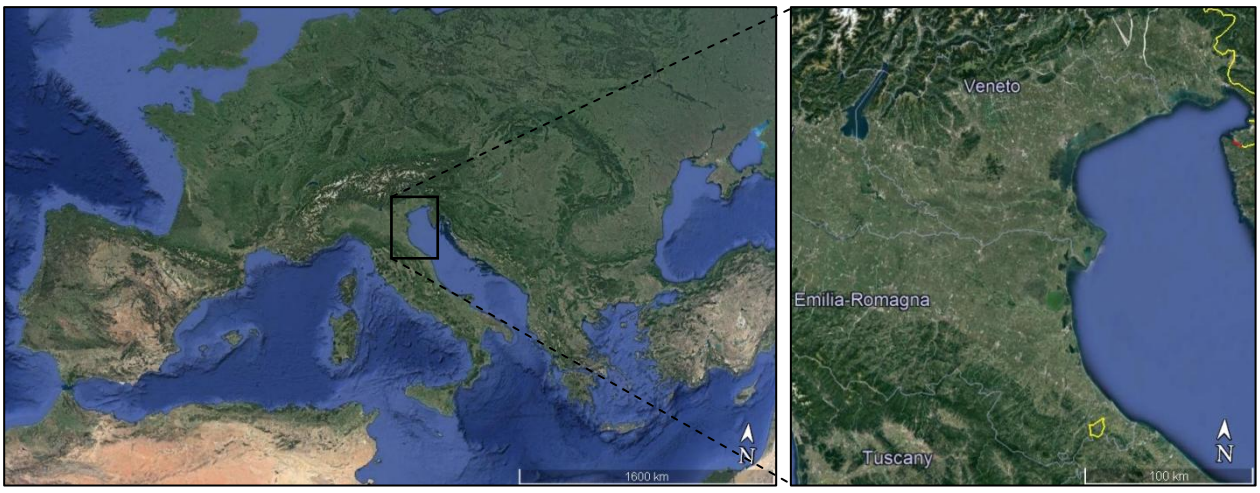

Figure 7 Location of the Emilia-Romagna littoral.

The most intense storm waves are generated from east to northeast and are associated to *Bora* weather conditions. These events are generally featured by large and steep waves. Surge events meanwhile mainly occur during *Scirocco* winds that blow from south to east, providing smaller but with a long wave period waves. This winds blowing on the entire extension of the Adriatic Sea, particularly during spring and autumn period. The region is particularly vulnerable to the intense coastal storms because of its low-ling coastal hinterland and the large amount of vulnerable beach front infrastructures for the touristic activities that are located along the entire Emilia-Romagna coasts. Overall, the regional coast is an environment compromised by urbanization and the intensive use of the territory, thus extremely vulnerable to marine pollution and erosion.

To counteract the erosion phenomenon that began from the early decades of the 1900s, over half of the Emilia-Romagna beaches (about 74 km), different defense structures were designed to protect the coast. The most common are the emerged detached breakwaters that defend about 40 km of coastline. The remaining 30 km are protected by revetments, low crested structures, submerged sand bag barriers and groins (Preti et al., 2009). Since the 1980s, the Emilia-Romagna Region has used a new defense strategy based on sand nourishments (Preti et al., 2002, Correggiari et al., 2011; Preti et al., 2011a; 2011b). As evidenced by Aguzzi et al (2016), 35% of the regional coast is in good condition, while the remaining 65% presents critical erosive conditions.

The net coastal sediment transport, as visible in Figure 8, has a predominant south-north direction with inversion tracts at convergence/divergence points generally coinciding with port infrastructures and river mouth (IDROSER Spa, 1996).

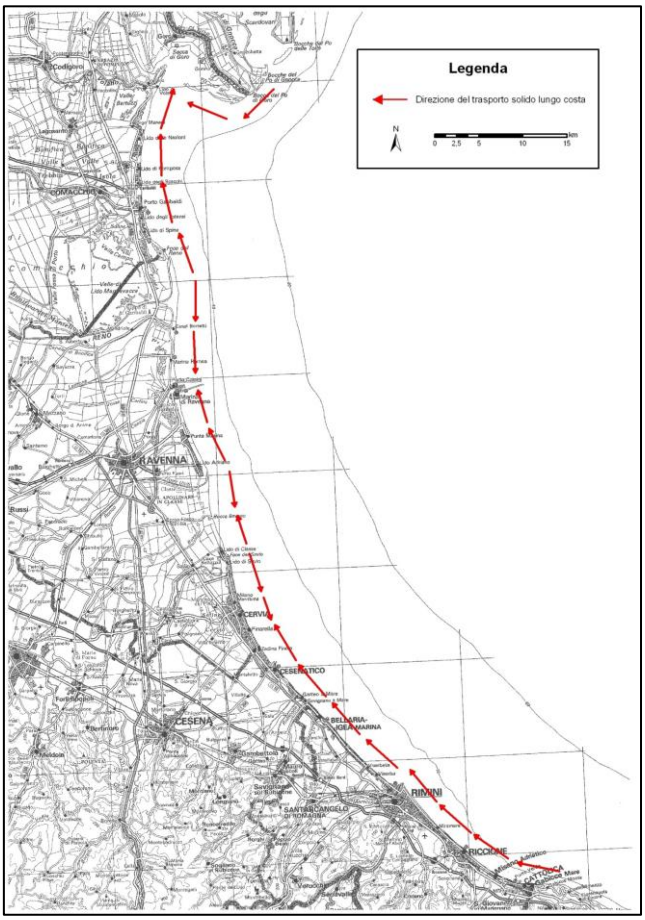

Figure 8 Sediment transport map of the Emilia-Romagna littoral. The red arrows indicate the local transport direction.

3.1.1 Cesenatico

The specific study area for the project is a 1km coastal stretch of the Emilia-Romagna littoral, located near the touristic town of Cesenatico.

Cesenatico municipality is a well-known touristic resort in the province of Forlì-Cesena. The coastline is approximately 7 km long and is divided by the harbour jetties and the different defences into a Northern and a Southern area (Figure 9).

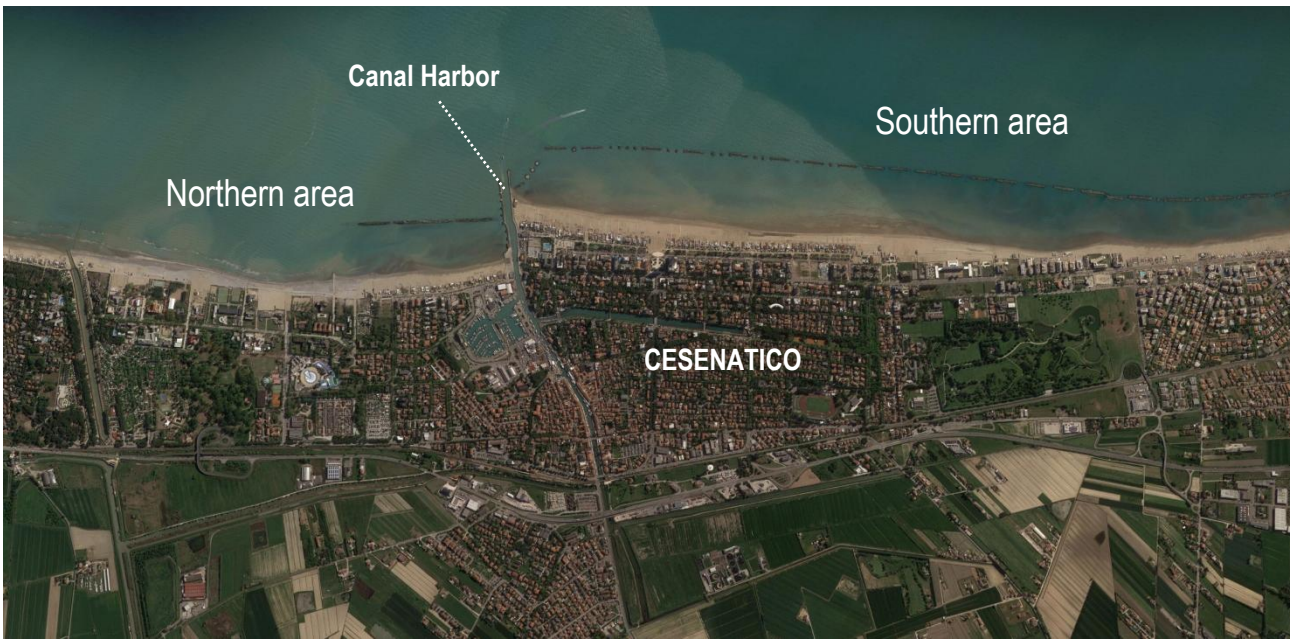

Figure 9 Aerial view of the Cesenatico site

Since the 70's the area suffered also for anthropogenic subsidence due to extraction of water for industrial and agricultural use. Flooding and erosion motivated the construction of the first defences:

- Cesenatico South: emerged (crest level: 1-1.5 m s.l.m) barriers in 1974;
- Cesenatico North: in 1978 Longard tubes were placed along the shoreline but were damaged by the sea and removed after a few years; in 1983 a nourishment (150'000 m3) was performed and geo-synthetic submerged barriers were built.

In 1982, extractions were forbidden by law and the lowering trend slowly decreased to the natural subsidence. Unfortunately the land lowering was already dramatic, i.e. 116 cm in the period 1950-2005, causing evident flooding and erosive problems.

Flooding became very frequent and the main pathways ware the beach overtopping and canal harbour intake, due to insufficient water drainage in the Tagliata-Porto canale system.
The national government therefore renewed the existing defences and planned new interventions:

- Center of Cesenatico: defence of the area immediately to the South of the Jetty with emerged barriers in 1997;
- Cesenatico North: Construction of a submerged (crest level: -0.5 m s.l.m) barrier 0.8 km long, 12 m wide, 250 m distant from the shoreline to replace the geosynthetic barrier. Nourishment with 160'000 m3 of sand. Removal of a 70 m long groin placed 400 m Northward of the jetty (2003-2005)
- Valverde, Southern adjacent beach: change of the layout of three emerged barriers, removal of 16

groins, construction of three new groins and nourishment with 160'000 m3 of sand (2003-2005); removal of a stone revetment with beneficial effects on the beach stabilisation. Due to the relatively little distance among the beach and the barriers, the interaction among the structures and the seabed induced erosive tendencies and rip-currents formations.

The following specific defences to high water events were designed by the Regional Authority in 2005 (Brath, 2007):

- construction of a sea gate, "Porte Vinciane" (Figure 10), 2.0 m high a.s.l., closing the canal harbour for water level exceeding 0.9 m a.s.l.; to face sedimentation at the entrance of the canal harbour, dredging operations have to be performed usually twice per year or exceptionally after intense storms;
- set-up of a pumping system in connection with "Porte Vinciane", whose operating capacity of 18 m3/s is much greater than what is necessary to drain an extreme rain event; in case of combined flood and sea storm with closure of the sea gate, it is assumed that the plant can still drain into the sea up to 8 m3/s, whereas the rest has to be discharged by Canale Tagliata;
- widening of Canale Tagliata (new section 20 m wide, slopes 1:2, height of river walls 3 m a.s.l) to assure the outflow up to the reference discharge of 90 m3/s, based on the indication of the "Bacini Romagnoli" Authority;
- set-up of a sewer-drain by-pass system of the railway and streets crossing Canale Tagliata;
- increasing the potential (from 10 to 17 m3/s) of the pumping system of the Canale Tagliata; the plant collect the water drained from the low-lying areas of Cervia and Cesenatico;
- construction of a series of lamination basins;
- construction of a gate on the Canale Vena, upstream the Porto Canale;
- control and upgrade (in terms of section and height) of channel banks and streets crossing the channels.

To protect the low-lying urban areas, the Municipality built a soil dike (Figure 10) in 2005, integrated into the urban use of the back beach, 20 m wide, 1 m high, 1.4 km long, starting from the southern jetty (extending Southward). The estimated costs of all these works exceeds 30 MEuro.

Figure 10 Mitigation measures: the "Gardens of Cesenatico": dike behind bathing facilities; sea gate in correspondence of the Canal Harbour.

The main periodical beach maintenance consists of:

- a seasonal dune 1.4 m high during the winter time to defend the bathing facilities. Its width is variable from point to point but it is always sufficiently wide to ensure a resistance to the storm events.
- yearly nourishments that are typically carried out Northward and Southward of the port of about

16’000 and 20’000 m3/y respectively.

By assuming that the high water defense system detailed above is properly working, the two main failure conditions of the coastal system in Cesenatico are:

- beach erosion;
- impossibility to close the Porte Vinciane due to sedimentation at the gates and inside the canal harbour.

3.1.2 Study site

The specific study site consists of a 1 km costal stretch located near the Cesenatico town. In particular, the seaside Port of Cervia and Cesenatico are located at the site’s northern and southern boundary respectively (Figure 11).

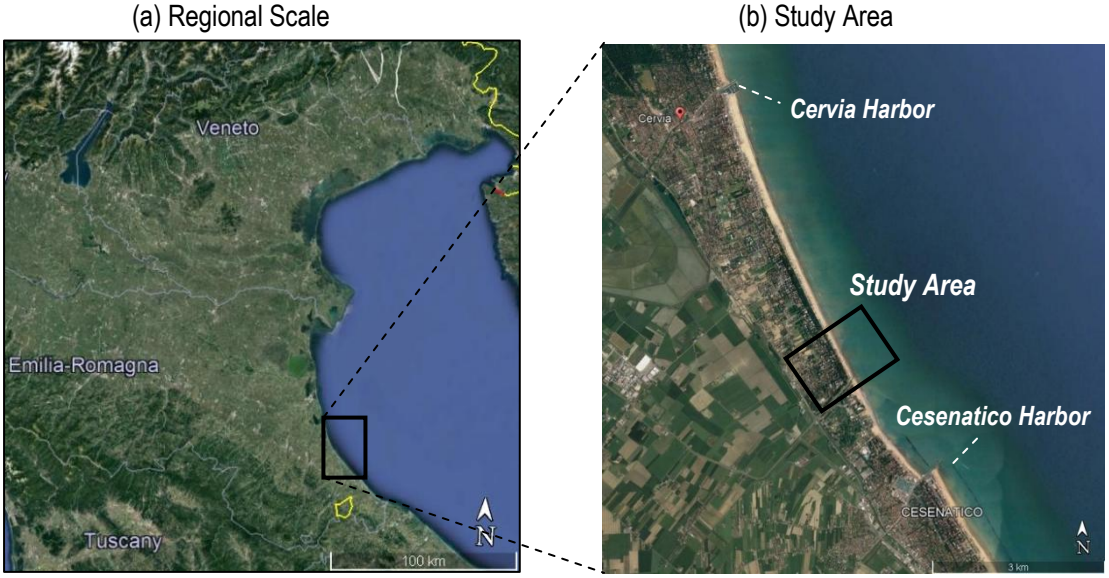

Figure 11 Cesenatico study site on the Adriatic Sea in Emilia-Romagna, Northern Italy.

This coastal stretch is an unprotected medium-fine sandy beach and, as most of the regional coastal areas, it is characterized by a low beach-face, with an average intertidal beach slope of around 2.5-3%. The bottom topography is characterized by submerged long-shore bars located near the coast which cause a greater dissipation of wave energy. The local net sediment transport is south-north oriented (Aguzzi et al., 2016).

3.2 **The two storms in Autumn2015**

The dataset used in the analysis was obtained during the winter 2015-2016, when two storm events occurred on the Emilia Romagna coasts. The storms caused flooding of the backward inhabited areas and numerous structural damages for most of the regional coasts. Before and after the storms topo-bathymetric measurements, along ten cross-shore sections, were performed by Arpae Emilia-Romagna. In this section, the meteorological and hydraulic storms condition, are described in detail.

3.2.1 *Wave height, period and direction*

A measurement buoy, named Nausicaa, is located off Cesenatico coasts. Wave height, wave direction, wave period and temperature data are measured up to 30 minutes and stored on the HydroMeteoClimate Service Database. Wave conditions for the first and the second event are shown in Figure 12 and Figure 13. The first is a double event, featured by two wave peaks close together. The waves increased rapidly on the later afternoon of the 21 November 2015 and reached the maximum value of 3.30 m on the 21 November 2015 at 23:00 UTC. Despite some missing data in the wave buoy record, it is possible to suppose a secondary wave rise on the morning of the following day thanks to the surge measured by the tide gauges located in the area of interest. The second peak occurred on the 26 November 2015 at 23:30 UTC with a height of 3.16 m. The storm waves were triggered by a Bora wind event (about 60° N), with cold winds from NE that reached about 20 m/s in Rimini and about 18 m/s in Ravenna.

The two peaks can be considered as two different storms. The first has an energy contribution of about 120.45 $m^2 \cdot h$, classified as moderate by Perini et al. (2011) while the second can be defined as significant because of its wave energy of about 181.85 $m^2 \cdot h$.

Due to adverse weather conditions, it was not possible to perform the beach relief immediately afterwards the first wave peak. For the sensitivity analysis the model was forced by the hydrodynamic conditions representative of both wave peaks. For this reason, the two peaks are considered as single case.

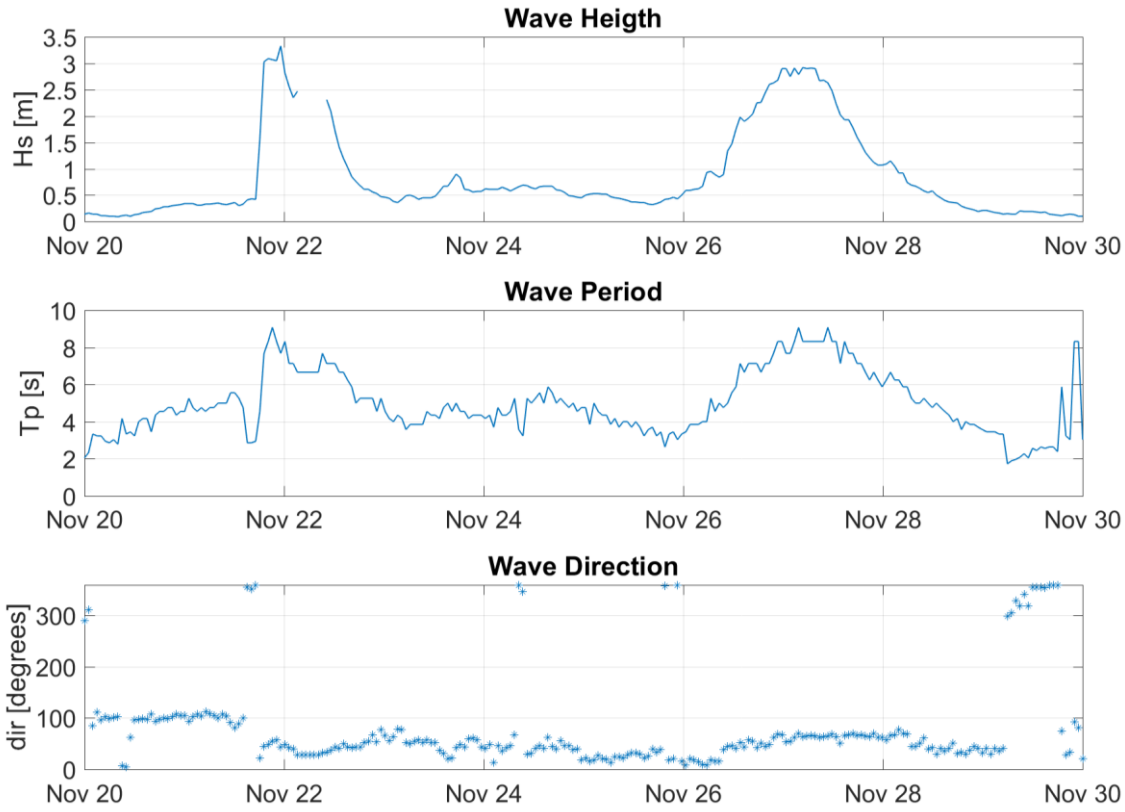

Figure 12 Wave height (first panel), Wave period (second panel) and Wave direction (third panel) retrieved by the Nausicaa buoy, located near Cesenatico. The data interval spans from 20 to 24 November 2015.

On the February 2016, a different event, with a lower wave energy of about 61.25 $m^2 \cdot h$ (moderate intensity), took place. The event started on the 27 February 2016 afternoon and reached a maximum wave height of 2.30 (Figure 13). The storm was generated by East-SouthEast wind that reached a wind speed of about 15 m/s at Rimini and Ferrara stations, named Scirocco.

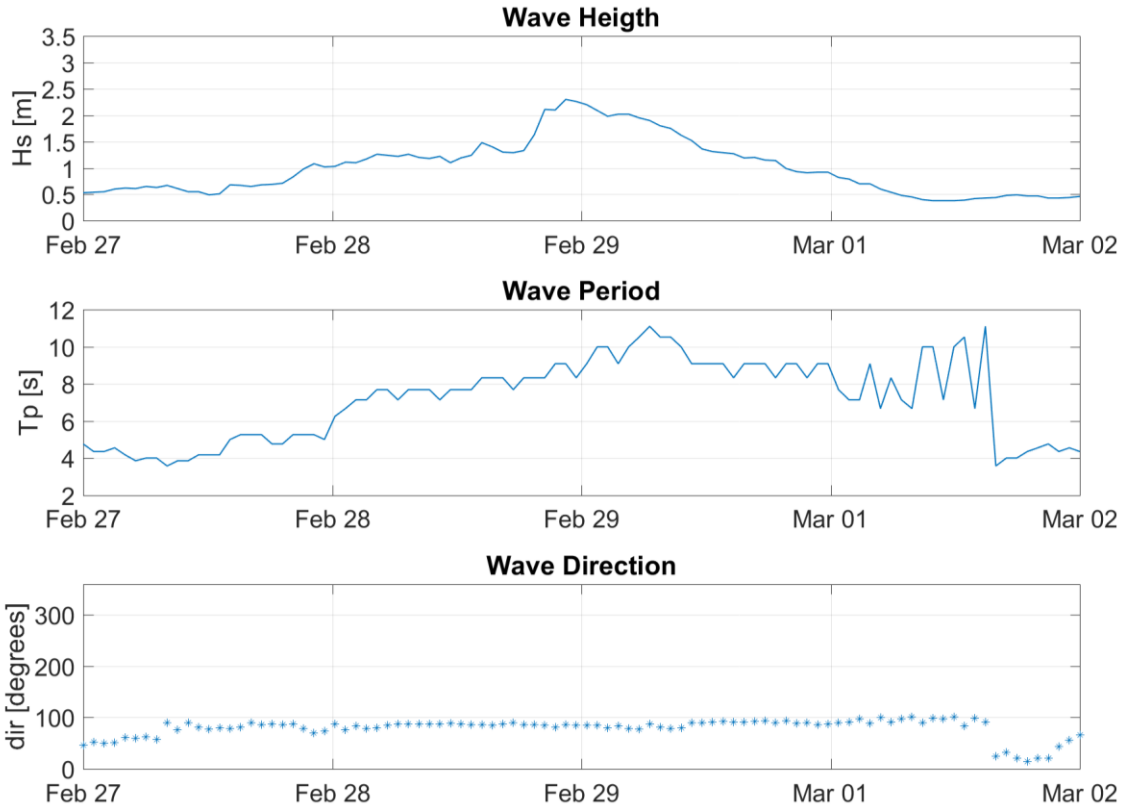

Figure 13 Wave height (first panel), Wave period (second panel) and Wave direction (third panel) retrieved by the Nausicaa buoy, located near Cesenatico. The data interval spans from 27 February to 02 March 2016.

3.2.2 Water levels

There are two tidal gauge stations close to the area of interest: Porto Garibaldi and Rimini stations. Figure 14 shows the respective distance between the water level stations and the Cesenatico study site.

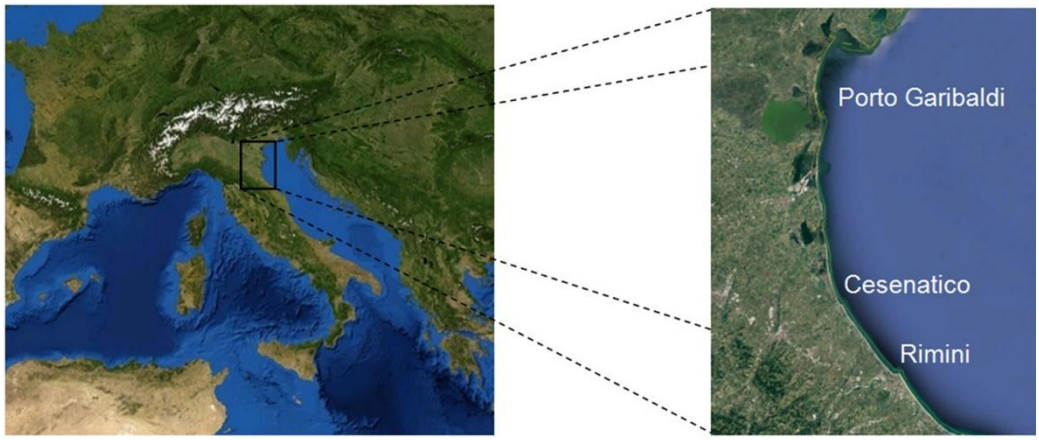

Figure 14 Location of the tide gauges of Porto Garibaldi and Rimini respect to the Cesenatico study area.

Both measurement stations will be used for generation of hydraulic conditions to forcing the XBeach model.

The tidal signal on Cesenatico was generated by an elaboration of tidal data forecasted by the model AdriaROMS. For the measurement stations of Rimini and Porto Garibaldi, the bias between the observed data and the forecasted data was calculated. Such correction was applied to simulated water levels extracted at Cesenatico. This data elaboration was performed for both the storm events.

As visible in Figure 15, the first peak in water level had a value of 0.58 m and occurred around 06:00 on November 22th UTC, about 7 hours later then the first wave peak (Figure 12). The sea level increase corresponding to the second wave peak is less evident.

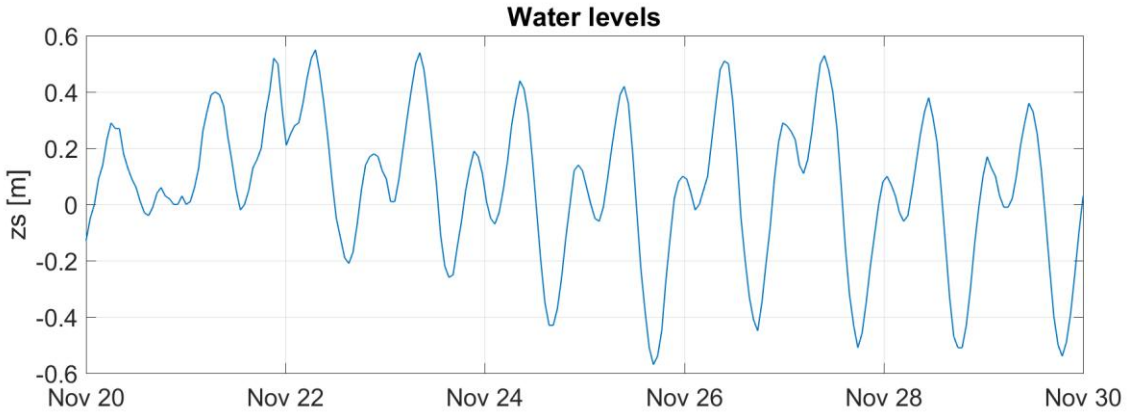

Figure 15 Water level boundary conditions imposed in the coastal model XBeach. Given the lack of a tide gauge close to Cesenatico, data were generated by the AdriaROMS (oceanographic model) forecasts. The data interval spans from 20 to 30 November 2015.

For the second storm, the water level reached the peak on 29 February 2016 at 1.300 UTC with a value of 0.81 m, as visible in Figure 16.

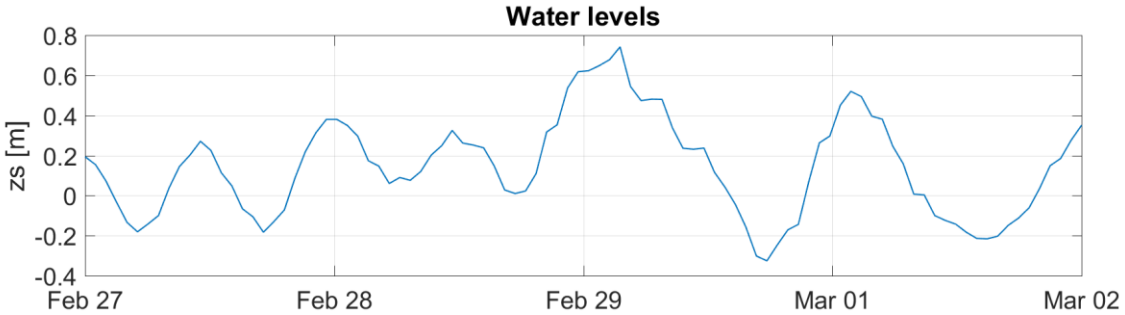

Figure 16 Water level boundary conditions imposed in the coastal model XBeach. Given the lack of a tide gauge close to Cesenatico, data were generated by the AdriaROMS (oceanographic model) forecasts. The data interval spans from 27 February to 02 March 2016.

3.3 **Morphological monitoring of the storms**

In this subsection, the available topo-bathymetric measurements are presented. At first, the pre- and post- storm reliefs used to calibrate the coastal model are presented, while secondly the beach profiles surveyed in the past and used for the final morphological analysis are described.

3.3.1 Beach profiles measurements: before and after storms

Topo-bathymetric reliefs of ten cross-shore beach profiles were carried out before and after the storms (Table 1). The cross-sections have a distance of about 100 m and extent up to a bottom depth of about 8m (Figure 17). Three of these sections were chosen in correspondence of existent sections which are part of the Regional Topo-Bathymetrical Network. Such network, managed by the Environmental Agency of Emilia-Romagna (Arpae) starting from the 80' years, consists of 251 cross-sections distributed along the entire regional littoral which are systematically surveyed.

Table 1 Dates in which the pre- and post- storm topo-bathymetric measurements of the beach profiles were carried out.

Storm event	Before storm relief	After storm relief
Event 1	19th November 2015	02th December 2015
Event 2	25th February 2016	02th March 2016

Both the emerged and submerged beach has been assessed, from the higher point of the beach up to depth of 8 m. In particular, landward the relief was extended until the first un-erodible point and if present, the winter dune is opportunely surveyed, defining the dune foot points and the peak of the structure. Figure 18 shows some pictures of the Cesenatico beach surveys.

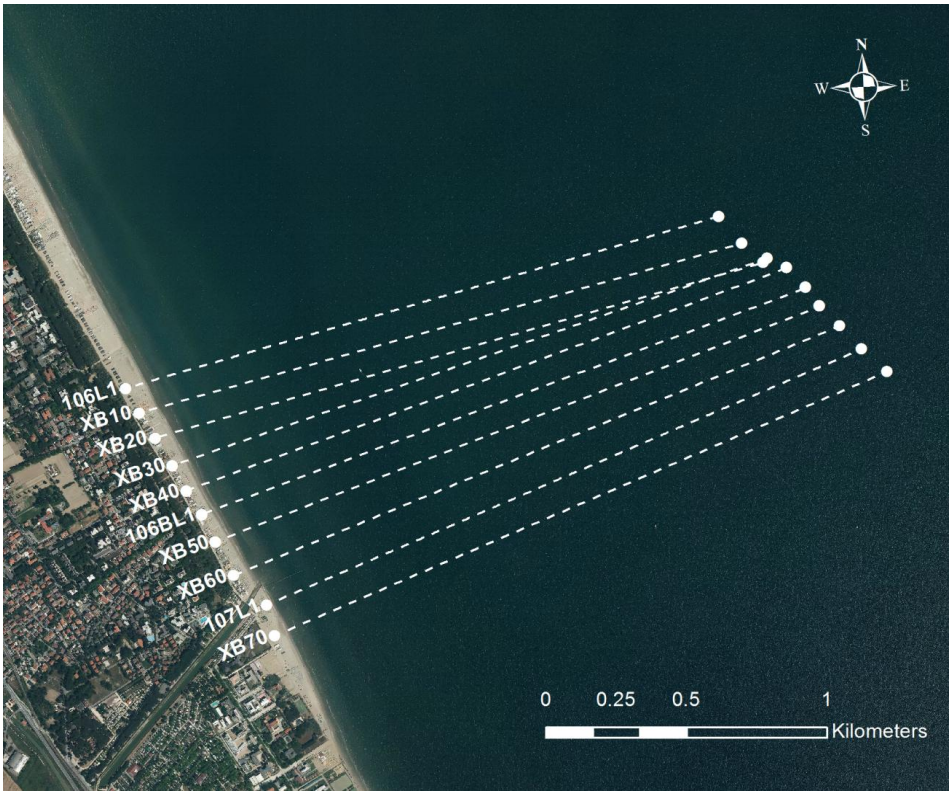

Figure 17 Locations of the 10 cross-shore sections that are monitored before and after the storms.

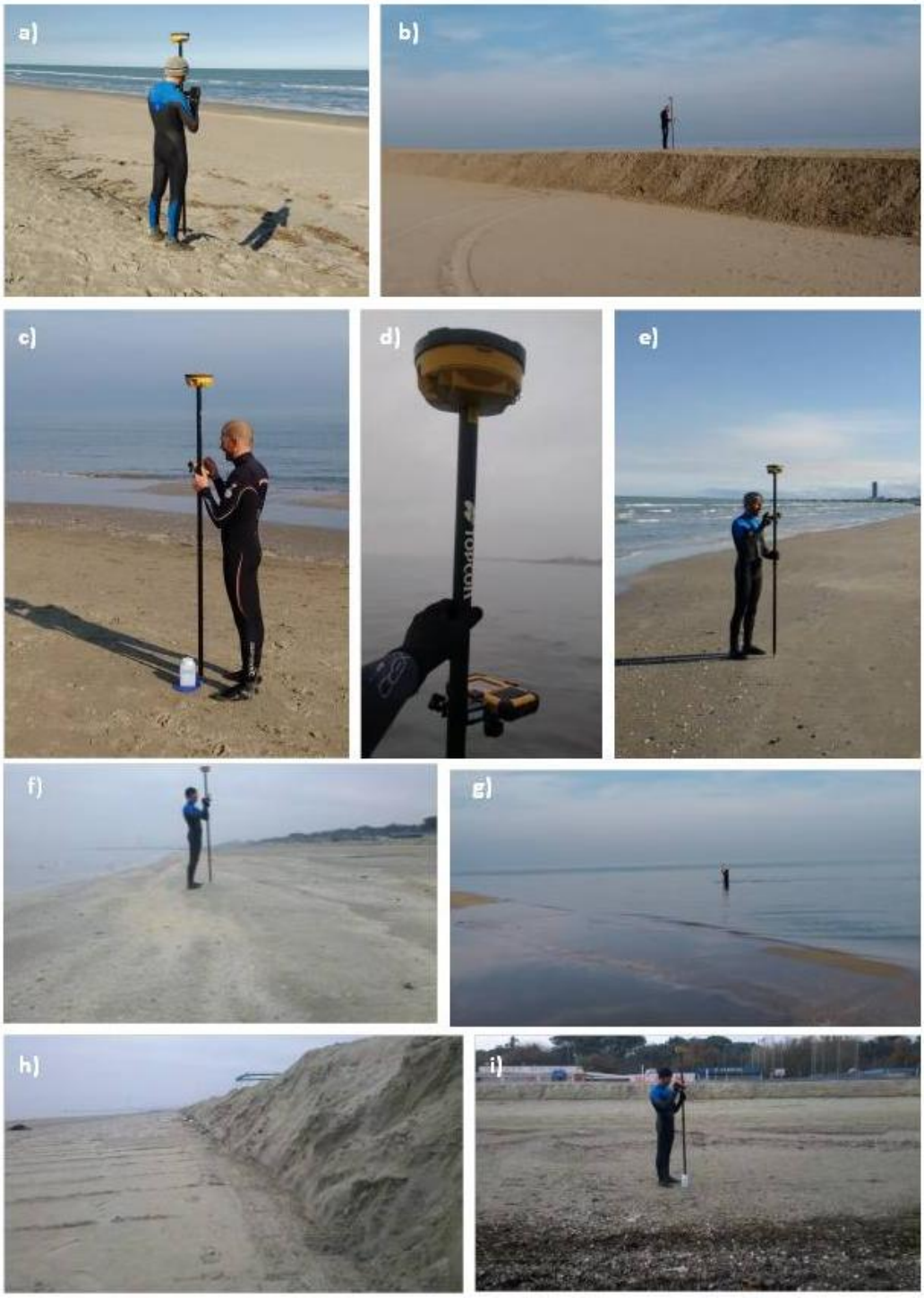

Figure 18 Topo-bathymetrical surveys of the emerged and submerged beach at Cesenatico study site.

Depending on the morphological configuration, different measurement tools and acquisition methods were adopted:

- *Emerged profile/ up to depth of 1m*. The survey was carried out using a dual-frequency GNSS geodetic receiver manually delivered by an operator. Plano-altimetric positioning was performed with the NRTK differential satellite receiver. The planimetric measurements were referenced to the national ETRF2000-RDN geodetic system and projected into the UTM32N chart plot. Quotas,

initially referenced to the ellipsoid ETRF2000, have been converted to orthometric dimensions using the Arpae leveling scales. The data acquisition was performed on points with reciprocal distance of 2-5 m.

- *Submerged profile between depth of 1m and 8m*. The survey was carried out using a double-frequency GNSS geodetic receiver coupled with echo sounder single-beam with single frequency (210 Khz), with a P01540 transducer having 10 ° opening of the beam, mounted on a special vessel. Instrument interfacing, NMEA string coupling, latency management, data acquisition, and navigation were performed using NavPro software. Plano-altimetric positioning was performed using the NRTK differential satellite receiver with the help of the positioning service provided by the national network of permanent Netgeo stations.

Chapter 4 Sensitivity Analysis of the morphological model

4.1 Introduction

In this chapter, the sensitivity analysis of the morphological model XBeach is presented. The aim was to investigate the effect of several input parameters on the model forecasts and hence provide some indications on the model uncertainties. The study also allowed to achieve a suitable calibration for the study area.

4.2 Background

When applying a suite of numerical models to provide coastal forecasts of flooding and inundation, it is essential that we are conscious of the uncertainties existent in the models. In a rapid decision support system, as the early warning system it is, the knowledge of these uncertainties is crucial to give an accurate indication of the forecasts reliability.

De Moel et al. (2012) state that there is quite some uncertainty in the flood damage simulations, which is rooted in the uncertainty of the input data and model assumptions (Merz et al., 2004; Merz and Thieken, 2009; Apel et al., 2008; De Moel & Aerts, 2011). These sources of uncertainty can relate to both epistemic uncertainty (incomplete knowledge), or aleatory uncertainty (natural variability) (see e.g. Apel et al., 2004).

Quite often, some or all of the model inputs are subject to sources of uncertainty, including errors of measurement, absence of information and poor or partial understanding of the driving forces and mechanisms (Der Kiureghian & Ditlevsen, 2009). Furthermore, the model itself can introduce uncertainty depending on his parameter setting, particularly with the setting of the individual parameters, which are used as input for the model (Heuvelink, 1998). In this way, a numerical model can be highly complex, and as a result its relationships between inputs and outputs may be poorly understood.

Besides, when a numerical modeling chain, applied on the extensive domain of meteorological, oceanographic and coastal fields is adopted, the uncertainties sources and their propagation within the models become a more complex element to define. The understanding of the uncertainty related to each model of the chain is required.

As stated by Bart (2017), with an approaching storm, it is important to give a sufficiently fast and reasonable result instead of providing an exact value. However, for the storm impact application to become operational, it is important to have a good knowledge of the model uncertainties and how they are propagated through the modeling chain.

For this purpose, different approaches were followed in the coastal applications for the analysis of the uncertainty propagation.

Bayesian methods, that assumed that both the model and the data were potentially inaccurate, were applied to surf zone processes (Plant and Holland, 2011a, 2011b) as well as sediment transport (Plant and Stockdon, 2012) to investigate the specific errors and uncertainty for each output variable and model parameter. The limitation of this approach is the need of a great amount of observation data and specific assumptions about the nature of the errors.

In many other cases, a different method that studies how the uncertainty in the output of a mathematical model or system (numerical or otherwise) can be apportioned to different sources of uncertainty in its inputs (Saltelli, 2002; Saltelli et al., 2008) was followed. This method, named Sensitivity Analysis (SA), is a valuable tools for identifying important model parameters, testing the model conceptualization, and improving the model structure. It helps to apply the model efficiently and to enable a focused planning of future research and field measurement (Sieber & Uhlenbrook 2005).

The sensitivity analysis is an instrument for assessment of the input parameters with respect to their impacts in the model output and it is useful for the model validation, the model development and last but not least for the analysis of the uncertainty. The goal of SA is to characterize how model outputs respond to changes in input, with an emphasis on finding the input parameters to which outputs are the most sensitive (Saltelli et al., 2000a; Kennedy and O'Hagan, 2001). This approach accounts only for the uncertainty in the model's input values and parameters, not in the model's structure (i.e. existence and functional form of dependencies between variables, etc.) (e.g. O'Hagan, 2012).

Several studies have broadly reviewed and classified the large number of approaches to performing a sensitivity analysis (Saltelli et al., 2000b, 2004; Helton and Davis, 2003; Oakley and O'Hagan, 2004; Frey and Patil, 2002; Christiaens & Feyen, 2002) proving their potential and their alternative fields of application.

One of the simplest and most common approaches is that of changing one-factor-at-a-time (OAT), to see what effect this produces on the output (Murphy et al. 2004). This analysis customarily involves the process to moving one input variable, keeping others at their baseline (nominal) values, then, returning the variable to its nominal value, and repeating for each of the other inputs in the same way. Sensitivity will be then measured by monitoring the behavior of the model output to the parameters variation. In this way, by changing one variable at a time and keeping all other variables fixed to their baseline values, any change observed in the output will unambiguously be due to the single variable changed and there is an increase of the comparability of the results (Saltelli & Annoni, 2010). As stated by Uusitalo et al. (2015) if the output value changes only little, the output is robust to changes in parameter values within the model indicating a relatively small uncertainty about the value. If, on the other hand, the value of the variable changes markedly when we change some parameters in the model within their reasonable range, this indicates that there is large uncertainty about the variable's value.

As performed by several modellers (McCall et al., 2010; Vousdoukas et al., 2011; Vousdoukas et al., 2012; Harley et al., 2011; Splinter and Palmer, 2012; Buckley and Ryan, 2013; Verheyen et al., 2014) the approach of the sensitivity analysis was adopted in this study to improve our understanding of the internal uncertainties related to the parameters of the morphological model XBeach involved in the

Early Warning System. In the context of this thesis, the sensitivity analysis was presented only for the morphological model XBeach, which is the final model of the numerical chain.

Such a study allows to investigate the influence of the settings of the single parameters on the output, defining a degree of uncertainty for each parameter. The models typically contain free model parameters which in many cases require careful and considered 'tuning' at new locations to ensure optimal model performance. On the other hand, the prediction of coastal morphological change using numerical models is a challenging task (e.g., Roelvink & Broker 1993; Vousdoukas et al. 2009) because to achieve the model validation/calibration it is important to have access to a large amount of data which are not always available.

Many studies focused on the quantification of uncertainty bounds for numerical modelling used in coastal engineering attempting to examine the sources of these uncertainties associated to the morphological coastal processes. Errors propagating through morphological response forecasts have been examined (Baart et al., 2011) to have an estimation of the uncertainty in input data and model parameters.

XBeach is the current `state-of-the-art' model used to predict changes in coastal morphology arising due to storms (Roelvink et al., 2009) and owns a large number of free model parameters that can be varied by the user. Most of these parameters are associated with physical processes such as sediment transport, wave motion or bottom updating while another part of them describe the numerical behavior.

The model has already been validated against extensive large-scale flume data sets including short and long wave distributions, return flow, orbital velocities, concentrations and profile change during dune erosion events. An essential part is an avalanching mechanism which allows a surprisingly accurate description of the evolution of the upper profile and dune face. XBeach developers have already defined default settings for all parameters in order to facilitate XBeach as a legal dune safety assessment model in the Netherlands (Kolokythas et al., 2016). However, the model is improved continuously. Continuous improvement feeds the need of continuous validation of the model results, performance and consistency.

The XBeach skillbed (Deltares organization; http://oss.deltares.nl) tries to fulfill this need by running a range of tests including analytical solutions, laboratory tests and practical field cases every week with the latest code (Deltares, 2017).

Many XBeach calibrations were achieved thanks to one-at-a-time variation to determine sensitive parameters, in order to define the "optimal" parameterization of the model using a skill measure (Callaghan et al., 2013; Pender and Karunarathna, 2013; Roelvink et al., 2009; Stockdon et al., 2014).

An XBeach calibration for a coastal stretch of the Emilia-Romagna Region, northern Italy, was carried out by Harley et al. (2016) as part of the FP7-MICORE project activities (www.micore.eu). The analysis investigated the 31 October 2012 storm that occurred on the Adriatic Sea and was performed along 11 beach profiles located at Lido di Classe. It concentrated on a number of XBeach parameters deemed critical to wave run-up and beach/dune erosion processes. The optimized parameter set consisting of smax=0.8, eps=0.1, gamma=0.42 and facua=0.15 (Harley et al., 2016) is applied on the operational model XBeach that was integrated in the coastal Early Warning System of the Emilia-Romagna Region.

However, the results of the studies carried out by Splinter et al. (2012) and Callaghan et al. (2013) showed that the XBeach model requires site-specific calibration and that calibration to multiple erosion events is necessary. Splinter et al. (2012) showed that the sensitive model XBeach requires rigorous site-specific calibration while Callaghan et al. (2013) found that the model requires calibration using multiple erosion events to provide great performance for erosion forecasts.

Moreover, a study that goes beyond the more usual comparison of outright model performance but examines issues around the need for site-specific calibration, concluded that the modellers must be cautious when transferring the XBeach model with calibrated parameter values that were not specifically derived at the location of interest, even when calibrated using extensive datasets at adjacent locations (Simmons et al., 2017).

This study focuses on a coastal zone and two storm events different from those analyzed by Harley et al. (2016) and leads to a specific calibration of the model, based on a preliminary sensitivity analysis according with Murphy et al. (2004) to evaluate the uncertainty of each model parameter.

The aim of this chapter is to determine the hydraulic and morphological parameters that significantly affect the model prediction. The sensitivity analysis is carried out by varying a single input parameter and by comparing the output results, to define an explicit correlation between the fixed input and the forecasted variables.

A few parameters have a significant impact on the morphological evolution and have been calibrated based on the observed morphological evolution. The calibrated model provides the users with more accurate predictions than using the default settings.

4.3 **Methods and material**

The analysis was made by applying a two-step approach. Firstly, a sensitivity analysis, to define the input parameters that mostly affect the results, was carried out. In the second part, the model performance related to the most relevant parameters was assessed in order to define an optimized model setup.

4.3.1 Numerical Model setup

XBeach was run in 1D conditions along real cross-sections. In order to generate the input bathymetry, topo-bathymetric measurements are used (described in Chapter 3). An optimized grid based on a minimum number of points per wave length was obtained with the help of the functions of the Open Earth Toolbox. The model grids were created with minimal dimension of 1 m in the emerged beach and a maximum distance of 10 m offshore, where larger grid cells can be applied.

XBeach was forced by hydrodynamic conditions, measured during the storm events. Measurement data are derived from the Nausicaa buoy and the tide gauges located near Cesenatico. A description of the available data can be found in Chapter 3. Wave conditions were imposed in spectral way through the JONSWAP spectrum (Hasselmann et al. 1973) while for the sea state conditions were used the observed sea levels time series.

The simulations related to the first event started on the 20 November 2015 at 00:00 UTC and finished on the 30 November 2015 at 00:00 UTC while for the second event, the model run with a duration of

four days since 27 February 2016 at 00:00 UTC. For each event, the features of the simulations are summarized in Table 2

Table 2 Set-up of XBeach simulations for the storm events.

Storm event	Start Date	End Date	Duration [hour]
Event 1	20th Novembre 2015 00:00	30th Novembre 2015 00:00	240
Event 2	27th February 2016 00:00	02th March 2016 00:00	144

4.3.2 Parameters and simulations

A "reference" simulation, where each parameter was kept to its default value as defined by Roelvink et al., 2010, was carried out for both the storm events. Then, a set of physical and numerical parameters was defined. In particular, the physical variables concerns sediment transport, short wave action, shallow water equations and bottom updating.

The "one-at-the-time" approach (Simmons et al., 2015) was followed. For each simulation, only one parameter was varied within its validity range with respect to the "reference" simulation. The hydraulic conditions were kept the same for all simulations. For the sensitivity analysis the following simulations have been performed (Table 3).

Table 3 Description of all the simulations carried out for the sensitivity study. A brief description, the default values and the validity range of each varied parameter, are reported.

Process	Parameter	Description	Simulations	Default	Range of value	Unit
Sediment transport	*cmax*	Maximum allowed sediment concentration	10	0.1	0.0 - 1.0	-
	smax	Maximum Shields parameter for equilibrium sediment concentration	9	-1.0	-1.0 - 3.0	-
	Lws	Switch to enable long wave stirring	2	1	0 - 1	-
	facua	Calibration factor time averaged flows due to wave skewness and asymmetry	9	0.1	0 - 1	-
Short wave action	*break*	Type of breaker formulation	3	roelvink2	roelvink1, Baldock, Roelvink2, roelvink_daly, janssen	-
	gamma	Breaker parameter in Baldock or Roelvink formulation	11	0.55	0.4 – 0.9	-
	turb	Switch to include short wave turbulence	3	bore_averaged	none, wave_averaged, bore_averaged	-
	fw	Short wave friction factor	21	0	0 - 1	-
	delta	Fraction of wave height to add to water depth	8	0	0 - 1	-

Continue in the next page

Follow by the previous page

Process	Parameter	Description	Simulations	Default	Range of value	Unit
Shallow water equation	*eps*	Threshold water depth above which cells are considered wet	12	0.005	0.001 - 0.1	m
	umin	Threshold velocity for upwind velocity detection and for vmag2 in equilibrium sediment concentration	5	0.0	0.0 - 0.2	m/s
	bedfriccoef	Bed friction coefficient	6	0.002 manning	3.5e-05 - 0.9	-
Bottom updating	*wetspl*	Critical avalanching slope under water (dz/dx and dz/dy)	9	0.3	0.1 - 1.0	-
	dryslp	Critical avalanching slope above water (dz/dx and dz/dy)	5	1.0	0.1 - 2.0	-

4.3.3 Evaluation method

The simulations were analyzed in term of morphological response, based on the output variables. In order to evaluate the morphological evolution of the intertidal beach profile, in this thesis the shoreline retreat ΔR and the erosion V_{ero} were investigated. Moreover the runup $R_{2\%}$ was considered as useful indicator of the possible flooding of the inhabited areas located behind the beach.

There are different methods in order to evaluate the eroded volumes. In this thesis, the eroded volume (V_{ero}) is the erosion, used in literature, measured above the MSL as a volume for linear meter ($m^3\ m^{-1}$). The shoreline retreat (ΔR) is defined as the displacement of the zero points of the profile in reference to the initial zero point. Therefore, the shoreline retreat is defined as a distance and a negative value indicates an advancement.

For each calculation step, the runup was evaluated by XBeach, as the higher point reached by the water during the swash. For this analysis, the runup 2% was considered as representative indicator. According to Sutherland et al. (2004) the model performance have be assessed by calculating the mean error (bias), accuracy (Root Mean Square Error) and skill (Brier Skill Score).

Bias is a measure of the difference in the central tendencies of the predictions and the observations. The basic equation for bias in the mean, used in this thesis, is the follows (7):

$$bias = \frac{\sum_1^n (z_m - z_p)^2}{n} \qquad (7)$$

Where n is the number of data points covered by both pre- and post storm measurements, z_m represents the measured beach profile while z_p is the modeled profile. Bias is used in this analysis in order to analyze the systematic error. A positive value of bias means that the bed level is higher in the computed data than the observed data while a zero bias indicates a good assessment of the morphological evolution.

Moreover, in this analysis, the accuracy of the forecasts was expressed through the Root mean square error ($RMSE$) that represents the average size of the difference between the computed data and the observations. The RMSE was evaluated as in equation (8):

$$RMSE = \sqrt{\frac{\sum_1^n (z_m - z_p)^2}{n}} \quad (8)$$

Finally the Brier Skill Score is commonly used as statistical indicator of the performance of the numerical model especially for morphological changes (Bugajny et al., 2013). Specifically, the classification used for this thesis is from Van Rijn (2003) in which a score below 0 is bad, a score between 0÷0.3 is poor, 0.3÷0.6 is reasonable/fair, 0.6÷0.8 is good and 0.8÷1.0 is an excellent performance. The correlation of the measured profiles (pre-storm z_b and post-storm z_p) and of the modeled profile (z_m) can be expressed as equation (9):

$$BSS = 1 - \left(\frac{\langle |z_m - z_p|^2 \rangle}{\langle |z_p - z_b|^2 \rangle} \right) \quad (9)$$

A negative value of this index means that the simulation is no better than predicting zero bed level change and it is worse than predicting zero bed level changes.

In the present study, bias, RMSE and BSS values were estimated considering the profile section above the mean sea level (MSL=0 m). The behavior of sand bars was not analyzed while the main focus has been the hydro-morphological response of the zone above the shoreline that is primary for the Early Warning System.

In the next subsections, the simulations results are presented. For each parameter shoreline retreat, eroded volumes and runup 2% are summarized in a table. Subsequently, for the parameters that have a significant impact on morphological evolution, the value of the statistical indicator ($bias$, $RMSE$ and BSS) are showed. The outcomes related to the most relevant parameters are supported by a beach profile plot. For completeness, the plots related to all parameters are reported in APPENDIX A.

4.4 Reference simulation vs observed data

In this subsection, the results of the reference simulations are presented. For simplicity, the results for a single cross-section (106BL1) can be found. For both events, the simulations result in a beach erosion of about 17$m^3 \cdot m$-1. Depending on the different initial beach slope, for the 20th November 2015 a shoreline retreat of about 7 m takes place while for the second case an advancement occurs (about 4 m). For both storms, the waves impact the dune face and a quantity of sediment is transported offshore. The model outputs and the observed variables are summarized in Table 4.

Table 4 Reference simulations results compared to the observed data. The measurements of the runup are not available. The final column indicates the model performance with a statistical indicator (BSS).

Storm event	Modeled ΔR [m]	Observed ΔR [m]	Modeled V_{ero} [$m^3 \cdot m^{-1}$]	Observed V_{ero} [$m^3 \cdot m^{-1}$]	Modeled $R_{2\%}$ [m]	BSS
20th November 2015	7.85	-3.90	17.45	2.07	0.97	-3.32

28th February 2016	-3.71	-3.60	17.49	1.80	0.95	-6.96

With the default settings, XBeach overestimate the erosion during overwash conditions and results in a negative BSS which indicates a *bad* model performance according to the classification of Van Rijn (2003). Beach profile evolution measured and simulated (default settings) is shown in Figure 19 and Figure 20.

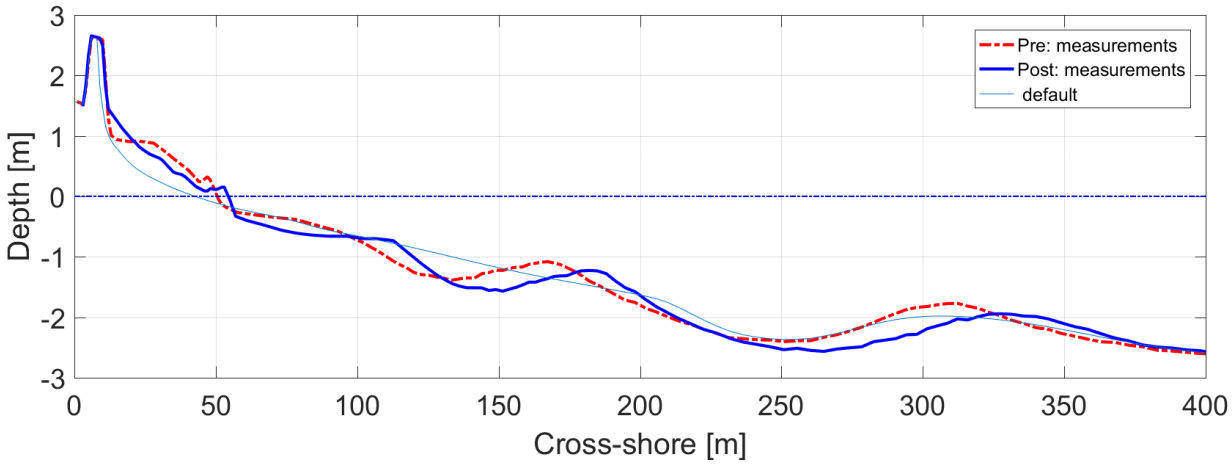

Figure 19 Development of the bed level simulated by the reference simulation (thin light blue line), for a single cross-section. The dashed line represents the initial beach profile while the thick blue line indicates the observed final profile. The simulation is referred to the event of 20 November 2015.

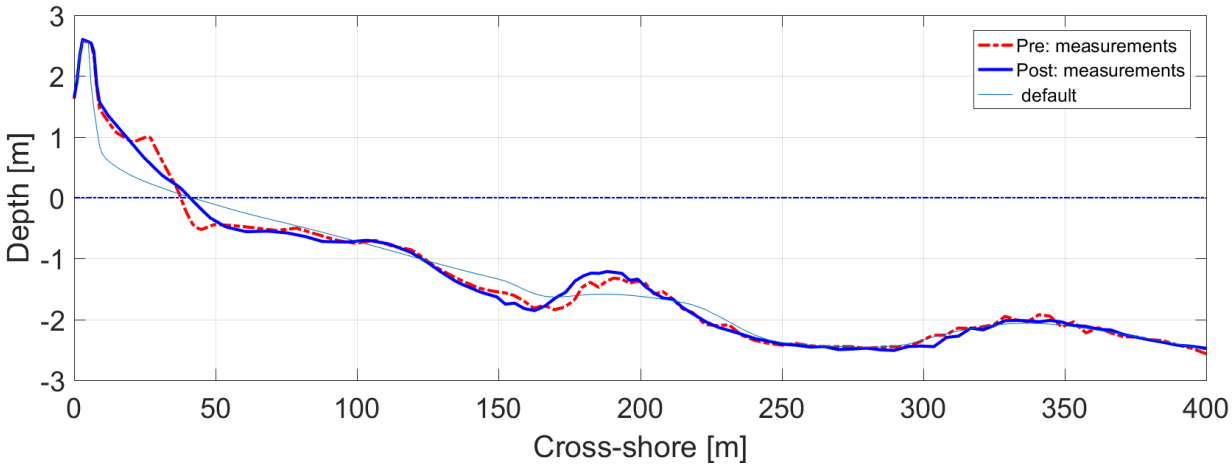

Figure 20 Development of the bed level simulated by the reference simulation (thin light blue line), for a single cross-section. The dashed line represents the initial beach profile while the thick blue line indicates the observed final profile. The simulation is referred to the event of 27 February 2016.

4.5 **Sensitivity analysis of the morphological response**

This subsection describes the results of the sensitivity analysis of the XBeach model. The results are grouped in refer to the physical processes that are influenced. Especially, sediment transport, short wave action, shallow water equation and bottom updating were analyzed.

4.5.1 Sediment Transport

The first analysis focused on the parameters that influence the sediment transport process. In particular, $cmax$, $smax$, lws and $facua$ parameters were investigated.

For overwash and inundation the default settings of XBeach overestimate erosion. This is related to the sediment transport formulation implemented in XBeach (Soulsby-Van Rijn) that is not strictly valid for sheet flow conditions. In order to achieve a realistic behavior, the equilibrium sediment concentration is limited through an artificial upper boundary defined with $cmax$ and $smax$ parameters.

The impact of the maximum allowed sediment concentration ($cmax$), imposed as upper boundary for the equilibrium sediment transport, is hardly represented by the model. Simulations with different values of this parameter will results in comparable erosion volumes (about 17 $m^3 \cdot m^{-1}$ for both the events) and shoreline retreat. Table 5 shows the results of all simulations carried out with different values of $cmax$ parameter. Differently than expected, for both the storm events, changes in this concentration limiter doesn't affect sediment transport processes and hence the morphological variation of the bottom. Such limit, which is rather artificial without any solid physical basis, doesn't provide a reduction of the beach erosion. For all simulations, the waves impact the dune face and the eroded sediments are transported offshore.

Table 5 Morphological and hydraulic response of the beach profile due to the cmax parameter variation. For each parameter value shoreline retreat (ΔR) eroded volumes (V_{ero}) and runup ($R_{2\%}$) are presented. The results are summarized for the two storms.

	2015 Storm			2016 Storm		
cmax value	ΔR [m]	V_{ero} [$m^3\ m^{-1}$]	$R_{2\%}$ [m]	ΔR [m]	V_{ero} [$m^3\ m^{-1}$]	$R_{2\%}$ [m]
0.10	7.40	16.34	1.00	-3.37	17.52	0.99
0.20	7.65	16.66	0.97	-4.07	17.28	0.96
0.30	6.85	17.05	0.99	-3.92	16.73	0.96
0.44	7.50	16.89	0.98	-3.87	17.22	0.97
0.55	7.05	16.93	0.99	-3.47	17.64	0.96
0.60	7.65	17.20	0.99	-4.12	17.55	0.97
0.70	8.60	17.42	0.97	-4.11	17.82	0.98
0.80	7.70	17.29	0.99	-4.42	17.98	0.97
0.99	8.00	17.34	0.98	-4.71	17.35	0.96
1.00	7.45	16.50	0.98	-3.67	17.18	0.95

Another artificial sediment transport limiter is defined through the Shields parameter θ. The $smax$ keyword is a parametric solution. McCall et al (2010) found that the application of $smax$ may reduce the overestimation of the morphological changes; however that case was related to a barrier island. In this analysis, the differences in the model results are very slight, as visible in Table 6.

For all simulations with the Shield number limiter, the seaward dune avalanching occurs and the beach profile tends to get in equilibrium. A sand volume of about 17 m3·m-1 is transported offshore from the emerged beach.

Table 6 Morphological and hydraulic response of the beach profile due to the smax parameter variation. For each parameter value shoreline retreat (ΔR) eroded volumes (V_{ero}) and runup ($R_{2\%}$) are presented. The results are summarized for the two storms.

	2015 Storm			2016 Storm		
smax value	ΔR [m]	V_{ero} [$m^3\ m^{-1}$]	$R_{2\%}$ [m]	ΔR [m]	V_{ero} [$m^3\ m^{-1}$]	$R_{2\%}$ [m]
-1.00	7.35	17.20	0.98	-4.32	17.46	0.97
-0.50	8.55	18.37	0.97	-4.21	17.64	0.96
0.00	6.60	17.08	0.98	-4.32	17.3	0.97
0.05	8.05	16.09	0.97	-3.37	17.16	0.97
0.10	9.40	17.29	0.97	-3.96	17.48	0.97
0.15	9.15	17.19	0.97	-3.52	17.4	0.93
0.20	7.15	17.21	0.97	-3.57	17.28	0.96
0.25	7.00	16.67	0.98	-3.71	17.62	0.97
0.30	7.60	17.09	1.01	-4.11	17.77	0.97

Furthermore, by default, the long-wave stirring is included by the model in the sediment transport formulations. The equilibrium sediment concentration Ceq is related to the velocity magnitude (v_{mg}), which in turns depends on the wave stirring. It is possible to disregard this term for the velocity calculation by setting the keyword lws to 0. The morphological response, shown in Table 7, is similar when including and excluding the long-wave stirring. If the long-wave stirring is deactivated, a slightly greater erosion volume is estimated while the beach width remains the same.

Table 7 Morphological and hydraulic response of the beach profile due to the lws parameter variation. For each parameter value shoreline retreat (ΔR) eroded volumes (V_{ero}) and runup ($R_{2\%}$) are presented. The results are summarized for the two storms.

	2015 Storm			2016 Storm		
lws value	ΔR [m]	V_{ero} [$m^3\ m^{-1}$]	$R_{2\%}$ [m]	ΔR [m]	V_{ero} [$m^3\ m^{-1}$]	$R_{2\%}$ [m]
0.00	0.48	15.41	0.98	-5.01	15.26	0.96
1.00	7.60	16.65	0.98	-3.31	18.00	0.98

At last, the sediment transport rate is strongly affected by the wave shape. However, XBeach considers the wave energy of short waves as averaged over their length, and hence does not simulate the wave shape. To address this lack, wave asymmetry and skewness are parameterized in the model as a function of the Ursell number (see "Section 2.5.1"; Roelvink et al. 2010). The parameter $facua$ enhances the effect of predicted wave non- linearity, determining the wave asymmetry and skewness contribution to the sediment advection velocity. The lower the value of facua, the greater the erosion overestimation. In Table 8 are shown the results of the different simulations.

When using the default value of 0.1, seaward dune erosion and offshore sediment transport takes place. Contrariwise, an increase of the value leads an on-shore sediment transport and a sand accumulation on the emerged beach. The sensitivity of the model to $facua$ is most marked during the 20th November 2015 event where the higher value produces an erosion of 30 $m^3 \cdot m^{-1}$. The range of

XBeach predictions with a high and a low $facua$ are enormous. The range of volumes variation reaches 50 $m^3 \cdot m^{-1}$.

Table 8 Morphological and hydraulic response of the beach profile due to the facua parameter variation. For each parameter value shoreline retreat (ΔR) eroded volumes (V_{ero}) and runup ($R_{2\%}$) are presented. The results are summarized for the two storms.

	2015 Storm			2016 Storm		
facua value	ΔR [m]	V_{ero} [$m^3\ m^{-1}$]	$R_{2\%}$ [m]	ΔR [m]	V_{ero} [$m^3\ m^{-1}$]	$R_{2\%}$ [m]
0.10	6.85	16.28	0.98	-3.62	17.42	0.98
0.15	4.55	12.77	0.99	-8.08	13.39	0.99
0.20	0.20	8.72	0.99	-14.73	8.06	0.99
0.25	-5.95	2.39	1.00	-26.59	2.08	0.99
0.30	-13.20	-4.33	1.02	-28.91	-7.04	0.99
0.35	-14.41	-9.91	1.04	-30.05	-14.80	1.03
0.40	-30.08	-15.38	1.02	-30.91	-18.92	1.09
0.45	-33.03	-24.76	1.05	-31.96	-21.75	1.13
0.50	-33.31	-30.22	1.08	-36.58	-20.07	1.18

For the event of 27th February 2016, the variability range is lower but still consistent (40 $m^3 \cdot m^{-1}$). Figure 21 shows a linear trend of the volumes variation for the first case while for the second case it can be seen a slowdown of the rate of erosion for a facua value of 0.35. Moreover, looking at Figure 22 it can be seen that the shoreline retreat grows up with the $facua$ values since to become an advancement matched by a berm generation. A significant rise of the runup 2% is visible for the second storm, probably caused by the same generation.

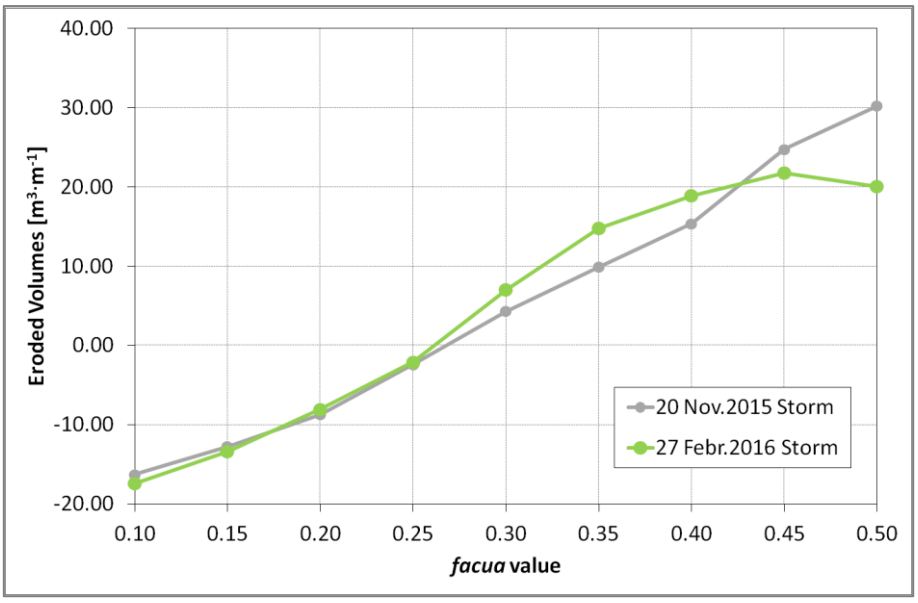

Figure 21 Morphological response of the beach profile in erosion, for different facua values.

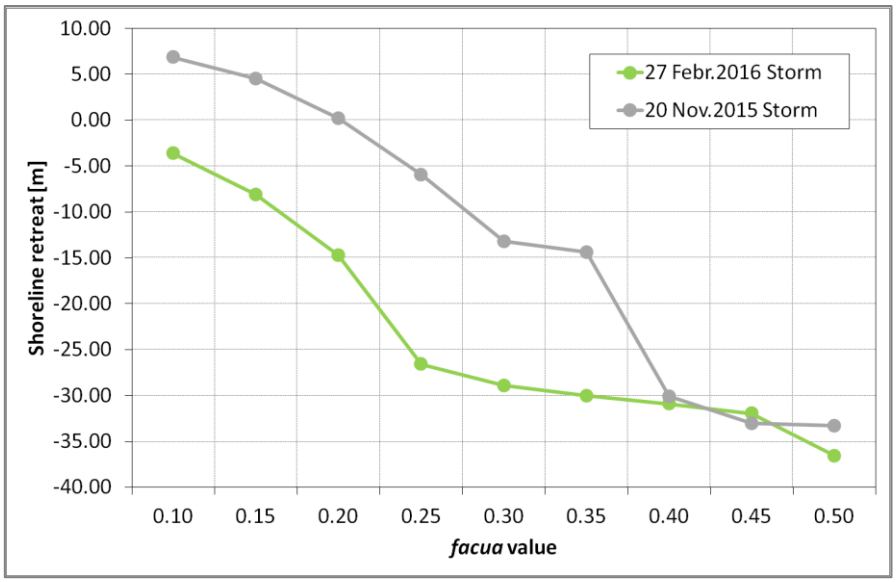

Figure 22 Morphological response of the beach profile in shoreline retreat, for different facua values.

4.5.2 Short Wave Action

The wave forcing in the shallow water momentum equation is obtained from a time dependent version of the wave action balance equation. In XBeach there are three short wave dissipation processes that can be accounted for: wave breaking (Dw), bottom friction (Df) and vegetation (Dv). In this subsection, the significant impact of a few parameters related to wave breaking and bottom friction dissipation is presented. The analysis focused on $break$, $gamma$, $turb$, fw and $delta$ parameters.

For the wave breaking calculation, five different wave breaking formulations are implemented and can be switched using the keyword $break$. For unsteady waves, by default the wave dissipation (kg/s2/s) is modeled using the formulation of Roelvink (1993) while the extended formulations of Roelvink (1993) and the formulation by Daly et al. (2010) are also implemented. The formulations by Baldock (1998) and Janssen & Battjes (2007) models the stationary wave. In this study, the unsteady waves formulations were investigated.

The adoption of the Daly formulation causes an intense erosion of the beach profile which extends up to the submerge beach. For the both storm cases, the waves impact the dune face and lumps of sediment slide on to the beach. During the first storm, the complete collapse of the dune occurs. The sand volume transported off-shore is more than twice of the other formulations. The simulations results are summarized in Table 9. Concluding, only the Daly formulation provides a substantial variation of the results.

Table 9 Morphological and hydraulic response of the beach profile due to the break parameter variation. For each parameter value shoreline retreat (ΔR) eroded volumes (V_{ero}) and runup ($R_{2\%}$) are presented. The results are summarized for the two storms.

	2015 Storm			2016 Storm		
break value	ΔR [m]	V_{ero} [$m^3\ m^{-1}$]	$R_{2\%}$ [m]	ΔR [m]	V_{ero} [$m^3\ m^{-1}$]	$R_{2\%}$ [m]
roelvink1	5.20	11.72	0.93	-4.86	13.41	0.93
roelvink2	7.80	16.97	0.97	-3.37	17.09	0.96
roelvink_daly	26.35	36.89	1.16	-6.27	26.44	1.04

In the formulation of dissipation due to wave breaking (Roelvink, 1993) the idea is to calculate the dissipation with a fraction of breaking waves (Qb) multiplied by the dissipation per breaking event. The maximum wave height is calculated as ratio of the water depth (h) plus a fraction of the wave height ($\delta Hrms$) using a breaker index (keyword: $gamma$). In the analysis, the $gamma$ value was varied between 0.4 and 0.9, respect to the default value of 0.55.

As visible in Table 10, for higher values a large erosion takes place. Gamma=0.65 is a limiter value for the collapse of the dune. Over this value, the dune is entirely eroded. As expected, varying the gamma parameter a significant variation of the runup 2% occurs. The breaker parameter is strictly related to the wave breaking and consequently to the runup process.

Table 10 Morphological and hydraulic response of the beach profile due to the gamma parameter variation. For each parameter value shoreline retreat (ΔR) eroded volumes (V_{ero}) and runup ($R_{2\%}$) are presented. The results are summarized for the two storms.

	2015 Storm			2016 Storm		
gamma value	ΔR [m]	V_{ero} [m^3 m^{-1}]	$R_{2\%}$ [m]	ΔR [m]	V_{ero} [m^3 m^{-1}]	$R_{2\%}$ [m]
0.40	-1.20	7.55	0.83	-7.73	10.44	0.89
0.45	1.00	9.73	0.88	-7.06	12.13	0.91
0.50	4.15	12.63	0.94	-6.37	14.34	0.95
0.55	7.75	16.73	0.98	-3.72	17.66	0.97
0.60	11.15	21.67	1.04	-1.87	21.48	1.02
0.65	13.95	29.47	1.08	1.09	26.87	1.04
0.70	17.85	38.10	1.14	3.04	33.59	1.07
0.75	35.70	48.32	1.16	10.67	38.55	1.08
0.80	49.95	50.80	1.14	23.81	43.13	1.06
0.85	50.45	50.80	1.16	32.85	44.63	1.01
0.90	50.50	50.80	1.13	-	-	-

Wave breaking induced turbulence at the water surface has to be transported towards the bed in order to affect the up-stirring of sediment. There are three possibilities to estimate the time averaged turbulence energy at the bed implemented in XBeach, which can be switched with $turb$ parameter. Table 11 shows the results obtained with the different estimation method. Including or excluding the short wave turbulence at the bed (keyword: $turb$), comparable morphological responses of the beach are forecasted. When a different value of $turb$ is selected, the eroded volumes slightly decrease while the shoreline position remains the same. However, the choice of this parameter is pretty complex because it represents a specific variable.

Table 11 Morphological and hydraulic response of the beach profile due to the turb parameter variation. For each parameter value shoreline retreat (ΔR) eroded volumes (V_{ero}) and runup ($R_{2\%}$) are presented. The results are summarized for the two storms.

	2015 Storm			2016 Storm		
turb value	ΔR [m]	V_{ero} [m^3 m^{-1}]	$R_{2\%}$ [m]	ΔR [m]	V_{ero} [m^3 m^{-1}]	$R_{2\%}$ [m]
bore_averaged	6.50	17.81	0.99	-3.36	17.56	0.99
none	7.75	11.03	0.99	-3.48	12.73	1.00
wave_averaged	8.25	11.81	0.98	-3.68	12.97	1.00

Most relevant conclusions can be obtained by the variation of the bed friction parameter (fw). The model performance considerably varies with different setting of fw. By default it is set to 0. The greater the value of fw, the lower the beach erosion. For the higher values the simulated final profile tends to the initial one. As visible in Figure 23, the model predicts a wide range of eroded volumes but it's interesting to note that this variation occurs for values between 0.00 and 0.25.

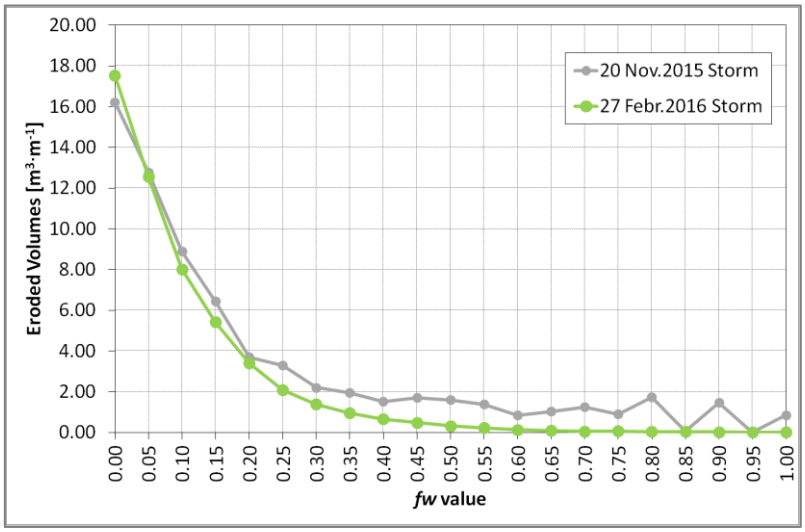

Figure 23 Morphological response of the beach profile in erosion, for different fw values

Table 12 Morphological and hydraulic response of the beach profile due to the fw parameter variation. For each parameter value shoreline retreat (ΔR) eroded volumes (V_{ero}) and runup ($R_{2\%}$) are presented. The results are summarized for the two storms.

	2015 Storm			2016 Storm		
fw value	ΔR [m]	V_{ero} [m^3 m^{-1}]	$R_{2\%}$ [m]	ΔR [m]	V_{ero} [m^3 m^{-1}]	$R_{2\%}$ [m]
0.00	7.60	16.22	1.00	-3.56	17.54	0.96
0.05	5.15	12.78	0.93	-5.66	12.55	0.92
0.10	2.10	8.89	0.86	-5.74	8.01	0.85
0.15	-1.35	6.44	0.80	-4.85	5.42	0.81
0.20	-1.15	3.69	0.76	-3.70	3.39	0.78
0.25	-2.70	3.29	0.74	-2.80	2.07	0.79
0.30	-3.55	2.20	0.75	-2.40	1.38	0.77
0.35	-4.55	1.94	0.72	-1.90	0.95	0.75
0.40	-4.05	1.52	0.71	-1.65	0.65	0.75
0.45	-4.30	1.70	0.70	-1.30	0.48	0.75
0.50	-3.70	1.60	0.69	-1.05	0.32	0.76
0.55	-4.45	1.37	0.68	-0.80	0.22	0.75
0.60	-3.30	0.84	0.68	-0.60	0.13	0.74
0.65	-4.45	1.04	0.65	-0.50	0.09	0.73
0.70	-4.80	1.25	0.65	-0.35	0.04	0.74
0.75	-4.75	0.89	0.65	-0.30	0.07	0.73
0.80	-4.05	1.72	0.66	-0.20	0.04	0.74
0.85	-3.30	0.07	0.65	-0.15	0.03	0.75
0.90	-4.50	1.46	0.66	-0.10	0.02	0.74
0.95	-3.20	0.00	0.65	-0.05	0.01	0.72
1.00	-4.45	0.86	0.66	-0.05	0.01	0.75

Another parameter that influences the results is *delta*. In the formulation of the dissipation due to wave breaking, the maximum wave height is calculated as ratio of the water depth (h) plus a fraction of the wave height (δH_{rms}, keyword: *delta*) using a breaker index γ (keyword: *gamma*). Secondly, the *delta* parameter influence the evaluation of the root mean squared velocity (u_{rms}) that is obtained from the wave group varying wave energy using linear wave theory. This parameter is set by default to 0.0 but it can be possible to set higher values, up to 1.

Table 13 Morphological and hydraulic response of the beach profile due to the delta parameter variation. For each parameter value shoreline retreat (ΔR) eroded volumes (V_{ero}) and runup ($R_{2\%}$) are presented. The results are summarized for the two storms.

	2015 Storm			2016 Storm		
delta value	ΔR [m]	V_{ero} [$m^3\ m^{-1}$]	$R_{2\%}$ [m]	ΔR [m]	V_{ero} [$m^3\ m^{-1}$]	$R_{2\%}$ [m]
0.00	-6.80	-16.40	0.98	-3.91	18.13	0.98
0.10	-9.10	-19.75	1.04	-3.06	19.63	0.98
0.20	-10.10	-22.09	1.06	-1.82	21.99	0.99
0.30	-12.20	-24.72	1.09	-0.52	25.67	1.07
0.40	-11.50	-30.69	1.18	0.28	29.67	1.09
0.50	-17.40	-36.28	1.22	4.18	33.91	1.11
0.60	-27.90	-44.23	1.24	10.94	37.84	1.16
0.70	-49.75	-50.80	1.28	31.60	44.44	1.09

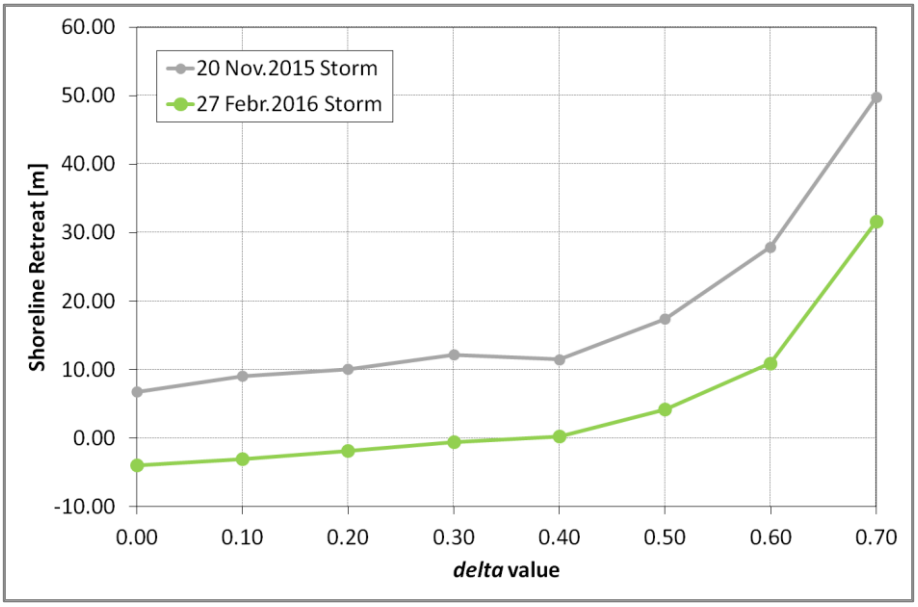

Figure 24 Morphological response of the beach profile as shoreline retreat, for different value of delta parameter.

4.5.3 Shallow Water Equation

The shallow water equations are used within the model to evaluate the low frequency waves and mean flows. To account for the wave induced mass-flux and the subsequent (return) flow these are cast into a depth-averaged Generalized Lagrangian Mean (GLM) formulation (Andrews and McIntyre, 1978, Walstra et al, 2000). The results presented in this subsection involve the numerical aspects of the shallow water equations that solve the water motions in the model (*eps*, *umin* and *hmin*) and the

physical parameter $bedfricceoff$ associated with mean currents and long waves. In order to avoid unrealistic behavior, in particular in very shallow water, some processes need to be controlled and limited. XBeach can be applied to a wide range of applications from laboratory scale up to super storm scale. The depth scale parameter allows to set-up the scale of the application. Eps, $umin$ and $hmin$ are depth scale related parameters.

The *eps* parameter, that determines whether points are dry or wet, can be varied between 0.001 and 0.1 m. The default value is set to 0.005. As it can be seen inTable 14, all simulations provide similar results for all the variables. The eroded volumes evenness shows that the model is not influenced by the *eps* parameter, probably because its thin range of variability is too little respect to the wave amplitude. This indicates that the method implement within the model is a stable method.

Table 14 Morphological and hydraulic response of the beach profile due to the eps parameter variation. For each parameter value shoreline retreat (ΔR) eroded volumes (V_{ero}) and runup ($R_{2\%}$) are presented. The results are summarized for the two storms.

	2015 Storm			2016 Storm		
eps value	ΔR [m]	V_{ero} [m^3 m^{-1}]	$R_{2\%}$ [m]	ΔR [m]	V_{ero} [m^3 m^{-1}]	$R_{2\%}$ [m]
0.001	-	-	-	-	-	-
0.005	7.85	16.81	0.97	-3.62	17.17	0.96
0.01	9.25	17.32	0.97	-4.12	17.09	0.94
0.02	8.45	16.48	0.98	-4.07	16.68	0.98
0.03	8.00	16.15	0.99	-3.32	17.10	0.98
0.04	8.10	16.07	0.98	-2.52	16.67	0.94
0.05	8.40	16.20	1.00	-3.12	16.47	0.96
0.06	7.45	15.68	0.97	-2.62	16.53	0.95
0.07	7.80	15.46	0.98	-3.21	15.94	0.99
0.08	7.35	14.73	0.98	-2.26	15.98	0.95
0.09	7.90	15.07	0.99	-3.21	16.09	0.95
0.10	6.70	13.78	0.96	-2.76	15.03	0.95

The second numerical parameter analyzed is $umin$. In the sediment transport formulations, the equilibrium sediment concentration (Ceq) is related to the velocity magnitude (v_{mg}), the orbital velocity (u_{rms}) and the fall velocity (w_s). Within the model a threshold is applied for the velocity magnitude, defined by the keyword $umin$. The $umin$ parameter is also used as limiter for the evaluation of the velocity related to the numerical scheme applied for the wave propagation. Table 15 shows comparable results for all simulations.

Table 15 Morphological and hydraulic response of the beach profile due to the umin parameter variation. For each parameter value shoreline retreat (ΔR) eroded volumes (V_{ero}) and runup ($R_{2\%}$) are presented. The results are summarized for the two storms.

	2015 Storm			2016 Storm		
umin value	ΔR [m]	V_{ero} [m^3 m^{-1}]	$R_{2\%}$ [m]	ΔR [m]	V_{ero} [m^3 m^{-1}]	$R_{2\%}$ [m]
0.00	8.50	16.89	0.98	-4.46	18.00	0.99
0.05	7.60	16.61	0.98	-3.41	17.37	0.98
0.10	8.20	17.07	0.97	-4.52	17.58	0.98
0.15	8.75	18.20	0.98	-3.67	16.94	0.98
0.20	7.25	17.23	0.99	-4.37	17.60	0.97

As mentioned above, also a physical parameter ($bedfriccoef$) was analyzed. The bed friction associated with mean currents and long waves is included via the formulation of the bed shear stress. There are five different formulations to determine the dimensionless bed friction coefficient c_f (keyword: $bedfriccoef$) implemented in XBeach. It is possible to varying the roughness of the bottom applying a variation of the dimensionless friction coefficient (c_f) or by the Chézy coefficient (C). The version of XBeach used in this thesis, Kingsday Release, has the implementation of the manning formulation with a value of 0.02. Manning can be seen as a depth-dependent Chézy value and a typical Manning value for sandy coasts would be in order of 0.02 $s/m^{1/3}$.

For this analysis the Chézy coefficient, that has a default value of 55 $m^{0.5}\cdot s^{-1}$, was applied. As expected, a reduction of the friction coefficient will result in more friction and thus less erosion. The friction value was varied between 30 and 70 $m^{0.5}\cdot s^{-1}$. As reported in Table 16, the simulations provide a volume variation of about of 13 $m^3\cdot m^{-1}$. The eroded volumes linearly increase as the $bedfriccoef$. For both events, a higher value of Chezy coefficient leads a landward movement of the shoreline, mostly visible for the first event.

Table 16 Morphological and hydraulic response of the beach profile due to the bedfriccoef parameter variation. For each parameter value shoreline retreat (ΔR) eroded volumes (V_{ero}) and runup ($R_{2\%}$) are presented. The results are summarized for the two storms.

	2015 Storm			2016 Storm		
bedfriccoef value	ΔR [m]	V_{ero} [m^3 m^{-1}]	$R_{2\%}$ [m]	ΔR [m]	V_{ero} [m^3 m^{-1}]	$R_{2\%}$ [m]
30	0.25	12.49	0.95	-6.57	13.93	0.96
40	5.53	16.97	0.96	-5.73	17.06	0.94
50	11.48	19.65	0.97	-2.58	20.27	0.94
55	12.28	22.54	0.97	-1.40	21.59	0.95
60	13.95	24.46	1.01	-1.63	22.47	0.95
70	18.25	26.84	0.97	-2.30	26.26	0.98

4.5.4 Bottom Updating

The last analysis focused on the parameter that affects the bottom updating. In particular, within the model two different critical slopes for avalanching are implemented. The behavior above and under the water is distinguished. To account for the slumping of sandy material from the dune face to the foreshore during storm-induced dune erosion avalanching (keyword: $avalanching$) is introduced to update the bed evolution. Avalanching is introduced via the use of a critical bed slope for both the dry and wet area (keyword: $wetslp$ and $dryslp$).

$Wetslp$ parameter represents the critical bed slope for the initiation of avalanching at the wet part of the profile and was varied between 0.2 and 1. The main morphological change concerns the dune erosion. The avalanching process is nearly avoided with the highest wetslp value. However the erosion of the beach is remarkable for all values. The simulations results are summarized in Table 17.

Table 17 Morphological and hydraulic response of the beach profile due to the wetslp parameter variation. For each parameter value shoreline retreat (ΔR) eroded volumes (V_{ero}) and runup ($R_{2\%}$) are presented. The results are summarized for the two storms.

	2015 Storm			2016 Storm		
Wetslp value	ΔR [m]	V_{ero} [m^3 m^{-1}]	$R_{2\%}$ [m]	ΔR [m]	V_{ero} [m^3 m^{-1}]	$R_{2\%}$ [m]
0.20	7.55	16.98	0.98	-5.06	17.72	0.95
0.30	9.25	17.86	0.99	-4.21	17.70	0.97
0.40	7.95	17.00	0.98	-3.26	17.77	0.96
0.50	8.90	17.22	0.98	-3.32	16.67	0.97
0.60	8.80	17.18	0.98	-2.17	16.99	0.95
0.70	9.00	17.31	0.97	-2.57	16.69	0.95
0.80	8.55	16.54	0.99	-3.07	16.33	0.96
0.90	8.95	16.96	0.98	-2.47	16.40	0.96
1.00	8.30	15.90	0.97	-2.27	16.19	0.95

For the dry part of the beach, the critical bed slope for the initiation of avalanching is defined with the keyword *dryslp*. The higher the value of , the higher the critical slope (Table 18). If the bed exceeds the relevant critical slope it collapses and slides downward (avalanching). For this reason, contrariwise to wet critical bed slope, when the value of *dryslp* is higher, a collapse of the dune occurs. The variation of this parameter doesn't impact the eroded volumes.

Table 18 Morphological and hydraulic response of the beach profile due to the dryslp parameter variation. For each parameter value shoreline retreat (ΔR) eroded volumes (V_{ero}) and runup ($R_{2\%}$) are presented. The results are summarized for the two storms.

	2015 Storm			2016 Storm		
Dryslp value	ΔR [m]	V_{ero} [m^3 m^{-1}]	$R_{2\%}$ [m]	ΔR [m]	V_{ero} [m^3 m^{-1}]	$R_{2\%}$ [m]
0.20	7.05	17.22	0.96	-4.66	17.71	0.98
0.50	7.85	16.75	0.97	-3.41	17.72	0.98
1.00	7.75	17.08	0.99	-4.87	17.07	0.97
1.50	7.90	18.26	0.99	-4.66	17.39	0.95
2.00	7.60	16.43	0.98	-3.97	17.16	0.96

4.6 Evaluation of the model performance and morphological calibration

A few input parameters provided a significant variability of the model predictions. Therefore, to avoid an unrealistic morphological prevision it's necessary to define their proper settings. For this purpose, the morphological results of the model are compared with the field data collected during the topo-bathymetrical measurements. In this subsection, the model performance for $facua$, $break$, $gamma$, fw, $delta$ and $bedfriccoef$ was evaluated through statistical indicators ($bias$, $RMSE$ and BSS). Subsequently, the calibration of fw parameter is presented.

4.6.1 *Facua parameter*

The default value of facua predicts an erosion overestimation that results in a negative BSS. Table 19 shows the model performance indicators evaluated for different values of facua parameter. The morphological skill of most of simulations can be defined as *bad*, according to the classification of Van Rijn (2003).

Table 19 Model performance indicators: BSS, RMSE and bias for different values of facua parameter.

	2015 Storm			2016 Storm		
facua value	Bias [m]	RMSE [m]	BSS [-]	Bias [m]	RMSE [m]	BSS [-]
0.10	-0.27	0.32	-2.49	-0.41	0.50	-6.93
0.15	-0.20	0.23	-0.82	-0.31	0.40	-3.93
0.20	-0.12	0.14	0.31	-0.20	0.28	-1.43
0.25	0.00	0.08	0.80	-0.11	0.20	-0.24
0.30	0.11	0.15	0.19	0.01	0.16	0.23
0.35	0.19	0.24	-1.06	0.09	0.20	-0.29
0.40	0.23	0.28	-1.73	0.12	0.20	-0.29
0.45	0.31	0.39	-4.21	0.10	0.17	0.06
0.50	0.35	0.44	-5.64	0.05	0.11	0.59

The bed levels predicted by the model for various value of facua for the first and the second event respectively are reported in Figure 25 and Figure 26. By increasing the facua value the erosion will be (partly) counteracted with an asymmetric onshore sediment transport. For the first event, a value of facua of 0.25 results in a good fit with measurement data. In particular, the value of 0.25 results in a BSS of 0.80 that indicates an *excellent* model performance while, for the second storm, the model is not able to predict the beach evolution in accurate way. The best performance is confirmed also by the lowest value of *bias* and *RMSE*.

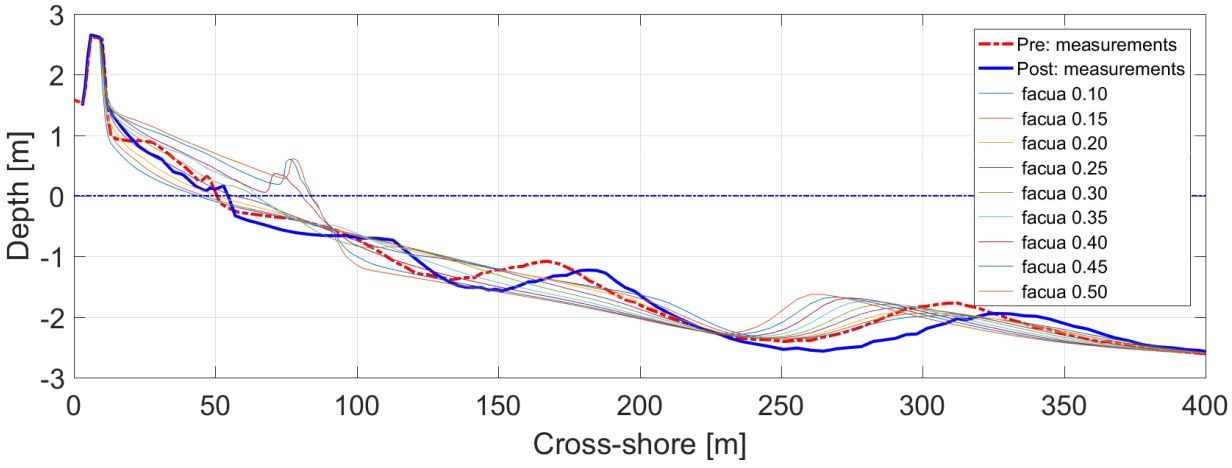

Figure 25 Post storm bed levels for a single cross-section for various values of facua, related to the storm event of the 20-24 November 2015. The forecasted beach profiles are compared to the observed post storm profile (blue line).

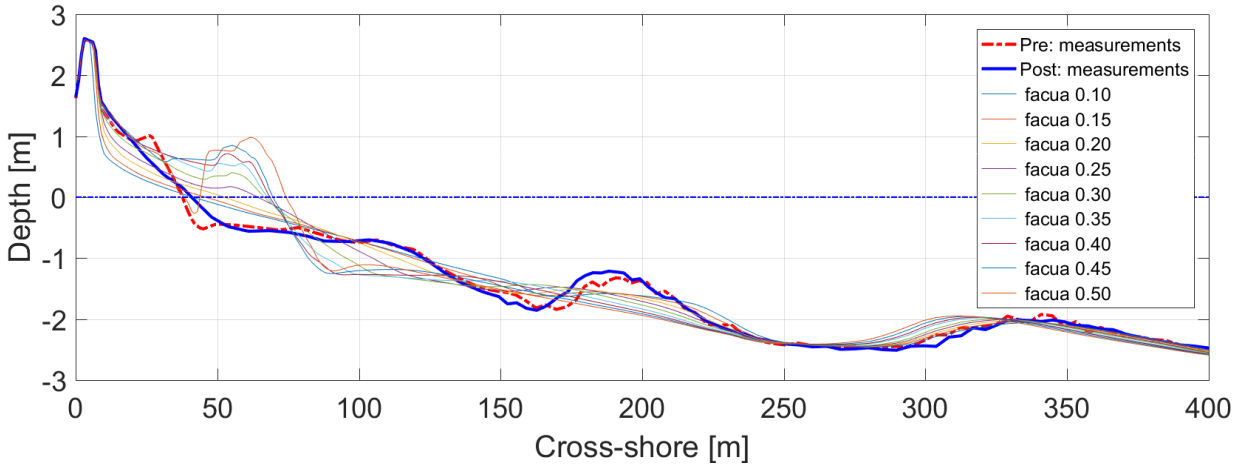

Figure 26 Post storm bed levels for a single cross-section for various values of facua, related to the storm event of the 27 February-02 March 2016. The forecasted beach profiles are compared to the observed post storm profile (blue line).

Interesting to see that the model predicts a berm generation when a too high value of facua is applied. Figure 27 shows the simulated beach profile with a facua value of 0.50, for the second storm. This behavior results in a good agreement between the modeled and the observed data above the mean sea level. However, the berm generation is not a realistic prediction.

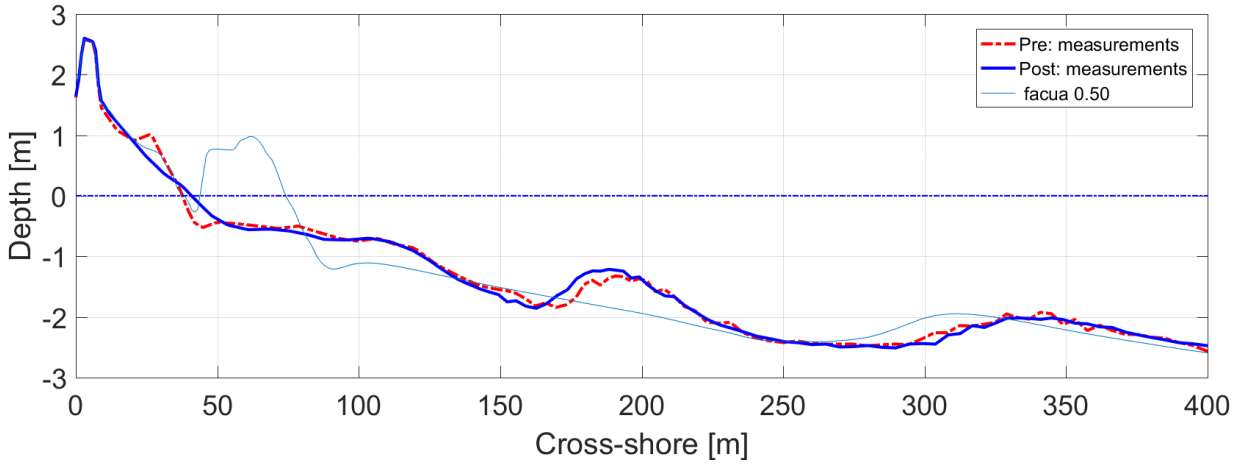

Figure 27 Discrepancy between the final beach profile, obtained with a facua value of 0.5, and the post storm measurements.

4.6.2 gamma parameter

As visible in Table 20, the BSS referred to the breaker parameter (*gamma*) simulations change rapidly. For the first event, a value of gamma 0.40 will result in the highest BSS, lowest bias and RMSE but it means a reasonable/fair score according to Van Rijn (2003). An excellent performance, for the analyzed storm cases, is not achieved. Therefore, a reduction of the default parameter shows better results and hence an improvement of the forecast model capability. The comparison between various simulated beach profiles and the observed measurements is displayed in Figure 28 and Figure 29.

Table 20 Model performance indicators: BSS, RMSE and bias for different values of gamma parameter.

	2015 Storm			2016 Storm		
gamma value	Bias [m]	RMSE [m]	BSS [-]	Bias [m]	RMSE [m]	BSS [-]
0.40	-0.09	0.12	0.46	-0.23	0.32	-2.17
0.45	-0.14	0.16	0.06	-0.28	0.36	-3.17
0.50	-0.20	0.23	-0.78	-0.33	0.42	-4.59
0.55	-0.28	0.33	-2.87	-0.41	0.51	-7.23
0.60	-0.39	0.47	-6.71	-0.51	0.64	-11.87
0.65	-0.55	0.68	-15.30	-0.65	0.81	-19.36
0.70	-0.73	0.88	-26.25	-0.84	1.00	-30.23
0.75	-1.05	1.20	-49.23	-0.99	1.15	-40.20
0.80	-1.31	1.46	-73.14	-1.18	1.33	-54.33
0.85	-1.42	1.55	-82.40	-1.30	1.45	-64.87
0.90	-1.49	1.61	-89.55	-	-	-

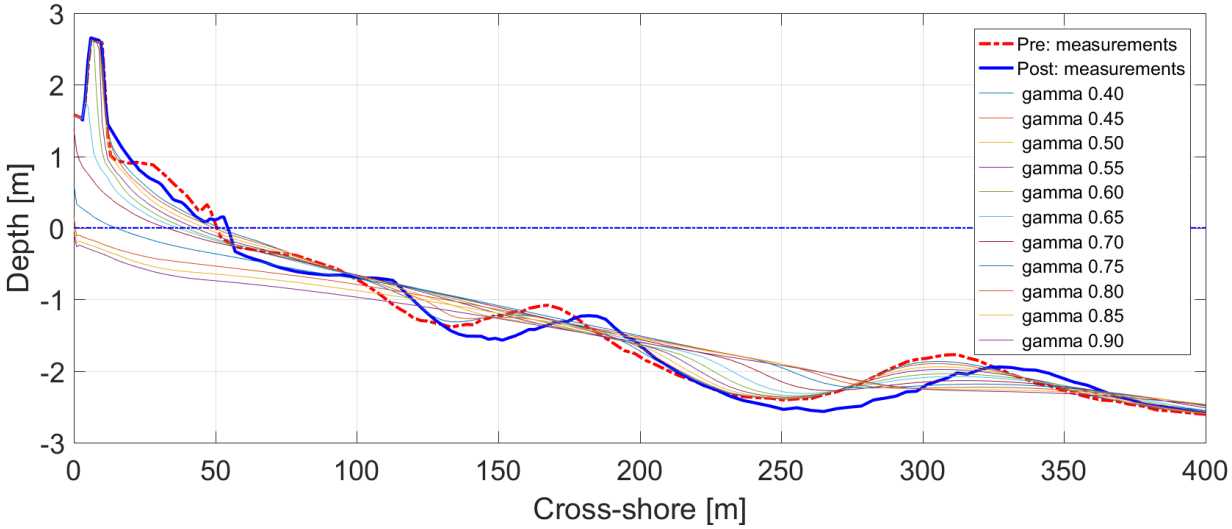

Figure 28 Post storm bed levels for a single cross-section for various values of gamma, related to the storm event of the 20-24 November 2015. The forecasted beach profiles are compared to the observed post storm profile (blue line).

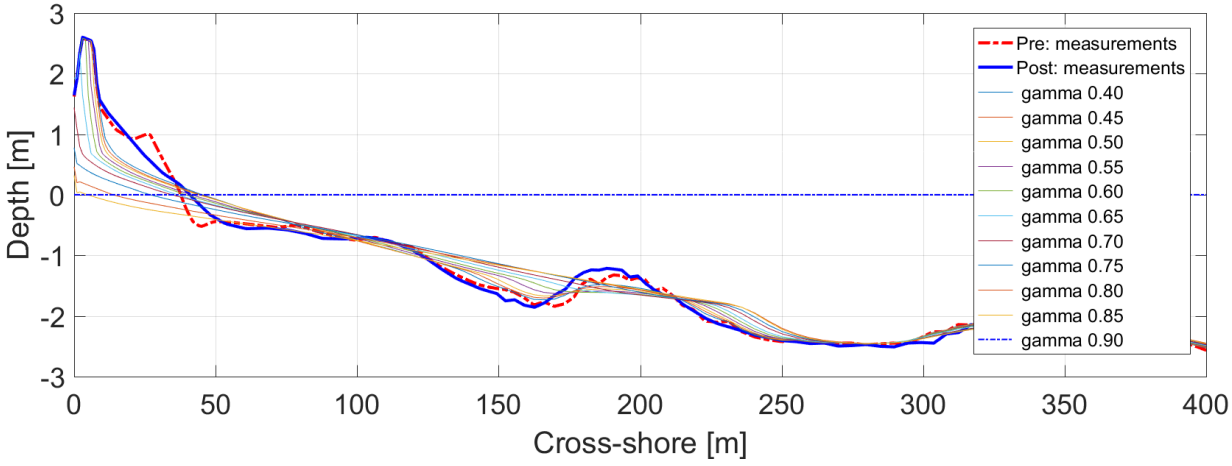

Figure 29 Post storm bed levels for a single cross-section for various values of gamma, related to the storm event of the 27 February-02 March 2016. The forecasted beach profiles are compared to the observed post storm profile (blue line).

4.6.3 *Break parameter*

Applying a different formulation to evaluate the dissipation due to wave breaking, the BSS are all negative. A slight improvement is provided by the formulation of Roelvink (1993) rather than the default formulation, while the use of the Daly et al. (2010) approach produces a strong reduction of the accuracy of the prediction. No setting of this parameter is able to model the morphological changes in accurate way, as visible in Figure 30 and Figure 31.

Table 21 Model performance indicators: BSS, RMSE and bias for different values of break parameter.

	2015 Storm			2016 Storm		
Break value	Bias [m]	RMSE [m]	BSS [-]	Bias [m]	RMSE [m]	BSS [-]
roelvink1	-0.18	0.21	-0.59	-0.30	0.38	-3.63
roelvink2	-0.29	0.34	-2.96	-0.40	0.49	-6.57
roelvink_daly	-0.78	0.91	-27.95	-0.65	0.77	-17.72

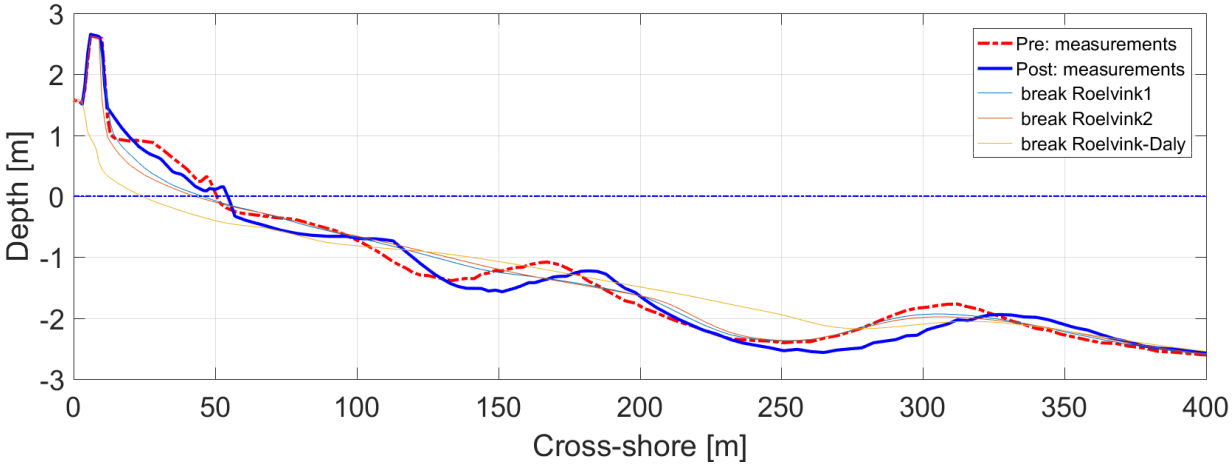

Figure 30 Post storm bed levels for a single cross-section for various values of break, related to the storm event of the 20-24 November 2015. The forecasted beach profiles are compared to the observed post storm profile (blue line).

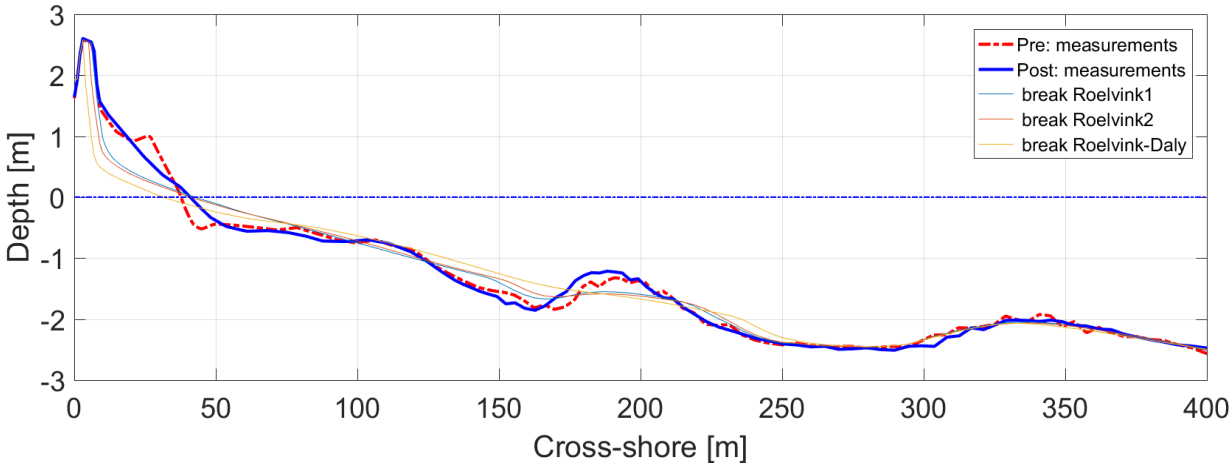

Figure 31 Post storm bed levels for a single cross-section for various values of break, related to the storm event of the 27 February-02 March 2016. The forecasted beach profiles are compared to the observed post storm profile (blue line).

4.6.4 *Delta parameter*

Also for *delta* parameter, that had shown a strong impact on the model results, all the simulations provide negative BSS (Table 22). Moreover, the model performance gets worse when the default value is changed. The bias and RMSE value grow with the value, indicating that the model capability can't be improved with the variation of this parameter. The morphological behavior for various value of delta is indicated in Figure 32 and Figure 33.

Table 22 Model performance indicators: BSS, RMSE and bias for different values of delta parameter.

	2015 Storm			2016 Storm		
delta value	Bias [m]	RMSE [m]	BSS [-]	Bias [m]	RMSE [m]	BSS [-]
0.00	-0.27	0.32	-2.66	-0.43	0.54	-7.99
0.10	-0.34	0.42	-5.24	-0.46	0.57	-9.37
0.20	-0.39	0.49	-7.27	-0.52	0.65	-12.16
0.30	-0.45	0.55	-9.71	-0.62	0.76	-17.11
0.40	-0.57	0.72	-16.93	-0.73	0.88	-23.50
0.50	-0.70	0.84	-23.59	-0.85	1.00	-30.64
0.60	-0.92	1.07	-38.62	-0.98	1.12	-38.44
0.70	-1.35	1.48	-74.88	-1.32	1.45	-65.21

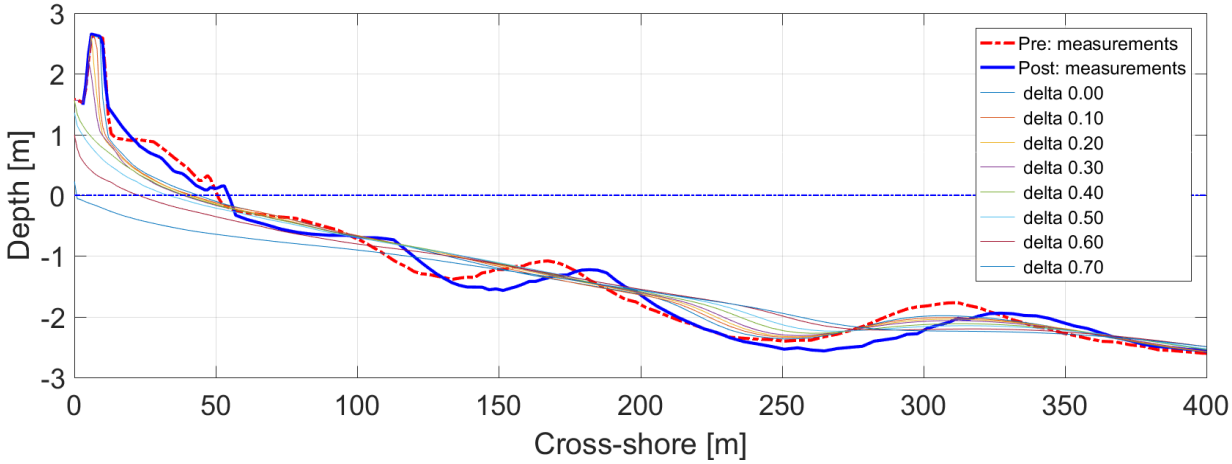

Figure 32 Post storm bed levels for a single cross-section for various values of delta, related to the storm event of the 20-24 November 2015. The forecasted beach profiles are compared to the observed post storm profile (blue line).

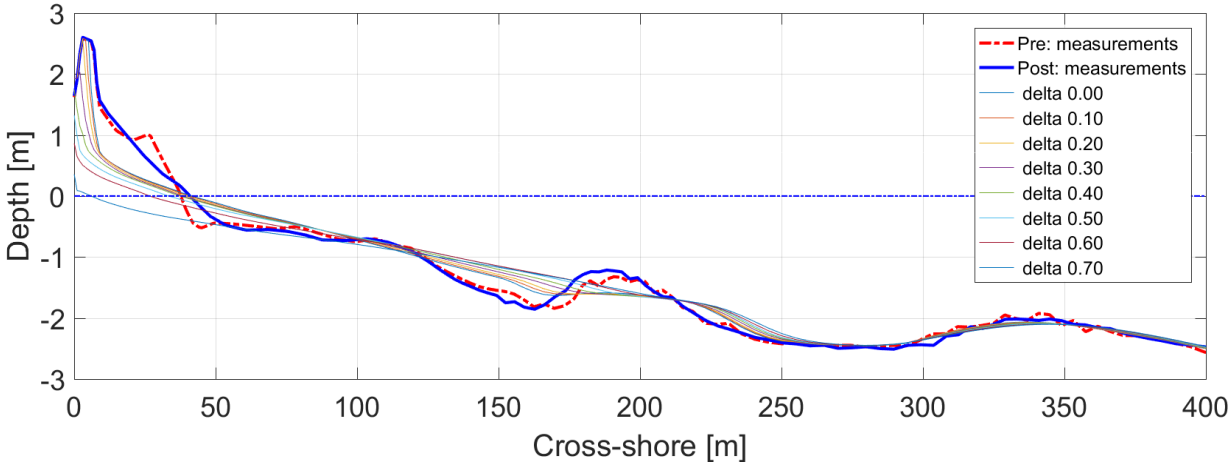

Figure 33 Post storm bed levels for a single cross-section for various values of delta, related to the storm event of the 27 February-02 March 2016. The forecasted beach profiles are compared to the observed post storm profile (blue line).

4.6.5 *Bedfriccoef parameter*

The sensitivity analysis has shown that the results were considerably influenced by the bottom friction coefficient (*bedfriccoef*). For both cases, a lower value of the Chezy value corresponds to a better performance of the model. Nevertheless, the value of 0.30 that provides the better results is not a commonly used bed friction value for sandy bottom. In Table 23 the model performances are summarized while in Figure 34 and Figure 35 the beach profile evolution due to different value of bedfriccoef is shown.

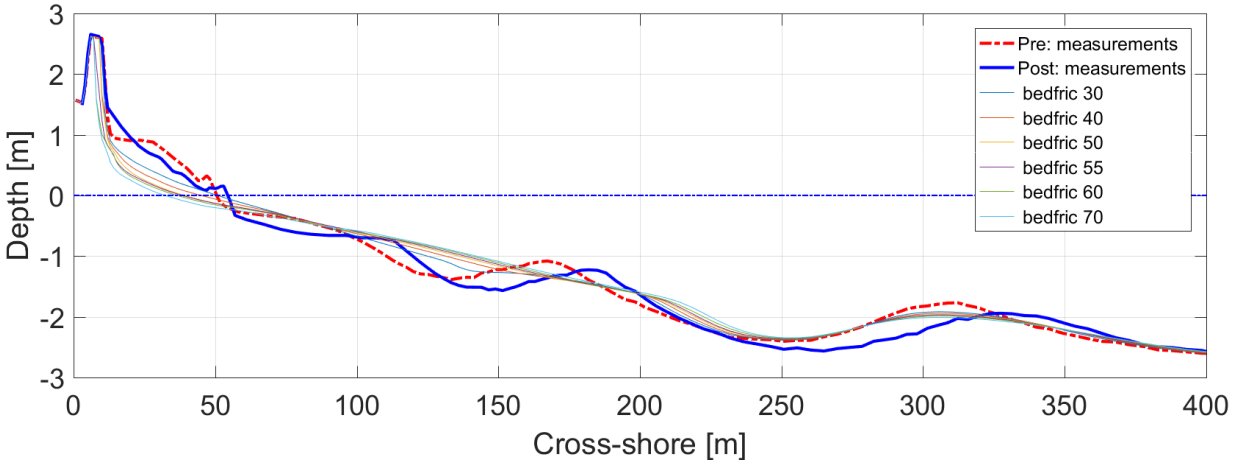

Figure 34 Post storm bed levels for a single cross-section for various values of bedfriccoef, related to the storm event of the 20-24 November 2015. The forecasted beach profiles are compared to the observed post storm profile (blue line).

Table 23 Model performance indicators: BSS, RMSE and bias for different values of bedfriccoef parameter.

	2015 Storm			2016 Storm		
bedfriccoef value	Bias [m]	RMSE [m]	BSS [-]	Bias [m]	RMSE [m]	BSS [-]
30	-0.19	0.24	-1.03	-0.32	0.41	-4.31
40	-0.28	0.34	-2.95	-0.40	0.50	-6.86
50	-0.35	0.40	-4.69	-0.48	0.60	-10.17
55	-0.40	0.48	-6.88	-0.51	0.63	-11.69
60	-0.45	0.54	-9.13	-0.54	0.67	-12.97
70	-0.51	0.61	-11.87	-0.64	0.78	-17.92

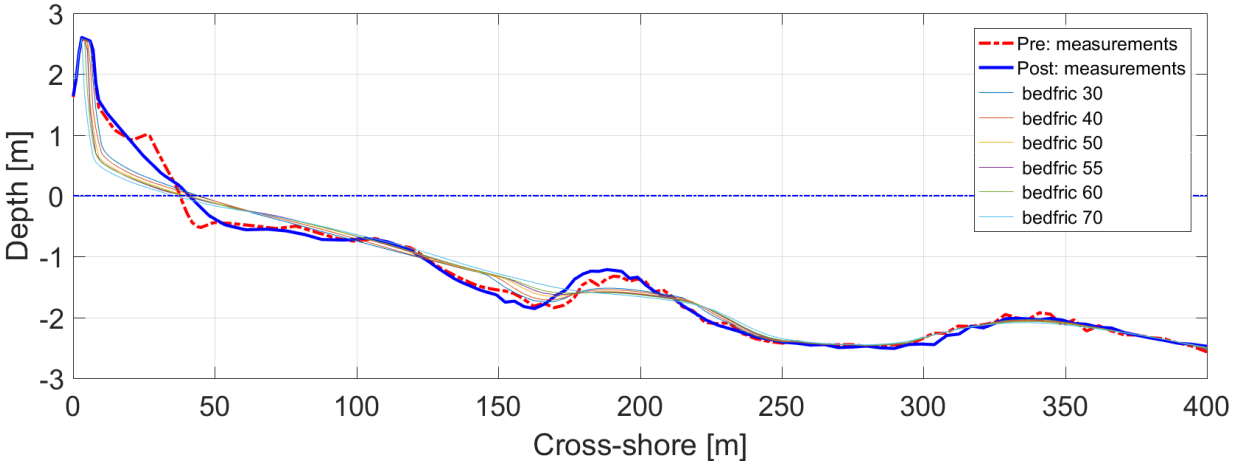

Figure 35 Post storm bed levels for a single cross-section for various values of bedfriccoef, related to the storm event of the 27 February-02 March 2016. The forecasted beach profiles are compared to the observed post storm profile (blue line).

4.6.6 Fw parameter

The best morphological skill is achieved with the setting of the bottom friction coefficient (fw). The value of 0.20 produces excellent skill for both the storm events. With the suggested fw value a BSS of 0.87 and a bias of -0.021 m are achieved in forecasting the impact of the storm of the 20th November 2015 and a BSS of 0.80 and a bias of -0.04 for the 27th February 2016 storm. A value of facua of 0.20 results in a good fit with measurement data. The model performance indicators are summarized in Table 24.

Table 24In conclusion, the analysis shows that the morphological results are calculated accurate and thus it is assumed that a fw setting of 0.20 can be a proper value for both the study cases. Figure 36 and Figure 37 show the good fit of this set-up with the observed measurements for both the events.

Table 24 Model performance indicators: BSS, RMSE and bias for different values of fw parameter.

	2015 Storm			2016 Storm		
fw value	Bias [m]	RMSE [m]	BSS [-]	Bias [m]	RMSE [m]	BSS [-]
0.00	-0.27	0.32	-2.47	-0.41	0.51	-7.04
0.05	-0.20	0.23	-0.92	-0.28	0.37	-3.19
0.10	-0.12	0.15	0.19	-0.17	0.22	-0.49
0.15	-0.07	0.10	0.64	-0.10	0.13	0.48
0.20	-0.02	0.06	0.87	-0.04	0.08	0.80
0.25	-0.01	0.07	0.82	-0.01	0.09	0.74
0.30	0.01	0.08	0.79	0.01	0.11	0.62
0.35	0.01	0.11	0.59	0.03	0.13	0.51
0.40	0.02	0.12	0.53	0.03	0.14	0.38
0.45	0.02	0.12	0.53	0.04	0.15	0.28
0.50	0.02	0.12	0.49	0.05	0.16	0.24
0.55	0.02	0.12	0.47	0.05	0.16	0.16
0.60	0.04	0.13	0.43	0.05	0.17	0.13
0.65	0.03	0.13	0.41	0.05	0.17	0.07
0.70	0.03	0.13	0.40	0.05	0.17	0.04
0.75	0.03	0.11	0.55	0.05	0.17	0.08
0.80	0.02	0.12	0.47	0.05	0.18	0.02
0.85	0.05	0.16	0.12	0.06	0.18	0.03
0.90	0.02	0.11	0.59	0.06	0.18	0.01
0.95	0.05	0.16	0.12	0.06	0.18	-0.02
1.00	0.03	0.13	0.40	0.06	0.18	0.00

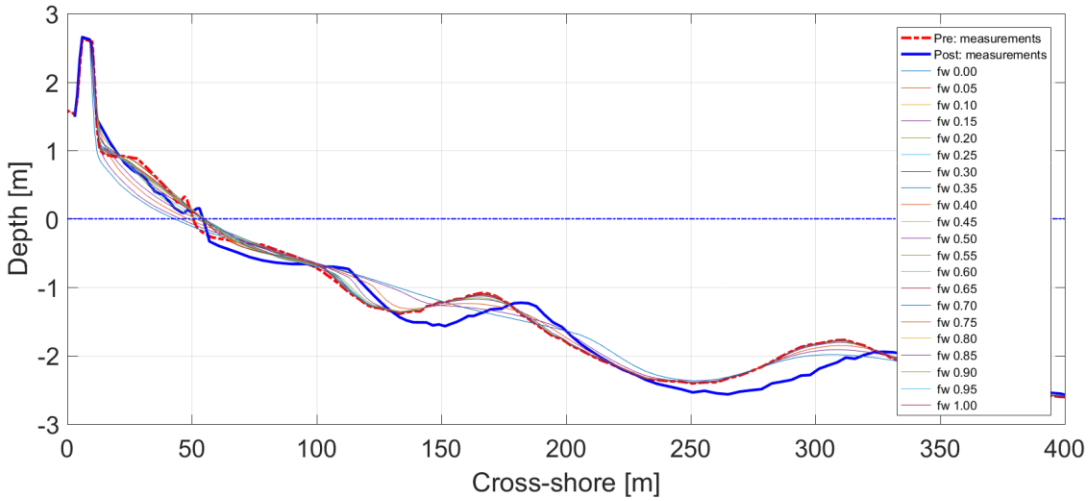

Figure 36 Post storm bed levels for a single cross-section for various values of fw, related to the storm event of the 20-24 November 2015. The forecasted beach profiles are compared to the observed post storm profile (blue line).

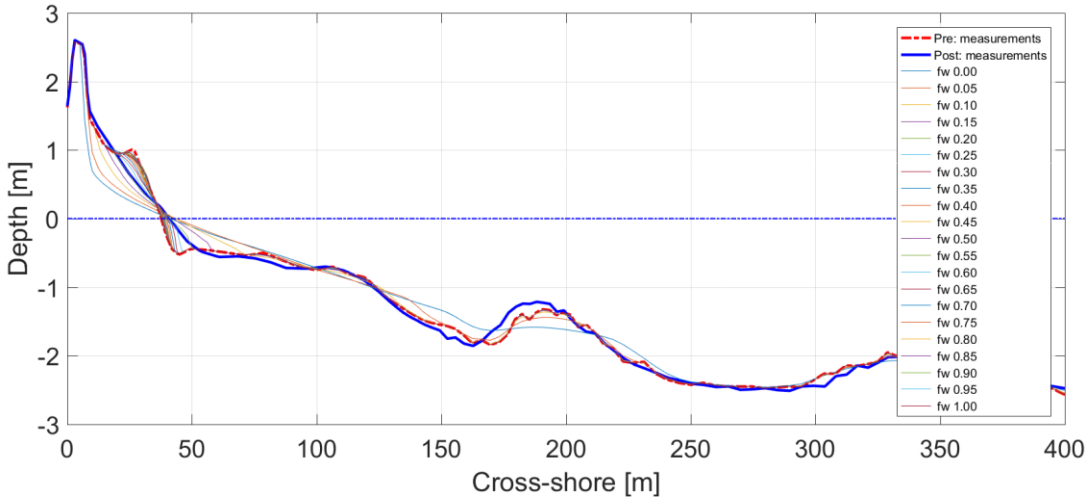

Figure 37 Post storm bed levels for a single cross-section for various values of fw, related to the storm event of the 27 February-02 March 2016. The forecasted beach profiles are compared to the observed post storm profile (blue line).

4.7 **Conclusions**

When using a numerical model to predict the morphological response during a storm event, it is essential to be conscious of the uncertainties that are propagated within the model. The sources of these uncertainties can be numerous. As demonstrated by several study, the physical and non-physical settings of the coastal model will strongly affect the output variables showing the need for a proper calibration. In this chapter, the effect of the variation of several input parameters was analyzed following the approach of the sensitivity analysis. Two storm events were investigated.

Firstly, the results of the reference simulation (default values) showed that XBeach overestimates the erosion, during overwash conditions. The reference simulation provides overestimation of eroded volumes that are about an order of magnitude higher than the measured values. This might be related to the sediment transport formulation that is not strictly valid for sheet flow conditions (Nederhoff, 2014).

Such morphological overestimation gives a first indication of the model uncertainties related to the parameters. A wrong calibration of the model, for the study area, provides inaccurate forecasts. Therefore, the knowledge of the higher uncertainties associated to each model parameter is required for improving the model performance.

The model is constantly evolving and improving. Recent insights reveal that the behaviour of the intertidal beach is key and that often XBeach tends towards a berm slope much flatter than observed. This problem is addressed in subsequent versions of XBeach but unfortunately not in the version applied (version 18. revision 4691, also known as the 'Kingsday' release). Therefore, in this thesis, the sand bars behavior was not been evaluated.

A few parameters, all related to the wave breaking process, have shown a strong impact on the morphological evolution of the beach profile. In the area of application, the input parameters that mostly affect the model results are $facua$ (wave shape), $gamma$ (breaker parameter), $delta$ (fraction of the wave height), $break$ (dissipation formulation), fw (bottom friction), and $bedfriccoef$ (bed friction). In Table 25 the output variations of the shoreline retreat and the eroded volumes are summarized. For each parameter, the higher values of the BSS are also reported.

Table 25 Results variation of shoreline retreat and eroded volumes, related to the variation of the most significant model parameters. The last two columns indicate the best BSS achieved, for both the storm events.

parameter	Shoreline Retreat variation [m]		Eroded Volumes variation [m3m-1]		Best BSS [-]	
	Storm 1	Storm 2	Storm 1	Storm 2	Storm 1	Storm 2
facua	40.16	32.96	46.50	37.49	0.80	0.20
break	21.15	1.41	25.17	13.03	-0.59	-3.63
gamma	51.70	40.58	43.25	34.19	0.46	-2.17
fw	12.05	3.51	15.36	17.53	0.87	0.80
delta	42.95	35.51	34.40	26.31	-2.66	-7.99
bedfriccoef	18.00	4.27	14.35	12.33	-1.03	-4.31

The BSS values indicate that the model is not able to reproduce the morphological evolution in accurate way except for facua and fw parameters. In particular, when a bottom friction value (fw) of 0.20 is adopted, the model outputs and the observed data are in good agreement.

The model shows good performance for both the storm events and thus it is assumed that a fw setting of 0.20 is a proper value for this case study. Nevertheless, a realistic range for the bottom friction parameter for sandy profiles would be 0.05-0.10 (Trouw et al., 2012). The chosen value is somewhat above the usual range suggesting that for low-lying beach profiles, the wave breaking dissipation due to the bottom is a primary process. For both cases, to achieve an accurate representation of the natural processes, this dissipation term needs to be higher than the usual value range.

In conclusion, the analysis highlighted that it is possible to model the morphological evolution in accurate way with the default settings and calibration of only one parameter. Figure 38 and Figure 39 show the final profiles, for both the events, with the default configuration and the setting of the fw parameter to 0.2.

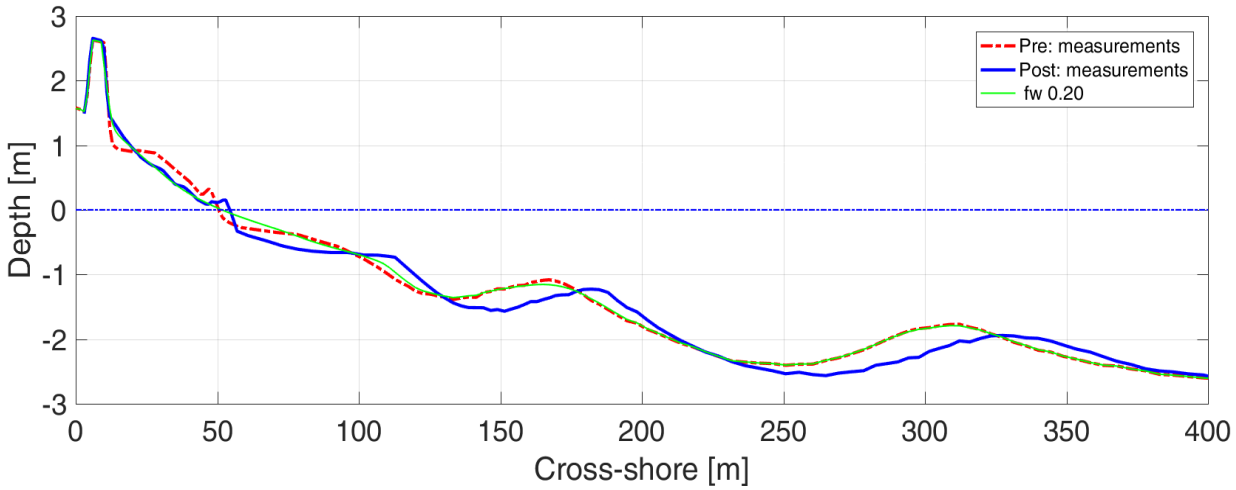

Figure 38 Post storm bed levels for a single cross-section for fw=0.2, related to the storm event of the 20-24 November 2015. The forecasted beach profile is compared to the observed post storm profile (blue line).

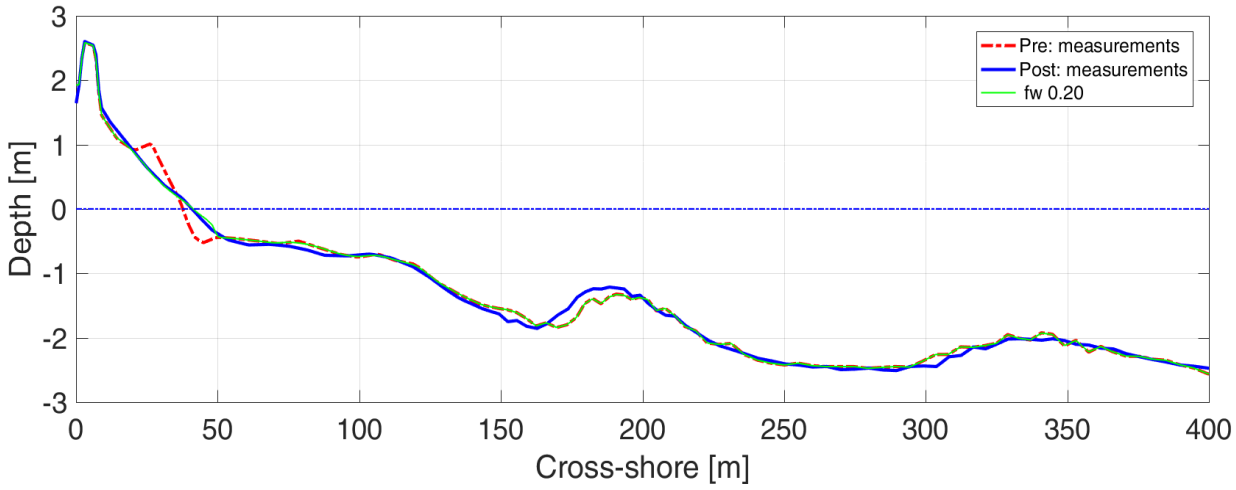

Figure 39 Post storm bed levels for a single cross-section for fw=0.2, related to the storm event of the 27 February-02 March 2016. The forecasted beach profile is compared to the observed post storm profile (blue line).

Chapter

5 Estimate of the uncertainty by means of the ensemble approach

5.1 Introduction

When a series of models are used in cascade for the meteorological, oceanographic and coastal predictions, one has to keep in mind that uncertainties associated to each model component propagate through the numerical chain with a collective effect on the final forecasts accuracy. In this chapter, the study of how these uncertainties propagate and affect the forecasts is presented. The numerical modeling chain is composed by the meteorological model COSMO, the wave model SWAN, the oceanographic model ROMS and the coastal model XBeach. In order to give some indications of the uncertainty associated to the forecasts, the study was carried out by means of the "ensemble" approach.

5.2 Background

Flooding due to coastal storms presents a significant threat to coastal structures, properties and human safety. Worldwide, storms and hurricanes cause severe damages along many coastal areas and several countries already developed and implemented flood forecast systems (e.g. Flather, 2000; Verlaan et al., 2005; Daniel et al., 2009; Lane et al., 2009; Werner et al., 2009; Ji et al., 2010). The forecasting systems aim to mitigate this threat by providing advance warning of dangerous events, so that protective actions can be taken. Usually, the coastal flood warnings are based on wind, wave and storm surges forecasts produced by meteorological, oceanographic and coastal models.

The Regional Agency for Prevention, Environment and Energy of Emilia-Romagna (Arpae) is responsible for issuing coastal flood warnings for the Emilia-Romagna Region, which overlooks the northern Adriatic Sea (Italy). The Emilia-Romagna Early Warning System (EWS) is a state-of-the-art coastal forecasting system, composed by an operational cascade of numerical models, to provide a forecast up to 72 hours ahead of the sea level height along the entire coastal region (Harley et al., 2016). The EWS is composed of the meteorological model COSMO (developed by the COSMO Consortium; www.cosmo-model.org), the wave/oceanographic models SWAN (Ris et al., 1994) and ROMS (Chiggiato and Oddo, 2006), and the coastal model XBeach (Roelvink et al., 2009).

An operational storm surge forecast needs to be provided in a fast way for early decision-making. However, the accuracy of storm surge forecast is likely to be affected by the uncertainties arising from the weather forecast (Ding et al., 2016). The interactions between atmospheric, oceanic and coastal processes are poorly understood, resulting in large uncertainties in the predictions of coastal flooding, in particular, under extreme conditions (Baart, 2011; Zou, 2009). Storm surges are driven by the weather, which is expected to be the dominant source of surge forecast uncertainty. As known from the Chaos theory (Lorenz, 1965), atmosphere is a chaotic system. Small errors in the initial conditions of a numerical weather prediction (NWP) model grow rapidly and affect predictability; forecasted

atmospheric conditions are then affected by errors (Paccagnella 2012). The awareness of the chaotic nature of the atmosphere, and the further awareness of the errors we inevitably make, has led to the development of a branch of numerical forecasting based on a probabilistic concept: the ensemble forecasting.

NWP models are deterministic, giving a single output value for each variable, without any indication of the amount of uncertainty or expected variation around this value. An ensemble modelling approach addresses this issue by producing not one but several forecasts with the same likelihood to be the correct one. Each forecast uses slightly different initial conditions and/or boundary conditions and/or model physics, with the aim of sampling the range of forecast results which are consistent with the uncertainty in the forecast (Palmer et al., 2004). The ensemble approach allows to estimate the probabilities of various outcomes and to quantify the associated uncertainties by producing a sample of alternative/possible future atmospheric states. Furthermore, it is also possible to assess how the uncertainty propagates from meteorological forecasts to coastal modeling (overtopping and coastal flood), thereby improving our understanding of the reliability of results (Zou and Reeve, 2009; Dance and Zou, 2010).

Scientifically, probabilistic forecasts are seen as being much more valuable than single forecasts "because they can be used not only to identify the most likely outcome but also to assess the probability of occurrence of extreme and rare events. Furthermore, probabilistic forecasts issued on consecutive days are also more consistent than corresponding single forecasts" (Buizza, 2008).

The ensemble modelling approach has been widely used in meteorology (e.g. Marsigli et al., 2001, Buizza et al., 2005; Bowler et al., 2008; and references therein) and storm surge studies (Horsburgh et al., 2008; Flowerdew et al., 2010, Ding et al., 2016), but much less so far in coastal engineering.

Moreover, regional EPSs exist, which are nested into global EPS to provide EPS forecasts on a smaller spatial scale. An example is COSMO-LEPS, the limited-area ensemble system developed at ARPAE-SIMC and operational since 2002 (Marsigli et al., 2001, 2008). COSMO-LEPS produces, twice a day, 20 forecasts up to 120 h.

Buizza (2005) proved that Ensemble forecasting is a successful way of dealing with the inherent uncertainty of weather and climate forecasts. An example of extended ensemble approach which includes wave, tide and surge models is The Met Office Global and Regional Ensemble Prediction System (MOGREPS), which has recently become operational in the UK (Flowerdew et al., 2010). Moreover, an ensemble prediction system for operational forecasting of storm surge in the northern Adriatic Sea is presented and applied to 10 relatively high storm surge events by Mel and Lionello (2014). Multi-model storm surge ensemble prediction has been performed for New York and the North Sea by Diliberto et al. (2011) and Siek et al. (2011), respectively. Operational and research flood forecasting systems around the world are increasingly moving towards using ensembles of Nearshore Wave Prediction System (NWPS), known as ensemble prediction systems (EPS), rather than single deterministic forecasts, to drive their flood forecasting systems (Cloke et al., 2009). Zou (2013) presents an integrated 'Clouds-to-Coast' ensemble modelling framework of coastal flood risk due to wave overtopping while the purpose of the study presented by Hawkens (2009) is to develop, demonstrate and evaluate probabilistic methods for surge, nearshore wave and coastal flood forecasting in England and Wales.

In order to investigate the propagation of the uncertainties, the purpose of the present study is to integrate meteorological models, regional hydrodynamic (waves, tides and surge) models and surf

zone hydrodynamic models in an ensemble prediction framework of coastal flood risk. It is also possible to assess how the uncertainty propagates from meteorological forecasts to coastal previsions and morphological changes, thereby improving our understanding of the reliability of forecasts.

In contrast to earlier studies of coastal flood risk (Zou et al., 2013; Mel and Lionello, 2014; Hawkens, 2009) this approach provides an analysis of results in terms of impact on coastal morphology. The main innovation of this study is indeed the use of hydraulic models extending through to action on beach morphology and flooding forecasts. The aim is to evaluate a deterministic-probabilistic modeling system for coastal flood forecasting in Emilia-Romagna as a tool to provide useful indications of the coastal forecast reliability. This study uses two different storm events that occurred in the winter 2015-2016 as test cases to illustrate the proposed approach.

5.3 Material and methods

To achieve the purpose of the analysis, the forecasts of the SIMC operational modeling chain, and the results from this ensemble integrated system were compared to the observations at defined locations. Furthermore, the use of the ensemble method as a tool to study and define the forecasts uncertainty was investigated. In particular, in this thesis, the extension of the ensemble method up to the coastal zone is presented. First, a description of both the deterministic and ensemble numerical systems is reported.

5.3.1 Deterministic framework system

The operational numerical modeling chain is composed of the meteorological model COSMO-I7 (www.cosmo-model.org), the wave/oceanographic models, SWAN (Ris et al., 1994), and ROMS (Chiggiato and Oddo,2006), and the coastal model XBeach (Roelvink et al., 2009) and provides a deterministic forecast up to 72 hour ahead. A global view of the operational chain is presented in Figure 40.

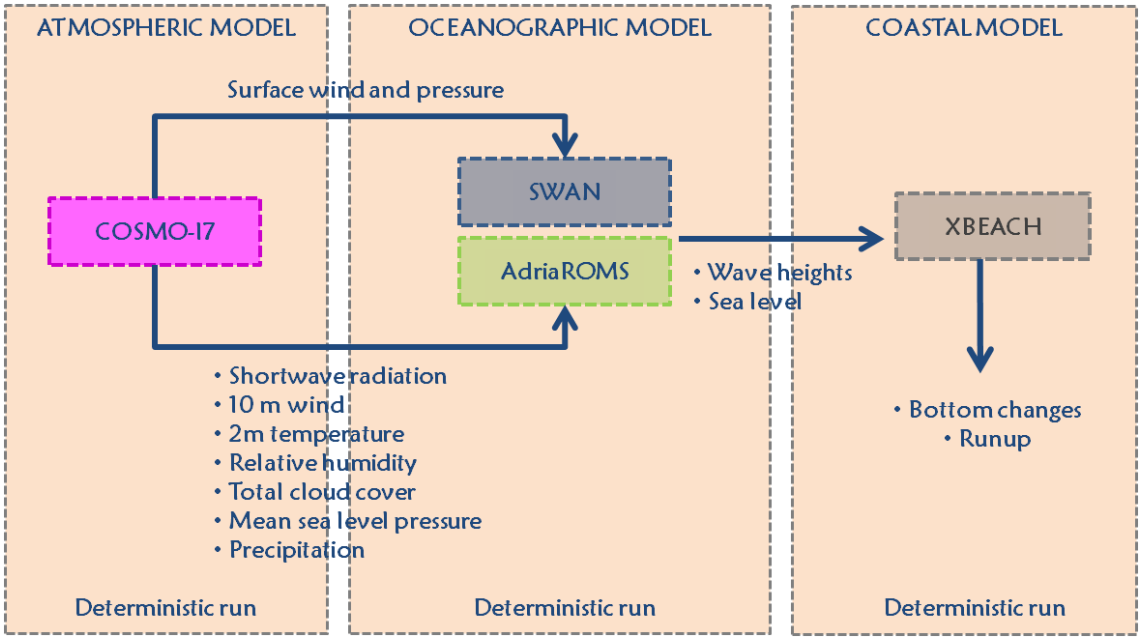

Figure 40 Integrated deterministic modelling framework.

The operational implementation of the COSMO model at Arpae-SIMC, consists of the 7 Km version of COSMO running over the Italian domain twice a day with a forecast range of 72 hours (COSMO I-7). The wave/oceanographic model SWAN and ROMS are driven by the weather forecast of COSMO-I7 model and provide the input data for the coastal model XBeach.

5.3.2 Ensemble framework system

To generate the ensemble system, the operational sea and coastal models were forced by the fields forecasted by the limited-area Ensemble Prediction System (COSMO-LEPS). For this thesis, the ensemble framework system was composed by the following models: the meteorological model COSMO-LEPS, the wave/hydrodynamic models SWAN and ROMS, and the morphological model XBeach (Roelvink et al., 2009). An extensive description of the models can be found in Chapter 2. The numerical models were linked, as visible in Figure 41, and applied to the given scenarios. COSMO-LEPS was developed at Arpae-SIMC on behalf of the COSMO consortium (Marsigli et al. 2001, Montani et al. 2011). In the construction of COSMO-LEPS, an algorithm selects a number of members, 16 in the operational configuration, (referred to as Representative Members, RMs) from the ECMWF global ensemble system (Marsigli et al., 2001; Molteni et al., 2001). Indeed, it consists of 16 integrations of the COSMO model running twice a day starting at 00:00 and 12:00 UTC, at 7 km of horizontal resolution and takes both initial and boundary conditions from the selected members of ECMWF ENS. Another deterministic integration is performed taking both initial and boundary conditions from ECMWF HRES, (the operational high resolution deterministic forecast of ECMWF) named COSMO-LEPS_Det.

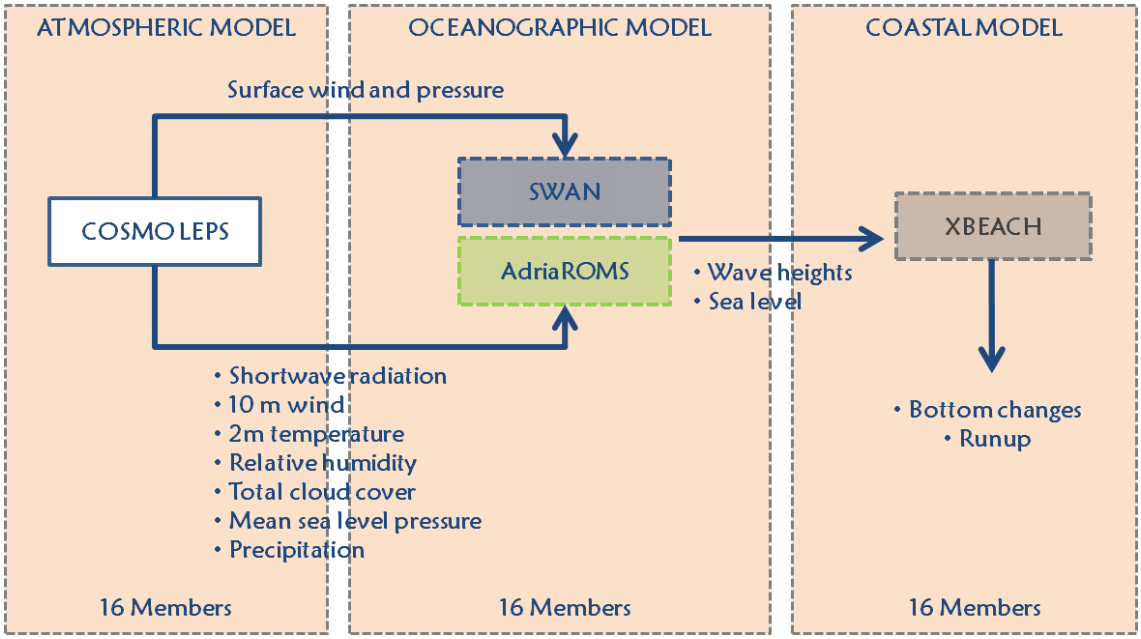

Figure 41 Integrated ensemble modelling framework.

Each of the members of the COSMO-LEPS system was used to provide the boundary conditions for the wave model SWAN and the oceanographic model implemented on the Adriatic Sea, AdriaROMS.

SWAN was run on the Italian domain, forced by the speed and direction of the 10 m wind obtained from the meteorological model. The wave model resolution is about 8 Km (1/12°) that is approximately equal to the meteorological model (7 Km horizontal resolution). This model produced

the boundary conditions for another higher resolution run, nested to focus over the Emilia-Romagna domain, which has a computational resolution of about 800 m. The wave conditions (significant wave height, mean direction, mean and peak period) forecasted by the model with a range of +72 hours, were extracted in correspondence of the edge of the transect profiles to generate the wave conditions to drive the coastal model.

Separately, the model AdriaROMS was run on the Adriatic domain, forced by astronomical tides derived from the OTIS database (Egbert and Erofeeva, 2002 TS3), by the oceanographic fields (salinity, temperature and currents) provided by the Mediterranean Ocean Forecast-ing system (MFS, Oddo et al., 2009) and by the fields COSMO (namely 10 m wind, mean sea level pressure, 2 m temperature, 2 m relative humidity, cloud cover, precipitation rate and short-wave solar radiation).

Finally, the outputs of these models, in particular wave and sea level conditions, were used to drive the coastal model XBeach, providing 16 different sea state conditions to force the model. XBeach was used to simulate the hydrodynamic and morphological conditions of the surf zone, along a single beach cross-section located in the study area of Cesenatico, described in Chapter 3. The XBeach model calibration, achieved with the sensitivity analysis of the model parameters (described in Chapter 4), was applied to the morphological model. Model calibration is performed to reduce at best the model uncertainties related to its possible different settings.

5.3.3 Storm cases

The analysis was applied to 2 storm events that occurred in the winter 2015-2016. A complete description of the storms is presented in Chapter 3. Due to the fact that the model forecast skill decreases over time the analysis covered a period of 4 days. The validation period of each storm is summarized in Table 26.

Table 26 Timing of the two storms analysis

Storm event	Start date	End date
20 November 2015 Storm	20-11-2015 00:00	24-11-2015 00:00
27 February 2016 Storm	27-02-2016 00:00	02-03-2016 00:00

5.3.4 Evaluation method

The analysis of the results is mainly based on comparing the model data with the observations. The computed wind fields were compared to the wind and to the mean sea level pressure by generating a wind map every 6 hours over the Italian domain. Further, the 10 m wind observations obtained by the land station of Cesenatico is considered in the analysis to validate the forecasts.

The comparison of the wave conditions were performed in correspondence of four measurements stations, marked in Figure 42 with a blue dot. In particular, the wave data were extracted at the Nausicaa Buoy location, 10 km from the Cesenatico coast and at three sea platforms named Garibaldi A., Angelina A. and Amelia A. It can be notice that the Garibaldi A. and the Amelia A. platforms are locate offshore while Angelina A. platform and the Nausicaa Buoy are placed near-shore.

Further, the sea level forecasts have been validated against the data obtained by the tidal gauges of Porto Garibaldi and Rimini. In Figure 42 the locations of the measurements stations for water levels is marked with yellow dots.

Finally, the morphological evolution of the beach profile was evaluated along 10 cross-sections located in the study area of Cesenatico, described in Chapter 3. Topo-bathymetrical surveys, along these sections, were performed before and after the storm events and are used as control data to validate the coastal model results.

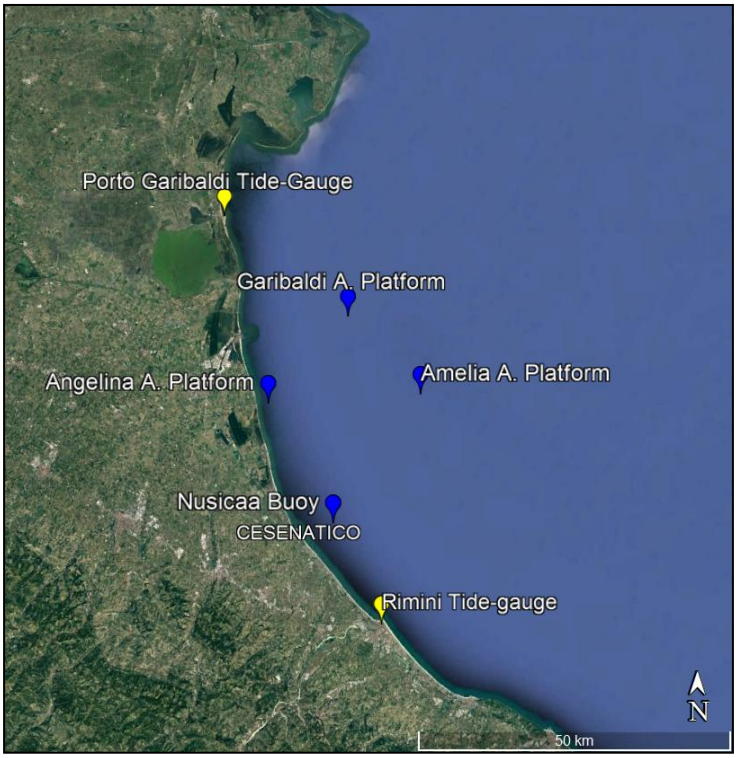

Figure 42 Location of the measurements stations of wave conditions and water levels, near the Cesenatico study site. The wave measurements stations, marked with blue dots, consist of the Nausicaa buoy and three sea platforms named Angelina A., Garibaldi A. and Amelia A. The Porto Garibaldi and Rimini tide gauges are marked with yellow dots.

The traditional deterministic forecast produces a single estimate of how each output will evolve as a function of time while the ensemble modeling approach produces not one but several forecasts. Each forecast uses slightly different initial conditions, boundary conditions and/or model physics, with the aim of sampling the range of forecast results consistent with the uncertainty in observations and in the modeling system itself. The availability of the probabilistic forecasts of the ensemble adds another dimension to the information available, offering the possibility to give useful indications of the forecasts uncertainty. By the ensemble outputs fields it is possible to define some statistical indicators as the mean and the spread of the ensemble members. The first is a simple mean of the parameter value between all ensemble members while the spread is calculated as the (non-biased) standard deviation of a model output variable, and provides a measure of the level of uncertainty in a parameter in the forecast. These statistical indicators can be linked to the forecast error, providing useful information of the forecasts reliability and accuracy. The range of different solutions in the forecast allows us to assess the uncertainty in the forecast, and how confident we should be in a deterministic forecast.

In the following sections the results of the individual models are discussed in more detail. The analysis of each storm events was organized as follows. First, the results of the deterministic chain were compared with the observations and then, the ensemble forecasts were evaluated. The propagation of the uncertainties through the model cascade is also discussed.

5.4 **The storm of 20 November 2015**

5.4.1 Deterministic forecasts

In this subsection, the verification of the deterministic run over a period of four days, from 20 to 24 November 2015, is presented.

First, the results from the meteorological model COSMO-I7 are compared with the ECMWF analysis, which has considered the most accurate representation of the atmospheric state. Maps of surface wind speed and mean sea-level pressure were generated every 6 hours to investigate the evolution of the weather conditions. In Figure 43 the most significant maps are presented while, for completeness, in APPENDIX B it can be found the 6 hours maps for the whole verification period.

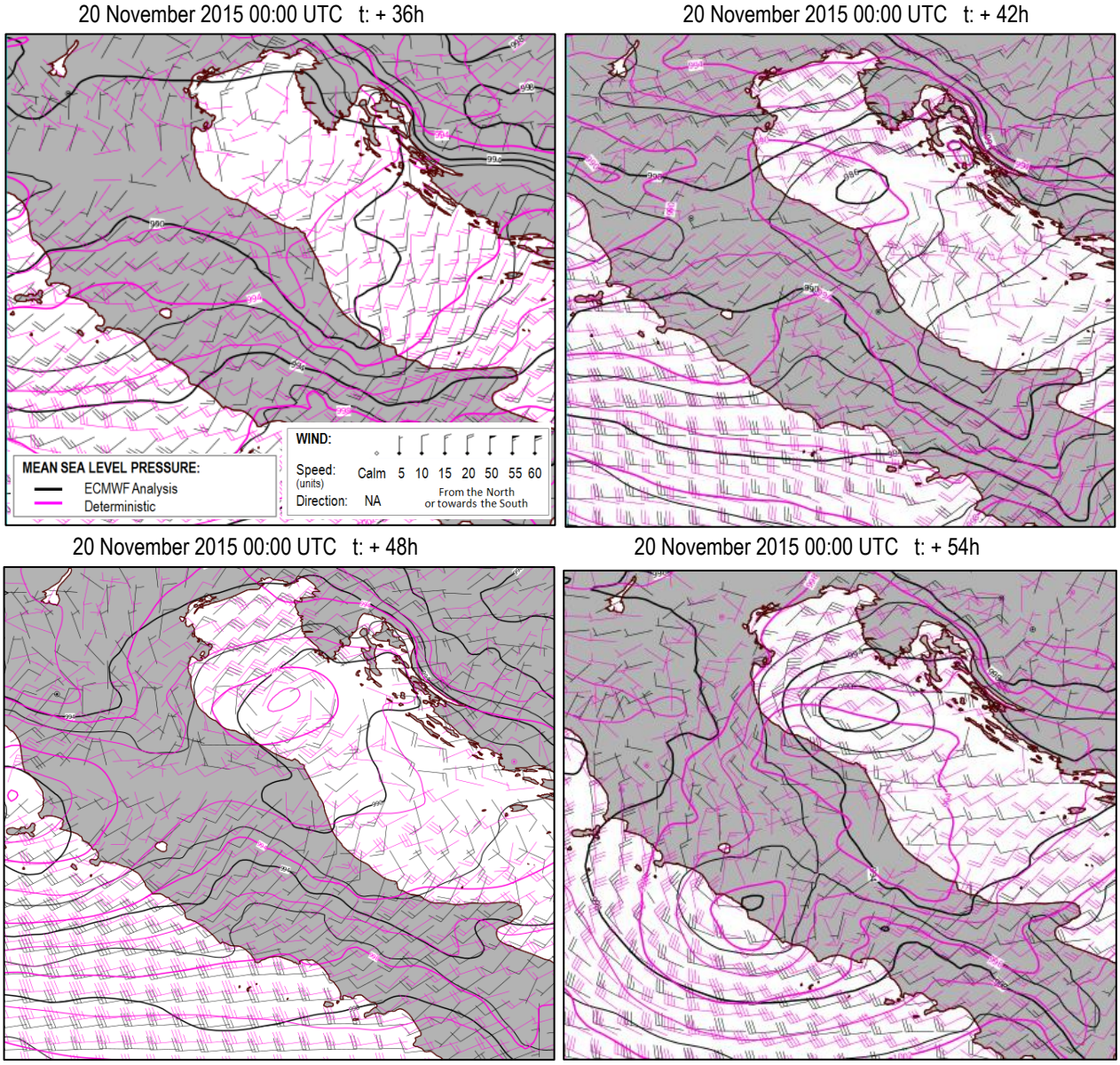

Figure 43 Mean sea level pressure and 10 m wind forecasts of 20-11-2015 at +36 h (upper left), +42h (upper rigth), +48 h (lower left) and +54 h (lower right). Comparison of the ECMWF analysis (black) and the deterministic run of COSMO-I7 (magenta).

The forecasts present a temporal delay in generating the minimum of mean sea level pressure in the northern Adriatic Sea, causing a temporal shift of the winds rotation.

Moreover, observed and predicted wave heights at different locations are compared. The location of the measurements stations is represented in Figure 42 of Section 5.3.4. Figure 44 shows the computed and observed wave heights at the four measurements sites. At the near-shore stations (Nausicaa Buoy and Angelina A. platforms) the wave heights are computed reasonably well, except for the peak of the storm where the computed variables are slightly smaller than the measurements.

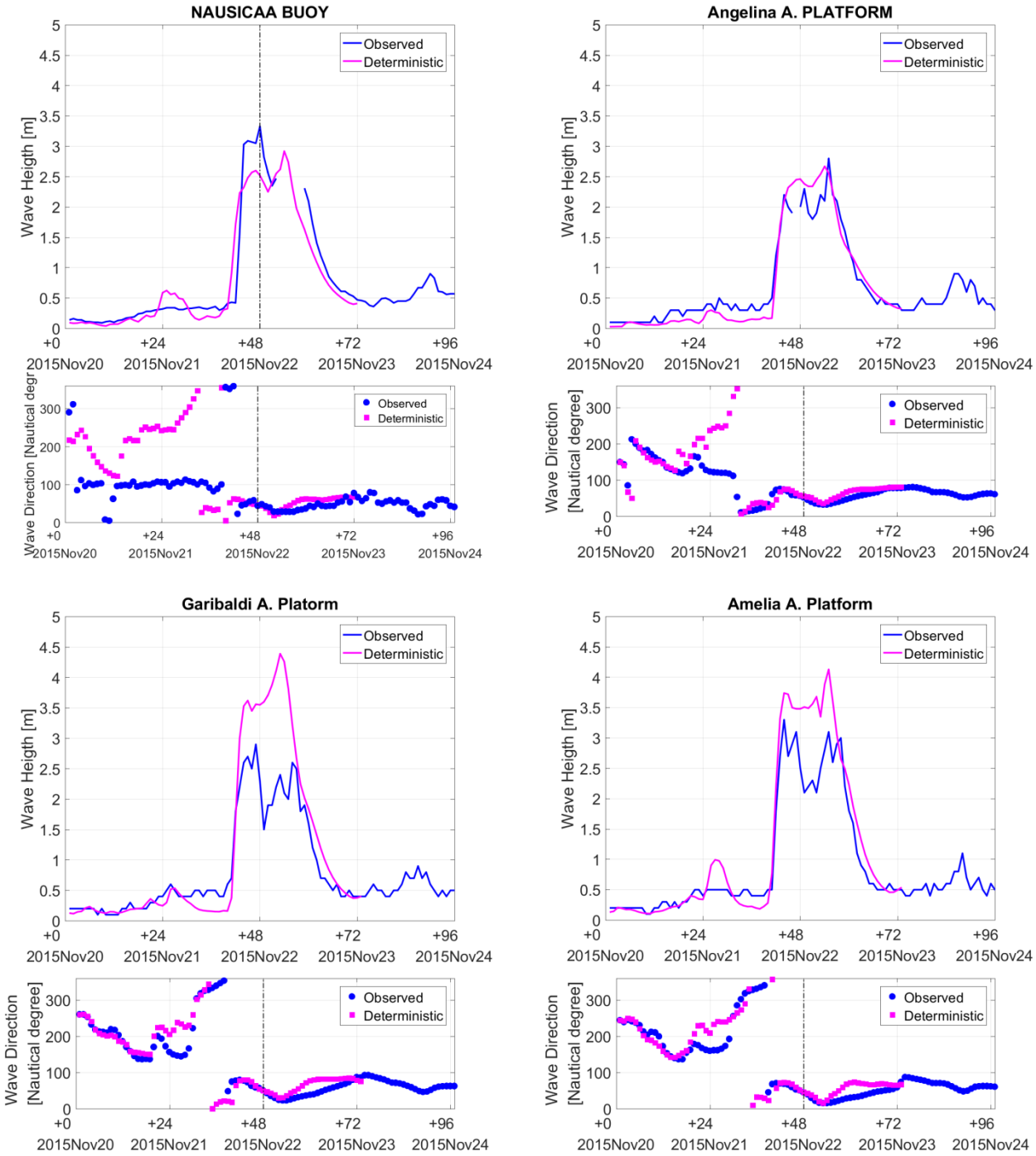

Figure 44 Comparison of computed wave heights (upper panel) and wave directions (lower panel) from the deterministic model SWAN (magenta line) with the measurements (blue) at four measurements stations indicated in Figure 42.

The data comparison at the offshore Garibaldi A. and Amelia A. platforms shows the opposite trend of overestimation of the peak of the storm (lower panels of Figure 44). The near-shore stations are probably influenced by the southwest-northeast oriented winds in correspondence of the local site of Cesenatico that were generated in advance. Globally, at all the measurements stations, the wave data are predicted with a good timing. The wave directions are predicted reasonably well at the off-shore stations while there is a discrepancy with the observations at Nausicaa buoy and at Angelina A. platform.

The 10 m wind speed and direction at the land station of Cesenatico, reported in Figure 45, show a good deterministic prediction, despite a fake peak after 24 hours from the start of the simulation. In addition, the wind direction is better predicted for more intense wind speeds.

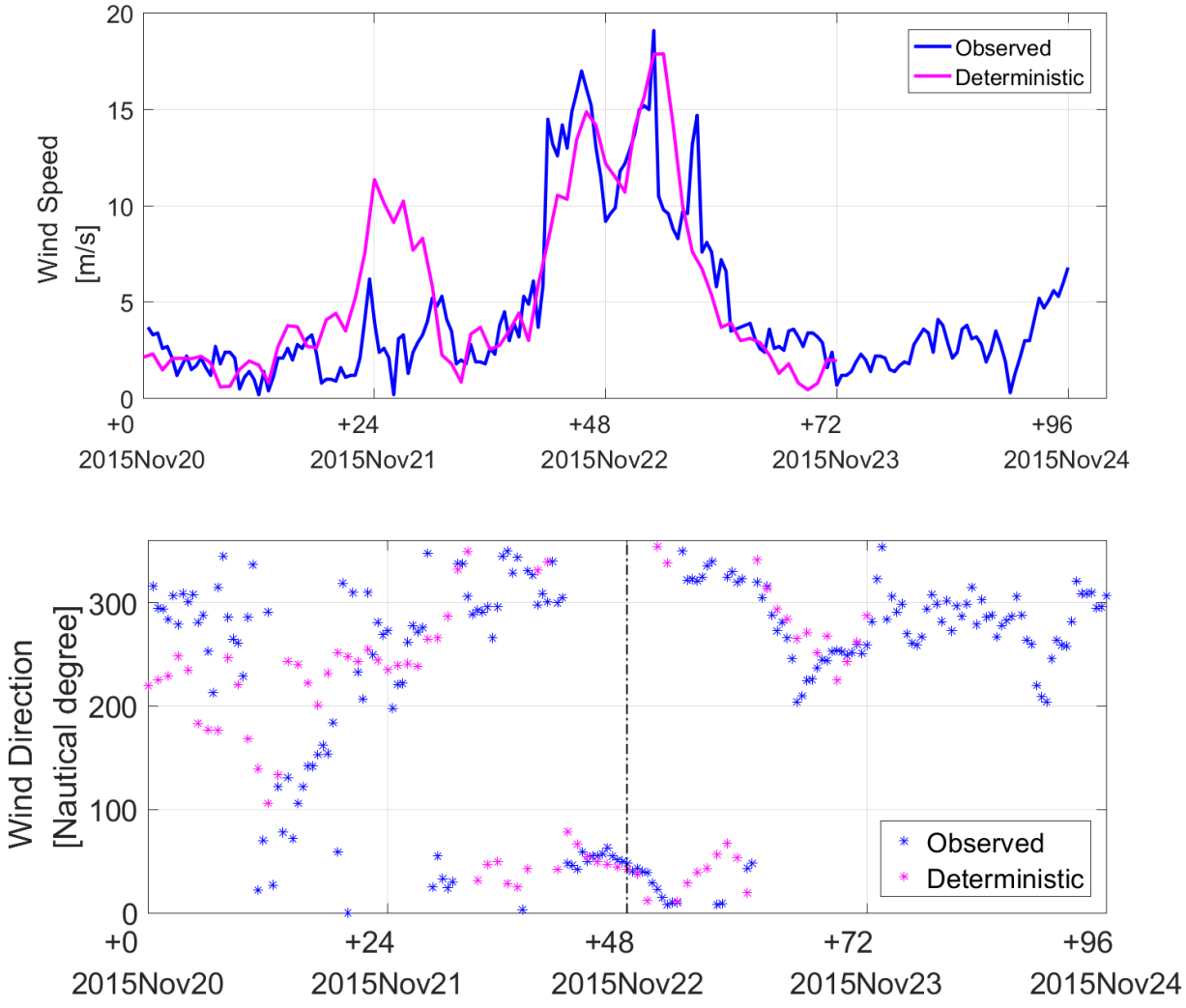

Figure 45 Comparison of 10 m wind speed (upper panel) and direction (lower panel) at the station of Cesenatico, relative to 20 November 2015. The deterministic forecasts of COSMO I-7 (magenta) are compared to the observations (blue).

Further, the model results of water levels were verified against the measurements obtained from the tide gauges of Porto Garibaldi and Rimini, located near the study area (reference in Chapter 3). Despite a slight underestimation Figure 46 indicates a good agreement between the model forecasts and the observations.

The final analysis focused on the coastal model results. The morphological behavior of the beach profile was compared to the observations obtained by the topo-bathymetrical reliefs carried out before and after the storm. A detailed description of the beach surveys is reported in Chapter 3. The lower panel of Figure 48 presents the bed level variations of the cross-shore beach profile displayed in the upper figure. Forecasted morphological variations are in good agreement with the observations.

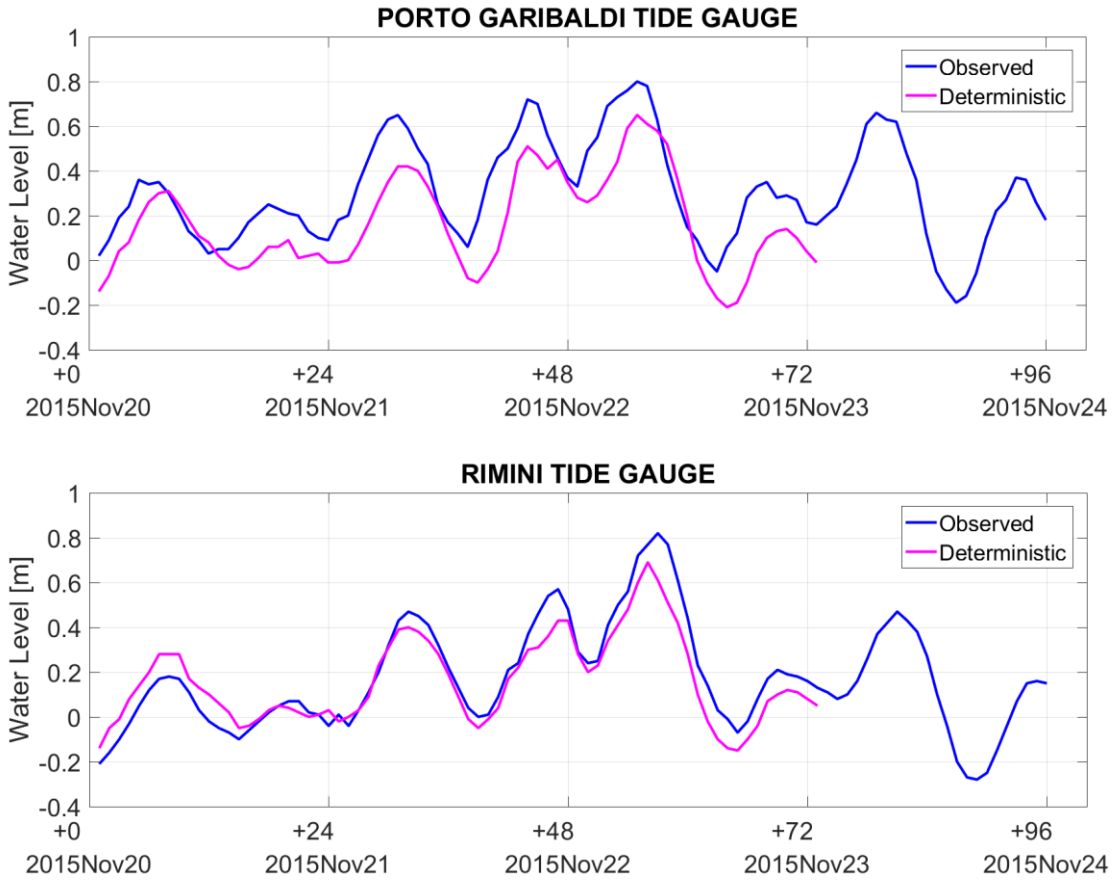

Figure 46 Comparison of water levels at tide gauges of Porto Garibaldi (upper panel) and Rimini (lower panel) related to 20 November 2015. The deterministic forecasts of Adria-ROMS (magenta) are compared with the observations (blue).

The eroded volumes evaluated for the beach profile above mean sea level, reported in Table 27, illustrate that globally XBeach is capable of reproducing the morphological response of the system in accurate way.

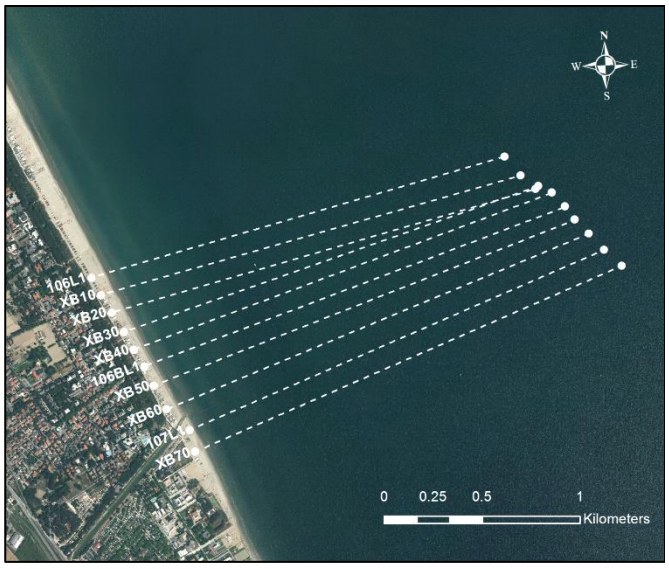

Figure 47 Location of the ten beach cross-sections at Cesenatico study site.

Beach profile name	Observed V_{ero} $[m^3 \cdot m^{-1}]$	Deterministic Forecast V_{ero} $[m^3 \cdot m^{-1}]$
106L1	3.59	3.77
XB10	3.32	4.00
XB20	3.9	2.98
XB30	2.76	2.99
XB40	3.42	2.97
106BL1	5.85	2.78
XB50	2.73	2.92
XB60	3.25	1.93
XB70	2.42	3.15
107L1	3.93	2.18

Table 27 Comparison of computed and observed eroded volumes above the mean sea level for the ten beach profiles showed in Figure 47.

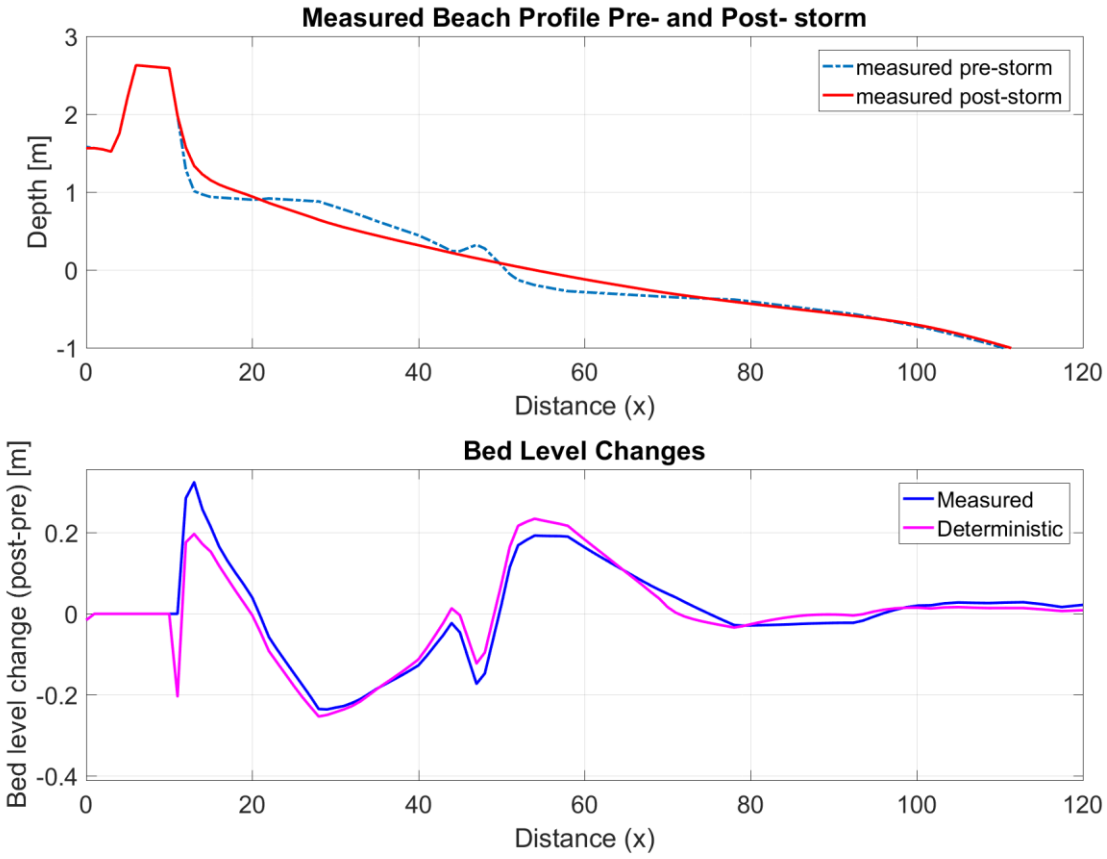

Figure 48 Morphological behavior of a single cross-section. The upper panel shows the pre- and post- storm measured beach profile. The lower panel presents the comparison of the deterministic forecasts of bed level changes, computed by XBeach model (magenta), and the observations (blue)

5.4.2 Ensemble modeling results

In this subsection, the verification of the ensemble modeling results for the period from 20 to 24 November 2015 is presented.

The wind and mean sea level pressure forecasts obtained from the deterministic run of the ensemble model COSMO LEPS are compared with the ECMWF analysis, as visible in Figure 49. Despite the fact that the weather conditions are globally well predicted a geographic displacement of the low-pressure system is visible resulting in a marked shift in the wind direction in the domain around the Cesenatico study site.

COSMO-LEPS predicts the minimum of the pressure moved to the north, providing a local wind recirculation on the Emilia-Romagna coasts with impact on the wave and tide models. Figure 50 shows the wave heights comparison at the near-shore stations located in correspondence of Nausicaa buoy and Angelina A. platform and the off-shore stations of Garibaldi A. and Amelia A. platforms.

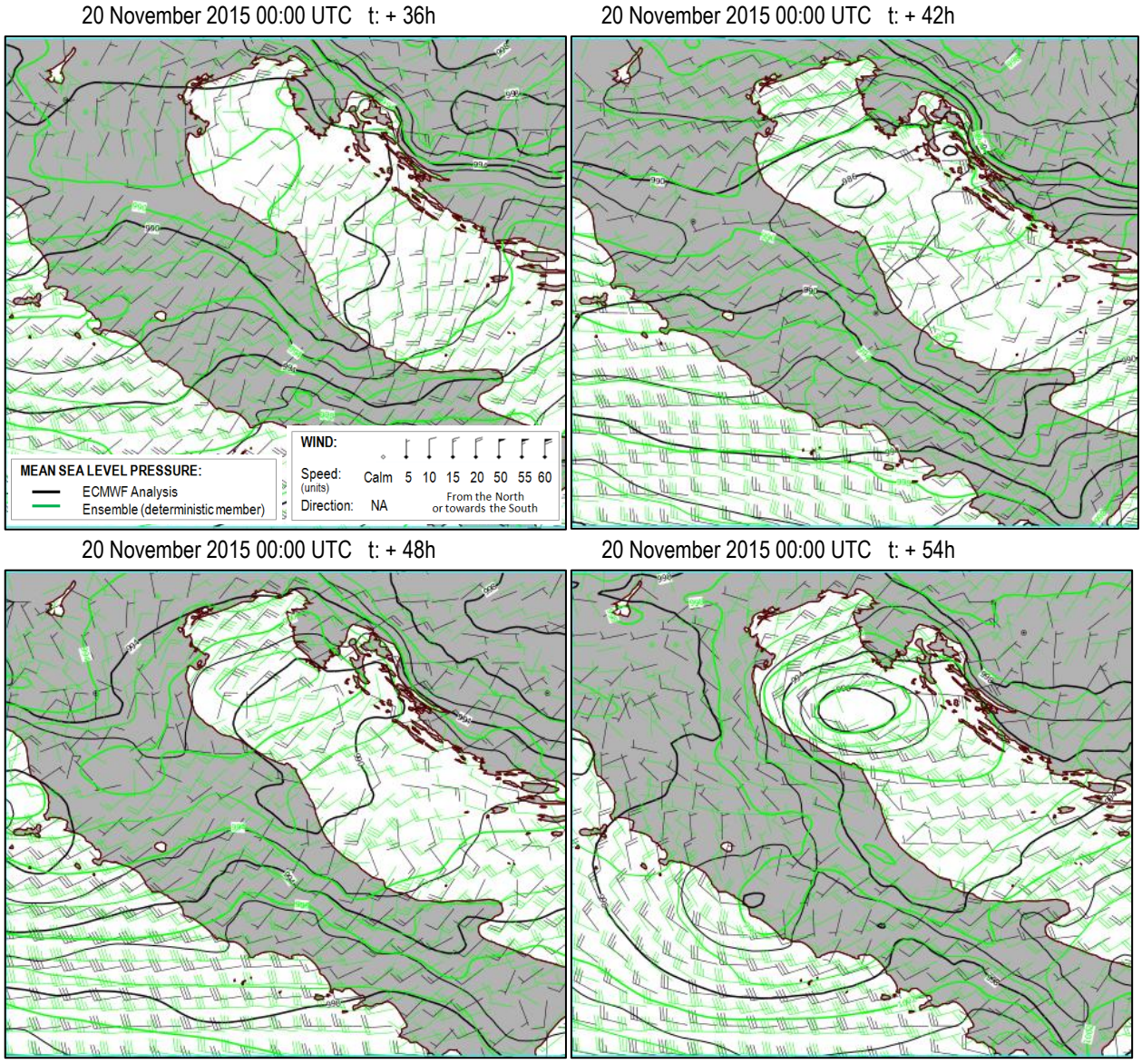

Figure 49 Mean sea level pressure and 10 m wind forecasts of 20-11-2015 at +36 h (upper left), +42h (upper rigth), +48 h (lower left) and +54 h (lower right). Comparison of the ECMWF analysis (black) and the deterministic run of COSMO-LEPS (green).

The location of the stations is indicated by Figure 42. The wave data comparison at the near-shore stations indicates that the wave heights are affected by the wrong local wind prediction. For these stations, the underestimation of the peak by the ensemble mean wave heights, represented with a dashed red line in the graphs, is evident.

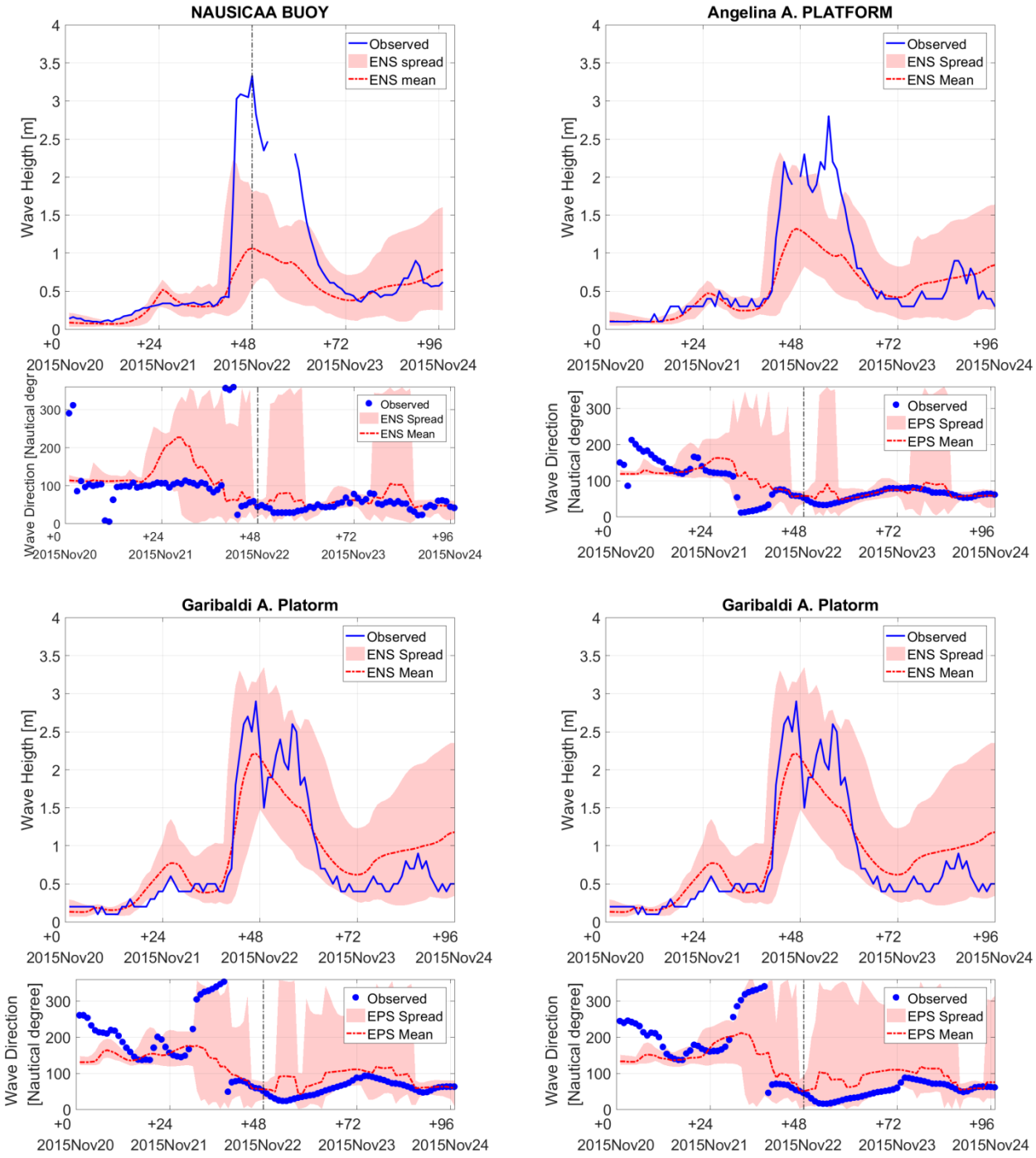

Figure 50 Comparison of computed wave heights (upper panel) and wave directions (lower panel) from the SWAN model (forced with the ensemble members of COSMO-LEPS) with the measurements (blue) at the four measurements stations indicated in Figure 42. The ensemble mean are presented with a dashed red line while the ensemble spread with a light red filled area.

At the offshore stations (Garibaldi A. and Amelia A.) the ensemble mean more accurately aligns with the observations. It's important to note that the ensemble modeling provides an indication of the forecast uncertainty by means the ensemble spread. The comparison with the measurements indicates

a good correspondence between the ensemble spread increase and the lower reliability of the forecast. At Garibaldi A. and Amelia A. platform, the ensemble spread is able to include the correct solution (observations) and the mean of the ensemble can be considered as good predictor of the wave height.

The wind direction and speed were also extracted at the land station of Cesenatico and are displayed in Figure 51. The wind speeds are averaged at each hour for the 16 ensemble members and are represented with a dashed red line in the upper panel. The ensemble mean forecast of the wind speed is below the observed data at the peak of intensity while exhibiting a very large growth in ensemble divergence (Figure 51, upper panel).The large divergence in the ensemble of the wave direction reflects a very unpredictable situation.

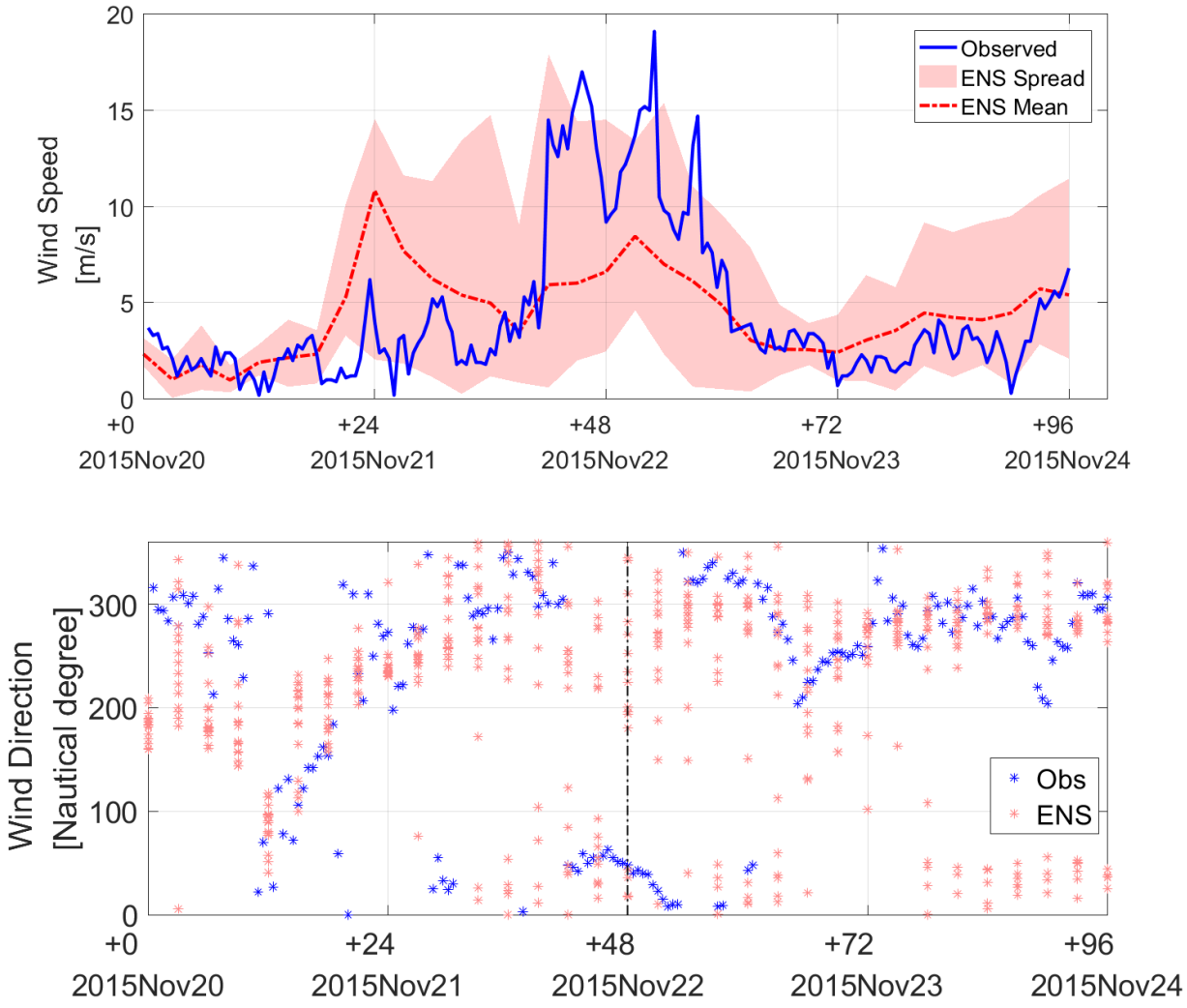

Figure 51 Comparison of 10 m wind speed (upper panel) and direction (lower panel) at the station of Cesenatico, relative to 20 November 2015. The ensemble members of COSMO LEPS, represented with their mean (red dashed line) and spread (light red area), are compared to the observations (blue).

For storm surge forecasting, the uncertainty in meteorological forcing is expected to dominate over uncertainties in the surge model formulation and initial state. The comparison graphs at the measurements station of Porto Garibaldi and Rimini show that, despite a general underestimation, the tidal trend is well predicted by the ensemble model. Moreover, the ensemble members are more diffused around the mean in correspondence of the peak of the event, indicating that the model is less able to accurately forecast the surge component.

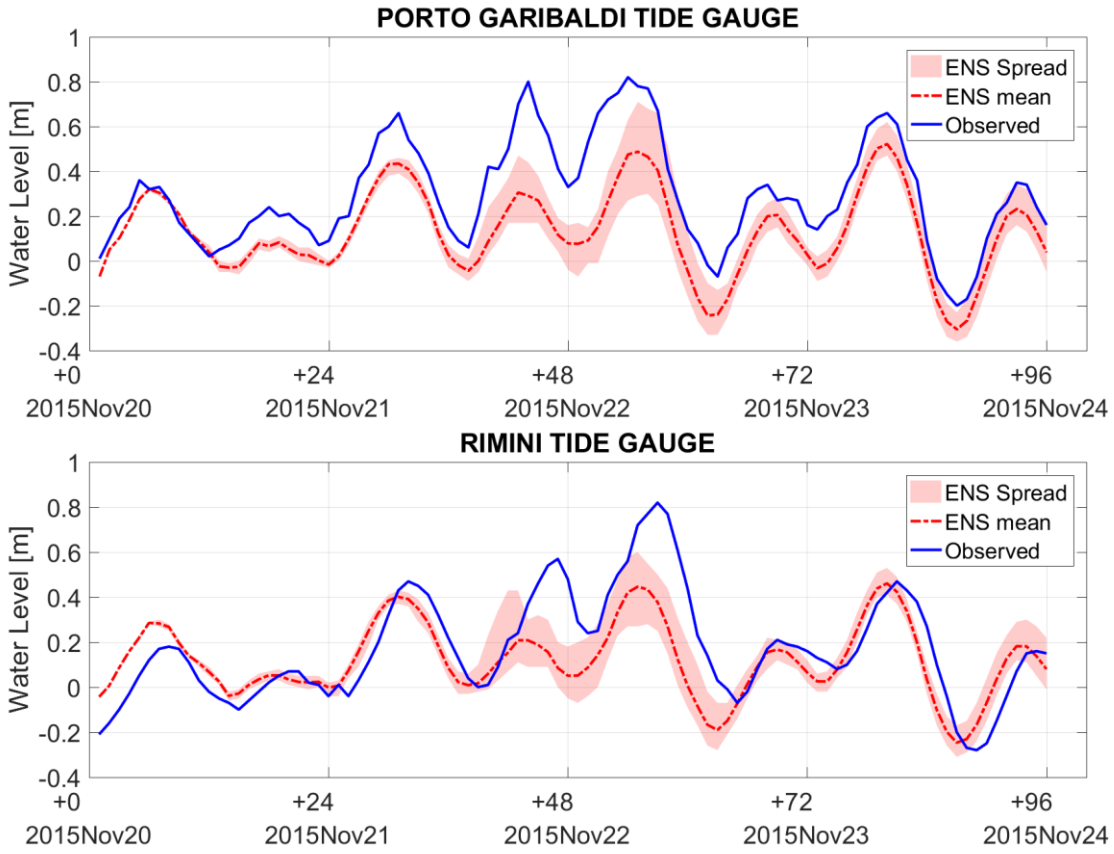

Figure 52 Comparison of water levels at tide gauges of Porto Garibaldi (upper panel) and Rimini (lower panel) related to 20 November 2015. The ensemble forecasts of AdriaROMS (light red) are compared with the observations (blue). The ensemble mean are represented by a dashed red line.

At the end, the outputs of the ensemble members of wave conditions and water elevations from the wave and oceanographic models (SWAN and AdriaROMS) are used to drive the coastal model XBeach. As expected, the underestimation of the oceanographic variables provides lower value of erosion rather than the observations.

Table 28 summarized the results of the eroded volumes above the mean sea level for ten beach cross-sections (Figure 53) at the study site of Cesenatico. The measured pre- and post- storm bed levels allow to have an instantaneous value of erosion for each cross-section, to validate the model performance. The morphological model XBeach was used to generate 16 different possible scenarios of final beach profiles.

As visible by Table 28, the ensemble mean of eroded volumes above mean sea level is not in good agreement with the observation, showing the effects of the under-prediction of the wave heights. The large spread in wave heights doesn't results in large deviation of the bed level ensemble members. Indeed, despite the larger deviation around the mean, the ensemble members present low energetic wave heights, which are not able to generate considerable erosion of the beach.

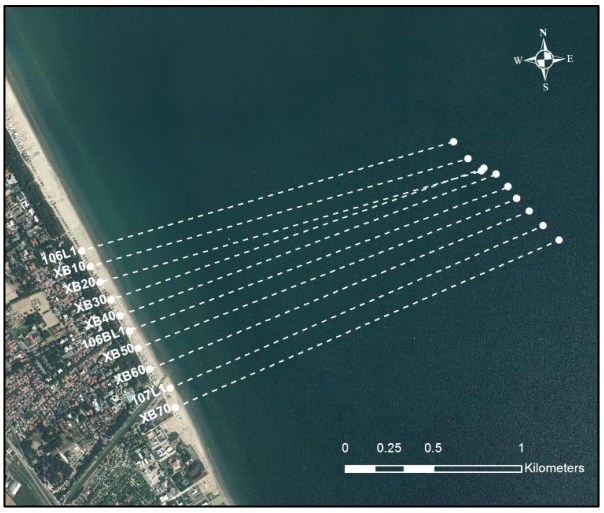

Figure 53 Location of the ten beach cross-sections at Cesenatico study site.

Beach profile name	Obs.	Det.	Ensemble forecasts		
	V_{ero} [$m^3 \cdot m^{-1}$]	V_{ero} [$m^3 m^{-1}$]	Min. V_{ero} [$m^3 m^{-1}$]	Mean V_{ero} [$m^3 \cdot m^{-1}$]	Max. V_{ero} [$m^3 \cdot m^{-1}$]
106L1	3.59	3.77	0.71	0.99	1.38
XB10	3.32	4.00	0.89	1.21	1.59
XB20	3.9	2.98	0.47	0.78	1.19
XB30	2.76	2.99	0.75	1.04	1.39
XB40	3.42	2.97	0.42	0.67	1.02
106BL1	5.85	2.78	0.85	1.19	1.58
XB50	2.73	2.92	0.22	0.4	0.77
XB60	3.25	1.93	0.53	0.79	1.15
XB70	2.42	3.15	0.35	0.63	1.09
107L1	3.93	2.18	0.62	0.87	1.18

Table 28 Comparison of computed and observed eroded volumes above the mean sea level for the ten beach profiles showed in Figure 53 . For the ensemble values the max and min of the EPS members are expressed with the average.

The lower panel of Figure 54 shows the bed level changes of a single cross-shore beach profile while the upper panel presents the beach profiles measured before and after the storm. The ensemble mean value (dashed red line) is substantially smaller than that observed. Moreover, the ensemble spread is not able to include the real solution but its increase indicates that the swash zone is the less predictable zone.

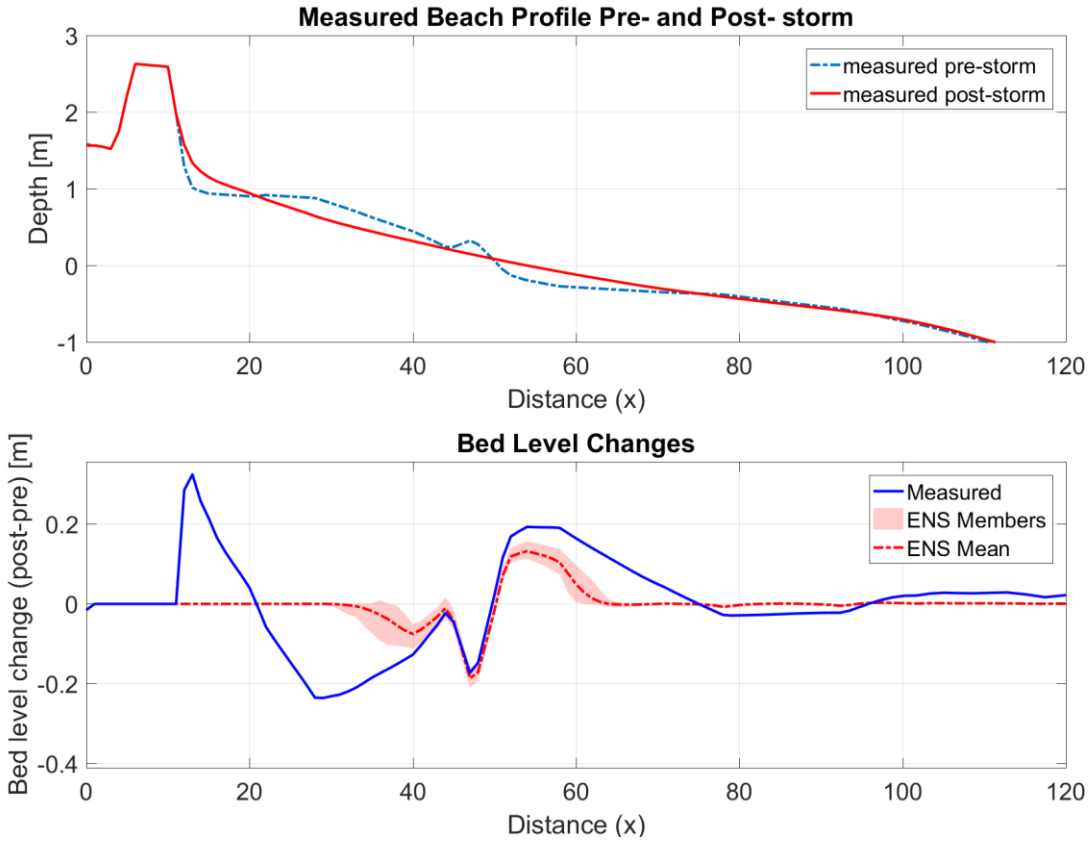

Figure 54 Morphological behavior of a single cross-section. The upper panel shows the pre- and post- storm measured beach profile. The lower panel presents the comparison of the ensemble forecasts of bed level changes, computed by XBeach, and the observations (blue). The ensemble mean are presented with a dashed red line while ensemble spread with a light red filled area.

5.5 The storm of 27 February 2016

A second storm event was investigated by means the ensemble approach. In the next subsections, the results of the deterministic and the ensemble runs, over the period from 27 February to 02 March 2016, are compared with the measurements.

5.5.1 Deterministic forecasts

The deterministic forecasts of COSMO-I7 are in good agreement with the ECMWF analysis. However, the wind and mean sea level pressure maps (Figure 55) indicates that COSMO-I7 predicts the minimum of the pressure over the Po valley in advance. In this way, locally it results in uncorrected wind directions over the Emilia Romagna coasts. Figure 55 presents the main significant wind maps that comparing the deterministic results (magenta) with the ECMWF analysis (black). The maps show the wind forecast on 27 February 2016, 36-, 42-, 48- and 54-hours ahead of the event.

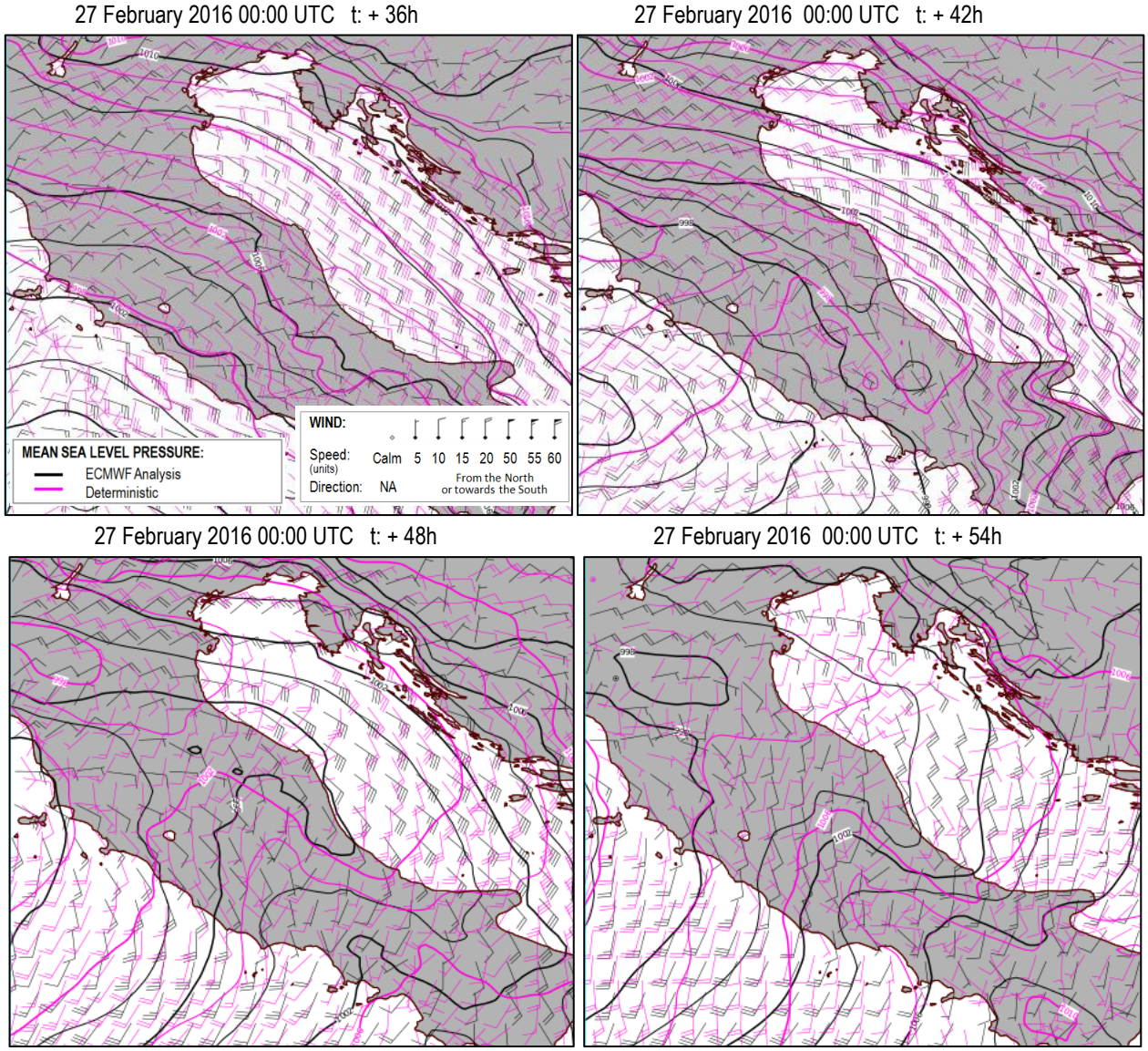

Figure 55 Mean sea level pressure and 10 m wind forecasts of 27-02-2016 at +36hours (upper left panel), + 42 hours (upper right panel), +48 hours (lower left panel) and +54 hours (lower right panel). Comparison of the ECMWF analysis (black) and the deterministic run of COSMO-I7 (magenta).

The comparison of deterministic forecasts (magenta) with the wind observations (blue) at the land station of Cesenatico is presented in Figure 56. The maximum of the wind speed is predicted in advance by the model while the graph of the wind directions shows a divergence of about 80 degrees until +48 hours. This result clearly reflects the same situation of the wind maps (Figure 55).

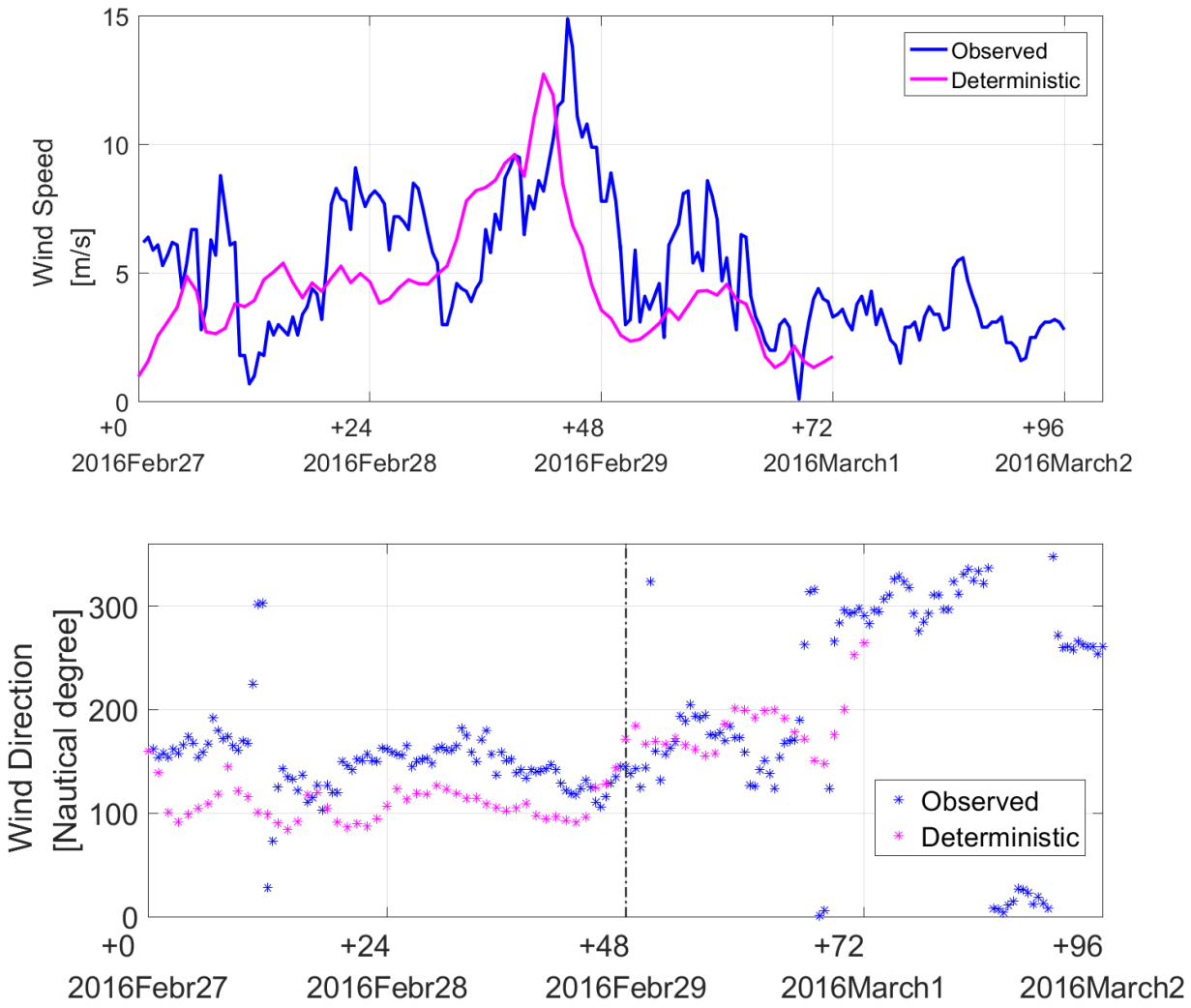

Figure 56 Comparison of 10 m wind speed (upper panel) and direction (lower panel) at the station of Cesenatico, relative to 27 February 2016. The deterministic forecasts of COSMO I-7 (magenta) are compared to the observations (blue).

Figure 57 illustrates the temporal variation of the predicted and observed wave heights and directions at selected locations which are indicated in Figure 42. The comparisons show a good agreement for waves at the near-shore measurement stations of Nausicaa Buoy and Angelina A. platforms but with an over-prediction during the storm peak. The wave height forecasts reach the storm peak in advance and decay more rapidly than the observations. This may simply reflect the model errors in wind predictions.

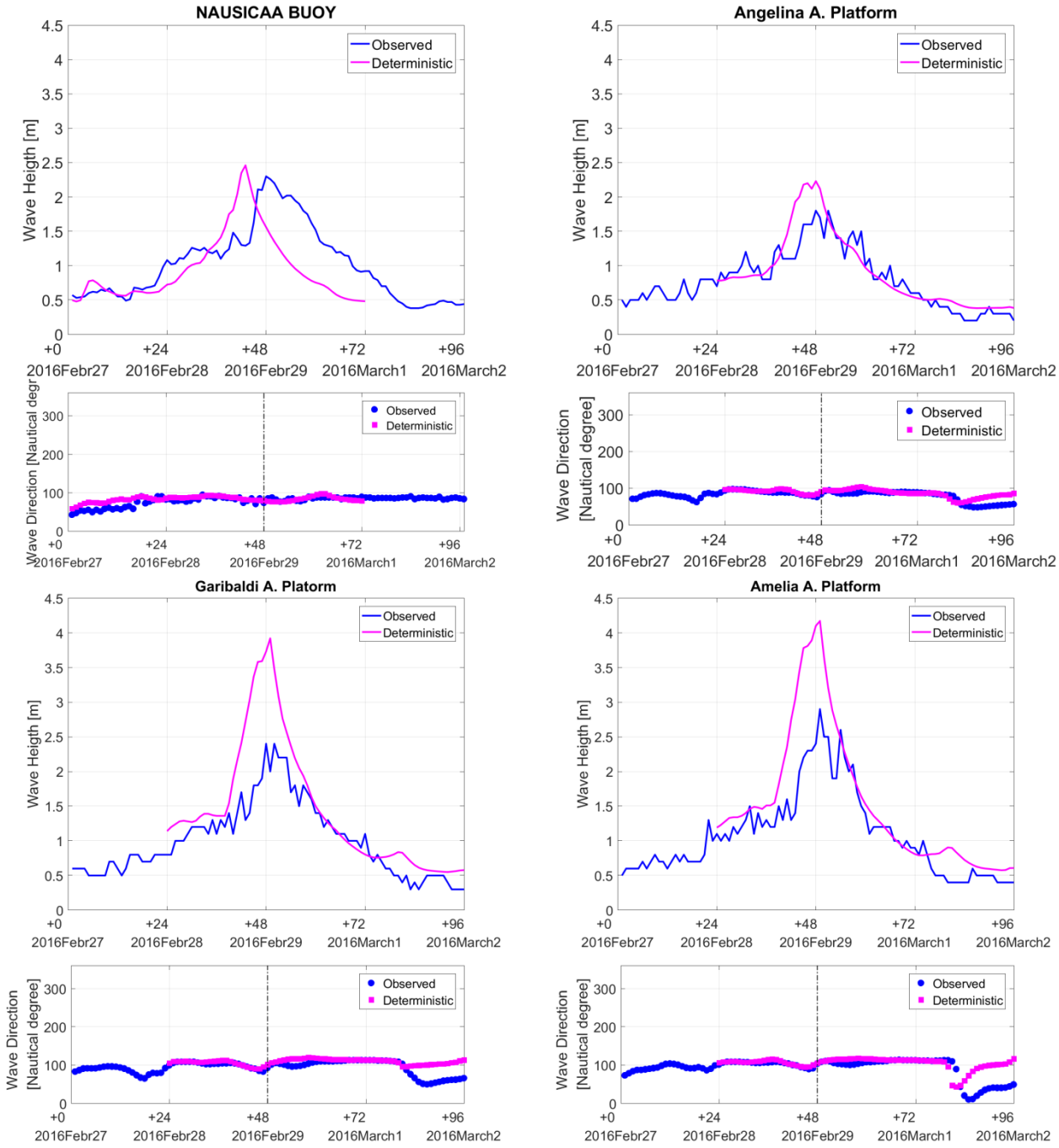

Figure 57 Comparison of computed wave heights (upper panel) and wave directions (lower panel) from the deterministic model SWAN (magenta line) with the measurements (blue) at four measurements stations indicated in Figure 42.

At the offshore measurements stations of Garibaldi A. and Amelia A., the COSMO-I7 model predicts higher wave peak and more rapid wave reduction with respect to the observations (Figure 57). For both the offshore platforms, the model provides a wave peak about twice of the observed. The accuracy of the wave results is largely dependent on the quality of wind data and hence the rapid dissipation of the wave energy, visible for all stations, can be correlated to the seaward winds predicted by the model during the storm peak.

Figure 58 shows the computed water levels at Porto Garibaldi and Rimini tide gauges, which are indicated in Figure 42, and clearly indicating that the model results don't fit with the observations. For

both the measurement stations, up to +42 forecasts, it is evident that the model fails to capture the tidal signal, showing the uncertainties in the oceanographic model. During the period of this thesis work, the oceanographic model AdriaROMS was forced by only 5 tidal components that probably were not sufficient to accurately represent the tide. To avoid this problem, the performance of the model was improved increasing the number of the tidal components from 5 to 8. The results presented in this thesis are performed with the old configuration of the model. Moreover, given the predominant role of the surge component on tide, it is difficult to separate the error in the meteorological data from the genuine surge although the signal in advance reflects the meteorological uncertainty.

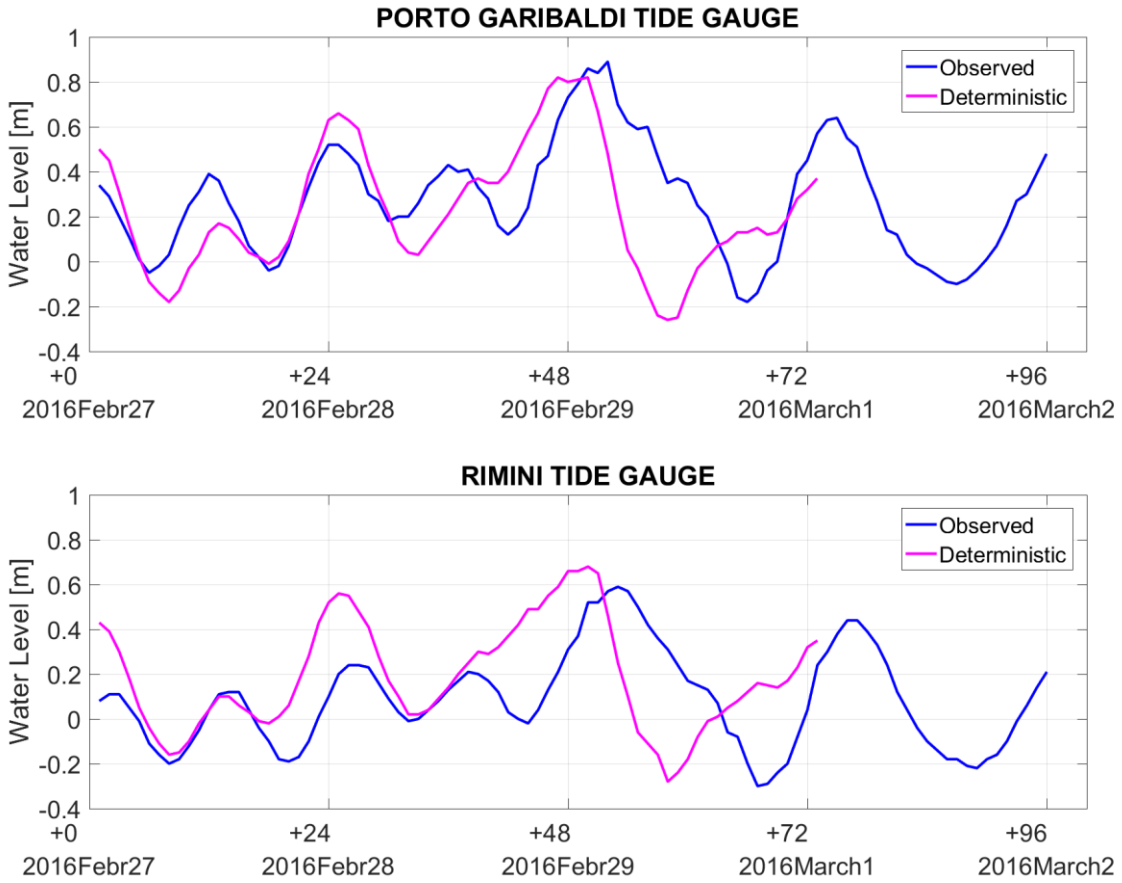

Figure 58 Comparison of water levels at tide gauges of Porto Garibaldi (upper panel) and Rimini (lower panel) related to 27 February 2015. The deterministic forecasts of AdriaROMS (magenta) are compared with the observations (blue).

The morphological variations of the beach profiles, predicted by the coastal model XBeach, were compared to the measured variation of the post-storm beach profile from the pre-storm profile. For most beach profiles, the model tends to underestimate the eroded volumes above the mean sea level, as reported in Table 29, where the deterministic forecast of erosion are compared with the observations. However, the order of magnitude of the results is acceptable. The comparison the bed level changes of a single cross-section (106BL1 profile), as can be seen in the lower panel Figure 60, shows the underestimation of the minimum and maximum of bed level variations and the tendency of the model to shift the erosion towards the upper beach profile.

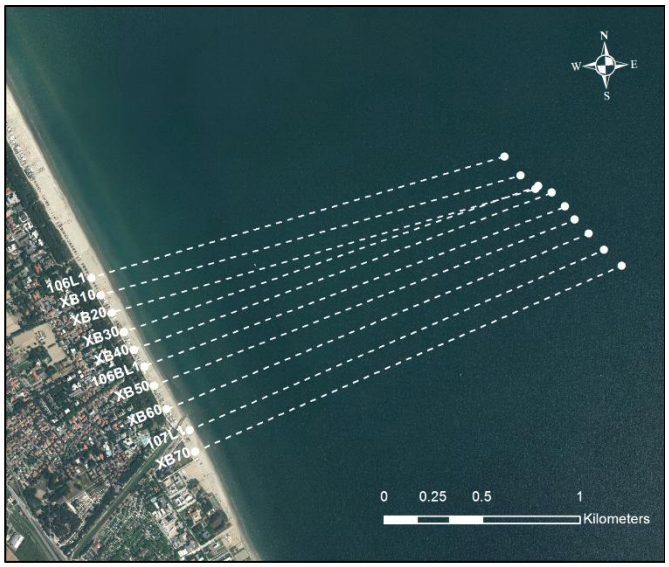

Figure 59 Location of the ten beach cross-sections at Cesenatico study site.

Beach profile name	Observed V_{ero} $[m^3 \cdot m^{-1}]$	Deterministic Forecast V_{ero} $[m^3 \cdot m^{-1}]$
106L1	1.02	1.83
XB10	3.37	1.53
XB20	1.21	1.51
XB30	1.63	1.10
XB40	1.31	1.16
106BL1	1.67	0.91
XB50	1.66	0.64
XB60	1.84	0.15
XB70	0.59	0.82
107L1	-5.03	1.27

Table 29 Comparison of computed and observed eroded volumes above the mean sea level for the ten beach profiles showed in Figure 59.

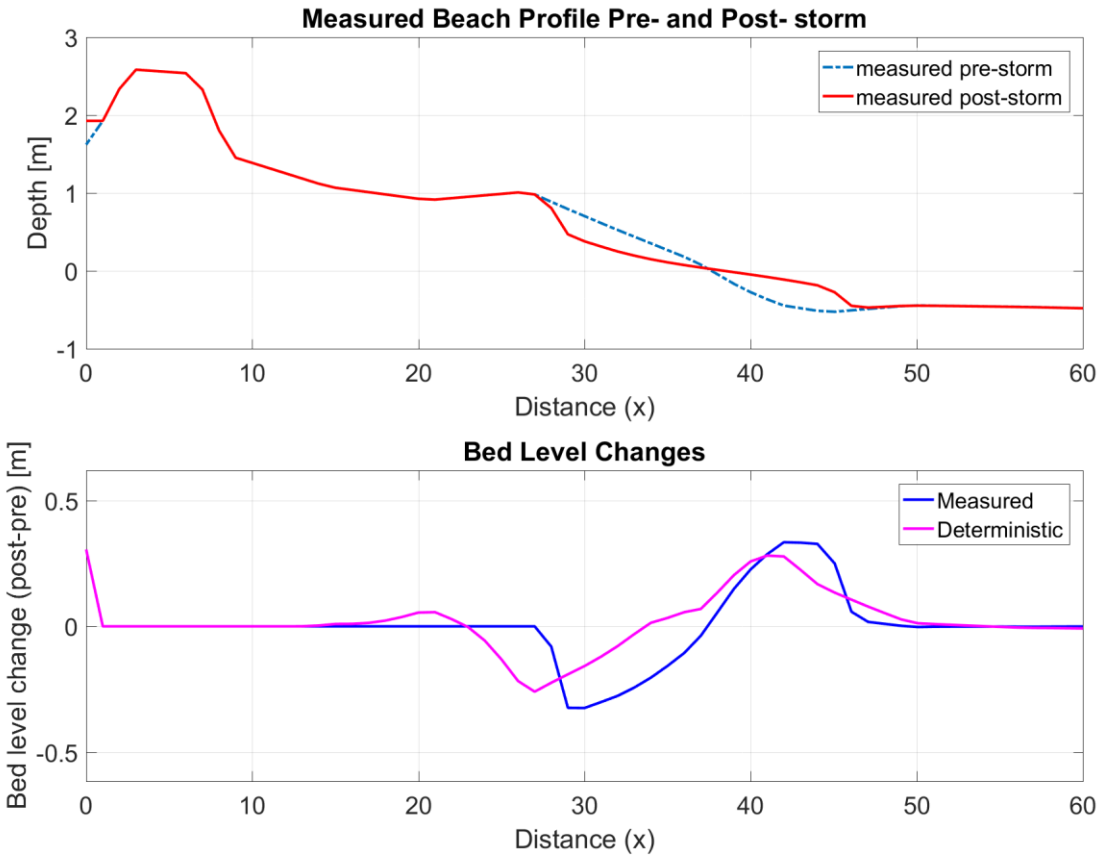

Figure 60 Morphological behavior of a single cross-section. The upper panel shows the pre- and post- storm measured beach profile. The lower panel presents the comparison of the deterministic forecasts of bed level changes, computed by the XBeach model (magenta) and the observations (blue).

5.5.2 Ensemble modeling results

The ensemble forecasts of wind and mean sea level pressure over the period from 27 February and 02 March 2016, on the Adriatic domain, are presented in Figure 61. Due to graphic limitation, the deterministic run of the ensemble model COSMO-LEPS (green line) is compared with the ECMWF analysis (black line). In the Northern Adriatic Sea, the forecasted wind fields fit the ECMWF analysis except during the wave storm, where the baric fields are different. Especially during the more intense wind forcing at +48 forecasts, a marked shift in the wind direction is visible in the limited domain considered here.

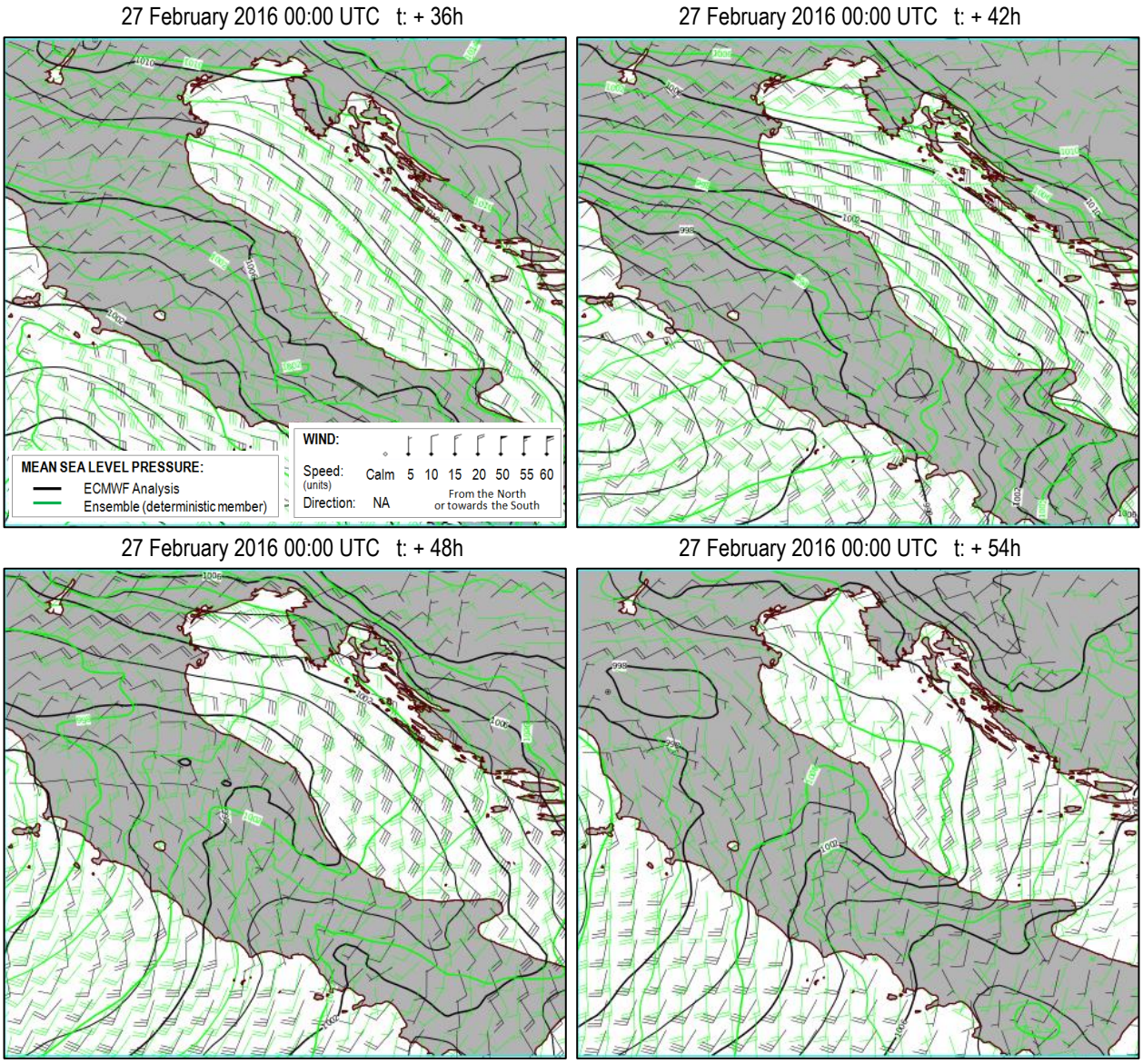

Figure 61 Mean sea level pressure and 10 m wind forecasts of 27-02-2016 at +36 h (upper left), +42h (upper rigth), +48 h (lower left) and +54 h (lower right). Comparison of the ECMWF analysis (black) and the deterministic run of COSMO-LEPS (green).

At the measurement station of Cesenatico the ensemble members of wind direction (light red) are at first slightly deviated by the observations (blue) while from T + 48 hours predictions, the observations fall within the range of the ensemble. The upper graph shows that the ensemble mean of the wind

speeds is in good agreement with the observation. In addition, the spread of the ensemble members is able to include the real solution.

The effects of the wind uncertainty are evident in the ensemble wave forecasts that are directly influenced by the wind field forecast. Figure 63 shows the temporal variation of the predicted wave heights and directions at the selected locations which are indicated in Figure 42. For all the measurements stations, the average values from the 16 ensemble members, denoted as 'Ensemble Mean', show that the storm peak is anticipated with a more rapid decrease of the wave intensity. This can be attributed to the wind forcing rotation. Especially at the offshore platforms, Garibaldi A. and Amelia A., the peak of the ensemble mean is higher than the observations. The ensemble forecast exhibit a very small variations in ensemble divergence for all the wave measurement stations.

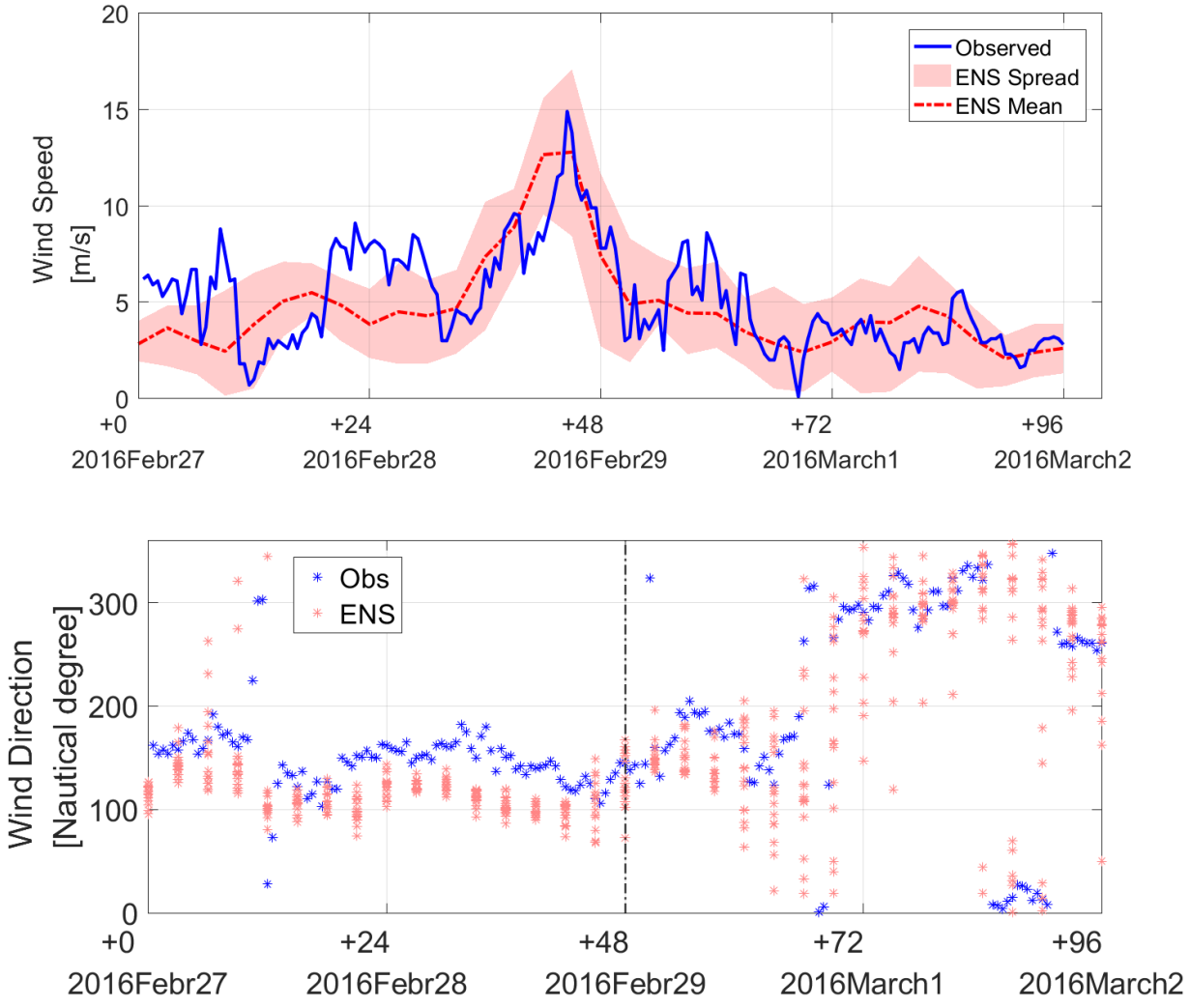

Figure 62 Comparison of 10 m wind speed (upper panel) and direction (lower panel) at the station of Cesenatico, relative to 27 February 2016. The ensemble members of COSMO LEPS, represented with their mean (red dashed line) and spread (light red area), are compared to the observations (blue).

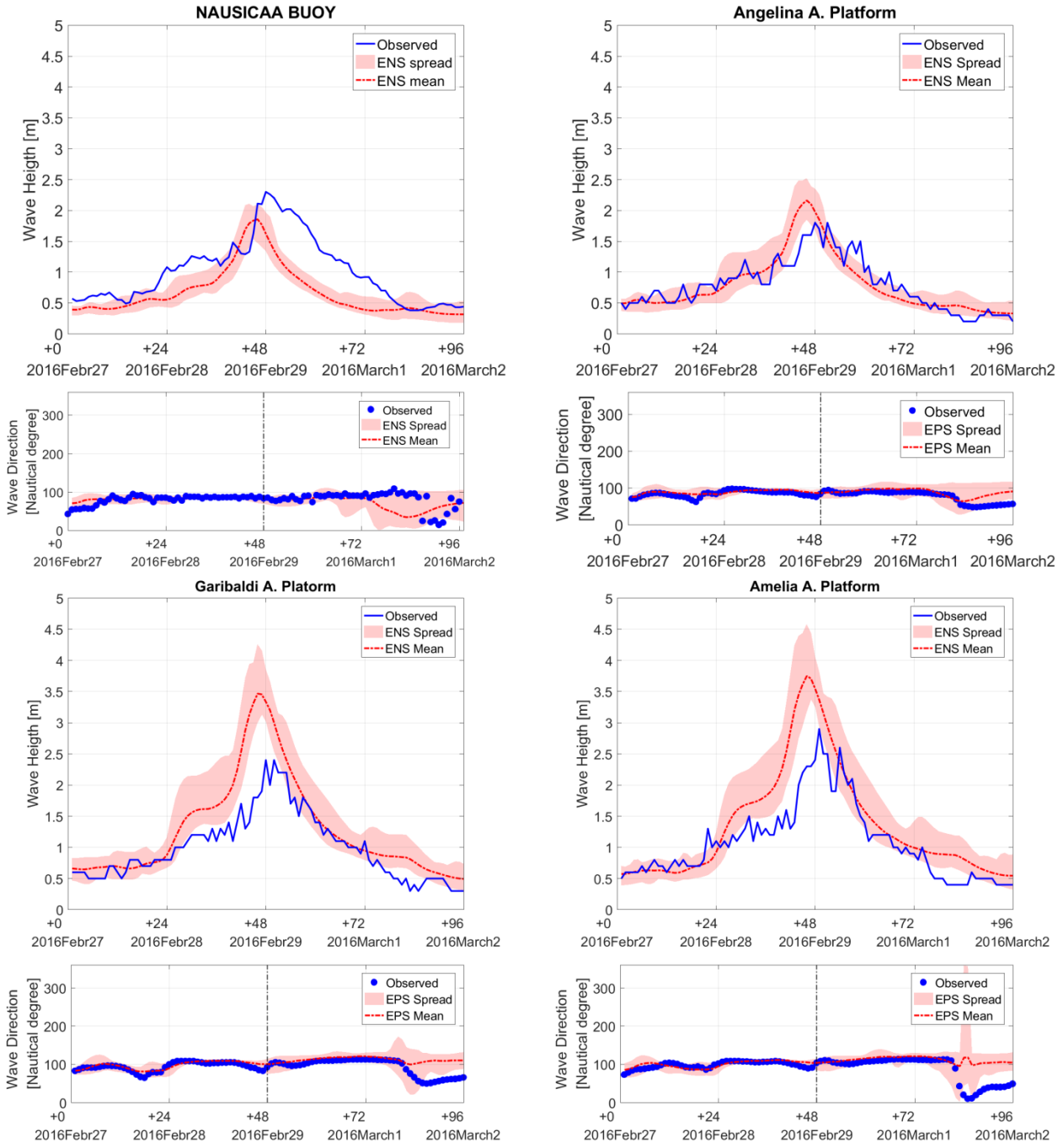

Figure 63 Comparison of computed wave heights (upper panel) and wave directions (lower panel) from SWAN (forced by the ensemble members of COSMO-LEPS) with the measurements (blue) at four measurements stations indicated in Figure 42. The ensemble mean are presented with a dashed red line while the ensemble spread with a light red filled area.

The verification of the water level forecasts are presented in Figure 64, where the computed data of water level are showed with the observations in correspondence of the measurement stations of Rimini and Porto Garibaldi. The location of the tide-gauges is indicated in Figure 42. The ensemble mean at both stations indicates that the water level forecasts are not represented in an accurate way.

During this storm, the tidal signal is clearly dominated by the surge. The mean of the ensemble members shows a tendency to anticipate the level variations. There are large differences not only in the forecast magnitude but also in its timing and shape. The range of solutions (ensemble spread)

widens in correspondence of the surge signal indicating a less predictable situation and a low degree of confidence in the forecast.

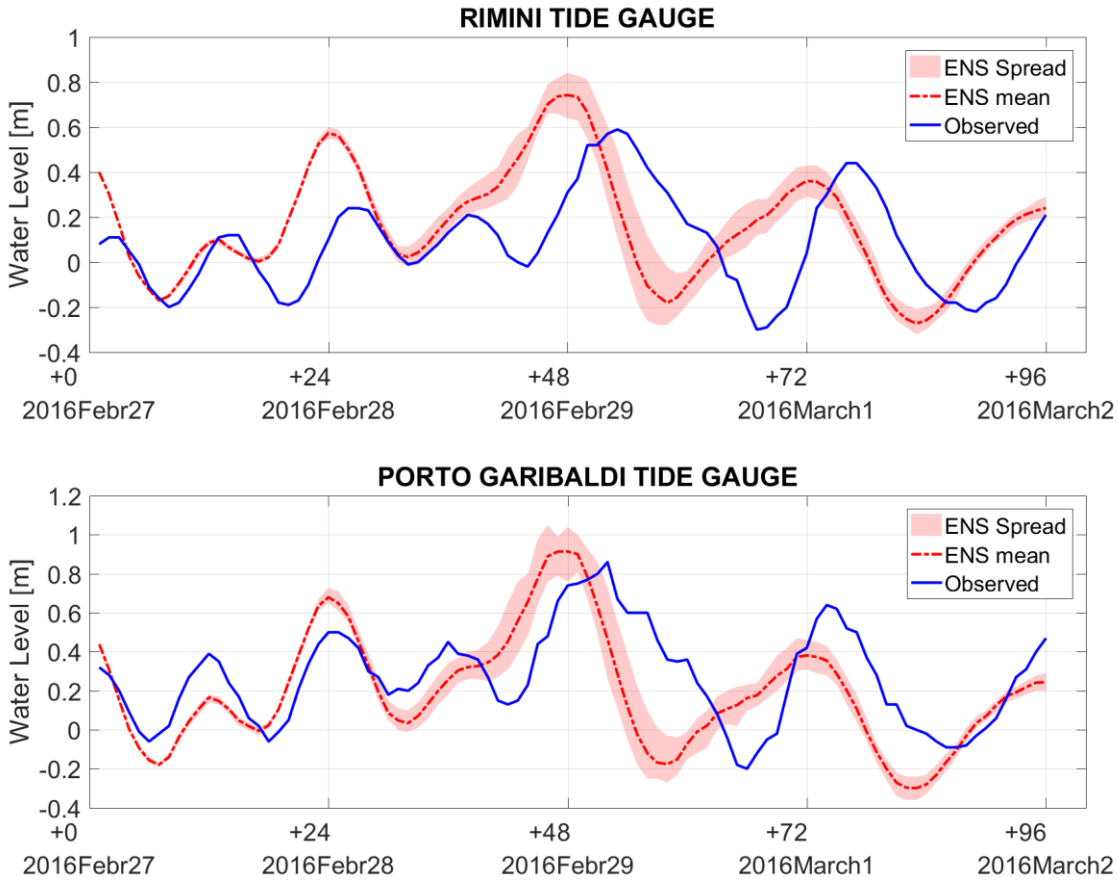

Figure 64 Comparison of water levels at tide gauges of Porto Garibaldi (upper panel) and Rimini (lower panel) related to 20 November 2015. The ensemble forecasts of AdriaROMS (light red) are compared with the observations (blue). The ensemble mean are represented by a dashed red line.

The outcomes of the ensemble members derived by the SWAN and AdriaROMS models are used to force the coastal model XBeach, providing an ensemble of probable morphological solutions. The ensemble forecasts of bed level variations for a single beach cross-section are presented with the measurements in Figure 65. The spread of the ensemble members is very limited around the mean value, which captures the minimum and maximum bed level changes. The deposit at the beach toe is well represented both as intensity and position with respect to the shore. The erosion of the intertidal beach is over-predicted and it is slightly shifted towards the upper beach profile. The models also predict erosion of the emerged beach, but the spread associated to this prediction is large, indicating a less accurate prediction.

The larger amount of erosion is clearly highlighted by calculating the eroded volumes above the mean sea level for each beach cross-section. Table 30 presents the computed and the measured eroded volumes for the ten transects interested by the XBeach model simulations, indicated in Figure 66. Contrariwise the tendency of the deterministic forecasts, the ensemble mean of eroded volumes is higher than the observations for most of beach profiles.

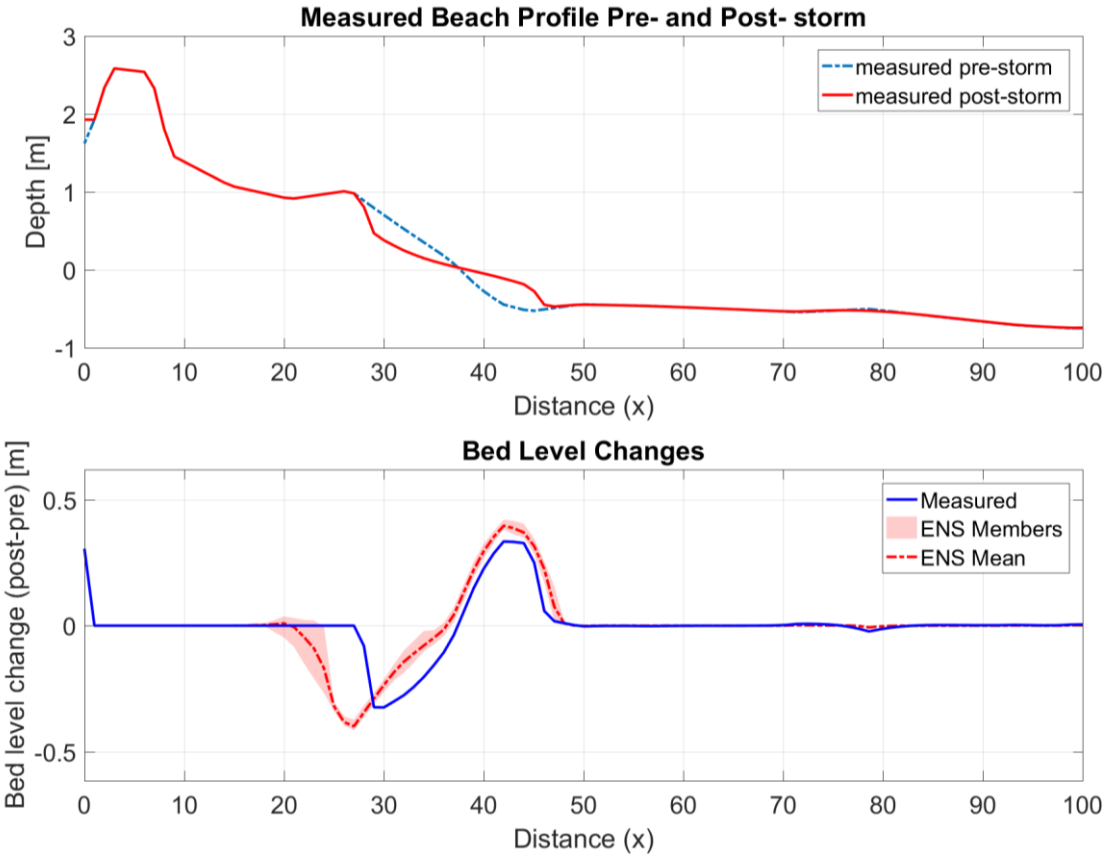

Figure 65 Morphological behavior of a single cross-section. The upper panel shows the pre- and post- storm measured beach profile. The lower panel presents the comparison of the ensemble forecasts of bed level changes, computed by the XBeach model, and the observations (blue). The ensemble mean are presented with a dashed red line while the ensemble spread with a light red filled area.

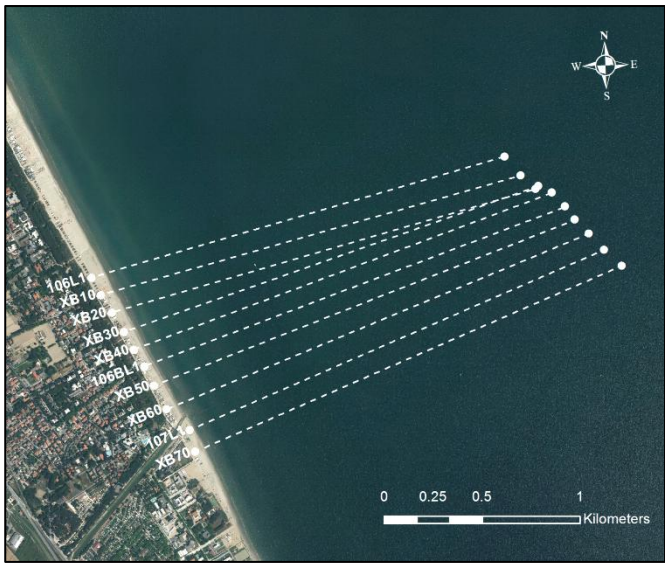

Figure 66 Location of the ten beach cross-sections at Cesenatico study site.

Beach profile name	Observed	Det.	Ensemble forecasts		
	V_{ero} [$m^3 \cdot m^{-1}$]	V_{ero} [$m^3 m^{-1}$]	Min. V_{ero} [$m^3 \cdot m^{-1}$]	Mean V_{ero} [$m^3 \cdot m^{-1}$]	Max. V_{ero} [$m^3 \cdot m^{-1}$]
106L1	1.02	1.83	2.33	2.49	2.6
XB10	3.37	1.53	2.51	2.65	2.79
XB20	1.21	1.51	2.59	2.73	2.85
XB30	1.63	1.10	2.36	2.49	2.6
XB40	1.31	1.16	2.32	2.48	2.61
106BL1	1.67	0.91	2.43	2.59	2.77
XB50	1.66	0.64	1.92	2.04	2.19
XB60	1.84	0.15	1.47	1.58	1.71
XB70	0.59	0.82	2.15	2.26	2.37
107L1	-5.03	1.27	1.68	1.72	1.8

Table 30 Comparison of computed and observed eroded volumes above the mean sea level for the ten beach profiles showed in Figure 66Figure 53 . For the ensemble values the max and min of the EPS members are expressed with the average.

5.6 **Discussion**

Meteorological forecasts of the deterministic model COSMO-I7 and of the ensemble system COSMO-LEPS were used to force two modeling chain composed by oceanographic, wave and coastal models, for two storm events occurred on the Emilia-Romagna region on the autumn2015-winter2016. COSMO-LEPS was used to generate a 16 member perturbed ensemble whose perturbations propagated up to the coastal morphology change simulations.

The deterministic wind forecasts of 20 November 2015 are in good agreement with the ECMWF analysis. This results in wave and morphological forecasts with a good level of accuracy. For water levels, the verification against observations shows a not negligible under-prediction of the whole signal. The ensemble forecasts of wave and tide are affected by the error in low level winds associated to the misplacement of the centre of a small scale low-pressure system. The ensemble mean of wave heights, compared to the off-shore platforms, appears to be more reliable than the deterministic forecast while at the near-shore stations the ensemble exhibits a very large growth in divergence around the mean that still under-predicts the storm peak.

As the deterministic forecasts, the tide and surge signals are not well represented by the ensemble members, which nevertheless display a large spread in correspondence of the wave peak. This case study indicates that the predicted magnitude and location of maximum bed level changes are well predicted by the deterministic model while the ensemble results are dominated by the under-prediction of the wave heights. It is relevant to note that, despite the uncertainty propagated by the meteorological model, the morphological forecasts are in agreement with the observed accumulation/erosion pattern and the predicted and observed eroded volumes present the same order of magnitude.

In the deterministic wind forecasts of 27 February, the anticipated formation of the mean sea level pressure minimum generates a corresponding anticipation of the peak in the wave height with a more rapidly decrease of the wave intensity. The mean of the ensemble wave forecasts is similar to the deterministic results but in addition holds the uncertainty information due to the spread in amplitude. The oceanographic model is not able to reproduce both the tidal and the surge variations in accurate way. The large divergence of the spread indicates that the period around the storm peak is the less predictable.

The combination of the effects of wave and water level forecasts is clearly visible in the morphological beach variation simulation. The maximum and the minimum bed level changes are better predicted by the ensemble members, which exhibit a larger spread in correspondence of the uncorrected erosion of the emerged beach, as visible in Figure 67. Also in the second storm, the forecasted morphological evolution of the beach profiles is in agreement with the observation.

The outcomes of both the storm events show that the accuracy of the forecasts of the wave (SWAN), oceanographic (ROMS) and morphological (XBeach) models is largely dependent on the quality in wind data. Therefore, the uncertainties of the wind and pressure fields generated from the meteorological model clearly propagated through to the predicted regional wave field.

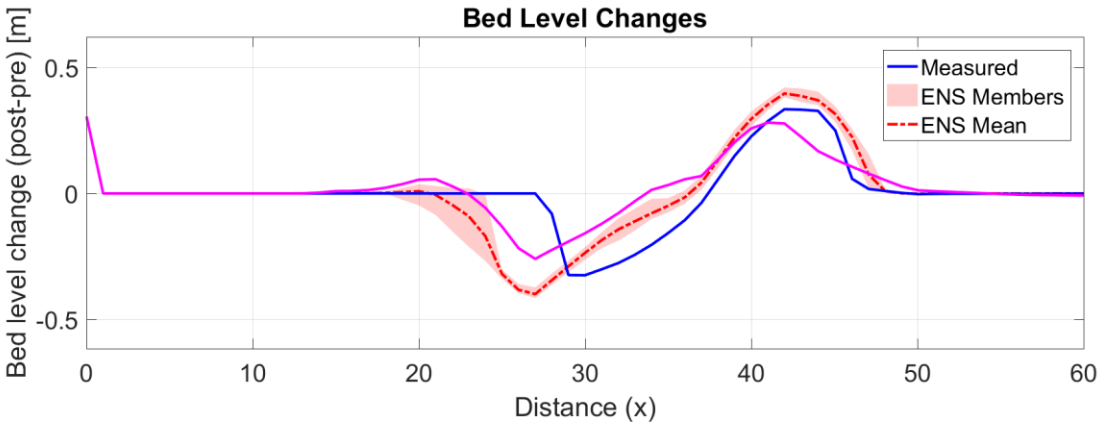

Figure 67 Morphological behavior of a single cross-section related to the storm of 27 February 2016. Comparison of deterministic (magenta) and probabilistic bed level changes (mean and spread) with the observations (blue).

The study of the two events indicates that, during the peak, the predicted waves at the off-shore stations are higher than the observation while at the near-shore stations the forecasted values are smaller than correspondent observations. The wind–wave relationship is much more complicated in the coastal region since waves are further affected by distance, coastal sheltering, fetch-limited wave growth, non-linear wave–wave interaction, bathymetric and other local effects, which would introduce further uncertainty into wave height predictions.

For water levels, the verification against observations almost always produces poor scores for both deterministic and probabilistic systems, because of the extra sources of error involved. It is important to take into account that the oceanographic model AdriaROMS is forced by 5 tidal constituents rather than 8 as the new version of the model. The comparison respect to the observations show that 5 astronomical components do not seems sufficient to correctly reproduce tides. Furthermore, an uncorrected setting of the boundary conditions seems to be the cause of the inaccurate forecast of the surge.

Finally, it is important to notice that the domain of the coastal model is considerably smaller than the meteorological domain. Therefore, as would be expected, the morphological forecasts are directly correlated to the local wave and surge data. In particular, the model is forced at the seaward boundary by the data extracted on the edges of the beach cross-sections.

Due to the availability of only the final morphological variation of the beach profile, instead of a temporal change, it wasn't possible to carry out a temporal analysis of the morphological ensemble forecasts. The comparison with the observation is a spatial analysis of the results.

5.7 **Conclusions**

In this study, the innovative approach to couple an Ensemble Meteorological prediction system, with marine wave and hydrodynamic (circulation, tides and surge) models and, at last, a surf zone hydrodynamic-morphological model is presented. The aim of the analysis is to investigate the propagation of the uncertainties within the numerical modeling chain up to the evaluation of coastal morphological changes due to marine storms.

The Early Warning system, operational at ARPAE SIMC Emilia-Romagna since December 2012 and developed as part of the MICORE project (Harley et al., 2011), is a state-of-the-art system for coastal flood forecasting with a time range of +72 hours. In the operational model suite all the models are run in deterministic mode that means only one run of each model component. Since a deterministic model run cannot give by itself any indication on the reliability of the forecast, the application of the ensemble approach is more and more frequently used especially for the meteorological applications. In this study, the limited area meteorological ensemble prediction system COSMO-LEPS was used to generate 16 different forecasts/members that were then used to force the wave model SWAN and the oceanographic model ROMS. Finally, the outputs of these models were used as input for the morphological model of the coastal zone XBeach. In this study, two storm events have been studied both occurred in the autumn 2015-winter 2016 on the Emilia-Romagna coasts.

The analysis of the results showed that, in both cases, the uncertainties of the wind and pressure fields, generated from the meteorological model, clearly propagated through to the marine models up to influence the coastal forecasts. The accuracy of the forecasts of the wave, oceanographic and morphological models is largely dependent on the quality of the wind data. For both cases the study shows the predominant role of the meteorological component in the overall error.

Despite the uncertainties in each model, and the uncertainty propagation from meteorological to coastal and surf zone models, the outputs of the ensemble modeling system are in agreement with the observed real sea state conditions, capturing the storm occurrence.

The XBeach results show that, for both storm events, the morphological variations are in agreement with the reality of the beach profile evolution. However, as expected, the morphological forecasts are affected by the uncertainties generated and propagated by the upstream models.

The two storm cases suggest that the deterministic forecast is not always the better prediction, exhibiting sometimes a remarkable mismatch with the observations. The outputs obtained by means of the ensemble approach supplies additional information on the reliability of the forecasts thanks to the increase or decrease of the ensemble spread. Especially for the second case, the mean of the ensemble members is more reliable than the deterministic forecast and the observations fall into the uncertainty band generated by the 16-different members.

As mentioned before, the ensemble spread is a good indicator of how the accuracy varies between different forecasting situations. In this study, the usefulness of the ensemble spread as a predictor of the forecast reliability is clearly demonstrated by the good correspondence between the forecast error and the ensemble spread. In particular, the increase of the ensemble spread, which corresponds to the peak of the events, indicates the lower forecast predictability.

This study highlighted how the strong downscaling from the atmospheric to the coastal model is a considerable source of uncertainties within the numerical modeling chain. Since XBeach domain is

definitely smaller than the atmospheric model domain, the coastal model is closely linked to the local scale structures which is well known to be the more difficult to forecast. As shown, a relatively small misplacement of the meteorological pattern can deteriorate the wind forecast and then can affect the results on the impact on coastal morphology.

In conclusion, the study demonstrated the capability to propagate probabilistic information through the forecasting system to site-specific near-shore wave conditions and it allowed to investigates how the uncertainties propagates through the models. The results are encouraging and suggested, as a future development, the possible optimization of the system by using a meteorological ensemble built in such a way to optimize the spread in terms of the surface variables used to drive the marine-coastal model components.

6 Conclusions

A coastal flooding forecasting system is generally composed of a cascade of numerical models that links meteorological, wave/oceanographic and coastal modeling domains. The interactions between atmospheric, oceanic and coastal processes are poorly understood, resulting in large uncertainties in the predictions of coastal flooding, in particular, under extreme conditions.

When constructing a forecasting system, we must take account that many sources of uncertainty are typically present and they are often difficult to fully understand. Being aware of the various sources of uncertainty may, however, help us to better understand how the uncertainties associated to each model component propagate through the numerical chain and affect the final forecasts accuracy.

Uncertainty in model formulation is certainly one of the most important factors which undermines confidence in forecasts. The mathematical and numerical approximations and the limitations of the models available to fully represent processes and mechanisms can also be significant for the accuracy of the forecast. Quite often, some or all of the model inputs are subject to sources of uncertainty, including errors of measurement, absence of information and poor or partial understanding of the driving forces and mechanisms. Furthermore, the model itself can introduce uncertainty depending on his parameter setting, particularly with the setting of the individual parameters, which are used as input for the model.

Moreover, in presence of nested models, computational domains and models resolution become a crucial point within a forecasting system. The overview of the sources of the uncertainties that are introduced and generated in the numerical models is presented in Figure 68. For the reasons described above, a numerical model can be highly complex, and as a result its relationships between inputs and outputs may be poorly understood.

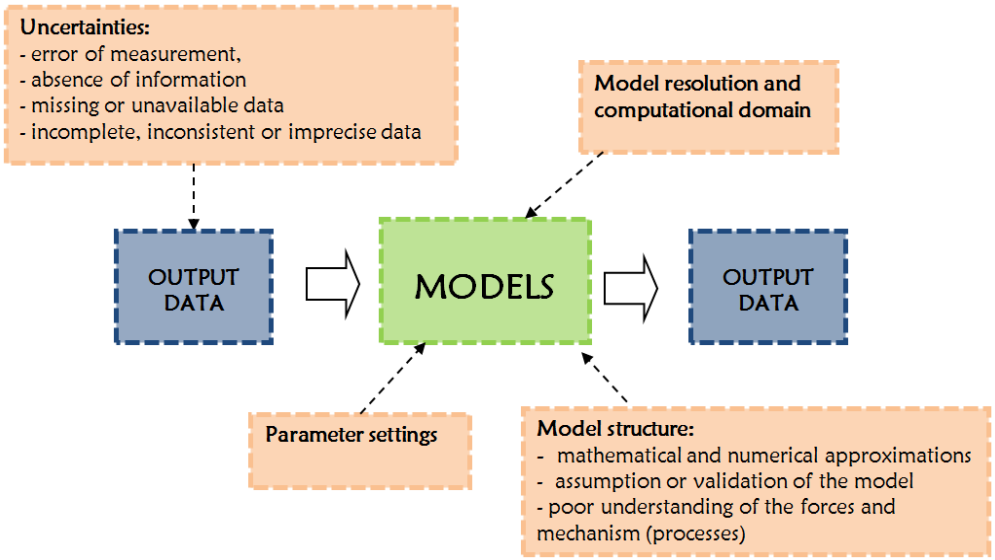

Figure 68 Scheme of Intrinsic (internal) and Extrinsic (external) uncertainty sources for numerical modeling systems

The need for predicting in accurate way the response of coasts to storms is rising steadily, because of the ongoing increasing usage of the coastal zone. However, it is difficult to understand the full range and interaction of uncertainties in the forecast systems. This is the basic concept of this project.

In this thesis, the meteorological model COSMO, the wave/oceanographic models SWAN and ROMS and the morphological model XBeach were integrated in order to investigate the propagation of the uncertainties within the numerical modeling chain.

6.1 Uncertainty Propagation

The Early Warning system, operational at ARPAE SIMC Emilia-Romagna since December 2012 and developed as a part of the MICORE project (Harley et al., 2011), is a state-of-the-art system for coastal flood forecasting with a time range of +72 hours. In the operational model suite all the models are run in deterministic mode that means only one run of each modeling component (see Chapter 2). A deterministic run gives a single output value for each variable, without any indication on the reliability of the forecast. To address this lack, the application of the ensemble approach is more and more frequently used especially for the meteorological applications.

The limited-area ensemble system developed at ARPAE-SIMC and operational since 2002 (Marsigli et al., 2001, 2008), named COSMO-LEPS, is a regional EPS, which is nested into the global ECMWF EPS to provide ensemble forecasts at higher resolution on a smaller spatial scale.

In order to investigate the propagation of the uncertainties within the numerical modeling chain, up to the evaluation of coastal morphological changes due to marine storms, the meteorological model COSMO-LEPS was used to generate 16 different members (i.e. model run) that were used to force the wave\oceanographic models SWAN and ROMS and hence the morphological model XBeach. The study focused on two different storm events both occurred in the autumn 2015-winter 2016 on the Emilia-Romagna coasts.

The results showed that, in both cases, the uncertainties of the forecasted wind and pressure field clearly propagated through to the wave and oceanographic models up to influence the coastal forecast. The accuracy of the forecasts of the oceanographic and morphological models is largely dependent on the quality in the driving forecasted wind data.

Even if the wind forecasts at the Adriatic basin scale give a good representation of the events, the misplacement of the centre of a small scale low-pressure system affects the forecasts of the downstream models. It is well known that the atmospheric predictability decreases with the size of the atmospheric circulations and processes to be forecasted; unfortunately sea storm events like those analyzed in this study are often linked to such kind of phenomena.

Despite the clear propagation of the uncertainties from the meteorological model, and the predominant role of its component in the overall error, in the overall the results of both the event simulations are in accord with the observed storm features.

Because of the strong under-prediction of the wave heights during the storm of November 2015, due to the local displacement of the low-pressure system and of the associated wind forecasts, only the results of the second events were chosen to summarize the outcomes of the study. Table 31 presents the mean absolute and percentage errors computed on the forecasts, for both the deterministic and the probabilistic system. Moreover, the last two columns exhibit the mean and the maximum of the

ensemble spread. All values are computed over the whole forecast period at local sites specified in table.

As visible in Table 31, the uncertainty associated with model predictions almost doubles while propagating from the wind field forecast to the wave height prediction. This result is a physically consistent feature given that the dimensionless wave height is approximately proportional to the square of wind speed in the open ocean. Furthermore, the oceanographic model exhibits significant uncertainties, probably because of the extra sources of error involved, related to the model structure.

Table 31 Mean percentage and absolute errors of the single forecasting models. The results of deterministic and ensemble forecasting are compared. The mean and the maximum of the ensemble spread are reported in the last two columns.

Model	Output Variable	Station	DETERMINISTIC		PROBABILISTIC			
			Mean Percentage Error	Mean Absolute error	Mean Percentage Error	Mean Absolute error	Mean Spread	Max Spread
Meteorological (COSMO)	Wind speed	Cesenatico station	8.80%	1.183 m/s	19 %	0.374 m/s	4.64m/s	9.01m/s
Wave (SWAN)	Wave height	Nausicaa Buoy	13.90%	0.220 m	31 %	0.339 m	0.36 m	0.81 m
Oceanographic (ROMS)	Sea level	Porto Garibaldi tide-gauge	40.20%	0.066 m	41 %	0.020 m	0.12 m	0.41 m
Morphological (XBeach)	Bed level changes (above MSL)	106BL1 Beach Profile	37,60%	0.015 m	6 %	0.0002 m	0.04 m	0.26 m

For this storm, large forecast errors exists in bed level changes obtained with the deterministic run while it is strongly reduced by means the ensemble approach. Despite the effects of the propagation of the uncertainties from the meteorological model, the morphological forecasts are in agreement with the reality of the accumulation/erosion processes.

The analysis of the two storms evidenced that the deterministic forecasts sometimes present a remarkable mismatch with the observations. The outputs obtained by means of the ensemble approach supplies additional information on the reliability of the forecasts, giving useful indication of the model errors.

The ensemble results demonstrated that the ensemble spread is a good indicator of how the accuracy varies between different forecasting situations. The good correspondence between the forecast error and the ensemble spread shows the usefulness of the ensemble spread as a predictor of the forecast reliability, which decreases when the spread increases.

6.2 **Morphological model uncertainties**

By means of a sensitivity analysis (SA) of the morphological model XBeach, the source of uncertainty related to the parameter setting was investigated. The goal of SA is to characterize how model outputs respond to changes in input, with an emphasis on finding the input parameters to which outputs are the most sensitive (Saltelli et al., 2000a; Kennedy and O'Hagan, 2001). This approach accounted only for the uncertainty in the model's input values and parameters, not in the model's structure (i.e. existence and functional form of dependencies between variables, etc.) (e.g. O'Hagan, 2012).

Several input parameters were varied from their default values, within their validity range (see Chapter 4). The morphological variation obtained with different parameter values was compared with the "reference" simulation where all the values were kept to its default value. Finally, the model performance has been assessed by calculating the mean error (bias), the accuracy (Root Mean Square Error) and skill (Brier Skill Score).

The outputs of the reference simulations highlighted a tendency to overestimate the erosion volumes using the default values. A few parameters, all related to the wave breaking process, have shown a strong impact on the morphological evolution of the beach profile, underlining that a variation on the input parameter values can significantly affect the final forecasts. Table 32 presents the parameters that impact significantly the outputs and the percentage error, corresponding to the maximum variation of the forecasts obtained with a different value of the parameter.

Table 32 Percentage error for the most sensitive parameter of the XBeach model. The values were calculated in correspondence of the larger variation in the forecasts by varying the parameter value.

parameter	Shoreline Retreat		Eroded Volumes	
	Storm 1	Storm 2	Storm 1	Storm 2
facua	-754%	-916%	1559%	1215%
break	775%	-1682%	-74%	-1368%
gamma	1015%	2234%	396%	2041%
fw	294%	-683%	98.10%	874%
delta	1175%	2554%	977%	2368%
bedfriccoef	567%	1196%	82%	1358%

By the analysis of the BSS values it is clear that the model is not able to reproduce the morphological evolution in an accurate way except for facua and fw parameters. In particular, when a bottom friction value (fw) of 0.20 is adopted, the model outputs and the observed data are in good agreement. The model shows good performance for both the storm events and thus it is assumed that a fw setting of 0.20 is a proper value for this case study.

The analysis shows that it is important to realize that different parameter settings of the coastal model XBeach can provide large output variations, defining therefore a significant source of uncertainties in the model itself. Despite efforts to improve process-based models such as XBeach with more accurate physical relations, currently the need for calibrating models is inevitable.

6.3 Integrated "Weather-Coastal" Ensemble System

Even if the use of ensemble flood forecasting is more and more becoming a widespread activity, the probabilistic approach is still novel for the coastal applications. This thesis presents a first approach to the extension of the ensemble forecasting system to the coastal scale, in particular applied to two different storm events occurred in the autumn2015-winter 2016 on the coasts of the Emilia-Romagna region.

The results show that the morphological variations are in agreement with the real beach profile evolution, indicating a fair performance of the coastal model within the numerical forecasting chain. As expected, the morphological forecasts are affected by the uncertainties generated and propagated by the upstream models. Especially, as concluded in the previous section, the morphological forecasts suffer from uncorrected wind However, the order of magnitude of the bed level variations is acceptable for both storms.

EPS are no the magic solution to estimating the uncertainty of future coastal flooding or erosion showing that a many further improvements are required but the study demonstrated the capability to propagate probabilistic information through the forecasting system to site-specific near-shore wave conditions and it allowed to investigate how the uncertainties propagate through the models.

The case studies mainly indicate that there may be added value in using flood forecasting systems based on ensemble prediction systems, rather than just on single deterministic forecasts. The combination of a properly calibrated morphological model forced by wind forecasts as accurate as possible may result in an adequate ensemble forecasting system for coastal warnings.

6.4 Further Research

At the end of this project, it is considered helpful to provide some considerations about the limits of the study and therefore some ideas for possible future developments:

- The results of the ensemble forecasting approach are encouraging and suggested, as a future development, the possible optimization of the system by using a meteorological ensemble built in such a way as to optimize the spread in terms of the surface variables used to drive the marine-coastal model components.
- The contribution to forecast uncertainty by all of the different components of the system is not yet fully estimated. In particular, the analysis of the morphological model XBeach has been focused only on the different parameter settings while other possible sources of uncertainty should be also taken into account. In this thesis, the model calibration was validated with the morphodynamic information available (pre- and post-storm bed levels). In the reality of an Early warning system, the morphological domain is based on a single beach profile measured even years before because of the lack of updated measurements. Therefore, it should important to be taken into account that there is a large uncertainty due to the uncorrected bathymetry used to provide the coastal warning. The implementation of different bathymetry as input to XBeach, within an ensemble forecasting system, is already started and it will be presented in future works.
- The present study has considered two single storm events that can illustrate forecast behavior in particular situations but an overall assessment requires representative statistics gathered over a variety of forecasting. For this reason, the presented considerations are not complete and generalizable even if some basic first conclusions related to the investigated storms. The presented methodology will be tested on other cases studies.
- The mismatch in water level results can be attribuited both to the uncertainty of the input data provided by the meteorological model COSMO, both to the inaccurate representation of the tide components within the numerical model AdriaROMS. To investigate and quantify the different error components, an harmonic analysis of the measured signal could be extremely interesting for the study.
- Data assimilation techniques are widely used for weather forecasting. Data assimilation (DA) is the process by which observational data is incorporated into numerical models to improve the definition of the initial model state. In meteorological models, data assimilation is commonly used to generate an optimal initial state to be used in subsequent forecasts through the use of a prior knowledge of the state (e.g. a previous forecast) and observational data obtained from satellites/weather stations etc. However, model error statistics that are needed for data assimilation experiments are generally unknown in coastal regions (Robinson et al. 1998, Echevin et al. 1998, Auclair et al. 2003). These are moreover likely to be strongly time-

dependent due to the short temporal scales of coastal dynamics. This is the reason why data assimilation has to be performed with a special care in these areas. A future development of this thesis should carefully consider the data assimilation approach applied to the coastal model.

Bibliography

Alovisi, J., Souch, C., & Toothill, J, 2007. Windstorm Kyrill: A glimpse into the future? Catastrophe risk management.

Apel, H., Thieken, A. H., Merz, B., & Blöschl, G., 2004. Flood risk assessment and associated uncertainty, Nat. Hazards Earth Syst. Sci., 4, 295–308, doi:10.5194/nhess42952004.

Apel, H., Merz, B., & Thieken, A. H., 2008. Quantification of uncertainties in flood risk assessments, Int. J. River Basin Management, 6, 149–162.

Auclair F., Marsaleix, P., & De Mey, P., 2003. Spacetime structure and dynamics of the forecast error in a coastal circulation model of the Gulf of Lions, Dyn. of Atm. and Oceans, 36, 309-346.

Baart, F., van der Kaaij, T., van Ormondt, M., van Dongeren, A., van Koningsveld, M., and Roelvink, J. A., 2009. Real-time forecasting of morphological storm impacts: a case study in the netherlands. Journal of coastal research, 2, 1617–1621.

Baart, F., van Gelder, P. H. A. J. M., & van Koningsveld, M., 2011. Confidence in real-time forecasting of morphological storm impacts, J. Coast. Res., 64, 1835–1839.

Bahremand, A., & De Smedt, F., 2008. "Distributed Hydrological Modeling and Sensitivity Analysis in Torysa Watershed, Slovakia". Water Resources Management. 22 (3), 293–408

Bajo, M. & Umgiesser, G., 2010. Storm surge forecast through a combination of dynamic and neural network models, Ocean Model., 33, 1–9.

Bart, L.J.C, 2017. Longterm modelling with XBeach: combining stationary and surf-beat mode in an integrated approach, PhD Thesis, uuid: e2550e2636c54a30afa1169e82b4b811

Basher, R., 2006. Global early warning systems for natural hazards: systematic and people-centred, Philos. T. R. Soc. A, 364, 2167– 2182,.

Battjes, J. A., & Gerritsen, H., 2002. Coastal modelling for flood defence. Phil. Trans. R. Soc. A, 360, 1461-1475.

Berlotti, L., Bidlot, J.R., Bunney, C., Cavaleri, L., Delli Passeri, L., Gomez, M., Lefevre, J.M, Paccagnella, T., Torrisi, L., Valentini, A., & Vocino, A., 2011. Performance of different forecast systems in an exceptional storm in the Western Mediterranean Sea, Q. J. Roy. Meteor. Soc., 138 , 34–55, doi:10.1002/qj.892.

Booij, N., Ris, R.C., & Holthuijsen, L.H., 1999. A third-generation wave model for coastal regions. Part I - Model description and validation. J. Geophys. Res. 104 (C4), 7649– 7666.

Bowler, N.E., Arribas, A., Mylne, K.R., Robertson, K.B. & Beare, S.E., 2008. The MOGREPS short-range ensemble prediction system, Q. J. R. Meteorol. Soc., 134, 703–722.

Buckley, M., Lowe, R. & Hansen, J., 2014. Ocean Dynamics, 64: 847. https://doi.org/10.1007/s10236 0140713x

Buizza, R., Houtekamer, P.L., Toth, Z., Pellerin, G., Wei, M. & Zhu, Y., 2005. A comparison of the ECMWF, MSC, and NCEP global ensemble prediction systems, Mon. Weather Rev., 133, 1076–1097.

Buizza, R., 2008. The value of probabilistic prediction, Atmospheric Science Letters, 9, 36–42.

Cacuci, D.G., 2003. Sensitivity and Uncertainty Analysis: Theory. I. Chapman & Hall.

Cacuci, D.G., IonescuBujor, M., & Navon, M., 2005. Sensitivity and Uncertainty Analysis: Applications to LargeScale Systems. II. Chapman & Hall.

Callaghan, D. P., Ranasinghe, R., & Roelvink, D., 2013. Probabilistic estimation of storm erosion using analytical, semiempirical, and process based storm erosion models, Coast. Eng., vol. 82, pp. 64–75.

Chiggiato, J. & Oddo, P., 2006. Operational Ocean Models in the Adriatic Sea: a skill assessment. Ocean Science, 4, 61-77.

Christiaens, K. & Feyen, J., 2002. Use of sensitivity and uncertainty measures in distributed hydrological modeling with an application to the MIKE SHE model, Water Resour. Res., 38, 1169, doi:10.1029/2001WR000 478, 2002.

Ciavola, P., Ferreira, O., Haerens, P., Van Koningsveld, M., Armaroli, C., Lequeux, Q., 2011. Storm impacts along European coastlines. Part 1: The joint effort of the MICORE and ConHaz Projects. Environmental Science & Policy 14 (7), 912–923.

Cloke, H.L. & Pappenberger F., 2009. Ensemble flood forecasting: a review, Journal of Hydrology, 375, 613–626.

Correggiari, A., Aguzzi, M., Remia, A. & Preti, M., 2011. Caratterizzazione sedimentologica e stratigrafica di giacimenti sabbiosi in Mare Adriatico settentrionale finalizzata all'individuazione delle aree di prelievo. Studi costieri, 19, 11-31.

Coumou, D. & Rahmstorf, S., 2012. A decade of weather extremes, Nature Climate Change, 2, 491–496, doi:10.1038/nclimate1452.

Czitrom, 1999. OneFactorataTime Versus Designed Experiments, American Statistician, 53 (2).

Dance, S.L., & Zou, Q.P., 2010. HESS opinions: Ensembles, uncertainty and flood prediction, Hydrol. Earth. Syst. Sci. Discuss., 7, 3591–3611.

Daniel, P., Haie, B., & Aubail, X., 2009. Operational forecasting of tropical cyclones storm surges at Meteo-France, Mar. Geodesy, 32, 233–242. http://dx.doi.org/10.1080/01490410902869649.

Deltares, 2017. XBeach skillbed report, revision 5280 status update trunk default, Report, Revision: 5280, pp. 94.

De Moel, H., Asselman, N. E. M., & Aerts, J. C. J. H., 2012. Uncertainty and sensitivity analysis of coastal flood damage estimates in the west of the Netherlands, Nat. Hazards Earth Syst. Sci., 12, 1045–1058, doi:10.5194/nhess1210452012.

De Moel, H. & Aerts, J. C. J. H., 2011. Effect of uncertainty in land use, damage models and inundation depth on flood damage estimates, Nat. Hazards, 58, 407–425, doi:10.1007/s1106901096756.

De Vet, P., 2014. Modelling sediment transport and morphology during overwash and breaching events, Technical report, MSc thesis, Delft University of Technology, Delft.

Der Kiureghian, A., & Ditlevsen, O., 2009. "Aleatory or epistemic? Does it matter?", Structural Safety. 31 (2): 105–112. doi:10.1016/j.strusafe.2008.06.020.

Di Liberto, T., Brian, A.C., Nickitas, G., Blumberg, A.F. & Taylor, A.A., 2011. Verification of a Multimodel Storm Surge Ensemble around New York City and Long Island for the Cool Season, Weather Forecasting, 26, 922–939. doi: http://dx.doi.org/10.1175/WAF-D-10-05055.1

Ding, X.L., Chen, Y.P., Pan, Y., & Reeve, D., 2016. Fast Ensemble Forecast of Storm Surge along the Coast of China. In: Vila-Concejo, A., Bruce, E., Kennedy, D.M., & McCarroll, R.J. (eds.), Proceedings of the 14th International Coastal Symposium (Sydney, Australia). Journal of Coastal Research, Special Issue, 75, 1077- 1081.

Dube, S., Jain, I., Rao, A., & Murty, T., 2009. Storm surge modelling for the Bay of Bengal and Arabian Sea, Nat. Hazards, 51, 3–27, doi:10.1007/s11069-009-9397-9, 2009.

Echevin V., De Mey, P. & Evensen, G., 2000. Horizontal and vertical structure of the representer functions for sea surface measurements in a coastal circulation model. J.Phys.Oceanogr., 30,2627-2635.

European Environment Agency, 2006. The changing faces of Europe's coastal areas, EEA Report No 6, ISBN 92-9167-842-2, 107 pp.

Ferrarin, C., Roland, A., Bajo, M., Umgiesser, G., Cucco, A., Davolio, S., Buzzi, A., Malguzzi, P., & Drofa, O., 2013. Tidesurge- wave modelling and forecasting in the Mediterranean Sea with focus on the Italian coast, Ocean Model., 61, 38–48, doi:10.1016/j.ocemod.2012.10.003.

Frey, H. & Patil, S., 2002. Identification and Review of Sensitivity Analysis Methods, Risk Analysis, 22, 553–578.

Flather, R., 2000. Existing operational oceanography, Coastal Eng., 41, 13–40.

Flowerdew, J., Horsburgh, K., Wilson, C. & Mylne, K., 2010. Development and evaluation of an ensemble forecasting system for coastal storm surges, Q. J. R. Meteorol. Soc., 136, 1444–1456.

Galarneau Jr., T. J., Davis, C. A., & Shapiro, M. A., 2013. Intensification of Hurricane Sandy (2012) through extratropical warm core seclusion, Mon. Weather Rev., 141, 4296–4321, doi:10.1175/MWR-D-13-00181.1.

Gonnert, G., Dube, S., Murty, T., & Siefert, W., 2001. Global storm surges: Theory observation and application. German Coastal Engineering Research Council, 623.

Harley, M., Armaroli, C. & Ciavola, P., 2011. Evaluation of XBeach predictions for a real-time warning system in Emilia-Romagna, Northern Italy, Journal of Coastal Research, 64, Proceedings of the 11th International Coastal Symposium, 1861-1865.

Harley, M. D. & Ciavola, P., 2013. Managing local coastal inundation risk using real-time forecasts and artificial dune placements, Coastal Engineering, 77, 77–90.

Harley, M. D., Valentini, A., Armaroli, C., Perini, L., Calabrese, L., & Ciavola, P., 2016. Can an earlywarning system help minimize the impacts of coastal storms? A case study of the 2012 Halloween storm, northern Italy, Nat. Hazards Earth Syst. Sci., 16: 209222.

Hasselmann, K., Barnett, T.P., Bouws, E., Carlson, H., Cartwright D.E., Enke, K., Ewing, J.A., Gienapp, H., Hasselmann, D.E., Kruseman, P., Meerburg, A., Mller, P., Olbers, D.J., Richter, K., Sell, W. & Walden, H., 1973. Measurements of wind-wave growth and swell decay during the Joint North Sea Wave Project (JONSWAP)' Ergnzungsheft zur Deutschen Hydrographischen Zeitschrift Reihe, 8, (12), 95.

Helton, J. & Davis, F., 2003. Latin hypercube sampling and the propagation of uncertainty in analyses of complex systems, Reliability Engineering and System Safty, 81, 23–69.

Heuvelink, G. B. M., 1998. Error propagation in environmental modelling with GIS, Taylor & Francis, London, UK.

Holthuijsen, L.H., Booij, N., & Herbers, T.H.C., 1989. A prediction model for stationary, short-crested waves in shallow water with ambient currents. Coast. Eng. 13, 23– 54.

Horsburgh, K.J., Williams, J.A., Flowerdew, J. & Mylne, K., 2008. Aspects of operational forecast model skill during an extreme storm surge event, J. Flood Risk Manage, 1, 213–221.

IDROSER Spa, 1996. Progetto di piano per la difesa dal mare e la riqualificazione ambientale del litorale della Regione Emilia-Romagna., Relazione generale, 365.

Ji, M., Aikman III, F., & Lozano, C., 2010. Toward improved operational surge and inundation forecasts and coastal warnings, Nat. Hazards, 53, 195–203. http://dx.doi.org/10.1007/s11069-009-9414-z.

Jongejan, R.B. & Ranasinghe, R., 2009. Establishing setback lines for land-use planning: A risk-informed approach (online). In: Coasts and Ports 2009: In a Dynamic Environment. (Wellington, N.Z.): Engineers Australia, 119-125.

Kinsela, M. and Hanslow, D., 2013, Coastal Erosion Risk Assessment in New South Wales: Limitations and Future Directions, in Proceedings of the NSW Coastal Conference, Port Macquarie.

Kennedy, M.C., O'Hagan, A., 2001. Bayesian calibration of computer models. J. R. Stat. Soc. Ser. B Stat. Methodol. 63, 425e464.

Knabb, R. D., Rhome, J. R., & Brown, D. P., 2005. Tropical cyclone report: Hurricane katrina, August 2005, National Hurricane Center, 23–30

Kobayashi, N., Tega, Y., and Hancock, M., 1996. Wave reflection and overwash of dunes. Journal of Waterway, Port, Coastal and Ocean Engeering, 122(3), 150-153.

Kolen, B., Slomp, R., & Jonkman, S., 2013. The impacts of storm Xynthia February 27–28, 2010 in France: lessons for flood risk management, Journal of Flood Risk Management, 6, 261–278, doi:10.1111/jfr3.12011

Kolokythas, G. K., Silva, R., Delgado Blanco, M.R., 2016. Morphological evolution of a bed profile induced by a storm event at the Belgian coast predicted by Xbeach model, in: The proceedings of the twenty-sixth (2016) International Ocean and Polar Engineering conference, Rhodes, Greece, 1239-1246.

Lagmay, A. M. F., Agaton, R. P., Bahala, M. A. C., Briones, J. B. L. T., Cabacaba, K. M. C., Caro, C. V. C., Dasallas, L. L., Gonzalo, L. A. L., Ladiero, C. N., & Lapidez, J. P., 2015. Devastating storm surges of Typhoon Haiyan, International Journal of Disaster Risk Reduction, 11, 1–12.

Lane, E., Walters, R., Gillibrand, P., & Uddstrom, M., 2009. Operational forecasting of sea level height using an unstructured grid ocean model, Ocean Modell, 28, 88– 96.

Lenhart, T., Eckhardt, K., Fohrer, N., & Frede, H.G., 2002. Comparison of two different approaches of sensitivity analysis, Physics and Chemistry of the Earth, 27(9), 645-654.

Lorenz, E.N., 1965. A study of the predictability of a 28-variable atmospheric model, Tellus, 17, 321-333.

Mariani, S., Casaioli, M., Coraci, E., & Malguzzi, P., 2015. A new highresolution BOLAM-MOLOCH suite for the SIMM forecasting system: assessment over two HyMeX intense observation periods, Nat. Hazards Earth Syst. Sci., 15, 1–24, doi:10.5194/nhess- 15-1-2015.

Marsigli, C., Montani, A., Nerozzi, F., Paccagnella, T., Tibaldi, S., Molteni, F. & Buizza, R., 2001. A strategy for high–resolution ensemble prediction. Part II: limited-area experiments in four alpine flood events, Quarterly Journal of the Royal Meteorological Society, 127, 2095–2115.

Marsigli, C., Montani, A., & Paccagnella, T., 2008. A spatial verification method applied to the evaluation of high-resolution ensemble forecasts, Meteorological Applications, 15, 125–143.

Martinelli L., Zanuttigh B., & Corbau C., 2010. Assessment of coastal flooding hazard along the Emilia Romagna littoral, IT, Coastal Engineering, 57, 11-12, 1042-1058.

McCall, R.T., Thiel, V., de Vries, J.S.M., Plant, N.G., Van Dongeren, A.R., Roelvink, J.A., Thompson, D.M., & Reniers, A.J.H.M., 2010. Two-dimensional time dependent hurricane overwash and erosion modeling at Santa Rosa Island. Coastal Eng, 57(7), 668–683. doi:10.1016/j.coastaleng.2010.02.006

Merz, B. & Thieken, A. H., 2009. Flood risk curves and uncertainty bounds, Nat. Hazards, 51, 437–458, doi:10.1007/s11069009 94526.

Merz, B., Kreibich, H., Thieken, A., & Schmidtke, R., 2004. Estimation uncertainty of direct monetary flood damage to buildings, Nat. Hazards Earth Syst. Sci., 4, 153–163, doi:10.5194/nhess4153 2004.

Molteni, F., Buizza, R., Marsigli, C., Montani, A., Nerozzi, F. & coauthors, 2001. A strategy for high-resolution ensemble prediction. Part I: definition of representative members and global-model experiments, Q. J. R. Meteorol. Soc., 127, 2069–2094.

Montani, A., Cesari, D., Marsigli, C. & Paccagnella, T., 2011. Seven years of activity in the field of mesoscale ensemble forecasting by the COSMO-LEPS system: main achievements and open challenges, Tellus A, 63, 605-624.

Morrow, B. H., Lazo, J. K., Rhome, J., & Feyen, J., 2014. Improving storm surge risk communication: Stakeholder perspectives, B. Am. Meteorol. Soc., 96, 35–48, doi:10.1175/BAMS-D-13- 00197.1, 2014.

Murphy, A. H. & Epstein, E. S., 1989. Skill scores and correlation coefficients in model verification, Monthly Weather Review, 117, 572–581.

Murphy, J.M., Sexton, D.M.H., Barnett, D.N., Jones, G.S., Webb, M.J., Collins, M. & Stainforth, D.A., 2004. Quantification of modelling uncertainties in a large ensemble of climate change simulations, Nature. 430, 768–772. Bibcode:2004 Natur.430.768M. PMID 15306806. doi:10.1038/nature02771.

Oakley, J. & O'Hagan, A., 2004. Probabilistic sensitivity analysis of complex models: a Bayesian approach, Journal of Royal Statistical Society Series B statistical Methodology, 66, 751–769.

O'Hagan, A., Buck, C. E., Daneshkhah, A., Eiser, J. R., Garthwaite, P.H., Jenkinson, D.J., Oakley, J.E. & Rakow, T., 2006. Uncertain Judgements: Eliciting Expert Probabilities, Chichester: John Wiley.

O'Hagan, A., 2012. Probabilistic uncertainty specification: overview, elaboration techniques and their application to a mechanistic model of carbon flux, Environ. Model. Softw., 36, 35-48.

Palmer, T.N., Doblas-Reyes, F.J., Hagedorn, R., et al., 2004. Development of a European multimodel ensemble system for seasonal-to-interannual prediction (DEMETER), Bull. Am. Meteorol. Soc., 85, 853–872.

Paul, B. K., 2009. Why relatively fewer people died? The case of Bangladeshs Cyclone Sidr, Nat. Hazards, 50, 289–304, doi:10.1007/s11069-008-9340-5.

Pender, D. & Karunarathna, H., 2013. A statisticalprocess based approach for modelling beach profile variability, Coast. Eng., 81, 19–29.

Perini, L., Calabrese, L., Deserti, M., Valentini, A., Ciavola, P., & Armaroli, C., 2011. Le mareggiate e gli impatti sulla costa in Emilia-Romagna 1946-2010. Bologna: Arpae Emilia-Romagna.

Perini L., Calabrese L., Lorito S., Luciani P. & Lorito, S., 2015. Il rischio da mareggiata in Emilia-Romagna: l'evento del 5-6 Febbraio 2015, Researchgate, available at https://www.researchgate.net /publication/301219671

Peterson, T. C., Hoerling, M. P., Stott, P. A., & Herring, S., 2013. Explaining extreme events of 2012 from a climate perspective, B. Am. Meteorol. Soc., 94, S1–S74.

Plant, N.G. & Holland, K.T., 2011a. Prediction and assimilation of surf-zone processes using a Bayesian network. Part I: Forward models, Coast. Eng., 58, (1), 119–130.

Plant, N.G. & Holland, K.T., 2011b. Prediction and assimilation of surf-zone processes using a Bayesian network. Part II: Inverse models, Coast. Eng., 58, (3), 256–266.

Plant, N.G. & Stockdon, H.F., 2012. Probabilistic prediction of barrier island response to hurricanes, Journal Geophys. Res. Earth Surf., 117, (3), 1-17.

Preti M., 2002. Ripascimento di spiagge con sabbie sottomarine in Emilia-Romagna. Studi Costieri, 5, 107-135.

Preti, M., De Nigris, N., Morelli, M., Monti, M., Bonsignore, F., & Aguzzi, M., 2009. State of the Emilia-Romagna littoral at 2007 and ten-years management plan, I quaderni dell'ARPA. Bologna. In Italian, abstract in English.

Preti, M., De Nigris, N., Morelli, & M., 2011. Il monitoraggio delle spiagge nel periodo 2002-2005. Studi costieri, 19, 35-87.

Preti, M., Aguzzi, M. Costantino, R., De Nigris, N. & Morelli, M., 2011. Il monitoraggio delle spiagge nel periodo 2007-2009. Studi costieri, 19, 137-198.

Ris, R.C., Holthuijsen, L.H., & Booij. N., 1994. A spectral model for waves in the near shore zone, Proc. 24th Int. Conf. Coastal Eng., Kobe, Oct. 1994, Japan, 68-78.

Ris, R.C., Booij, N., & Holthuijsen, L.H., 1999. A third-generation wave model for coastal regions. Part II - Verification. J. Geophys. Res. 104 (C4), 7667– 7681.

Robinson A.R., Lermusiaux, P.F.J. & Quincy Sloan III, N., 1998. Data assimilation. In The Sea, Volume 10, The Global Coastal Ocean: Processes and Methods, K.H. Brink and A.R. Robinson, eds. Wiley, New York, Chap 20.

Roelvink, J.A. & Broker, I., 1993. Cross-shore profile models, Coastal Eng., 21, (1‑3), 163‑191.

Roelvink, D., Reniers, A., van Dongeren, A., van Thiel de Vries, J., McCall, R., & Lescinski, J., 2009. Modelling storm impacts on beaches, dunes and barrier islands, Coast. Eng., 56, (11–12), 1133–1152.

Roelvink, D., van Dongeren, A., McCall, R., Hoonhout, B., van Rooijen, A., van Geer, P., de Vet, L., Nederhoff, K. & Quataert, E., 2015. XBeach Technical Reference: Kingsday Release. Model description and reference guide to functionalities, Deltares, UNESCOIHE Institute of Water Education and Delft University of Technology, 141. Available at https://oss.deltares.nl/web/xbeach/

Sacks, J., Welch, W.J., Mitchell, T.J., & Wynn, H.P., 1989. Design and Analysis of Computer Experiments. Statistical Science, 4, 409–435.

Saltelli, A., Chan, K., & Scott, E.M., 2000a. Sensitivity Analysis, John Wiley & Sons, Chichester.

Saltelli, A., Tarantola, S., & Campolongo, F., 2000b. Sensitivity Analysis as an Ingredient of Modeling, Statistical Science, 15, 377–395.

Saltelli, A., 2002. Sensitivity Analysis for Importance Assessment, Risk Analysis, 22, (3), 1–12.

Saltelli, A., Tarantola, A., Campolongo, F., & Ratto, M., 2004. Sensitivity Analysis in Practice. A Guide to Assessing Scientific Models, John Wiley and Sons, Chichester.

Saltelli, A., Ratto, M., Andres, T., Campolongo, F., Cariboni, J., Gatelli, D., Saisana, M., & Tarantola, S., 2008. Global Sensitivity Analysis: The Primer. John Wiley & Sons.

Saltelli, A., & Annoni, P., 2010. How to avoid a perfunctory sensitivity analysis, Environmental Modeling and Software, 25, 1508–1517

Siek, M., & Solomatine, D.P., 2011. Optimized dynamic ensembles of multiple chaotic models in predicting storm surges, Journal of Coastal Research, 64, 1184–1188. Szczecin, Poland, ISSN 0749-0208.

Simmons, J.A., Marshall, L.A., Turner, I.L., Splinter, K.D., Cox, R.J., Harley, M.D., Hanslow, D.J. & Kinsela M.A., 2015. A more rigorous approach to calibrating and assessing the uncertainty of coastal numerical models. In: Australasian Coasts & Ports Conference 2015: 22nd Australasian Coastal and Ocean Engineering Conference and the 15th Australasian Port and Harbour Conference. Auckland, New Zealand: Engineers Australia and IPENZ, 2015: 821827.

Simmons, J.A., Harley, M.D., Turner, I.L. & Splinter, K.D. 2017. Quantifying calibration data requirements for coastal erosion models: how many storms is enough?, Coasts & Ports 2017 Conference – Cairns, 21-23 June 2017.

Slingo, J., Belcher, S., Scaife, A., McCarthy, M., Saulter, A., McBeath, K., Jenkins, A., Huntingford, C., Marsh, T., Hannaford, J., & Parry, S., 2014. The recent storms and floods in the UK, Tech. Rep., Met Office, UK.

Small, C. & Nicholls, R. J., 2003. A global analysis of human settlement in coastal zones, Journal of Coastal Research, pages 584-599.

Soulsby, R.L., 1997. Dynamics of Marine Sands, London: Thomas Telford Publications.

Splinter, K.D. & Palmsten, M.L., 2012. Modeling dune response to an East Coast Low, Mar. Geol., 329–331, 46–57.

Stephens, E. & Cloke, H., 2014. Improving flood forecasts for better flood preparedness in the UK (and beyond), The Geographical Journal, 180, 310–316, doi:10.1111/geoj.12103.

Stockdon, H.F., Thompson, D.M., Plant, N.G., & Long, J.W., 2014. Evaluation of wave runup predictions from numerical and parametric models, Coast. Eng., 92, 1–11.

Trouw, K., Zimmermann, N., Mathys, M., Delgado, R. & Roelvink, D., 2012. Numerical modeling of hydrodynamics and sediment transport in the surf zone: a sensitivity study with different types of numerical models, Proceedings of the International Conference on Coastal Engineering 2012, Santander, Spain.

USGCRP (2014). Moser, S. C., Davidson, M. A., Kirshen, P., Mulvaney, P., Murley, J. F., Neumann, J. E., Petes, L., & Reed, D., 2014. Coastal Zone Development and Ecosystems. Climate Change Impacts in the United States: The Third National Climate As¬sessment, Melillo, J. M., Terese, T.C., Richmond, and Yohe G. W., Eds., U.S. Global Change Research Program, 579-618.

Uusitalo, L., Lehikoinen, A., Helle, I., & Myrberg, K., 2015. An overview of methods to evaluate uncertainty of deterministic models in decision support, Environmental Modelling & Software, 63, 24-31

Van Rijn, L.C., 1984. Sediment transport, part III: bed forms and alluvial roughness, Journal of Hydraulic Engineering, 110, (12), 1733–1754.

Van Rijn, L.C., 2007. Unified View of Sediment Transport by Currents and Waves: part I and II, Journal of Hydraulic Engineering, 649–667.

Van Thiel de Vries, J.S.M., 2009. Dune erosion during storm surges. PhD thesis, Delft Unversity of Technology, Delft. ISSN 18775608

Verlaan, M., Zijderveld, A., de Vries, H., & Kroos, J., 2005. Operational storm surge forecasting in the Netherlands: developments in the last decade, Philos. Trans. R. Soc., 363, 1441–1453. http://dx.doi.org/10.1098/rsta.2005.1578.

Vousdoukas, M.I., Velegrakis, A.F. & Karambas, T.V., 2009. Morphology and sedimentology of a microtidal, beachrockinfected beach: Vatera Beach, Lesvos, NE-Mediterranean, Cont. Shelf. Res., 29, (16), 1937‑1947.

Vousdoukas, M.I., Almeida, L.P. & Ferreira, Ó., 2011. Modelling storm induced beach morphological change in a mesotidal, reflective beach using XBeach, J. Coast. Res., 64, 1916–1920.

Vousdoukas, M.I., Ferreira, Ó., Almeida, L.P. & Pacheco, A., 2012. Toward reliable stormhazard forecasts: XBeach calibration and its potential application in an operational earlywarning system. Ocean Dynamics, 62, 1001–1015.

Werner, M., Cranston, M., Harrison, T., Whitfield, D., & Schellekens, J., 2009. Recent developments in operational flood forecasting in England, Meteorological Applications, Wales and Scotland, http://dx.doi.org/10.1002/met.124.

World Ocean Review, 2017. The battle of the Coast. [Online]

Zou, Q.P., & Reeve, D.E., 2009. Modelling water from clouds to coast, Planet Earth, Natural Environment Research Council, August issue, 22–23. http://planetearth.nerc.ac.uk/features/story.aspx?id=52

APPENDIX A

Supportive material for Sensitivity Analysis of XBeach

In order to investigate the effect of several input parameters on the model forecasts and hence provide some indications on the model uncertainties, Chapter 4 presents the sensitivity analysis of the morphological model XBeach.

The analysis was made by applying a two-step approach. Firstly, a sensitivity analysis, to define the input parameters that mostly affect the results, was carried out. In the second part, the model performance related to the most relevant parameters was assessed in order to define an optimized model setup.

In Chapter 4 are presented the results of all the parameter investigated in the analysis, however, because of the limited space, only the plots related to the most sensitive parameters are reported. For completeness, in this appendix the plots related to all analyzed parameters can be found.

The plots present the comparison of the bed level evolution computed with different parameter values with the observations, after the storm impact. In particular, two storms occurred in autumn2015-winter2016 were investigated. A complete description of the storms can be found in Section 3.2 and Section 3.3 of Chapter 3. The discussions of each parameter results are presented in Chapter 4.

As the method followed in Chapter 4, graphs are reported separate towards the phenomena to which each parameter is related; sediment transport, short wave action, shallow water equation and bottom updating.

A.1 Sediment transport

A.1.1 Cmax parameter

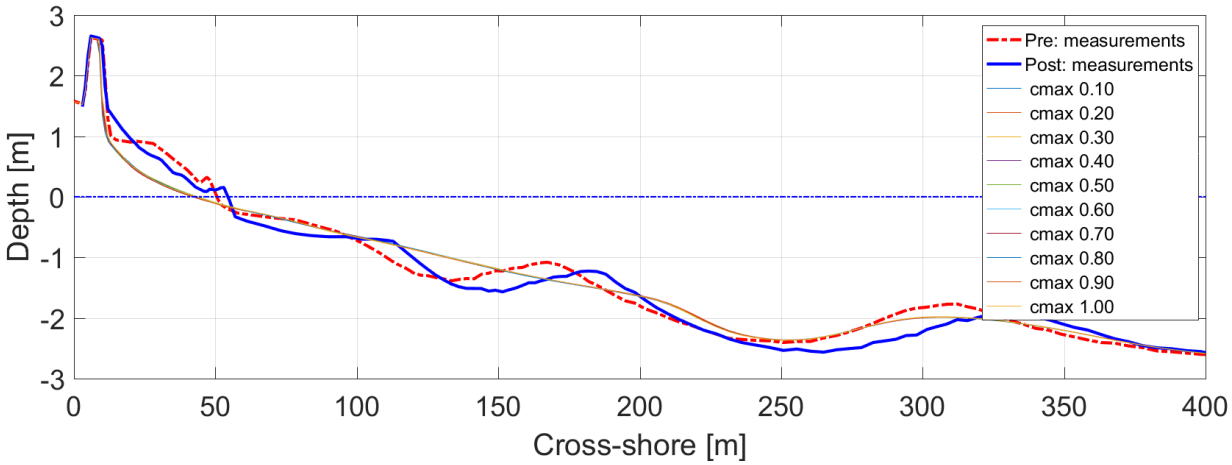

A 1Post storm bed levels for a single cross-section for various values of cmax, related to the storm event of the 20-24 November 2015. The forecasted beach profiles are compared to the observed post storm profile (blue line).

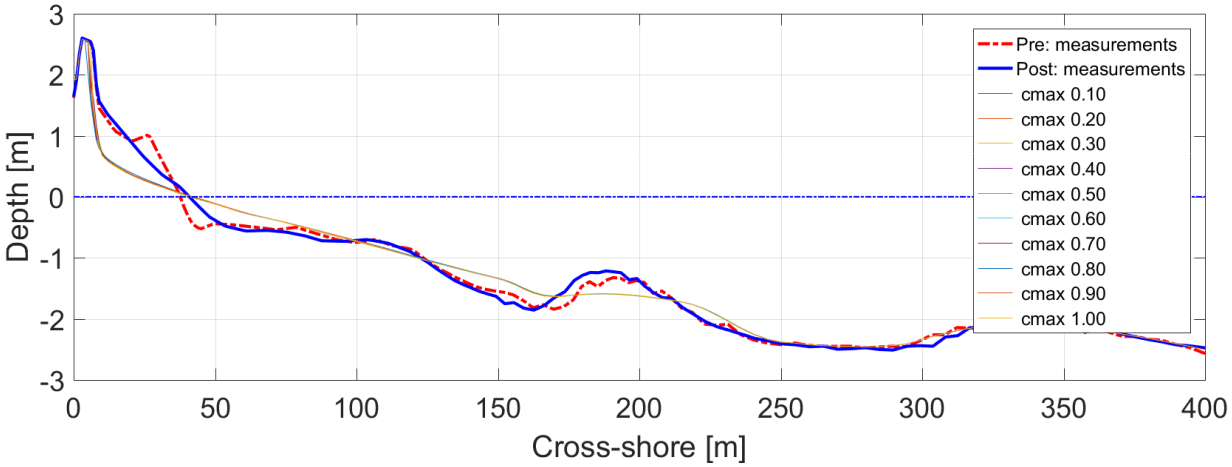

A 2 Post storm bed levels for a single cross-section for various values of cmax, related to the storm event of the 27 February-02 March 2016. The forecasted beach profiles are compared to the observed post storm profile (blue line).

A.1.2 Smax parameter

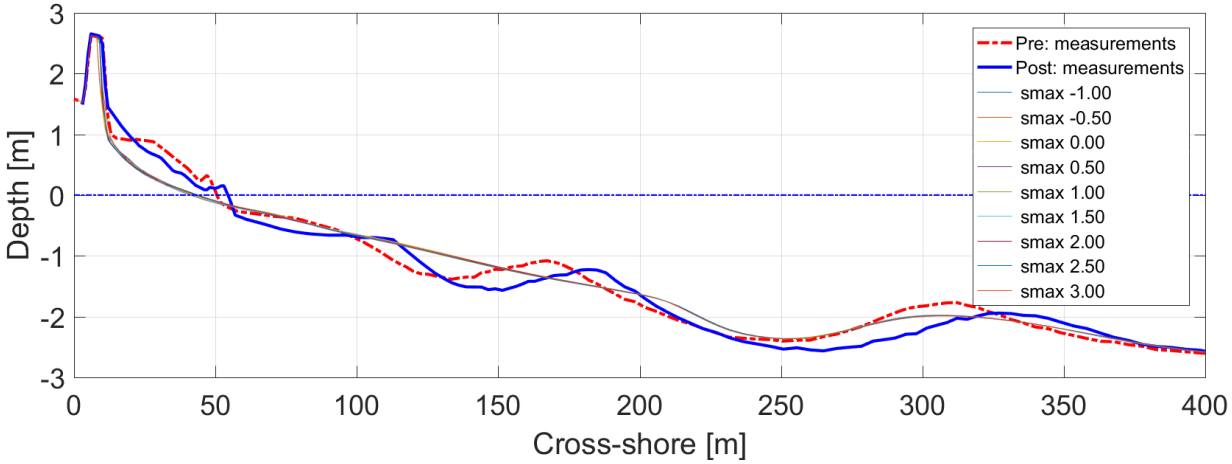

A 3 Post storm bed levels for a single cross-section for various values of smax, related to the storm event of the 20-24 November 2015. The forecasted beach profiles are compared to the observed post storm profile (blue line).

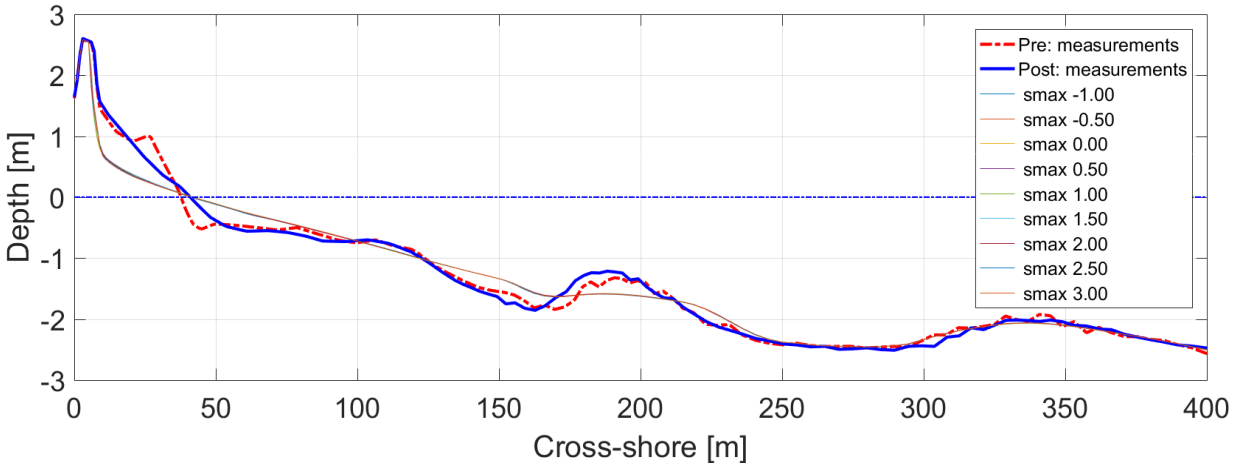

A 4 Post storm bed levels for a single cross-section for various values of smax, related to the storm event of the 27 February-02 March 2016. The forecasted beach profiles are compared to the observed post storm profile (blue line).

A.1.3 Lws parameter

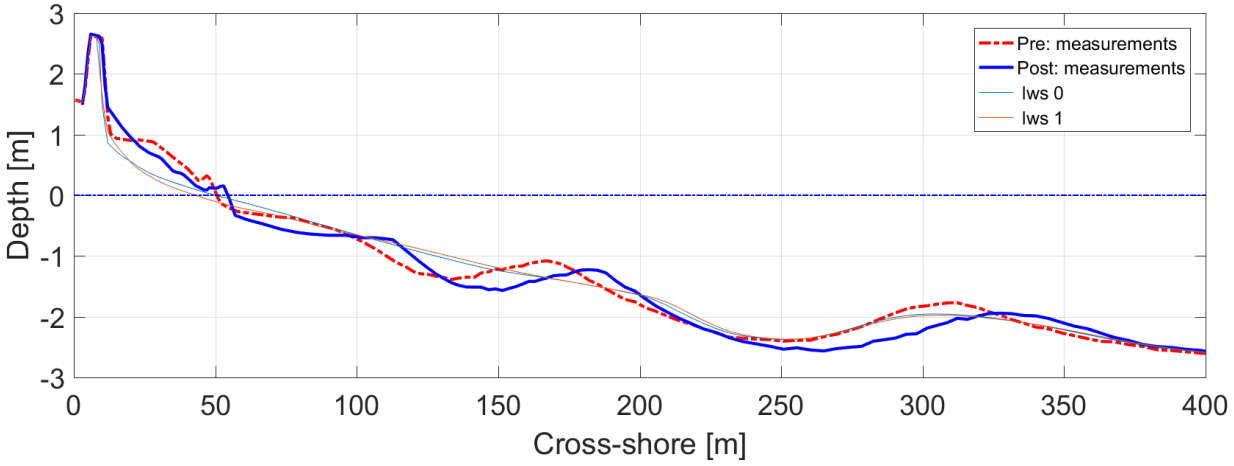

A 5 Post storm bed levels for a single cross-section for various values of lws, related to the storm event of the 20-24 November 2015. The forecasted beach profiles are compared to the observed post storm profile (blue line).

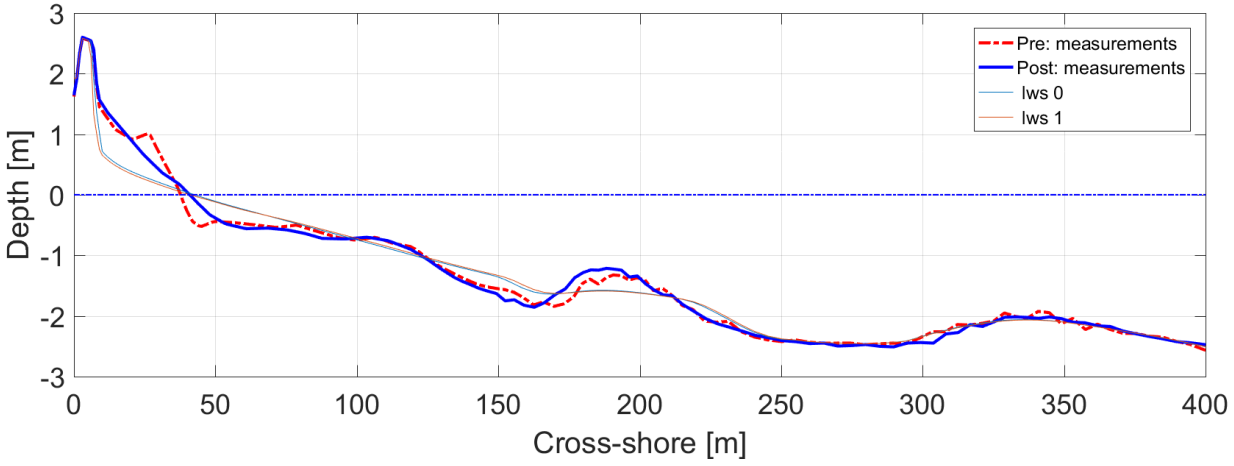

A 6 Post storm bed levels for a single cross-section for various values of lws, related to the storm event of the 27 February-02 March 2016. The forecasted beach profiles are compared to the observed post storm profile (blue line).

A.1.4 Facua parameter

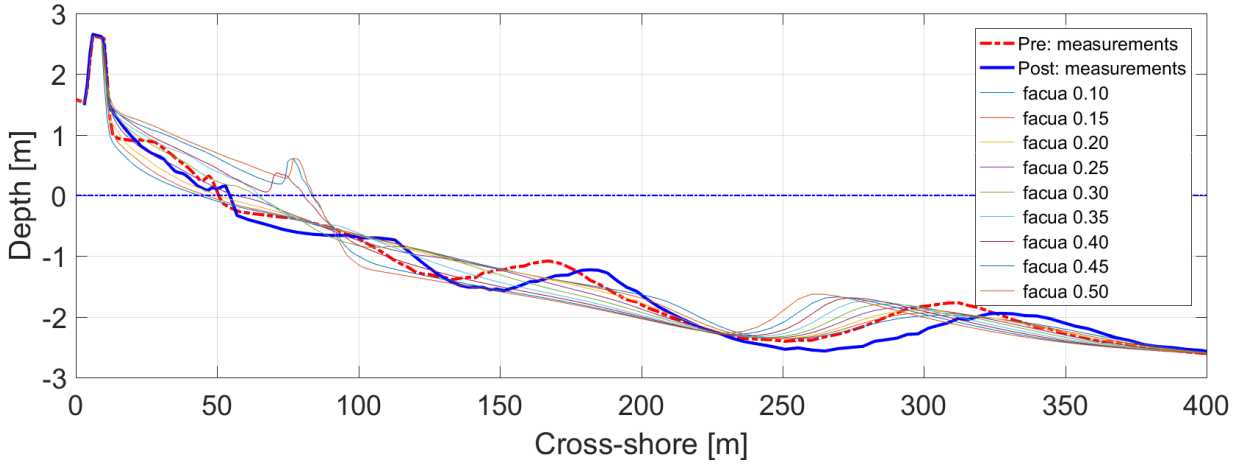

A 7 Post storm bed levels for a single cross-section for various values of facua, related to the storm event of the 20-24 November 2015. The forecasted beach profiles are compared to the observed post storm profile (blue line).

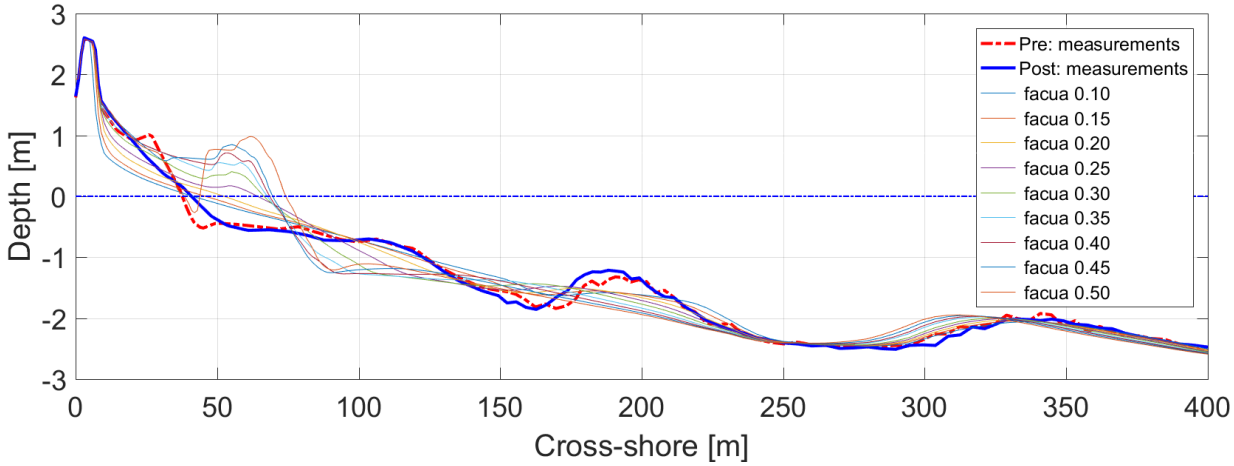

A 8 Post storm bed levels for a single cross-section for various values of facua, related to the storm event of the 27 February-02 March 2016. The forecasted beach profiles are compared to the observed post storm profile (blue line).

A.2 Short wave action

A.2.1 Break parameter

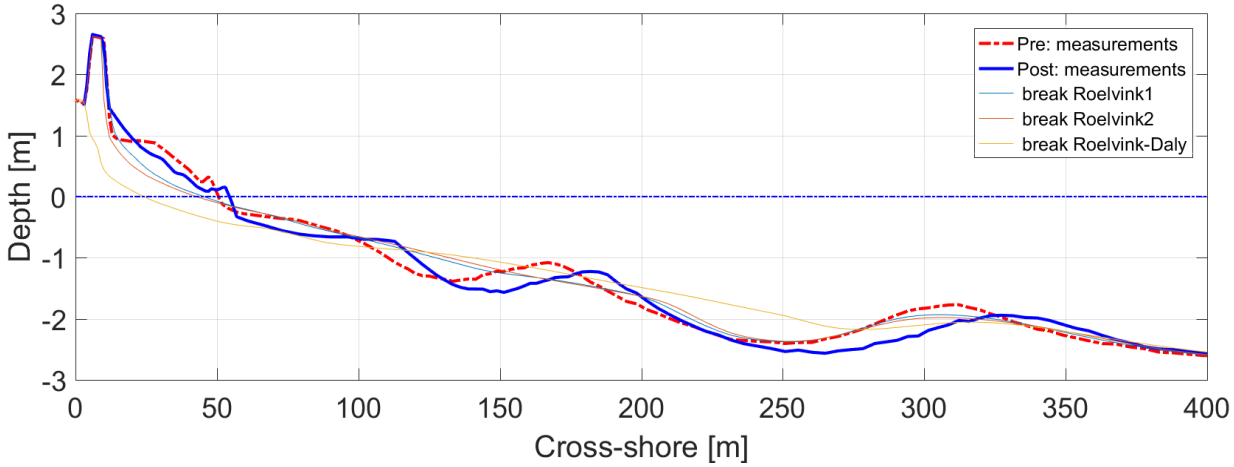

A 9 Post storm bed levels for a single cross-section for various values of break, related to the storm event of the 20-24 November 2015. The forecasted beach profiles are compared to the observed post storm profile (blue line).

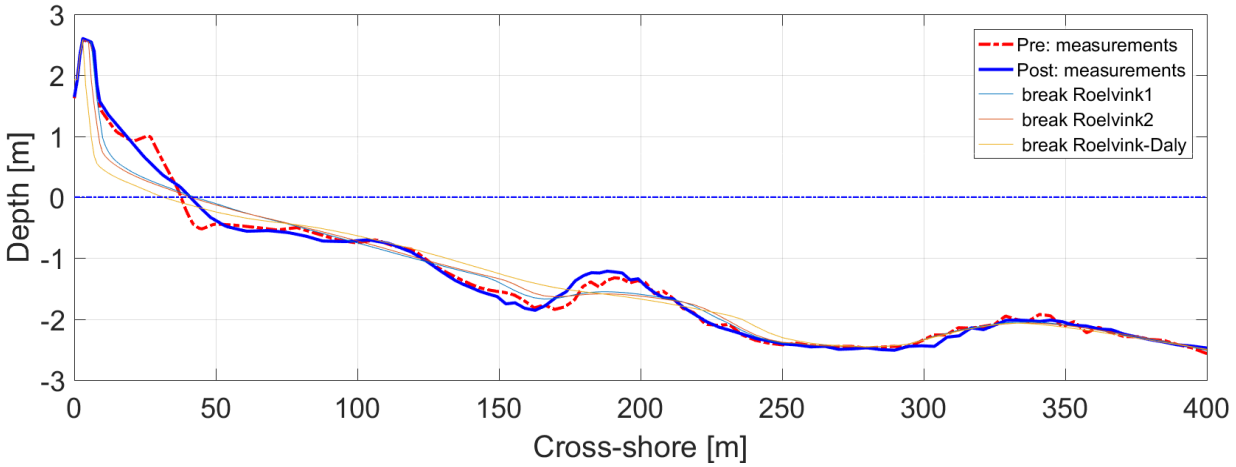

A 10 Post storm bed levels for a single cross-section for various values of break, related to the storm event of the 27 February-02 March 2016. The forecasted beach profiles are compared to the observed post storm profile (blue line).

A.2.2 Gamma parameter

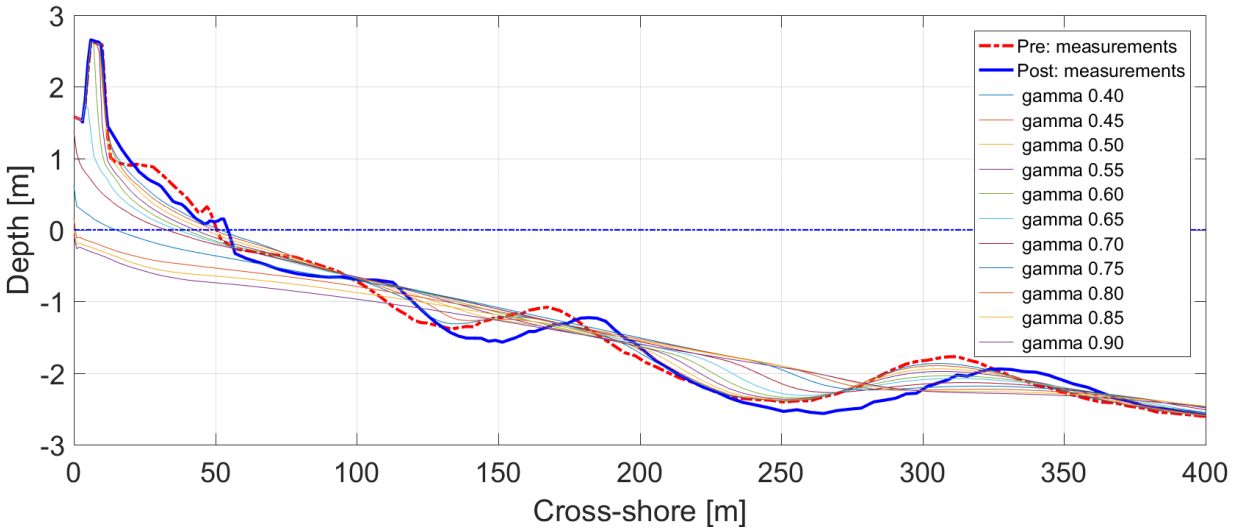

A 11 Post storm bed levels for a single cross-section for various values of gamma, related to the storm event of the 20-24 November 2015. The forecasted beach profiles are compared to the observed post storm profile (blue line).

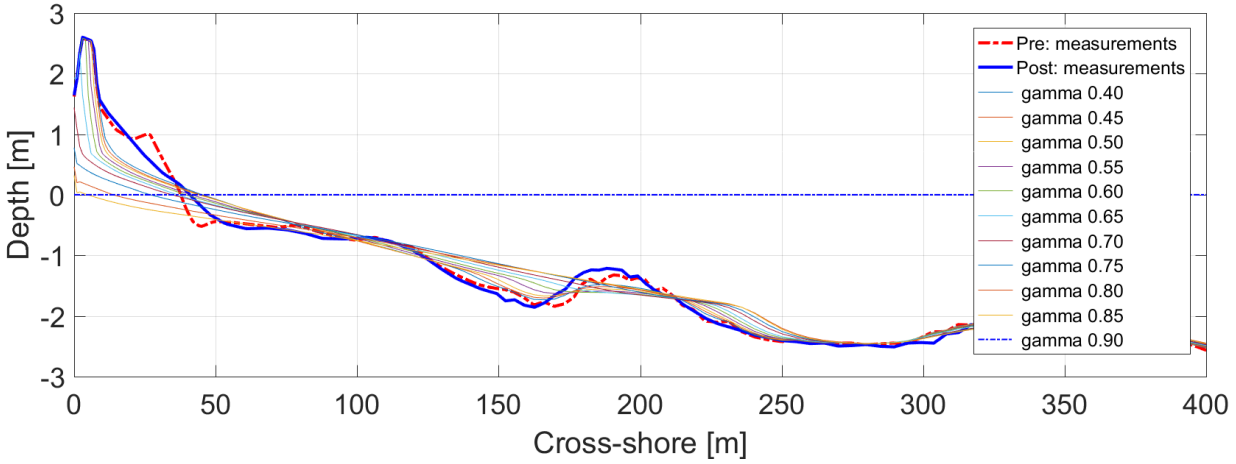

A 12 Post storm bed levels for a single cross-section for various values of gamma, related to the storm event of the 27 February-02 March 2016. The forecasted beach profiles are compared to the observed post storm profile (blue line).

A.2.3 Turb parameter

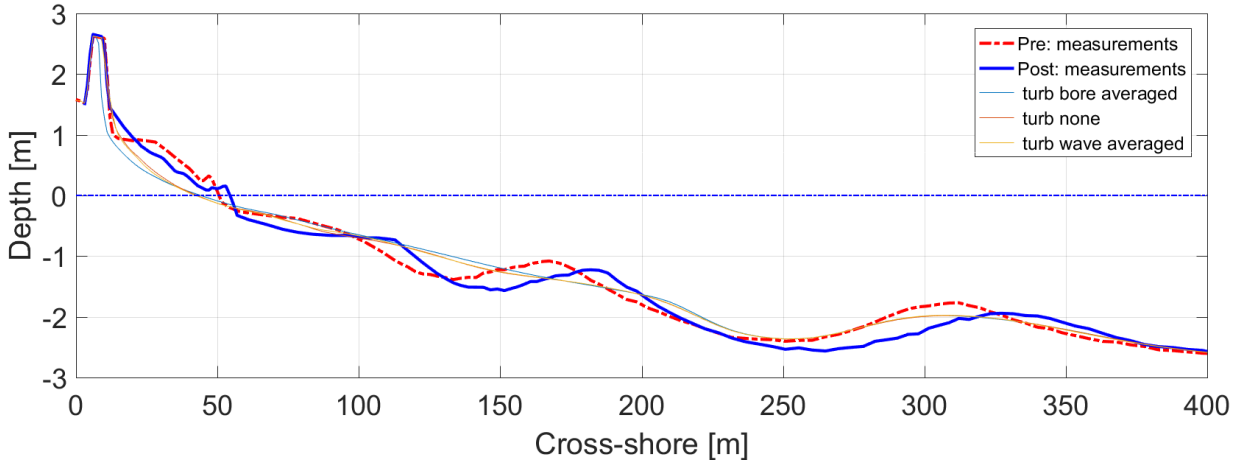

A 13 Post storm bed levels for a single cross-section for various values of turb, related to the storm event of the 20-24 November 2015. The forecasted beach profiles are compared to the observed post storm profile (blue line).

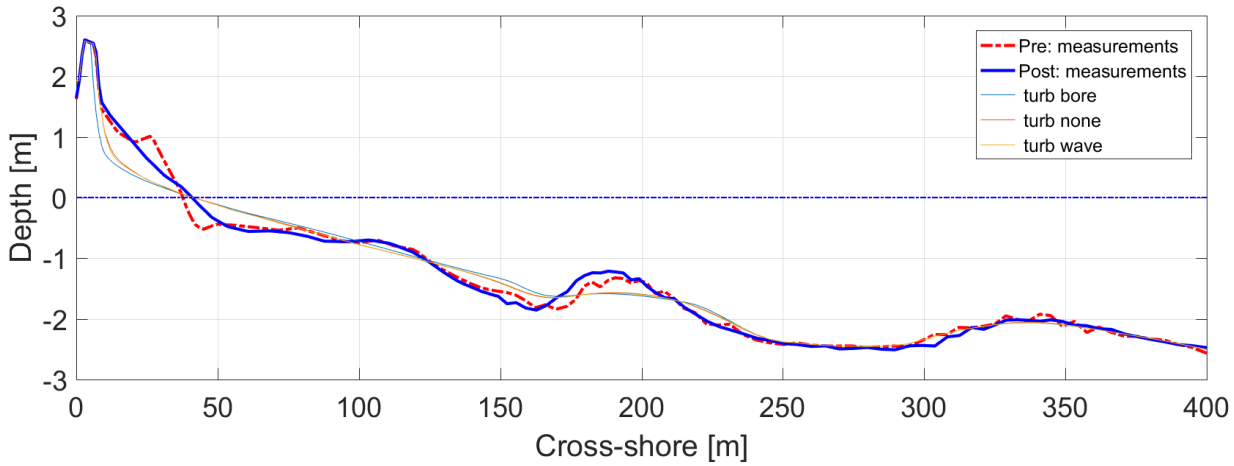

A 14 Post storm bed levels for a single cross-section for various values of turb, related to the storm event of the 27 February-02 March 2016. The forecasted beach profiles are compared to the observed post storm profile (blue line).

A.2.4 Fw parameter

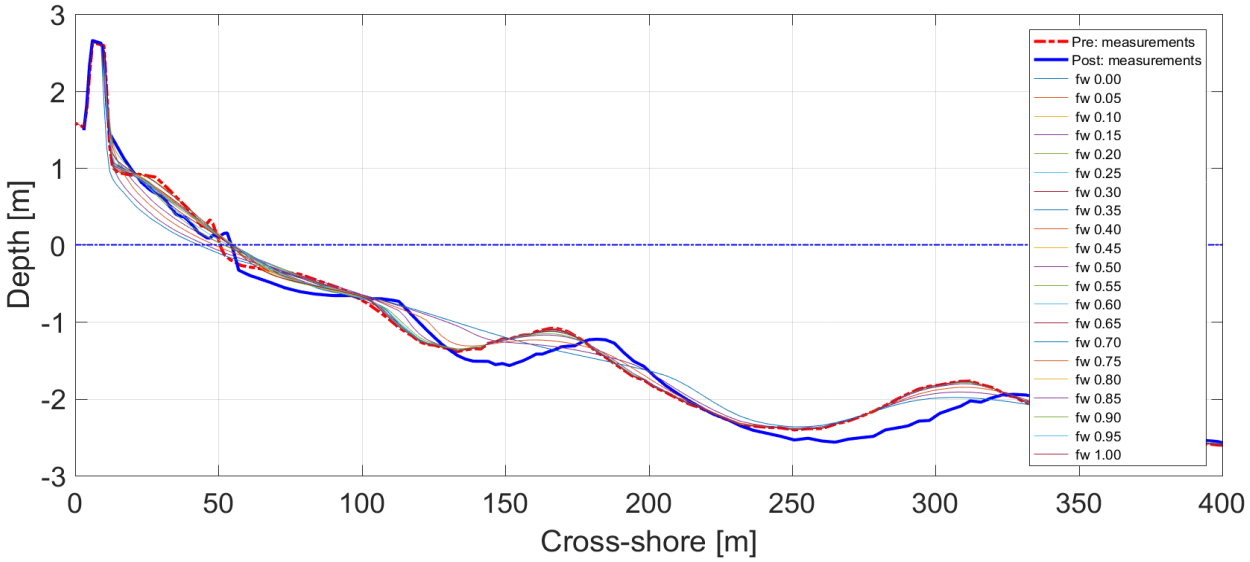

A 15 Post storm bed levels for a single cross-section for various values of fw, related to the storm event of the 20-24 November 2015. The forecasted beach profiles are compared to the observed post storm profile (blue line).

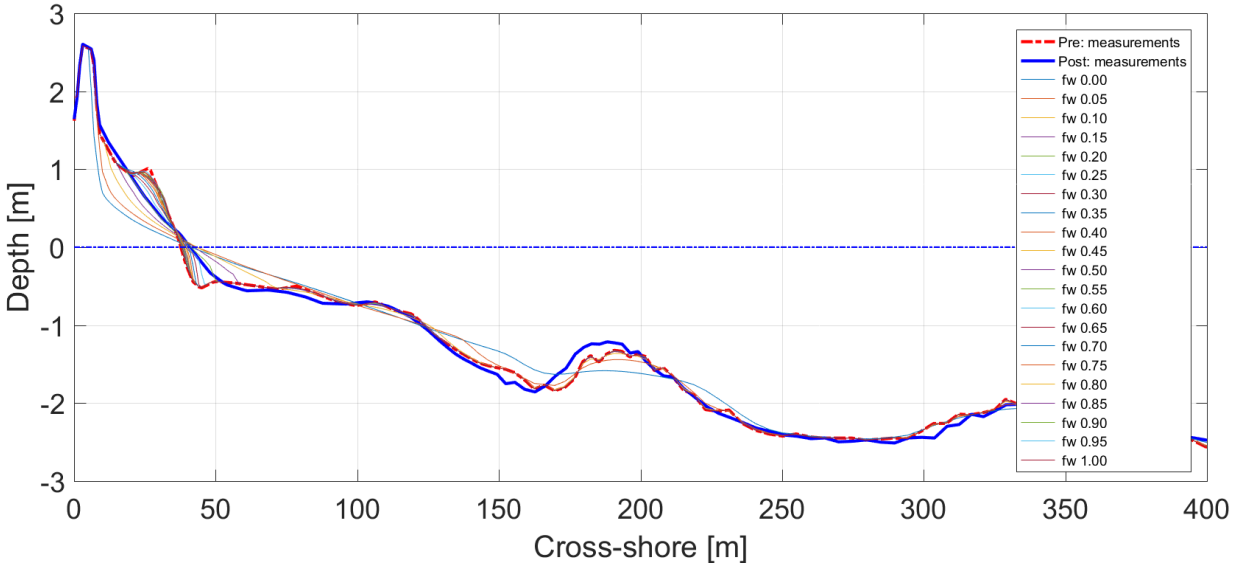

A 16 Post storm bed levels for a single cross-section for various values of fw, related to the storm event of the 27 February-02 March 2016. The forecasted beach profiles are compared to the observed post storm profile (blue line).

A.2.5 Delta parameter

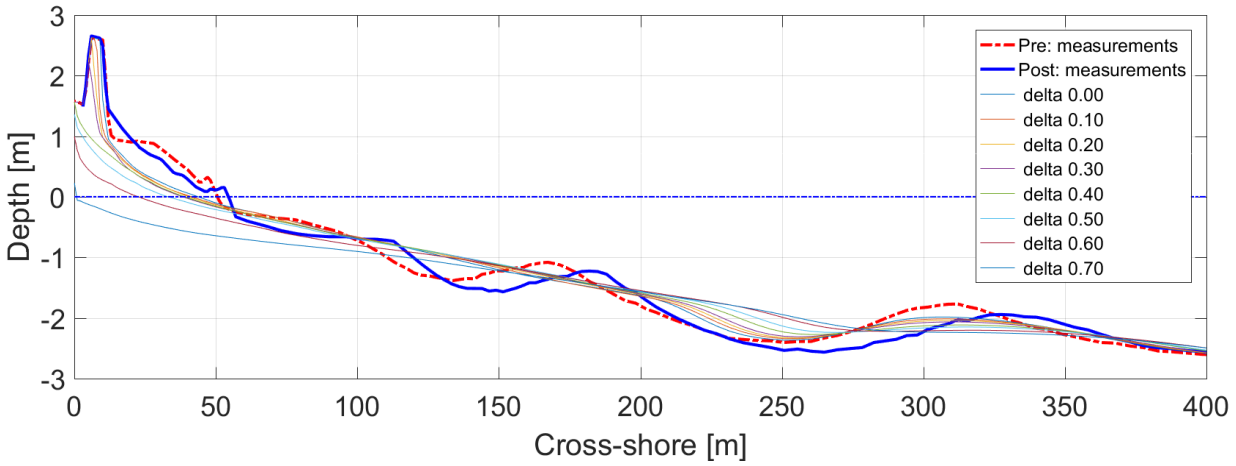

A 17 Post storm bed levels for a single cross-section for various values of delta, related to the storm event of the 20-24 November 2015. The forecasted beach profiles are compared to the observed post storm profile (blue line).

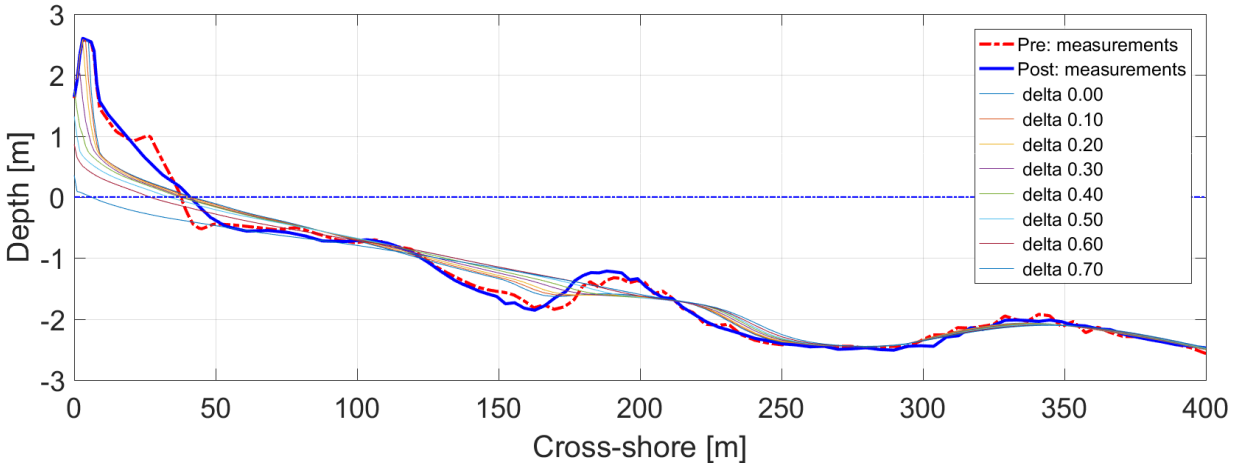

A 18 Post storm bed levels for a single cross-section for various values of delta, related to the storm event of the 27 February-02 March 2016. The forecasted beach profiles are compared to the observed post storm profile (blue line).

A.3 Shallow water equation

A.3.1 Eps parameter

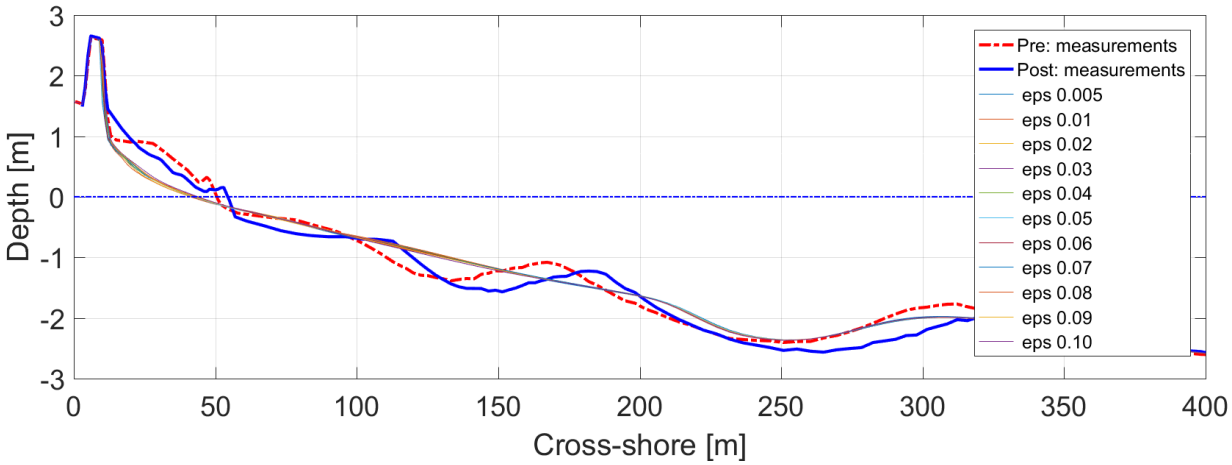

A 19 Post storm bed levels for a single cross-section for various values of eps, related to the storm event of the 20-24 November 2015. The forecasted beach profiles are compared to the observed post storm profile (blue line).

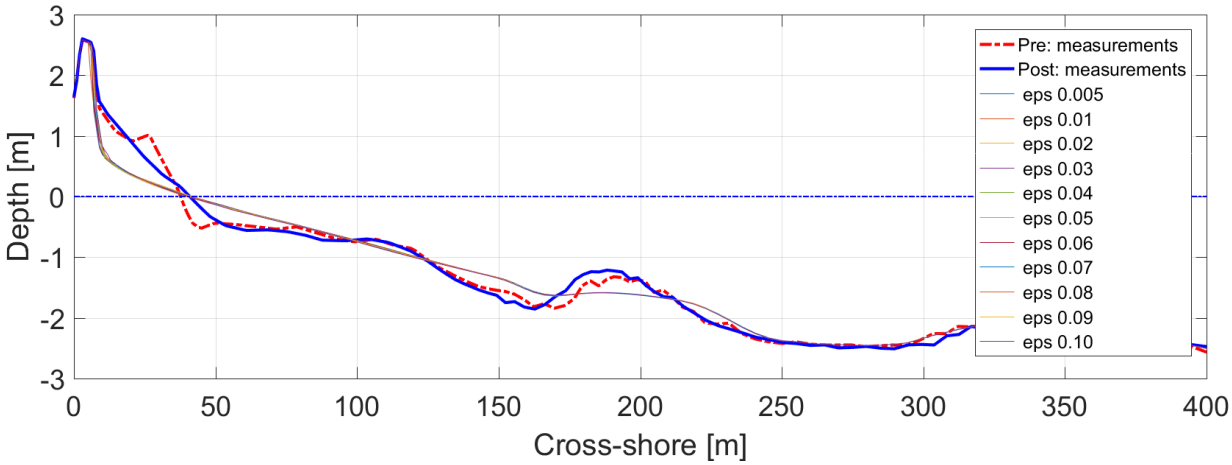

A 20 Post storm bed levels for a single cross-section for various values of eps, related to the storm event of the 27 February-02 March 2016. The forecasted beach profiles are compared to the observed post storm profile (blue line).

A.3.2 Umin

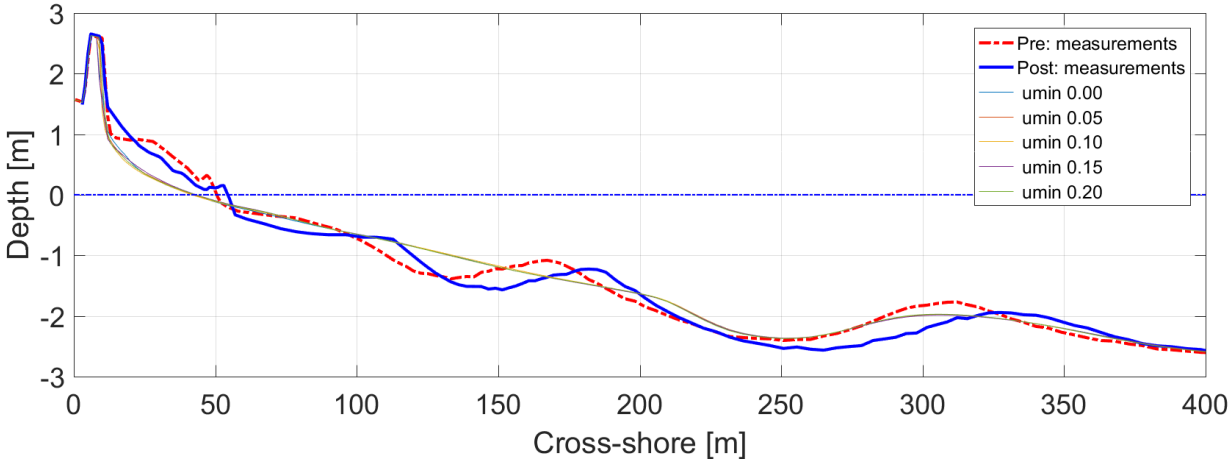

A 21 Post storm bed levels for a single cross-section for various values of umin, related to the storm event of the 20-24 November 2015. The forecasted beach profiles are compared to the observed post storm profile (blue line).

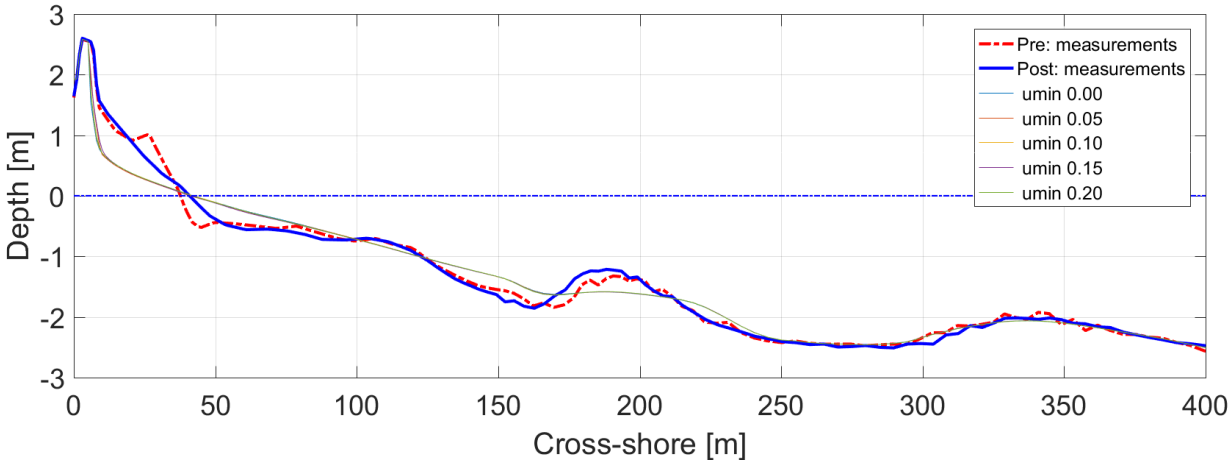

A 22 Post storm bed levels for a single cross-section for various values of umin, related to the storm event of the 27 February-02 March 2016. The forecasted beach profiles are compared to the observed post storm profile (blue line).

A.3.3 Bedfriccoef parameter

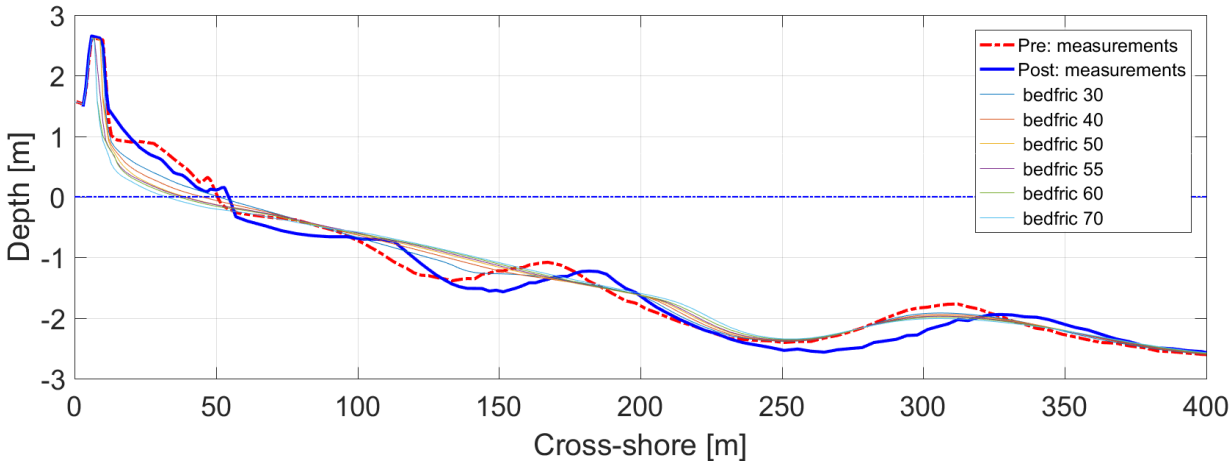

A 23 Post storm bed levels for a single cross-section for various values of bedfriccoef, related to the storm event of the 20-24 November 2015. The forecasted beach profiles are compared to the observed post storm profile (blue line).

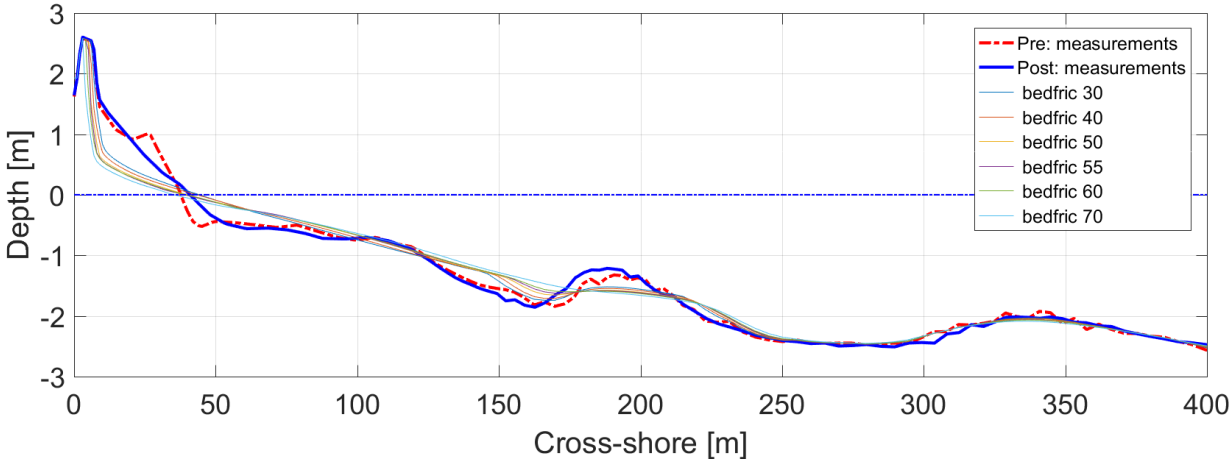

A 24 Post storm bed levels for a single cross-section for various values of bedfriccoef, related to the storm event of the 27 February-02 March 2016. The forecasted beach profiles are compared to the observed post storm profile (blue line).

A.4 Bottom updating

A.4.1 Wetslp parameter

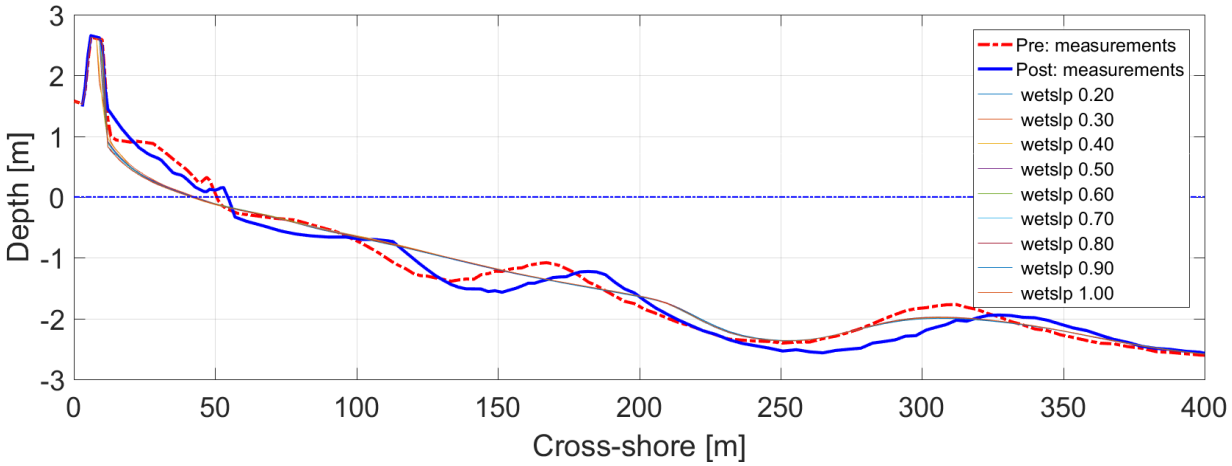

A 25 Post storm bed levels for a single cross-section for various values of wetslp, related to the storm event of the 20-24 November 2015. The forecasted beach profiles are compared to the observed post storm profile (blue line).

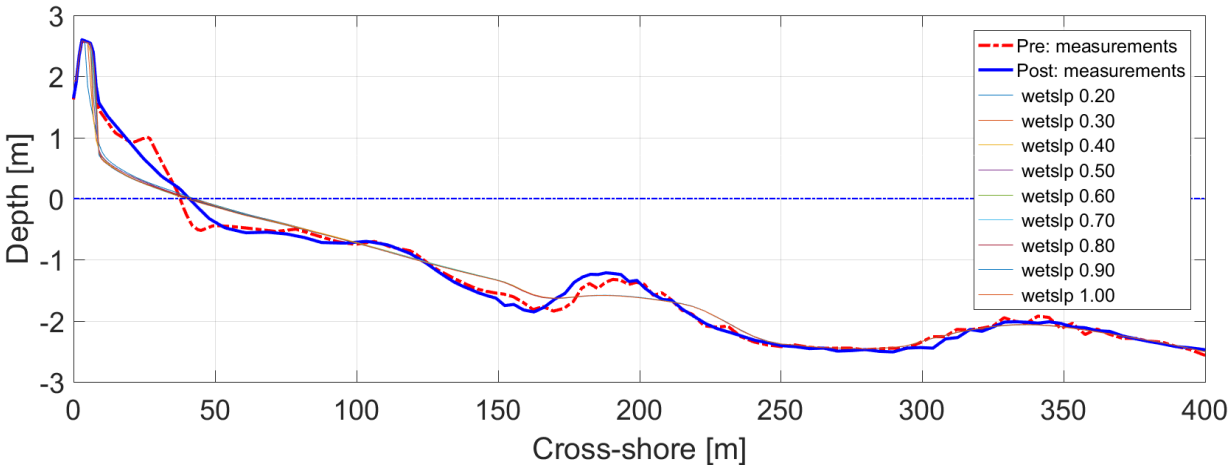

A 26 Post storm bed levels for a single cross-section for various values of wetslp, related to the storm event of the 27 February-02 March 2016. The forecasted beach profiles are compared to the observed post storm profile (blue line).

A.4.1 Dryslp parameter

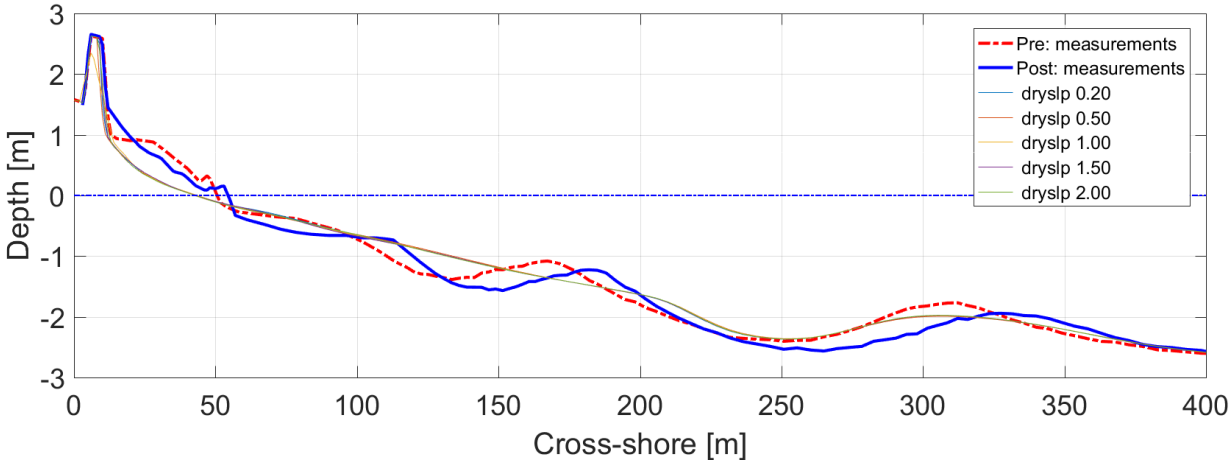

A 27 Post storm bed levels for a single cross-section for various values of dryslp, related to the storm event of the 20-24 November 2015. The forecasted beach profiles are compared to the observed post storm profile (blue line).

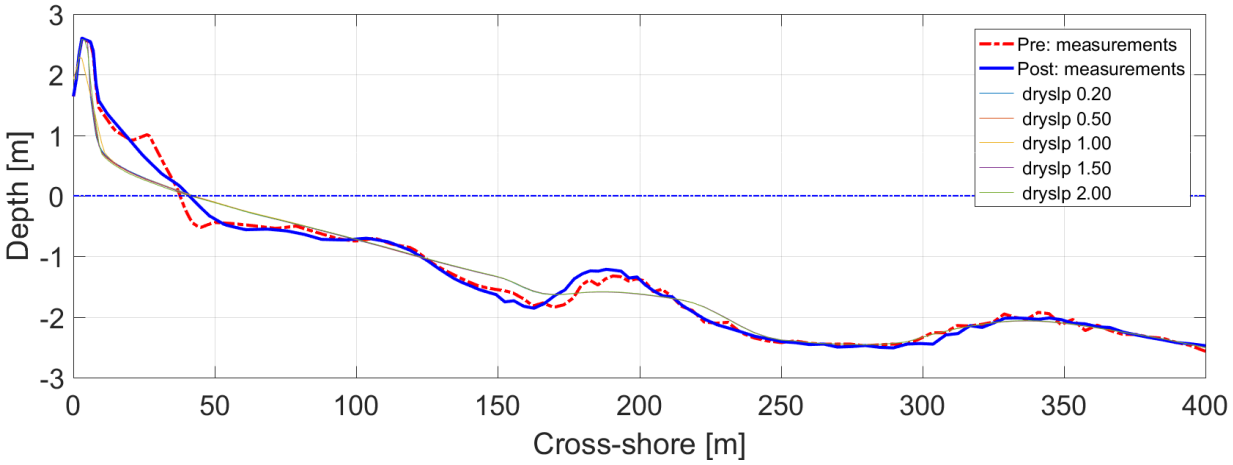

A 28 Post storm bed levels for a single cross-section for various values of dryslp, related to the storm event of the 27 February-02 March 2016. The forecasted beach profiles are compared to the observed post storm profile (blue line).

APPENDIX B

Wind and mean sea level pressure maps

The analysis of the propagation of the uncertainties within the numerical forecasting chain, composed by the meteorological model COSMO, the wave/oceanographic models SWAN and ROMS and the morphological model XBeach, is presented in Chapter 5. The purpose of the study is to integrate these numerical models in an ensemble prediction framework of coastal flood risk. Indeed, the analysis was carried out by means the ensemble method.

The analysis was applied to 2 storm events that occurred in the winter 2015-2016. A complete description of the storms is presented in Section 3.2 and Section 3.3 of Chapter 3.

The study contained different analysis steps, based on the comparison of the models forecasts with the observations at defined locations. In this appendix, the wind maps generated every 6 hours for both the period of verifications, which extend from 20 to 24 November 2015 and from 27 February to 2 March 2016, are presented. In Chapter 5 the significant maps corresponding to the peak of the storms can be found.

The wind and mean sea level pressure forecasts of the two storms are presented separated.

B.1 The storm of 20 November 2015

B.1.1 Deterministic Forecasts

In this subsection, the deterministic forecasts (COSMO I-7) of wind and mean sea level pressure, over the period from 20 to 24 November 2015, are presented. The forecasts are visualized with the ECMWF analysis represented in black (B 1, B 2 and B 3). The legend helps to read the maps.

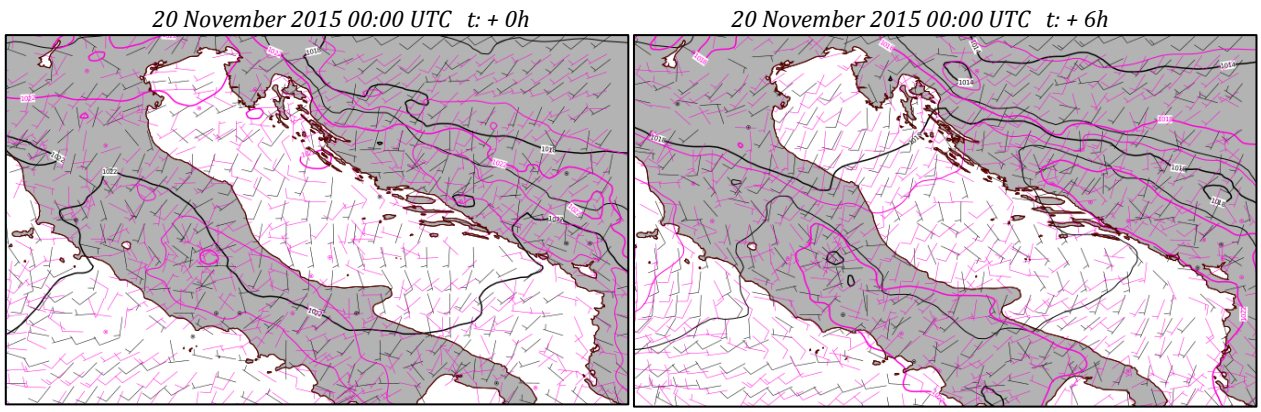

B 1 Mean sea level pressure and 10 m wind forecasts of 20-11-2015 at +0h and +6h.. Comparison of the ECMWF analysis (black) and the deterministic run of COSMO-I7 (magenta).

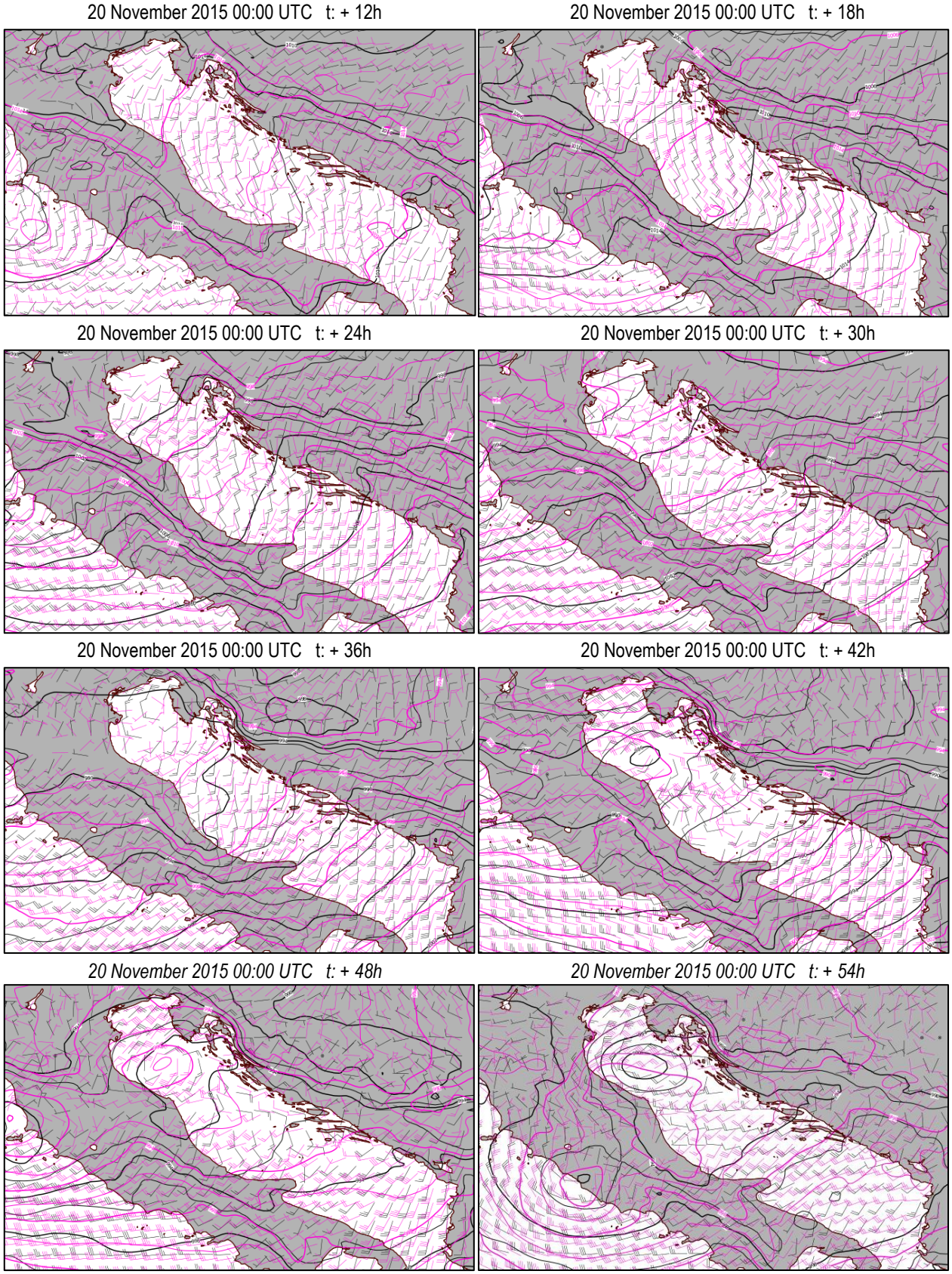

B 2 Mean sea level pressure and 10 m wind forecasts of 20-11-2015 from+12h to +54h. Comparison of the ECMWF analysis (black) and the deterministic run of COSMO-I7 (magenta).

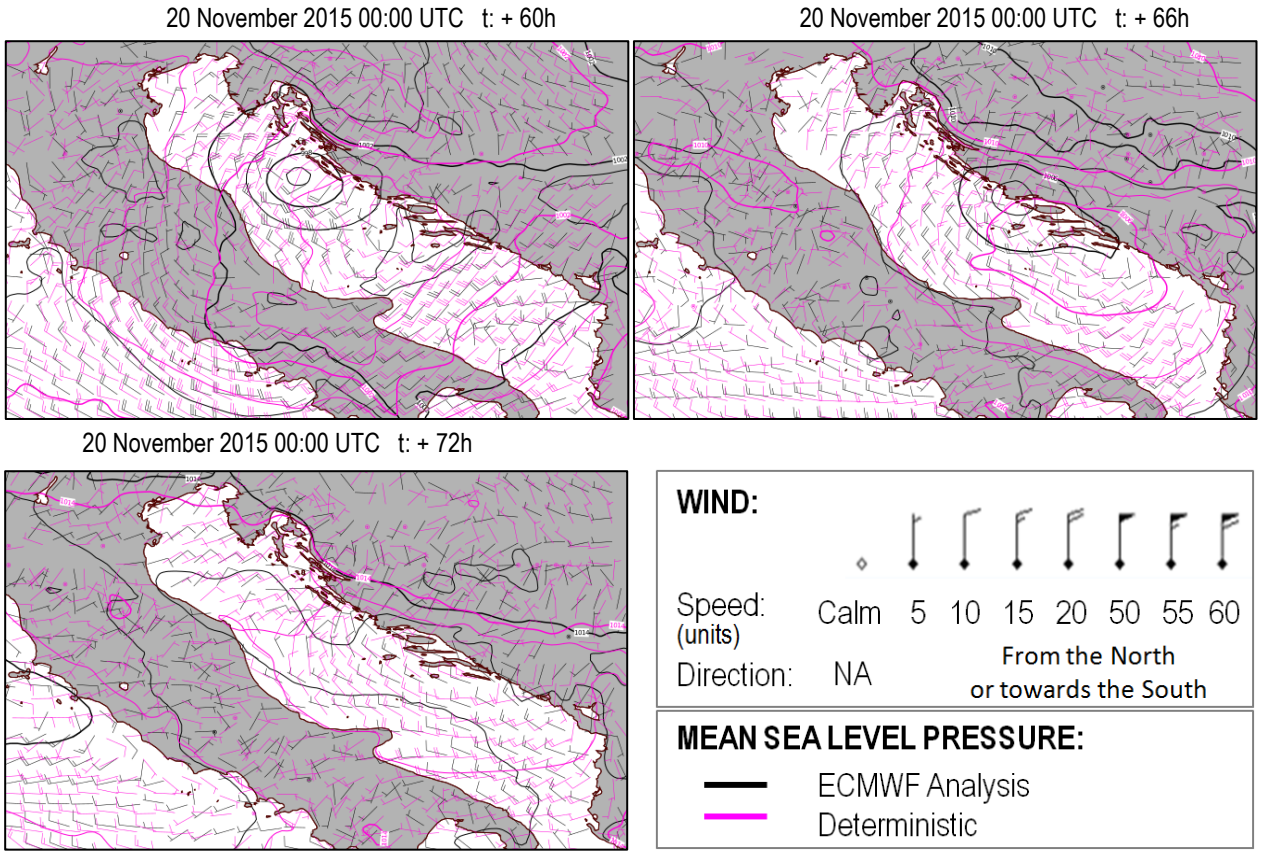

B 3 Mean sea level pressure and 10 m wind forecasts of 20-11-2015 from+60h to +72h. Comparison of the ECMWF analysis (black) and the deterministic run of COSMO-I7 (magenta).

B.1.2 Probabilistic Forecasts

In this subsection, the comparison maps of wind and mean sea level pressure forecasts obtained from the deterministic run of the ensemble model COSMO LEPS and the ECMWF analysis, over the period from 20 to 24 November 2015, are reported (B 4, B 5 and B 6). Due to graphic limitation, the deterministic run of the ensemble model COSMO-LEPS (green line) is compared with the ECMWF analysis (black line).The legend helps to read the maps.

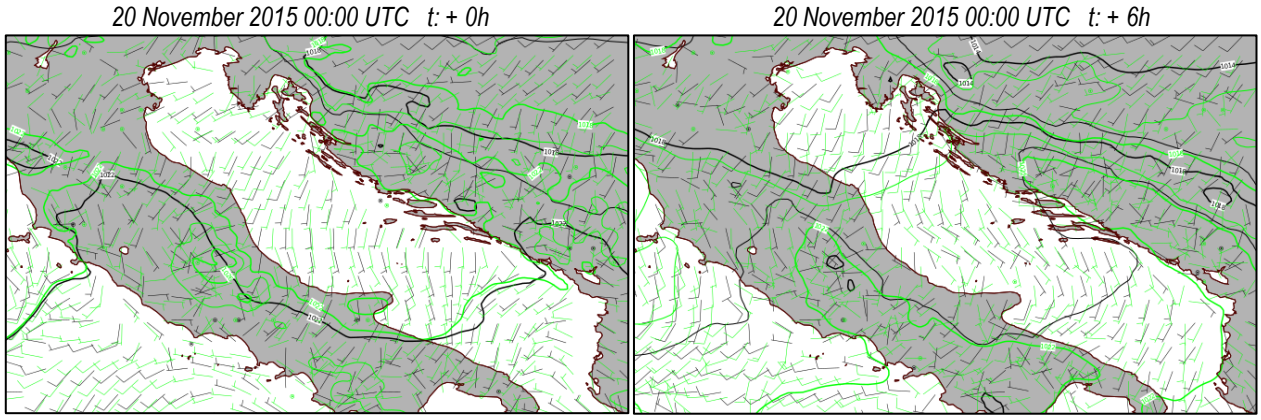

B 4 Mean sea level pressure and 10 m wind forecasts of 20-11-2015 at +0 h and +6 h. Comparison of the ECMWF analysis (black) and the deterministic run of COSMO-LEPS (green).

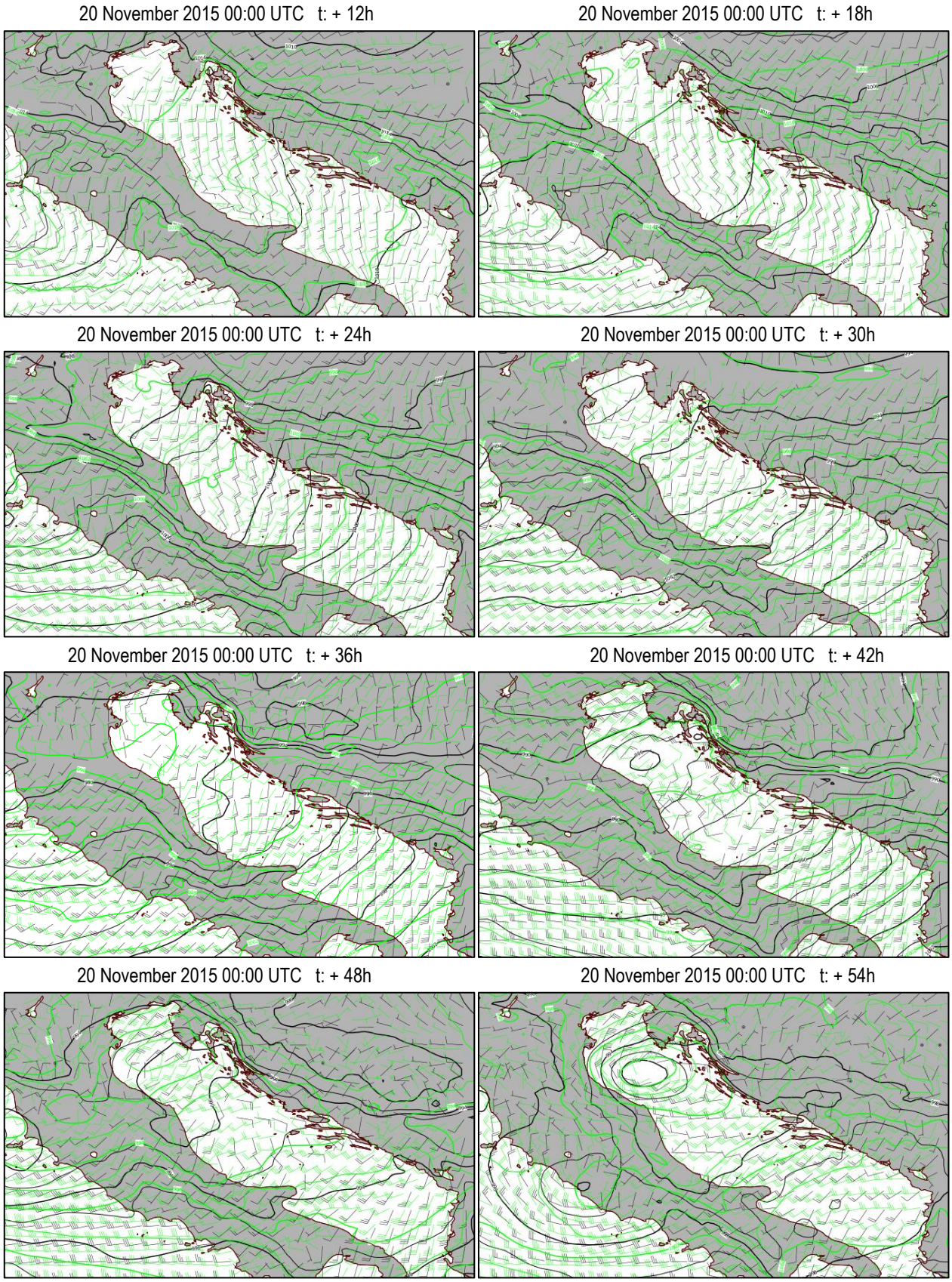

B 5 Mean sea level pressure and 10 m wind forecasts of 20-11-2015 from +12 h to +54 h. Comparison of the ECMWF analysis (black) and the deterministic run of COSMO-LEPS (green).

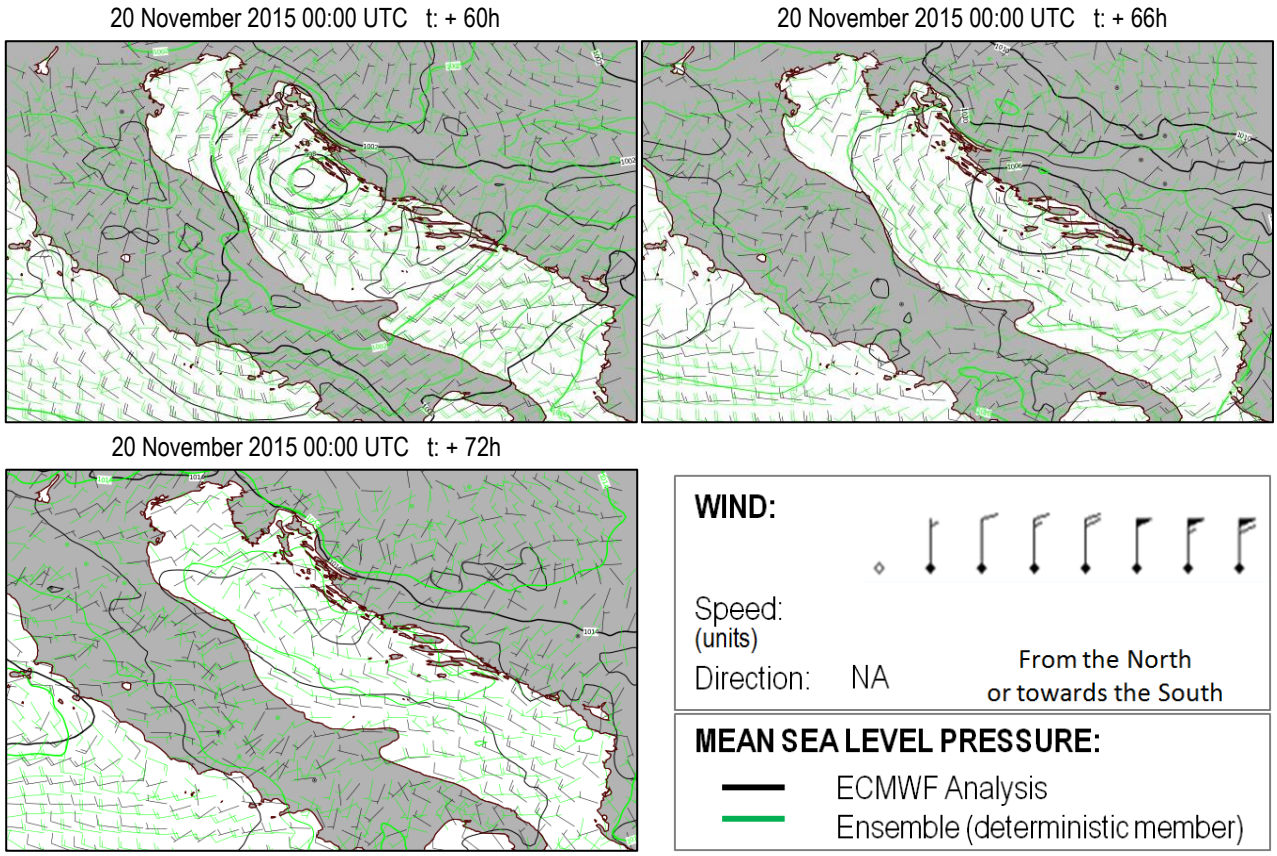

B 6 Mean sea level pressure and 10 m wind forecasts of 20-11-2015 from +60 h to +72 h. Comparison of the ECMWF analysis (black) and the deterministic run of COSMO-LEPS (green).

B.2 The storm of 27 February 2016

B.2.1 Period of verification: 27 February - 02 March 2016

In this subsection, the deterministic forecasts (COSMO I-7) of wind and mean sea level pressure, over the period from 27 February to 2 March 2016, are presented. The forecasts are visualized with the ECMWF analysis represented in black (B 7, B 8 and B 9). The legend helps to read the maps.

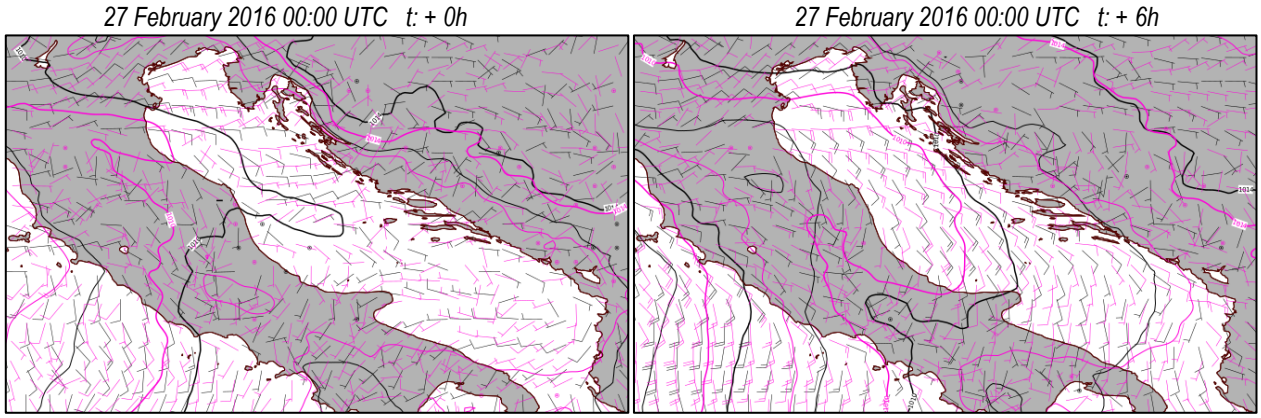

B 7 Mean sea level pressure and 10 m wind forecasts of 27-02-2016 at +0 h and +6 h. Comparison of the ECMWF analysis (black) and the deterministic run of COSMO-I7 (magenta).

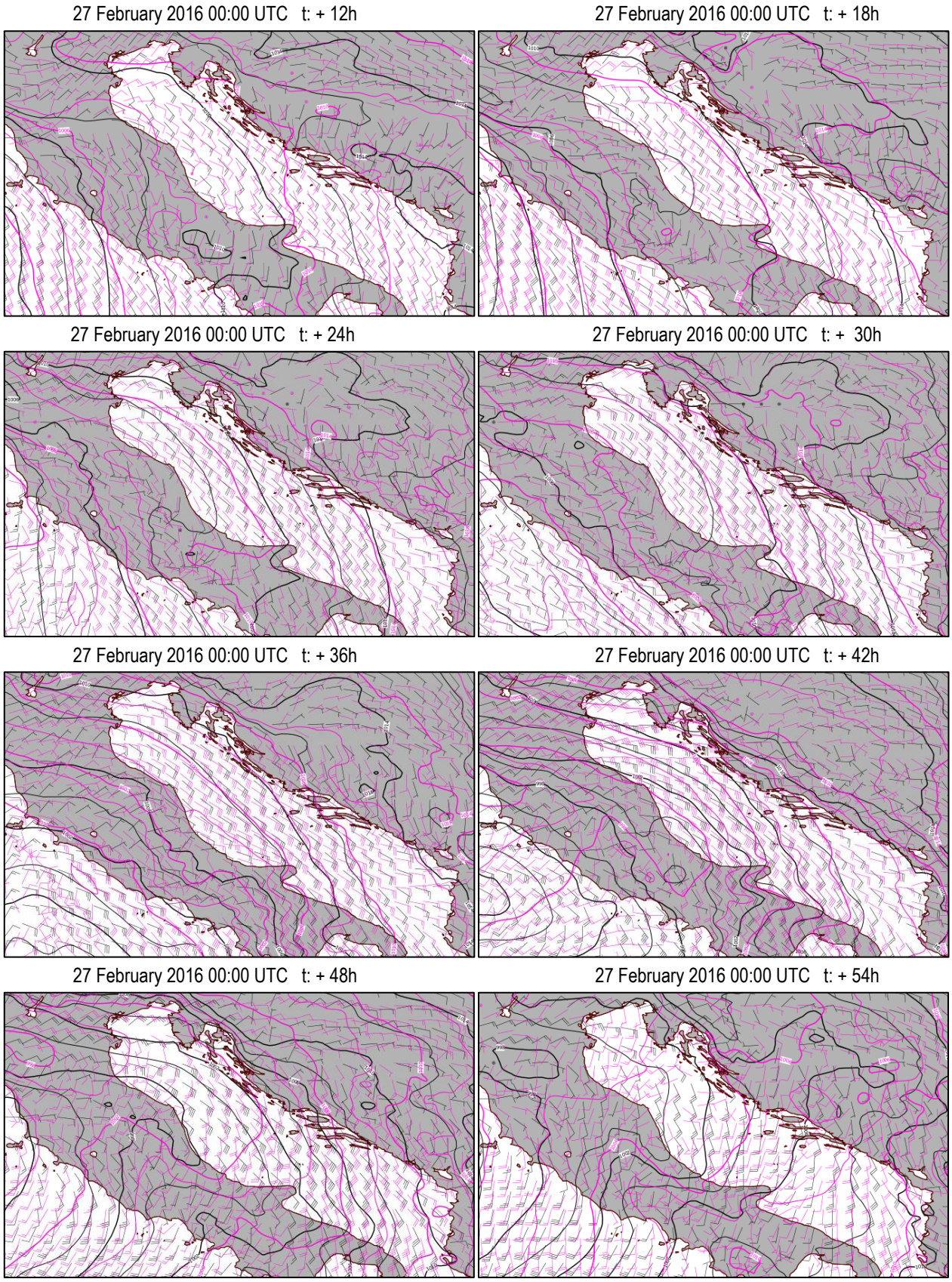

B 8 Mean sea level pressure and 10 m wind forecasts of 27-02-2016 from +12 h to +54 h. Comparison of the ECMWF analysis (black) and the deterministic run of COSMO-I7 (magenta).

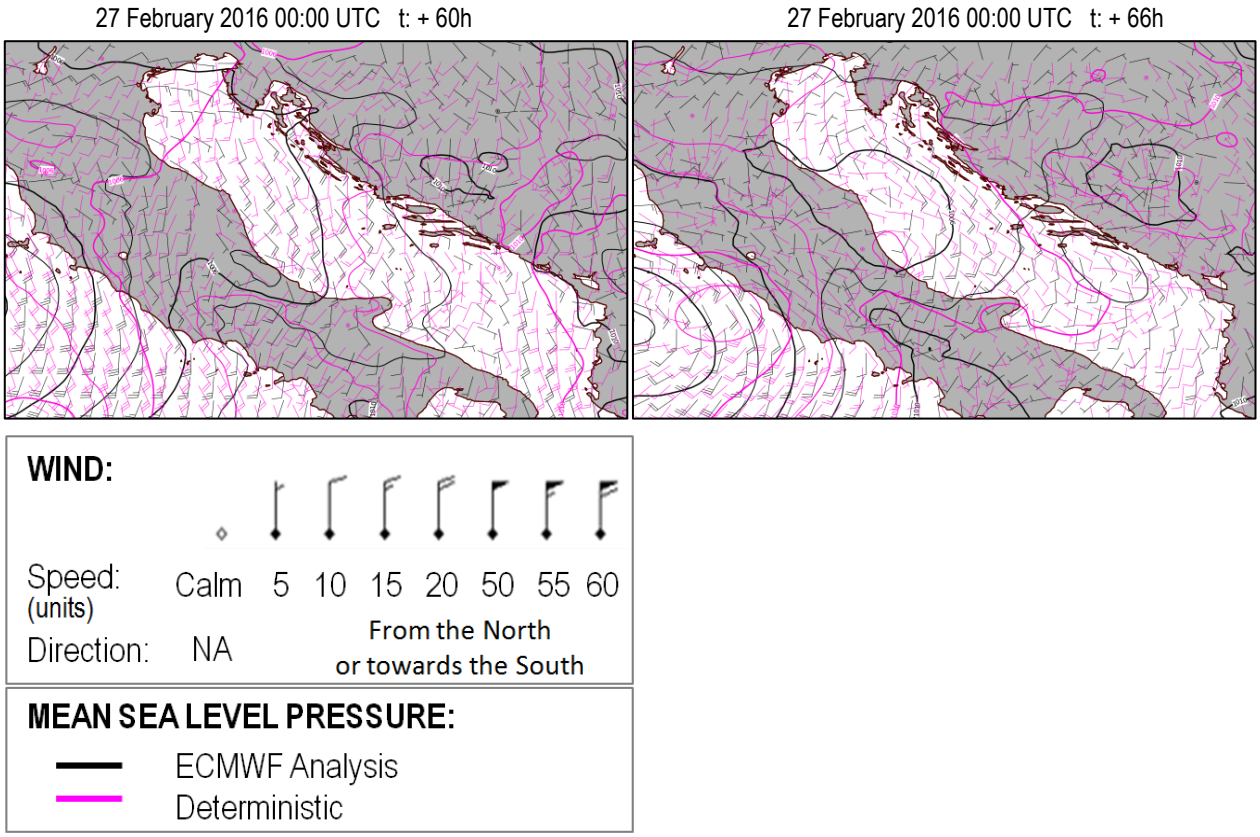

B 9 Mean sea level pressure and 10 m wind forecasts of 27-02-2016 at +60 h and +66 h. Comparison of the ECMWF analysis (black) and the deterministic run of COSMO-I7 (magenta).

B.2.2 Probabilistic Forecasts

In this subsection, the comparison maps of wind and mean sea level pressure forecasts obtained from the deterministic run of the ensemble model COSMO LEPS and the ECMWF analysis, over the period from 27 February to 2 March 2016, are reported (B 10, B 11 and B 12). Due to graphic limitation, the deterministic run of the ensemble model COSMO-LEPS (green line) is compared with the ECMWF analysis (black line).The legend helps to read the maps.

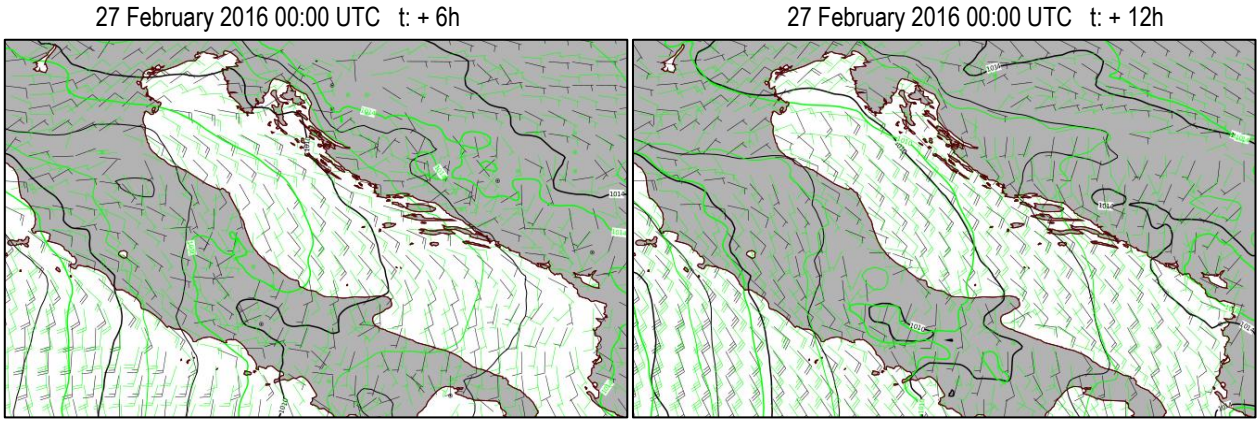

B 10 Mean sea level pressure and 10 m wind forecasts of 27-02-2016 at +6 and +12 h. Comparison of the ECMWF analysis (black) and the deterministic run of COSMO-LEPS (green).

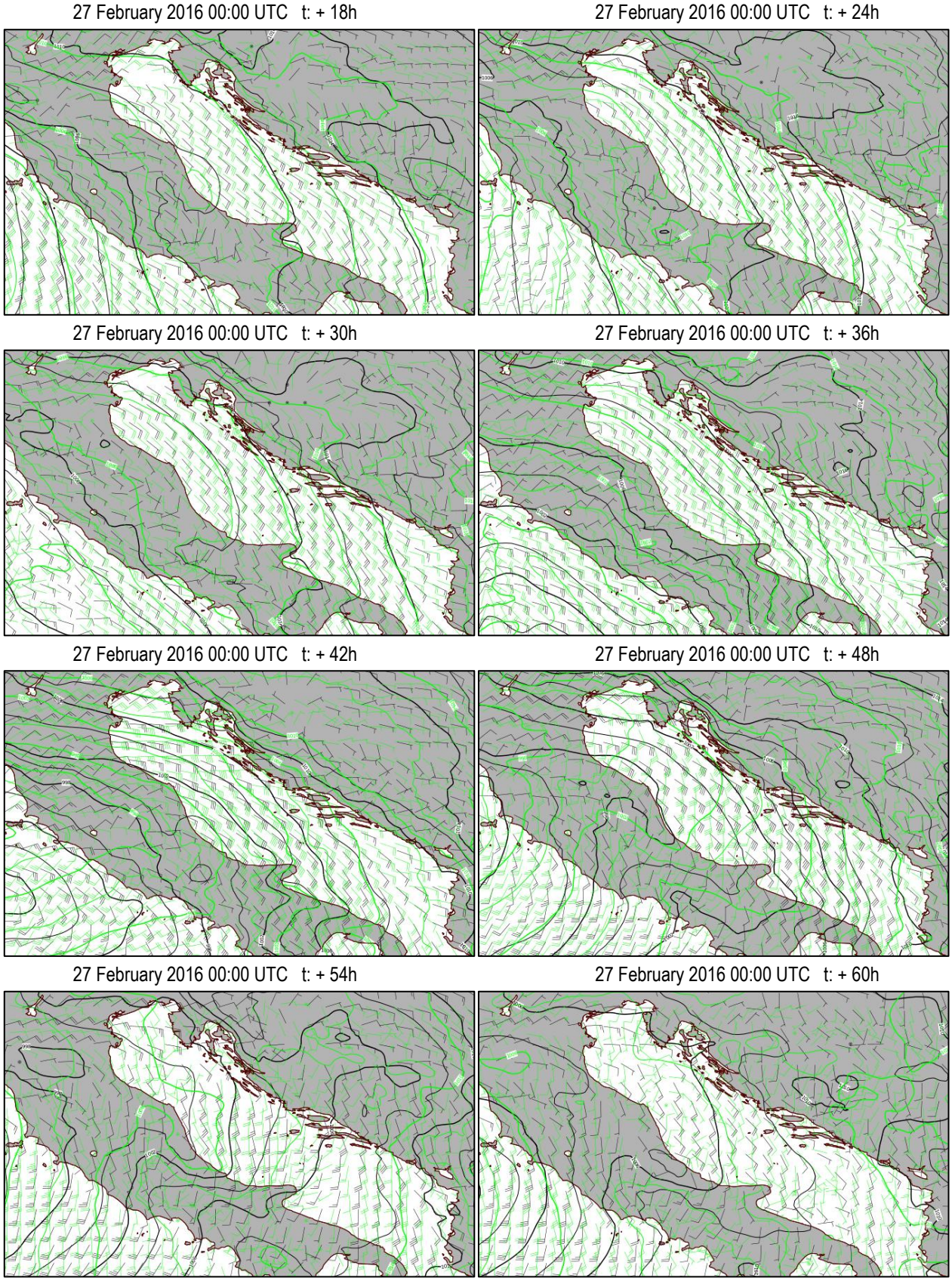

B 11 Mean sea level pressure and 10 m wind forecasts of 27-02-2016 from +18 to +60 h. Comparison of the ECMWF analysis (black) and the deterministic run of COSMO-LEPS (green).

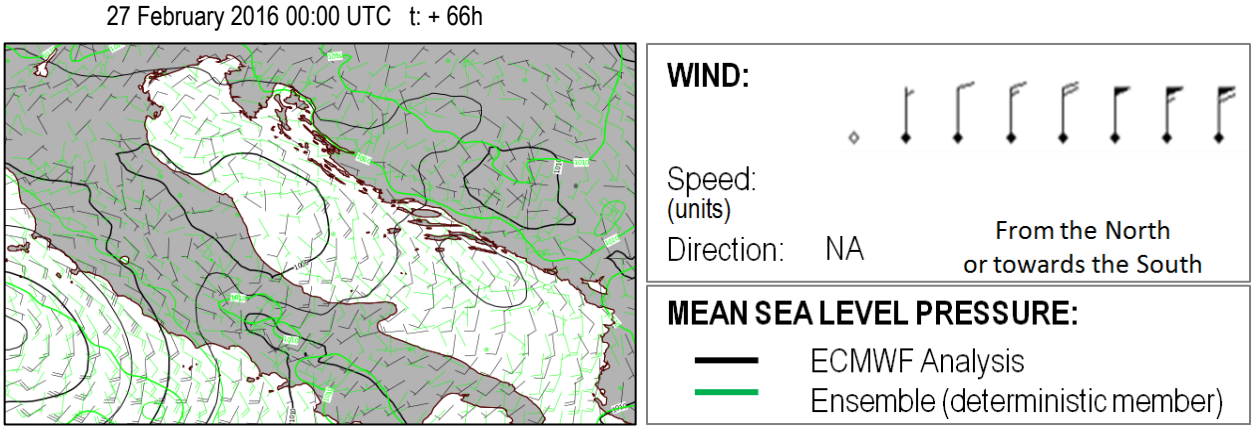

B 12 Mean sea level pressure and 10 m wind forecasts of 27-02-2016 at +66 h. Comparison of the ECMWF analysis (black) and the deterministic run of COSMO-LEPS (green).